

CPIMS 14

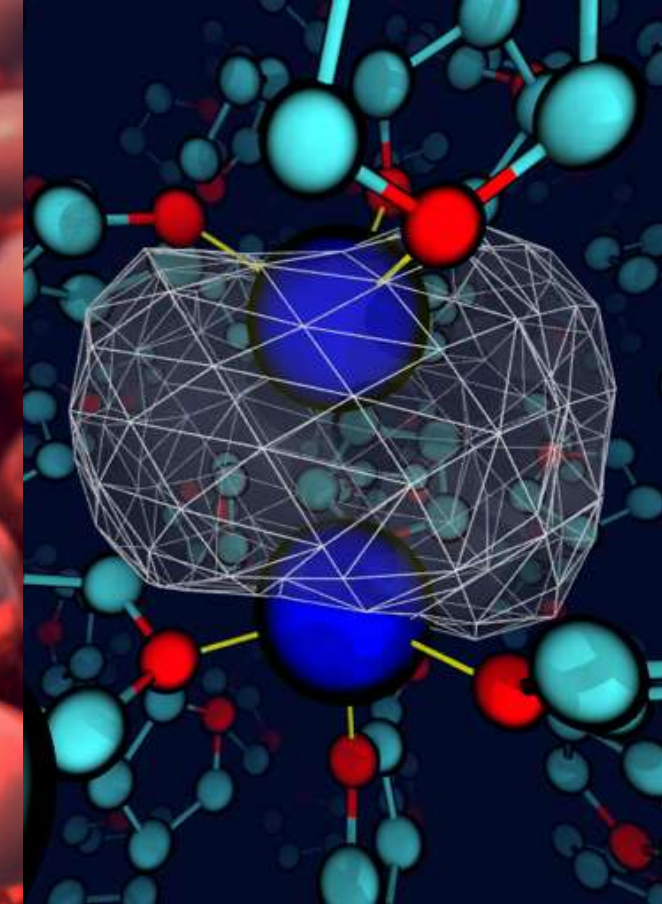
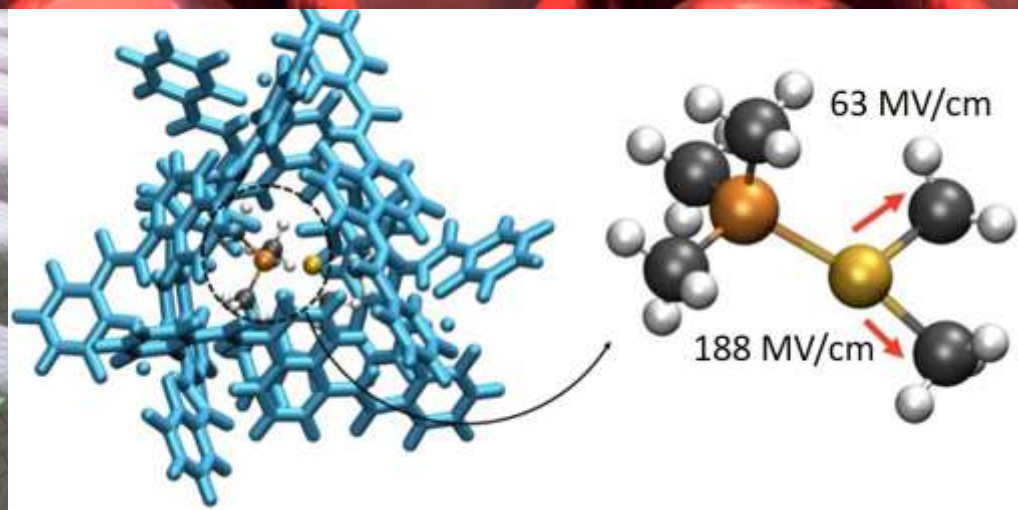
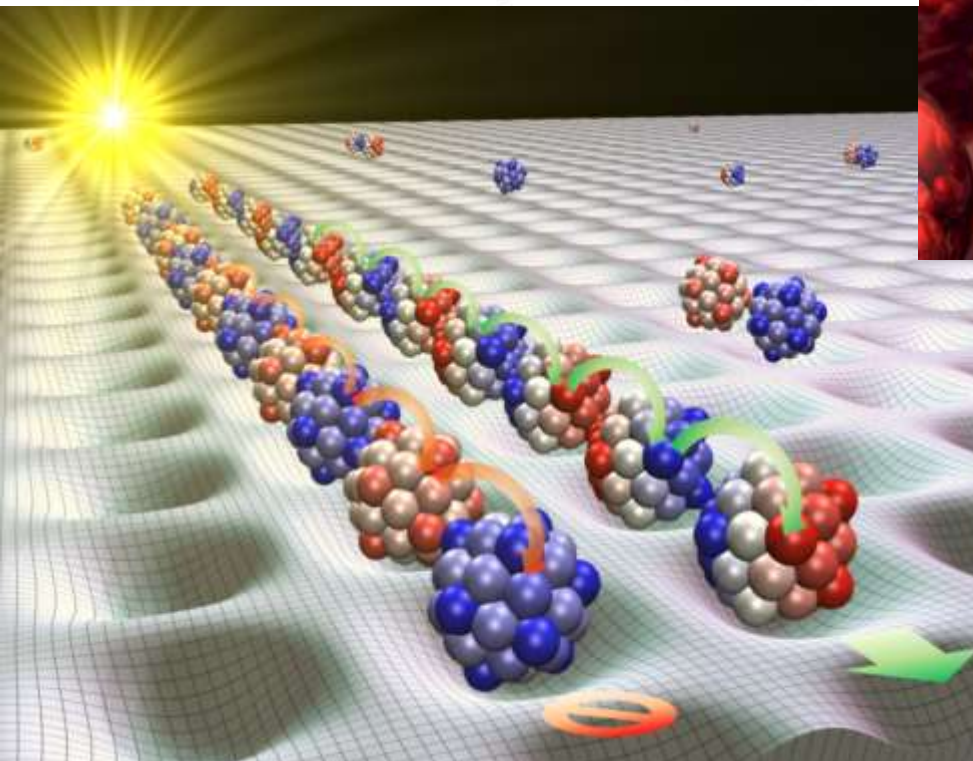
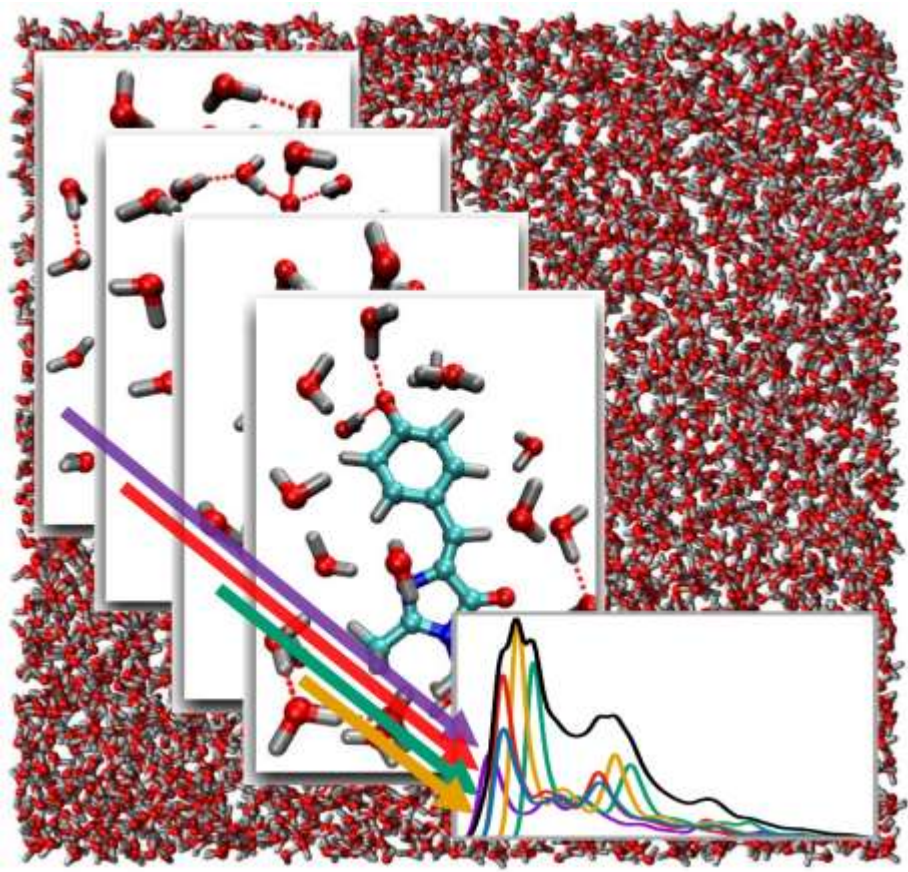
Fourteenth Condensed Phase and Interfacial Molecular Science (CPIMS) Research Meeting

Gaithersburg Marriott
Washingtonian Center
Gaithersburg, MD
October 14-17, 2018



U.S. DEPARTMENT OF
ENERGY

Office of
Science



Submitted by Christine M. Isborn (University of California, Merced)

For more information, see:

T. J. Zuehlsdorff and C. M. Isborn, "Combining the ensemble and Franck-Condon approaches for calculating spectral shapes of molecules in solution," *Journal of Chemical Physics* **148**, 024110 (2018). DOI: 10.1063/1.5006043

T. J. Zuehlsdorff, J. A. Napoli, J. M. Milanese, T. E. Markland and C. M. Isborn, "Unraveling electronic absorption spectra using nuclear quantum effects: Photoactive yellow protein and green fluorescent protein chromophores in water." *Journal of Chemical Physics* **149**, 024107 (2018). DOI: 10.1063/1.5025517

Abstract begins on page 60

Submitted by Bryan M. Wong (University of California, Riverside)

For more information, see N. V. Ilawe, M. B. Oviedo, and B. M. Wong, "Effect of quantum tunneling on the efficiency of excitation energy transfer in plasmonic nanoparticle chain waveguides" *Journal of Materials Chemistry C* **6**, 5857 (2018). DOI: 10.1039/c8tc01466c

Abstract begins on page 146

CPIMS 14

ABOUT THE COVER GRAPHICS

Submitted by E. Charles. H. Sykes (Tufts University)

For more information, see M. T. Darby, M. Stamatakis, A. Michaelides, and E. C. H. Sykes, "Lonely atoms with special gifts: Breaking linear scaling relationships in heterogeneous catalysis with single-atom alloys", *Journal of Physical Chemistry Letters* **9**, 5636 (2018). DOI: 10.1021/acs.jpcllett.8b01888. Reprinted with permission; Copyright (2018) American Chemical Society.

Abstract begins on page 128

Submitted by Teresa Head-Gordon (Lawrence Berkeley National Laboratory)

V. V. Welborn, L. R. Pestana and T. Head-Gordon, "Computational optimization of electric fields for better catalysis design", *Nature Catalysis* **1**, 649 (2018). DOI: 10.1038/s41929-018-0109-2

Abstract begins on page 1

Submitted by Benjamin J. Schwartz (University of California, Los Angeles)

For more information, see D.R. Widmer and B.J. Schwartz, "Solvents can control solute molecular identity," *Nature Chemistry* **10**, 910 (2018). DOI: 10.1038/s41557-018-0066-z

Abstract begins on page 122

Submitted by Christy F. Landes and Stephan Link (Rice University)

For more information, see S. R. Kirchner et al., "Snapshot hyperspectral imaging (SHI) for revealing irreversible and heterogeneous plasmonic processes" *Journal of Physical Chemistry C* **122**, 6865 (2018), DOI: 10.1021/acs.jpcc.8b01398

Abstract begins on page 88

Program and Abstracts for

CPIMS 14

Fourteenth Research Meeting of the
Condensed Phase and Interfacial Molecular
Science (CPIMS) Program

Gaithersburg Marriott Washingtonian Center
Gaithersburg, Maryland
October 14-17, 2017



U.S. DEPARTMENT OF
ENERGY

Office of
Science

Office of Basic Energy Sciences
Chemical Sciences, Geosciences & Biosciences Division

The research grants and contracts described in this document are supported by the U.S. DOE Office of Science, Office of Basic Energy Sciences, Chemical Sciences, Geosciences and Biosciences Division.

FOREWORD

This volume summarizes the scientific content of the Fourteenth Research Meeting on Condensed Phase and Interfacial Molecular Science (CPIMS) sponsored by the U. S. Department of Energy (DOE), Office of Basic Energy Sciences (BES). The research meeting is held for the DOE national laboratory and university principal investigators within the BES CPIMS Program to facilitate scientific interchange among the PIs and to promote a sense of program awareness and identity.

This year's speakers are gratefully acknowledged for their investment of time and for their willingness to share their ideas with the meeting participants.

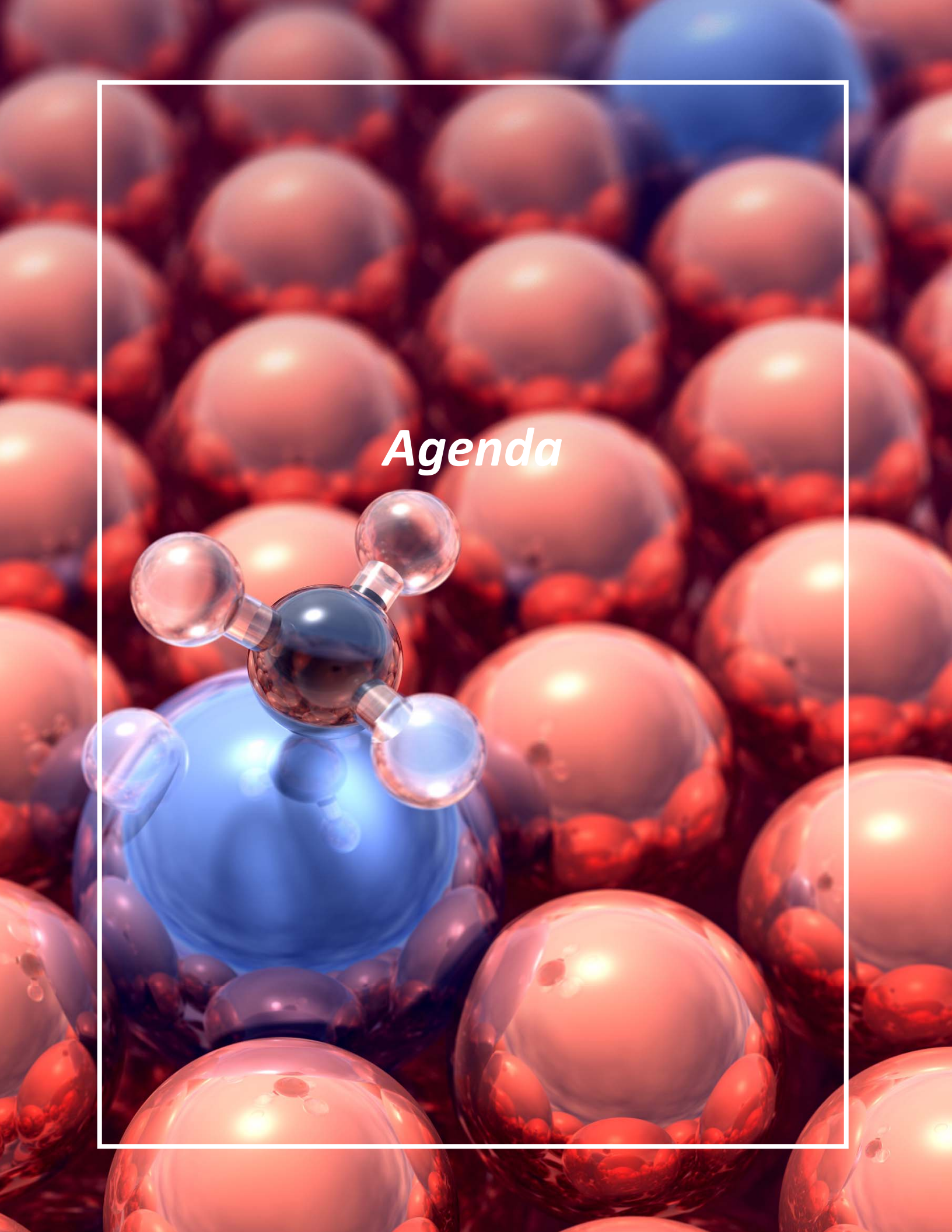
The abstracts in this book represent progress reports for each of the projects that receive support from the CPIMS program. Therefore, the book represents a snapshot in time of the scope of CPIMS-supported research. This past year brought an increase in support for the research grant portfolio, resulting in 15 new awards (including three DOE Office of Science Early Career Research Program Awards). These new efforts have been entered in the Table of Contents using [blue font](#). Because of strong synergistic ties to the research programs across the Chemical Sciences, Geosciences, and Biosciences Division, the CPIMS program provides co-funding for a number of projects whose abstracts are listed in this book. Of these, presentations will be given by Anastassia Alexandrova (co-funded with the Catalysis Science Program), Christine Isborn (co-funded with the Computational and Theoretical Chemistry Program), and Liang Shi (co-funded with the Computational and Theoretical Chemistry Program). Moreover, a presentation given by William Tisdale will include plans for his new project that is co-funded with the Physical Behavior of Materials Program in the Materials Science and Engineering Division at BES. Finally, since the inception of the CPIMS meeting series, participants who work in the field of radiation chemistry (and receive support from the Solar Photochemistry program) have attended; the CPIMS 14 agenda includes presentations from two speakers in this area: David Bartels and Jay LaVerne; their abstracts are contained in the Solar Photochemistry section of the abstract book.

A recent tradition is the use of the cover of this book to display research highlights from CPIMS investigators. This year, we have included six images on the cover. These images were selected from highlights and abstracts submitted by CPIMS investigators during the past two years. We thank the investigators for allowing us to place their images on the cover of this book, and we thank all CPIMS investigators who submitted research highlights. CPIMS Investigators are encouraged to continue to submit highlights of their results; we will continue to receive these stories of success with great pride.

We are deeply indebted to the members of the scientific community who have contributed valuable time toward the review of proposals and programs. These thorough and thoughtful reviews are central to the continued vitality of the CPIMS Program. We appreciate the privilege of serving in the management of this research program. In carrying out these tasks, we learn from the achievements and share the excitement of the research of the many sponsored scientists and students whose work is summarized in the abstracts published on the following pages.

Special thanks are reserved for the staff of the Oak Ridge Institute for Science and Education, in particular, Connie Lansdon. We also thank Teresa Crocket in the Materials Science and Engineering Division, Gwen Johnson in the Chemical Sciences, Geosciences, and Biosciences Division, and Kerry Hochberger in the Office of Basic Energy Sciences (via her support of the DOE Office of Science Early Career Research Program) for their indispensable behind-the-scenes efforts in support of the CPIMS program.

Gregory J. Fiechtner, Mark R. Pederson, and Jeffrey L. Krause
Chemical Sciences, Geosciences and Biosciences Division
Office of Basic Energy Sciences



Agenda

CPIMS 14



U.S. DEPARTMENT OF

ENERGY

Office of
Science

Office of Basic Energy Sciences

Chemical Sciences, Geosciences & Biosciences Division

Fourteenth Condensed Phase and Interfacial Molecular Science (CPIMS) Research Meeting Gaithersburg Marriott Washingtonian Center, Gaithersburg, Maryland

Sunday, October 14

- 3:00-6:00 pm **** Registration (Salons A-D) ****
6:00 pm **** Reception (No Host, Lobby Lounge) ****
6:30 pm **** Dinner (on your own) ****

Monday, October 15

- 7:30 am **** Continental Breakfast (Salon E) ****

All Presentations Held in Salon A-D

- 8:30 am *Update from BES Chemical Sciences, Geosciences, and Biosciences Division*
Bruce Garrett, DOE BES/Chemical Sciences, Geosciences, and Biosciences Division
- 9:00 am *Update from the CTC Program*
Mark Pederson, DOE BES/Computational and Theoretical Chemistry Program
- 9:10 am *Introductory Remarks and Program Update*
Gregory Fiechtner, DOE BES/CPIMS Program
- Session I** Chair: **Xue-Bin Wang**, Pacific Northwest National Laboratory
- 9:30 am *A Bottom-Up Cluster Approach to Solvation Effects on Ion Structure and Photochemistry*
Etienne Garand, University of Wisconsin
- 10:00 am *Unmasking the Mechanics of Proton Defect Accommodation and Transport in Water with Cluster Spectroscopy*
Mark Johnson, Yale University, and **Ken Jordan**, University of Pittsburgh
- 10:30 am **** Break ****
- Session II** Chair: **Geraldine Richmond**, University of Oregon
- 11:00 am *Resolving Chemical Bond Dynamics at an Electrode Surface*
Tanja Cuk, University of Colorado, Boulder and Renewable and Sustainable Energy Institute (RASEI)
- 11:30 am *Hydronium/Water Dynamics – Ultrafast 2D IR Chemical Exchange Spectroscopy*
Michael Fayer, Stanford University
- 12:30 pm **** Working Lunch (Salon E) ****

1:30 pm–2:30 pm Free/Discussion Time

Session III Chair: **Stephan Link**, Rice University

2:30 pm *Hot Carrier Assisted Chemistry on Nanoparticle Surfaces*

Christy Landes, Rice University

3:00 pm *Multimodal Characterization of Interfacial Dynamics through Raman Nanoscopy*

Patrick El-Khoury, Pacific Northwest National Laboratory

3:30 pm *Coherent Multiphoton Photoelectron Spectroscopy of Silver: How Plasmons are Born and Decay*

Hrvoje Petek, University of Pittsburgh

4:00 pm **** Break ****

Session IV: Overview of New Grants

Chair: **Adam Willard**, Massachusetts Institute of Technology

4:30 pm **Anastassia Alexandrova**, University of California, Los Angeles

4:45 pm **Ethan Crumlin**, Lawrence Berkeley National Laboratory

5:00 pm **Ismaila Dabo**, The Pennsylvania State University

5:15 pm **Michel Dupuis**, University at Buffalo

5:30 pm **Joel Yuen-Zhou**, University of California, San Diego

5:45 pm **Will Tisdale**, Massachusetts Institute of Technology

6:15 pm **** Working Dinner (Salon E) ****

Tuesday, October 16

7:30 am **** Continental Breakfast (Salon E) ****

Session V Chair: **James Rustad**, DOE/BES Geosciences Program

8:30 am *Voltage and Field Fluctuations Underlying Nucleation*

Shawn Kathmann, Pacific Northwest National Laboratory

9:00 am *Enhancing Rare Event Sampling in Molecular Simulations with Applications to Complex Systems*

Sapna Sarupria, Clemson University

9:30 am *Intrinsic to Collective Properties of Ions in Solution*

Christopher Mundy, Pacific Northwest National Laboratory

10:00 am *The Many-Body Expansion for Aqueous Systems Revisited*

Sotiris Xantheas, Pacific Northwest National Laboratory

10:30 am **** Break ****

Session VI Chair: **Christopher Fecko**, DOE/BES Solar Photochemistry Program

11:00 am *How Big is the Hydrated Electron? Solvation Free Energy and Partial Molar Volume*
David Bartels, Notre Dame Radiation Laboratory

11:30 am *Radiation Stability of Aromatic Compounds*
Jay LaVerne, Notre Dame Radiation Laboratory

Overview of a New Grant:

12:00 pm **Munira Khalil**, University of Washington, and **Niranjan Govind**, Pacific Northwest National Laboratory

12:15 pm ***** Working Lunch (Salon E) *****

1:15 pm–3:00 pm Free/Discussion Time

Session VII Chair: **Aurora Clark**, Washington State University

3:00 pm *Experimental Probes of Solvation Dynamics and Chemical Reactivity in Heterogeneous Environments*

Musahid Ahmed, Lawrence Berkeley National Laboratory

3:30 pm *Modeling the Optical Spectroscopy of Molecules in Solution: Ionic, Vibronic, and Nuclear Quantum Effects*

Christine Isborn, University of California, Merced

Session VIII **Overview of New Grants**

Chair: **Neeraj Rai**, Mississippi State University

4:15 pm **Liang Shi**, University of California, Merced

4:30 pm **Francesco Paesani and Wei Xiong**, University of California, San Diego

4:50 pm **Jim Pfaendtner**, University of Washington

5:05 pm **Mark Maroncelli**, The Pennsylvania State University

5:30 pm ***** Reception (No Host, Lobby Lounge) *****

6:00 pm ***** Dinner (on your own) *****

Wednesday, October 17

7:30 am **** Continental Breakfast (Salon E) ****

Session IX Chairs: **Viviane Schwartz and Chris Bradley**, DOE/BES Catalysis Science Program

8:30 am *Single-Atom Alloy Catalysts: Born in a Vacuum, Verified in a Reactor, and Understood In Silico*

E. Charles H. Sykes, Tufts University

9:00 am *Transport, Crystallization, and Isotope Exchange in Nanoscale Water Films I: Unravelling Interface versus Bulk Effects*

Bruce Kay, Pacific Northwest National Laboratory

9:30 am *Transport, Crystallization, and Isotope Exchange in Nanoscale Water Films II: Exploring Supercooled Water in “No-Man’s Land” via Transient Heating*

Greg Kimmel, Pacific Northwest National Laboratory

10:00 am *Chemical Transformations Confined in Nanoparticles and Droplets*

Kevin Wilson, Lawrence Berkeley National Laboratory

10:30 am *Closing Remarks*

Gregory Fiechtner, DOE Basic Energy Sciences

11:00 am **** Meeting Adjourns ****

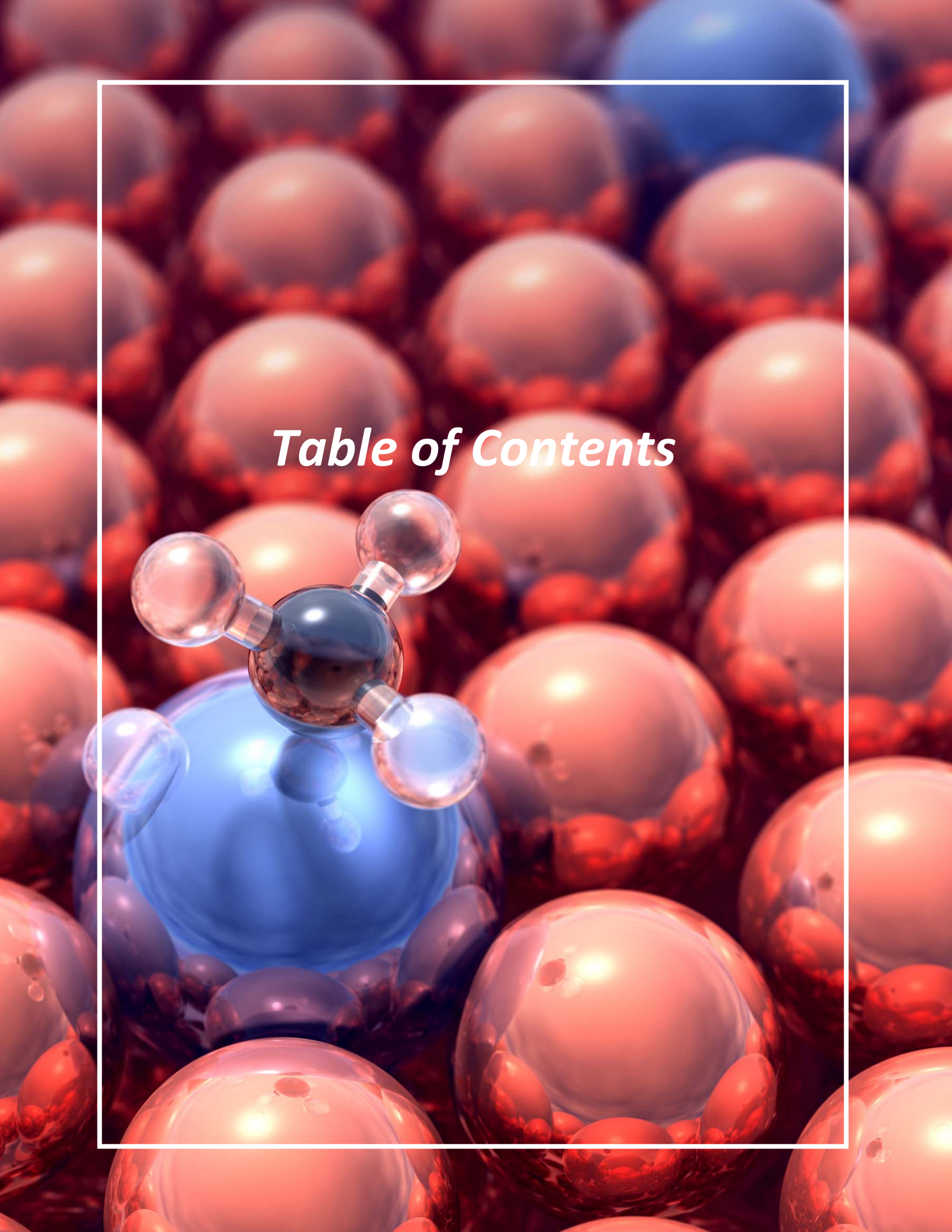


Table of Contents

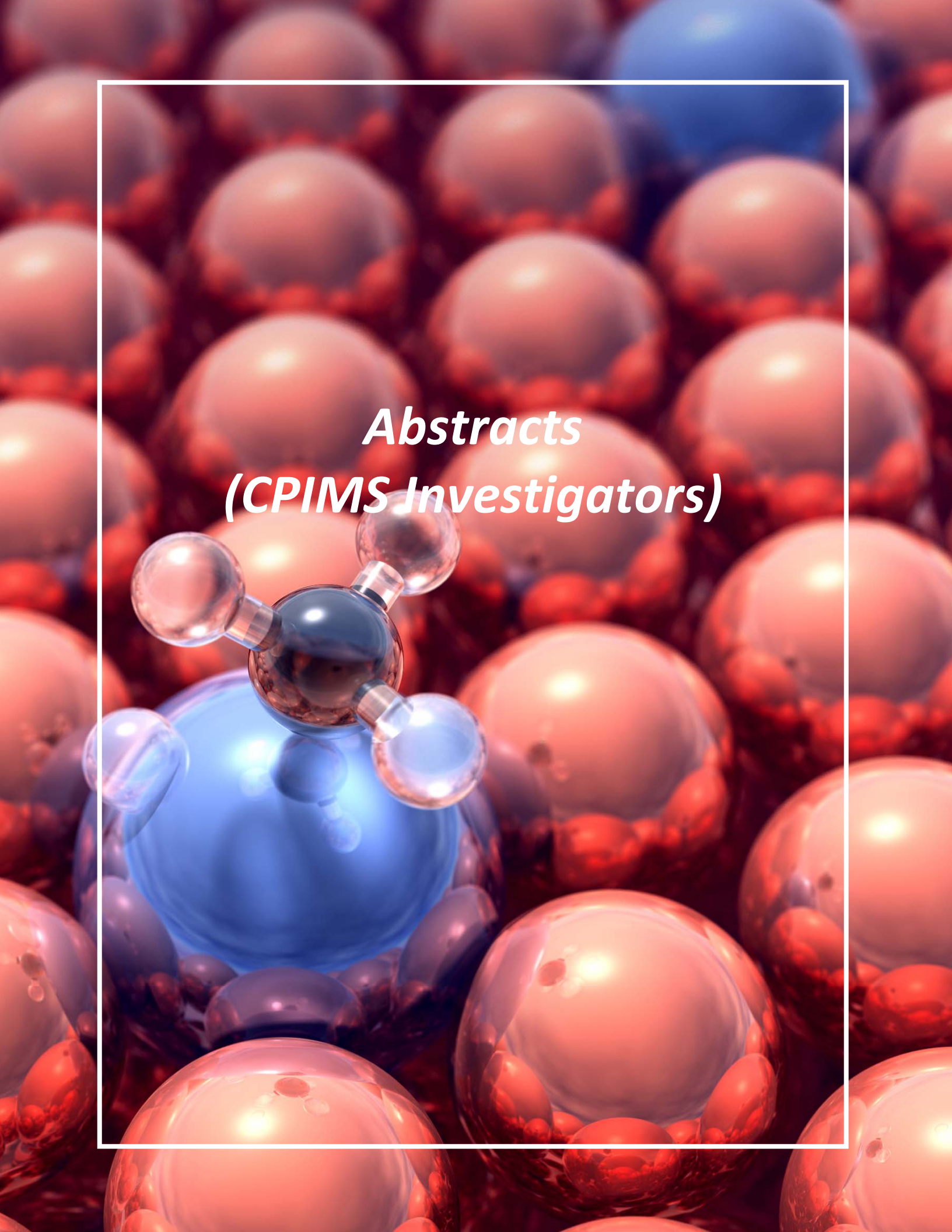
TABLE OF CONTENTS

FOREWORD.....	ii	
AGENDA.....	iii	
TABLE OF CONTENTS.....	vii	
ABSTRACTS.....	1	
CPIMS Principal Investigator Abstracts (New Awards in Blue Font)		
<i>Chemical Transformations in Bulk Aqueous Solutions and Near Interfaces</i> Musahid Ahmed, Hendrik Bluhm, Teresa Head-Gordon, Richard Saykally and Kevin Wilson (Lawrence Berkeley National Laboratory).....		1
<i>Ensemble Representation for the Realistic Modeling of Cluster Catalysts at Heterogeneous Interfaces</i> Anastassia N. Alexandrova and Philippe Sautet (University of California, Los Angeles).....		5
<i>Controlling Aqueous Interfacial Phenomena of Redox-Active Ions with External Electric Fields</i> Heather C. Allen (The Ohio State University).....		7
<i>Visible Light Photo-Catalysis in Charged Micro-Droplets</i> Abraham Badu-Tawiah (The Ohio State University).....		10
<i>Probing Ion Solvation and Charge Transfer at Electrochemical Interfaces Using Nonlinear Soft X Ray Spectroscopy</i> L. Robert Baker (The Ohio State University).....		14
<i>Discovering the Mechanisms and Properties of Electrochemical Reactions at Solid/Liquid Interfaces</i> Ethan J. Crumlin (Lawrence Berkeley National Laboratory).....		18
<i>Observing the Molecular & Dynamic Pathway of Water Oxidation on Titania Surfaces</i> Tanja Cuk (University of Colorado, Boulder and Renewable and Sustainable Energy Institute).....		20
<i>Voltage-Dependent Deposition and Leaching at Electrocatalytic Solid–Liquid Interfaces</i> Ismaila Dabo and Susan B. Sinnott (The Pennsylvania State University).....		21
<i>Rate Theory of Ion Pairing at Liquid Interfaces</i> Liem X. Dang (Pacific Northwest National Laboratory).....		24
<i>Exploring New Diamond Surfaces with Precision Chemistry and Quantum Spectroscopy</i> Nathalie de Leon (Princeton University).....		28
<i>Charge Carrier Space-Charge Dynamics in Complex Materials for Solar Energy Conversion: Multiscale Computation and Simulation</i> Michel Dupuis (University at Buffalo).....		32

<i>Nanoporous Materials and Ionic Liquids: Dynamics, Structure, and Interactions</i> Michael D. Fayer (Stanford University).....	35
<i>Size Dependence of Liquid-Liquid Phase Separation in Aerosol Particles</i> Miriam A. Freedman (Pacific Northwest National Laboratory).....	39
<i>Fundamentals of Solvation under Extreme Conditions</i> John L. Fulton (Pacific Northwest National Laboratory).....	43
<i>A Cluster Approach to Understanding Solvation Effects on Ion Structure and Photochemistry</i> Etienne Garand (University of Wisconsin).....	47
<i>Methods for Addressing Strongly Heterogeneous and Far-From-Equilibrium Systems</i> Phillip L. Geissler, Teresa Head-Gordon, Kranthi Mandadapu and Kevin Wilson (Lawrence Berkeley National Laboratory)	51
<i>Laser Induced Dynamics, Reactions and Spectroscopy at Surfaces</i> Wayne P. Hess (PI) Alan G. Joly and Patrick Z. El-Khoury (Pacific Northwest National Laboratory)	55
<i>Improved Methods for Modeling Functional Transition Metal Compounds in Complex Environments: Ground States, Excited States, and Spectroscopies</i> Hrant P. Hratchian, Christine M. Isborn, Aurora Pribram-Jones, Liang Shi, and David A. Strubbe (University of California, Merced).....	59
<i>Development of Approaches to Model Excited State Charge and Energy Transfer in Solution</i> Christine Isborn (University of California, Merced), Aurora Clark (Washington State University) and Thomas Markland (Stanford University).....	60
<i>Unmasking the Mechanics of Proton Defect Accommodation and Transport in Water through Rational Control of Water Cluster Scaffolds</i> Kenneth D. Jordan (University of Pittsburgh) and Mark A. Johnson (Yale University)	64
<i>Nucleation Chemical Physics</i> Shawn M. Kathmann (Pacific Northwest National Laboratory)	68
<i>Structure and Reactivity of Ices, Oxides, and Amorphous Materials</i> Bruce D. Kay, R. Scott Smith, and Zdenek Dohnálek (Pacific Northwest National Laboratory)	72
<i>Probing and Controlling Electronic Correlations and Vibronic Coupling During Ultrafast Intramolecular Electron Transfer in Solvated Mixed Valence Complexes</i> Munira Khalil (University of Washington, Seattle), Niranjan Govind (Pacific Northwest National Laboratory), and Robert Schoenlein (SLAC National Accelerator Laboratory)	76

<i>Non-Thermal Reactions at Surfaces and Interfaces</i> Greg A. Kimmel and Nikolay G. Petrik (Pacific Northwest National Laboratory)	80
<i>2D IR Microscopy—Technology for Visualizing Chemical Dynamics in Heterogeneous Environments</i> Amber T. Krummel (Colorado State University)	84
<i>Mechanistic Investigations of Hot Carrier Induced Electrocatalysis by Single-Particle Spectroscopy</i> Christy F. Landes and Stephan Link (Rice University)	88
<i>Ion Solvation and Hydrogen Bonding in Liquid Electrolytes</i> Mark Maroncelli (The Pennsylvania State University) and Hyung Kim (Carnegie Mellon University)	92
<i>Intrinsic to Collective Properties of Ions in Solution</i> Christopher J. Mundy (Pacific Northwest National Laboratory)	94
<i>Probing the Structure and Dynamics of Water under Heterogeneous Nanoconfinement Through Ultrafast Vibrational Spectro/microscopy and Many-Body Molecular Dynamics</i> Francesco Paesani and Wei Xiong (University of California San Diego)	98
<i>Studies of Surface Adsorbate Electronic Structure and Femtochemistry at the Fundamental Length and Time Scales</i> Hrvoje Petek (University of Pittsburgh)	99
<i>Understanding Molecular Scale Chemical Transformations at Solid-Liquid Interfaces—Computational Investigation of Interfacial Chemistry in Electrolytes and Charged Interfaces</i> Jim Pfaendtner (University of Washington)	103
<i>Probing Condensed-Phase Structure and Dynamics in Hierarchical Zeolites and Nanosheets for Catalytic Upgradation of Biomass</i> Neeraj Rai (Mississippi State University)	104
<i>Molecular Structure, Bonding and Assembly at Nanoemulsion and Liposome Surfaces</i> Geraldine Richmond (University of Oregon)	107
<i>Enhancing Rare Events Sampling in Molecular Simulations</i> Sapna Sarupria (Clemson University)	111
<i>Equilibrium Structure and Dynamics of Aqueous Solutions and Interfaces</i> Richard Saykally, Musahid Ahmed, Phillip L. Geissler, Kranthi Mandadapu and Teresa Head-Gordon (Lawrence Berkeley National Laboratory)	114
<i>Molecular Theory and Modeling</i> Gregory K. Schenter (Pacific Northwest National Laboratory)	118
<i>Understanding Chemical Bond Dynamics in Liquids Using Mixed Quantum/Classical Molecular Dynamics Simulation</i> Benjamin J. Schwartz (University of California, Los Angeles)	122

<i>Development of Metal-Free Photocatalysts</i> Kevin L. Shuford (Baylor University)	126
<i>An Atomic-scale Approach for Understanding and Controlling Chemical Reactivity and Selectivity on Metal Alloys</i> E. Charles H. Sykes (Tufts University)	128
<i>Excitons in Low-Dimensional Perovskites</i> William A. Tisdale (Massachusetts Institute of Technology)	132
<i>Structural Dynamics in Complex Liquids Studied with Multidimensional Vibrational Spectroscopy</i> Andrei Tokmakoff (University of Chicago)	133
<i>Ab-initio Analysis of Molecular Interactions in Clusters and Bulk Systems</i> Marat Valiev (Pacific Northwest National Laboratory)	136
<i>Cluster Model Investigation of Condensed Phase Phenomena</i> Xue-Bin Wang (Pacific Northwest National Laboratory)	138
<i>Nonequilibrium Properties of Driven Electrochemical Interfaces</i> Adam P. Willard (Massachusetts Institute of Technology)	142
<i>Non-Empirical and Self-Interaction Corrections for DFTB: Towards Accurate Quantum Simulations for Large Mesoscale Systems</i> Bryan M. Wong (University of California-Riverside)	146
<i>Intermolecular Interactions in the Gas and Condensed Phases</i> Sotiris S. Xantheas (Pacific Northwest National Laboratory)	150
<i>The Emergent Photophysics and Photochemistry of Molecular Polaritons: A Theoretical and Computational Investigation</i> Joel Yuen-Zhou (University of California San Diego)	154
<u>Solar Photochemistry Principal Investigator Abstracts</u>	
<i>Fundamental Advances in Radiation Chemistry</i> David M. Bartels, Ian Carmichael, Ireneusz Janik, Jay A. LaVerne, and Sylwia Ptasińska (Notre Dame Radiation Laboratory)	155
<i>Radiation Stability of Aromatic Compounds</i> Jay A. LaVerne (Notre Dame Radiation Laboratory)	159
<i>Radiation Chemical Impacts on Nuclear Power</i> Jay A. LaVerne and David M. Bartels (Notre Dame Radiation Laboratory)	163
LIST OF PARTICIPANTS	167

The background is a dense field of glowing, semi-transparent spheres in shades of red, orange, and blue. In the lower-left foreground, a molecular structure is visible, consisting of several smaller spheres connected by thin rods, with a larger blue sphere at its center. The overall lighting is warm and vibrant, creating a sense of depth and energy.

Abstracts
(CPIMS Investigators)

Chemical Transformations in Bulk Aqueous Solutions and Near Interfaces

Musahid Ahmed (mahmed@lbl.gov) , Hendrik Bluhm (hbluhm@lbl.gov), Teresa Head-Gordon (thg@berkeley.edu), Richard Saykally (saykally@berkeley.edu), Kevin Wilson (krwilson@lbl.gov)

*Lawrence Berkeley National Laboratory, Chemical Sciences Division,
One Cyclotron Road, Berkeley, CA 94720*

Program Scope

Aqueous solutions and their interfaces govern important phenomena in the environment and in numerous technical applications, but the molecular scale processes in the bulk and at the interfaces, such as evaporation, are often not yet understood. The goal of this program is to investigate the fundamental interactions and reactions in aqueous solutions and their interfaces through the development and application of state-of-the-art experimental and theoretical methods.

Progress Report

Properties of Aqueous Solution/Oxide Interfaces. Bluhm and coworkers have investigated liquid/solid interfaces using *operando* APXPS to directly probe the energy level positions at the electrochemically active interface between intrinsic and doped hematite and a KOH solution. The particular goal here is to elucidate factors that reduce the efficiency of photoelectrochemical devices. The performance of a photoelectrochemical device is determined in large part by the heterogeneous interface between the photoanode and the electrolyte, which was characterized directly under operating conditions. APXPS is a non-contact probe of local electrical potentials which allows the direct measure of the band alignment at the semiconductor/electrolyte interface as a function of solar illumination, applied potential, and doping, through the observation of shifts in the photoelectron peak positions. The measurements showed the absence of in-gap states in the hematite/KOH system, in contrast to previous measurements using indirect methods.

Probing directed chemistry via non covalent interactions in ionic liquids (IL). This is a new thrust in this program, established by Ahmed and coworkers. We have built micro-droplet and “open space” reactors which are amenable to multiple probing via photon spectroscopies, while its flow configuration lends itself to continuous rapid monitoring of the complex reaction mixtures via ambient ionization based mass spectrometry. An “open space” configuration localizes chemical reactions on interfaces or can be “self-contained” and does not impose constraints that can occur from encapsulation, pre-processing steps or the need for scaffolds. During the past year, we have acquired a terahertz time domain spectrometer and coupled it to our “open space reactor” which has also been adapted to an ambient ionization ion trap mass spectrometer. To complete the suite of probe methods, we have built a silicon wafer based attenuated total reflection spectrometer, which allows direct probing of chemical reactions in an “open space” configuration. Preliminary results have been obtained on an IL interaction with water via near-infrared fingerprinting of the first overtone of water’s symmetric O-H stretch that changes with evaporation over time, that agree with bulk liquid phase mixing measurements. Open space reactors were also visualized by optical microscopy by encapsulating [EMIm]⁺BF₄⁻ droplets in squalane oil and stabilized with titania nanoparticles.

Water evaporation from liquid microjets. Saykally and coworkers have exploited liquid microjet technology to study the details of water evaporation, free from the obfuscating effects of condensation that have plagued previous studies. The most important practical result of this ongoing work is the quantification of the water evaporation coefficient (0.6), which has been highly controversial, and is a critical parameter in models of climate and cloud dynamics. Ammonium sulfate, the most common ionic solute in atmospheric aerosols, has been shown to have no statistically significant effect on the rate, whereas sodium perchlorate effected a 25% reduction. The presence of acetic acid—a surface active component of natural aerosols—was likewise shown not to effect significant changes in the evaporation rate. However, the evaporation coefficient of 1.0 M HCl exhibited a 60% decrease relative to pure water, while that for 0.1 M HCl exhibited a 45% increase relative to pure water. These surprising results suggest a large perturbation in the surface structure induced by either hydronium ions adsorbing to the water surface or by the presence of a $\text{Cl}^- \cdots \text{H}_3\text{O}^+$ ion-pair moiety in the interfacial region. Interestingly, simulations by Mundy et al predict a high degree of ion pairing for HCl at the interface, whereas HBr behaved quite normally. Preliminary studies of sodium hydroxide solutions yield results indistinguishable from water. Those results need to be examined in further detail however.

Reactivity and Nanoconfinement. Head-Gordon and coworkers have been developing rational, physical concepts that are more predictive in designing desired catalytic outcomes, by calculating electric field values relevant to the reactant and transition states of different types of catalysts. We have illustrated how electric fields have been used to computationally optimize biocatalytic performance of a synthetic enzyme for Kemp elimination, and how they are used as a unifying descriptor for catalytic design across a range of homogeneous and heterogeneous catalysts including catalysis of reductive elimination from gold complexes confined in supramolecular capsules. While focusing on electrostatic environmental effects may open new routes toward the rational optimization of efficient catalysts, much more predictive capacity is required of theoretical methods to have a transformative impact in their computational design – and thus experimental relevance – when using electric field alignments in the reactive centers of complex catalytic systems. This included the validation of meta-GGA functionals that are similar in quality to much more expensive hybrid functionals, the importance of combining DFT with nuclear quantum effects (NQEs) in the condensed phase such as liquid water, and the use of a spatially resolved two phase entropy analysis for calculating the solvation entropies via trajectories of reactant and transition state ensembles.

Future Plans

Diels-Alder reactions in ionic liquids. Ahmed and coworkers will use hydrogen bond-rich ILs to probe Diels-Alder type reactions. It has been suggested that the ILs should be described as a 3D network of cations and anions, where each ion is surrounded by several counter ions. This can result in reorganization and reorientation of the solvent around the solute, and reduces possibilities of solvation, making the dynamics very different from traditional ion-pair association and dissociation. We seek to track these processes with spectroscopies being developed in this program while evaluating the outcome of a reaction in terms of product via mass spectrometry in a multimodal manner. Our target system is the reaction between a furan (diene) and maleic anhydride (dienophile) in the IL $\text{BMIM}^+ \text{BF}_4^-$. If successful, these methods can be extended beyond ILs which are highly viscous into the domain of anhydrous liquid

electrolytes, recently demonstrated in the room-temperature cycling of fluoride-ion electrochemical cells. (Davis et al. Science (accepted))

The Effects of Nanoconfinement on Diels-Alder type Reactions. The experimental investigations by Ahmed et al. will go hand-in-hand with theoretical studies of Diels-Alder reactions by the Head-Gordon Lab, who is currently deploying *ab initio* meta-GGAs with NQEs to quantify how altered solvent properties between confining interfaces can be utilized to direct new reactive chemistry. Earlier theoretical studies on the Diels-Alder reaction have provided mechanistic insight into the role of water, showing that the hydrophobic effect drives the cycloaddition by reducing hydrophobic surface area of the diene and the dienophile construct, combined with enhanced hydrogen bonding between water and reactant molecules in the transition state and better solubility of the reactants. We are using metadynamics to calculate the free energy barriers of the most feasible reaction pathways involving the endo-cis and endo-trans structures of the transition states in the case of the Diels-Alder reaction. By systematically calculating the free energy barriers of the reactions as a function of the confinement conditions, while at the same time mapping the water physical properties (viscosity, density fluctuations, hydrogen bonds, vibrational spectra, etc.) to that degree of confinement, we can provide a phase diagram of the catalytic properties of confined water and to derive guidelines of how to control reactivity using confinement. We also propose to connect this theoretical study to the droplets or nanoparticles performed in the Wilson group.

Interplay of the Chemical Reactivity between the Bulk and Surface, and under Nanoconfinement in Aqueous Systems. Wilson et al. will explore the interplay between bulk and interfacial reactions and the influence of confinement on the products and mechanisms of chemical reactions in aqueous environments. The motivation for this work comes from chemical transformations in realistic systems, where processes rarely occur in a single phase and often involve transport and reactions across interfaces and the bulk. Here we propose to examine the chemical coupling of bulk and interfacial processes to examine how reaction mechanisms and rates are modified in systems that have simple interfaces and dimensions that are small compared to the characteristic reaction diffusion lengths. The reaction-diffusive length $L_{rxn}=D\tau$ is the average distance a molecule travels prior to reaction. L_{rxn} depends upon the diffusion constant (D) and τ , the chemical lifetime (i.e. concentration/bimolecular rate constant). For highly reactive species, such as hydroxyl radicals in an organic liquid, L_{rxn} is only a couple of nanometers. Less reactive molecules can also exhibit short L_{rxn} in semisolid or glassy environments due to diffusive confinement. It is our hypothesis that for reaction containers (e.g. droplets or nanoparticles) that have substantial surface area and dimensions that are on the order of L_{rxn} , reactants increasingly sample the container walls (i.e. interfaces), where surface orientation and reduced solvent coordination can substantially alter transition states, rates, and mechanisms from those observed in the bulk liquid.

Towards a Complete Understanding of CO₂ – Carbonate Systems. Saykally and coworkers will continue to perfect microjet-based mixing system for generating of short lived species, e.g. carbonic acid, for study by X-ray spectroscopy, using both XAS and XPS, and the newly operational soft X-ray free electron lasers at Trieste and elsewhere, as this rapidly evolving technology permits. They will apply this technology to the study of hydration and hydrolysis of carbon dioxide, nitrogen oxides, and sulfur oxides, including temperature dependence, in collaboration with LBNL beamline scientists and theoreticians. They will study the properties of aqueous carbonic acid, and its interactions with Ca²⁺ and Mg²⁺ ions to nucleate solid

carbonate phases. Fundamental insights gained from these studies are expected to facilitate the development of CO₂ sequestering schemes based on saline aquifer burial. Similar investigations of nitrogen and sulfur oxides will be explored. The planar liquid jet technology will continue to be perfected for use in nonlinear optics studies of interfaces, specifically addressing the interesting reversed fractionation of carbonates observed in XPS experiments and the interesting evaporation rate effects observed for HCl. These systems will be addressed by XFEL SHG and SFG, as the available technology(at Trieste) permits.

Publications Acknowledging DOE BES CSBG Support:

- S. Belsare, V. Pattni, M. Heyden, and T. Head-Gordon, *J. Phys. Chem. B* **122**, 5300 (2018).
- S. S. Chacon, M. García-Jaramillo, S.Y. Liu, M. Ahmed, M. Kleber. *Soil Biology & Biochemistry*, **119**, 101 (2018).
- A. C. Carr, L. E. Felberg, V. A. Piunova, J. E. Rice, T. Head-Gordon, W. C. Swope, *J. Chem. Theory Comput.* **121**, 2902 (2017).
- X. Chen, D. Aschaffenburg, T. Cuk, *Chem. Comm.* **53**, 7254 (2017).
- X. Chen, D. Aschaffenburg, T. Cuk, *J. Mat. Chem. A* **5**, 11410 (2017).
- X. Chen, S. Choing, D. Aschaffenburg, C.D. Pemmaraju, D. Prendergast T. Cuk, *J. Am. Chem. Soc.* **139**, 1830 (2017).
- C.B. Gopal, S.C. Lee, M. Garcia-Melchor, Y. Shi, M. Monti, Z. Guan, R. Sinclair, H. Bluhm, A. Vojvodic, W.C. Chueh, *Nat. Comm.* **8**, 15360 (2017).
- O. Karslioglu, H. Bluhm, In: “Operando Studies in Heterogeneous Catalysis”, Springer Series in Chemical Physics, Vol. XIV, Eds.: I.M.N. de Groot, J.W.M. Frenken, pp. 31-57 (2017).
- R.K. Lam, J.W. Smith, A.M. Rizzuto, O. Karslioglu, H. Bluhm, R.J. Saykally, *J. Chem. Phys.* **146**, 094703 (2017).
- R. K. Lam, et al., *Chem. Phys. Lett.* **703**, 112 (2018).
- R.K. Lam, et al., *Phys. Rev. Lett.* **120**, 023901 (2018).
- R.K. Lam, O. Shih, J.W. Smith, A.T. Sheardy, A.M. Rizzuto, D. Prendergast, R.J. Saykally, *J. Chem. Phys.* **146**, 249902 (2017).
- D.L. McCaffrey, S.C. Nguyen, S.J. Cox, H. Weller, A.P. Alivisatos, P.L. Geissler, R.J. Saykally, *PNAS* **114**, 13369 (2017).
- H. Mizuno, A.M. Rizzuto, R.J. Saykally, *J. Phys. Chem. Lett.* **9**, 4753 (2018).
- K. Pollock, H. Q. Doan, C. Stanton, T. Cuk, *J. Phys. Chem. Lett.* **8**, 922 (2017).
- A.M. Rizzuto, E.S. Cheng, R.K. Lam, R.J. Saykally, *J. Phys. Chem. C* **121**, 4420 (2017).
- L. Ruiz Pestana, O. Marsalek, T. E. Markland, T. Head-Gordon, *J. Phys. Chem. Lett.* **9**, 5009 (2018).
- J.W. Smith, R.J. Saykally, *Chem. Rev.* **117**, 13909 (2017).
- L. Trotochaud, A.R. Head, O. Karslioglu, L. Kyhl, H. Bluhm, *J. Phys.: Cond. Matt.* **29**, 053002 (2017).
- V. Vaissier Welborn, L. Ruiz Pestana, T. Head-Gordon, *Nature Catalysis* **1**, 649 (2018).
- V. Vaissier, S. C. Sharma, K. Schaettle, T. Zhang, T. Head-Gordon, *ACS Catalysis* **8**, 219 (2018).
- V. Vaissier Welborn, T. Head-Gordon, *J. Phys. Chem. Lett.* **9**, 3814 (2018).
- C.H. Wu, B. Eren, H. Bluhm, M.B. Salmeron, *ACS Catalysis* **7**, 1150 (2017).
- J. Yao, D. Lao, X. Sui, Y. Zhou, S. K. Nune, X. Ma, T. P. Troy, M. Ahmed, Z. Zhu, D. J. Heldebrant, X-Y Yu, *Phys. Chem. Chem. Phys.* **19**, 22627 (2017).

Ensemble representation for the realistic modeling of cluster catalysts at heterogeneous interfaces

PI: Anastassia N. Alexandrova^{1,3}

co-PI: Philippe Sautet^{1,2,3}

¹*Department of Chemistry and Biochemistry, and* ²*Chemical and Biomolecular Engineering, University of California, Los Angeles.* ³*California NanoSystems Institute. 607 Charles E. Young Drive East, Los Angeles, CA 90095-1569, USA*

e-mail: ana@chem.ucla.edu

When a catalytic interface is amorphous and dynamic, reaction conditions set it in motion. Under the influence of high temperatures and partial pressures of gasses, a strong restructuring of the interface can take place, and the motion continues concurrently with the catalyzed reaction. This opens hundreds of possibilities for how the surface may look like, and what active sites it may expose and use in catalysis at any instance. Modeling this reality requires a paradigm shift toward statistical mechanics and ensemble representation of heterogeneous catalytic interfaces. This constitutes the scope of our project.

We currently focus on oxide surfaces decorated with clusters of transition metals, as catalysts of the reaction of dehydrogenation, hydrogenation, and hydrogenolysis. Our team is developing efficient algorithms to access the accurate ensemble states of the catalyst, and short-cut reactivity descriptors that would allow characterization of the ensemble activity without exhaustive mechanistic studies. The work features close collaborations with experimental partners, such as Stefan Vajda at Argonne National Laboratory.

In a number of preliminary studies (in vast majority of times collaborative with experimentalists), we demonstrated that sub-nano surface-supported catalytic clusters covered with adsorbates generally have many low-energy isomers accessible at elevated temperatures of catalysis. Moreover, they easily interconvert, visiting dozens of structural forms in as little as 1 ns (Alexandrova JPCLet 2017). Every intermediate during the catalyzed reaction is characterized by different ensemble of the catalyst states. By working closely with experimental partners, we showed that all practically-important properties of cluster catalysts can be correctly modeled only within a statistical ensemble representation, and only in this way can these simulations agree with experiment. For example, the simplest properties such as ionization potential and heat capacity of clusters vary strongly as an ensemble average at changing temperatures (Fig. 1A, Alexandrova JCTC 2015). Cluster sintering on the support (one of the prime mechanisms of catalyst deactivation) is strongly influenced by structural diversity in the ensemble, as we showed for clusters of Pd, PtPd, and PtZn on various oxides (Alexandrova JCP 2011, ACS Catal 2012, JPCC 2013). Size-dependent catalytic activity of small Pt clusters on oxides for dehydrogenation of alkanes is governed by families of metastable states accessible at high T and coverage with reagents, and not seen in the simulations based on the global minima (Alexandrova ACS Catal 2017). Furthermore, we pointed at specific higher-energy metastable isomers that dominate catalysis instead of the most stable global minimum (Fig. 1B, Sautet JACS 2018; Alexandrova ACS Catal 2017). In oxidative dehydrogenation of alkanes on deposited Cu and Pd oxide clusters, we detected several different types of dynamics: the ensemble of catalyst states changes as a function of the bound intermediate, the oxidation state of the catalytic metal changes as a function of T, and cluster fluxionality is (i) composition- and oxidation state-dependent, and (ii) responsible for experimentally-observed selectivity. We see that fluxionality can be too much, too little, or just right for the desired selectivity, and thus constitutes a level of cluster catalyst design (Fig. 1C, Alexandrova, submitted to Nat. Catal.). Selectivity and poisoning resistance as a function of cluster size and nature of dopants is also a property that develops only under reaction conditions as the corresponding ensemble of many states emerges (Fig. 1D, Alexandrova JACS 2017).

We face a number of outstanding questions in this new field. For example, How does the change in the cluster structure combines with the elementary reaction steps along the catalytic pathway? At what moment of the reaction does such a cluster structure change operate? What is the respective rate of cluster rearrangement and bond forming/breaking processes in the reactant? Does cluster dynamics directly

couple to the reaction coordinate? Can there be multiple active sites of varying activity? Can there be multiple different catalytic mechanisms present simultaneously, collectively giving experimentally observable properties? Can we catch non-Arrhenius behavior of our catalysts? How to design a cluster catalyst that would not look catalytic at preparation conditions, but would develop the desired state at the reaction conditions? Etc.

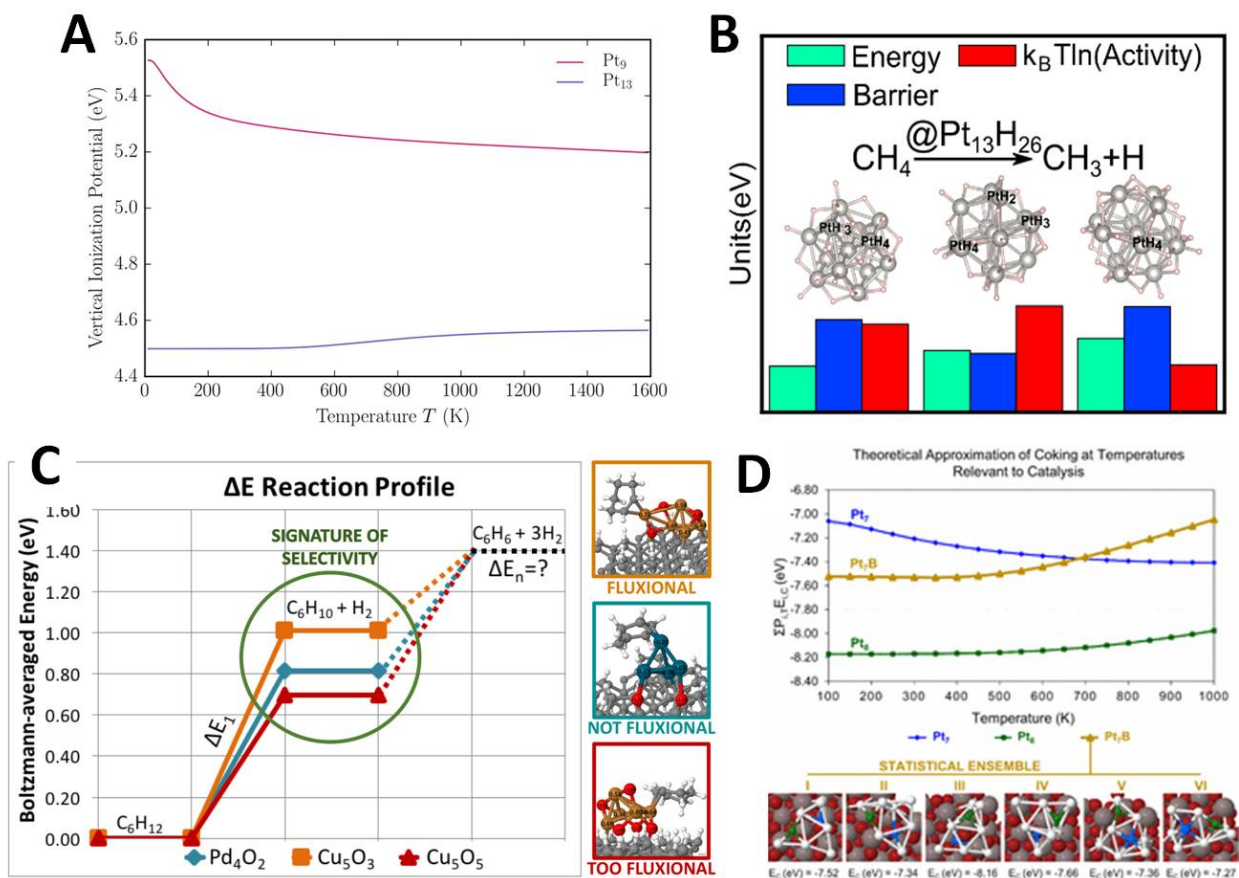


Figure 1. (A) Calculated ionization potential for Pt_9 and Pt_{13} in the gas phase as a function of temperature, showing strong variations as the statistical ensemble expands with temperature (Alexandrova et al. JCTC 2015). (B) In the ensemble of Pt clusters covered with H in the gas phase, the second most thermally-accessible isomer is 500 times faster in catalyzing methane dehydrogenation than the global minimum (Sautet, JACS 2018). (C) Cu_xO_n and Pd_xO_m on diamond are exceptionally selective for oxidative dehydrogenation of cyclohexane, producing cyclohexene and benzene, respectively. Cu owes the selectivity to partial reduction at reaction temperatures and reduced structural fluxionality that comes with it (Alexandrova, submitted to Nat. Catal. 2018). (D) Coking resistance of Pt clusters on Al_2O_3 during dehydrogenation is predicted and experimentally confirmed to be mitigated by adding B to the cluster, but the effect is only seen in simulations when the ensemble of cluster states is expanded toward the catalytically-relevant temperature regime (Alexandrova, JACS 2017).

There are no publications to report because this is a new award, with a start date of September 1, 2018.

Condensed Phase and Interfacial Molecular Science

Heather C. Allen

Ohio State University, Department of Chemistry and Biochemistry

100 West 18th Ave, Columbus OH 43210

Program Scope

Controlling Aqueous Interfacial Phenomena of Redox-Active Ions with External Electric Fields. There is a critical need to develop a thorough mechanistic understanding of interfacial hydration of redox ions and solvent organization with and without externally applied fields. Iron (II) / iron (III) is one such redox couple that is pervasive in our natural environment. Furthering our understanding of water-mediated iron speciation at interfaces provides fundamental knowledge relevant to geochemical and energy-related phenomena including mineral dissolution and energy infrastructure. Literature precedents suggest that an externally applied electric field will influence ion hydration properties, ion pairing, ion speciation and complexation, and interfacial water organization at the air/aqueous interface. We know that, of the studied alkali and alkaline earth metal ions, ions and water are not distributed homogeneously at interfaces, and it is therefore the current expectation that multivalent cations with co-anions will spontaneously form an electrical double layer, thereby aligning water in the diffuse layer. This phenomenon will be explored with aqueous iron salts. Here we also study iron ions and their preferred speciation including the role interfacial water has on mediating the speciation process, in addition to the solvation shell water within the interface, and in the bulk. An additional goal for the proposed research is to show beyond proof of concept experiments, a fundamental understanding of the organization of, and induced by, redox ions Fe(II) and Fe(III) with and without externally applied electric fields at the hydrophobic air /water interface. In these studies we design and employ vibrational sum frequency generation (VSFG) spectroscopic, glancing angle, and polarized Raman spectroscopic, surface tension and ²⁴¹Am-based surface potentiometric experiments. Expected outcomes include instrumentation development important to understanding redox ions at aqueous surfaces, electric field effects, and advances in surface-sensitive spectroscopy, and constant depth reflection spectroscopy.

Recent Progress

Bulk Fe(III) speciation undergoes hydrolysis reactions and polynuclear compound formation. Yet at the air/water interface, iron(III) chloride appears to undergo speciation at a different kinetic rate compared to bulk kinetics. Thus, our first two years on this project has been devoted to understanding this difference and in defining a potential surface species. The work collected under close-to-equilibrium conditions, *"Iron(III)-Chloro Complex observed at the Air/Aqueous Interface using Vibrational Sum Frequency Generation Spectroscopy"*, was recently submitted. In addition, we are currently delineating the temporal aspect of FeCl₃ speciation with an expected submission in December of 2018 that addresses the difference from bulk versus surface kinetics.

For the equilibrium experiments, we observed an enhancement of molecular ordering of water dipoles at the surface, indicative of an electrical double layer (EDL) of hydronium and Cl^- ions at a bulk concentration

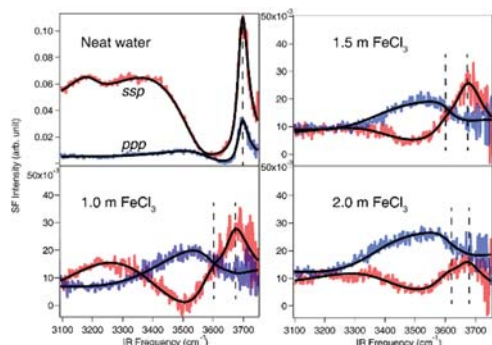


Figure 1. Polarized sum frequency generation spectroscopic measurements of air/aq. FeCl_3 solutions to reveal symmetry of the solvation shell water at the interface.

of 0.5 molal FeCl_3 in aqueous solution - yet only for this low concentration. We determined that for the more concentrated FeCl_3 solutions, $\text{FeCl}_2(\text{H}_2\text{O})_4^+$ ions maintain a significant presence at the surface (see Fig. 1). Its centrosymmetric configuration is consistent with a dramatic decrease in the VSG intensity in the OH stretching region. VSG spectra indicate that the OH group of the surface water molecules bound to the dangling OH is weakly hydrogen bonded to the chlorine of the $\text{FeCl}_2(\text{H}_2\text{O})_4^+$ ion, and gives rise to a peak at $\sim 3600 \text{ cm}^{-1}$. We also observe a 40 cm^{-1} red-shift to $\sim 3660 \text{ cm}^{-1}$ of the dangling OH from the water molecule that straddles the air-aqueous interface and is part of the first solvation shell of the $\text{FeCl}_2(\text{H}_2\text{O})_4^+$ surface complex. We therefore conclude that the first solvation shell and the bound water molecules of the $\text{FeCl}_2(\text{H}_2\text{O})_4^+$ ions exist at the air/aqueous interface at concentrations at and above 1.0 molal FeCl_3 .

of 0.5 molal FeCl_3 in aqueous solution - yet only for this low concentration. We determined that for the more concentrated FeCl_3 solutions, $\text{FeCl}_2(\text{H}_2\text{O})_4^+$ ions maintain a significant presence at the surface (see Fig. 1). Its centrosymmetric configuration is consistent with a dramatic decrease in the VSG intensity in the OH stretching region. VSG spectra indicate that the OH group of the surface water molecules bound to the dangling OH is weakly hydrogen bonded to the chlorine of the $\text{FeCl}_2(\text{H}_2\text{O})_4^+$ ion, and gives rise to a peak at $\sim 3600 \text{ cm}^{-1}$. We also observe a 40 cm^{-1} red-shift to $\sim 3660 \text{ cm}^{-1}$ of the dangling OH from the water molecule that straddles the air-aqueous interface and is part of the first solvation shell of the $\text{FeCl}_2(\text{H}_2\text{O})_4^+$ surface complex. We therefore conclude that the first solvation shell and the bound water molecules of the $\text{FeCl}_2(\text{H}_2\text{O})_4^+$ ions exist at the air/aqueous interface at concentrations at and above 1.0 molal FeCl_3 .

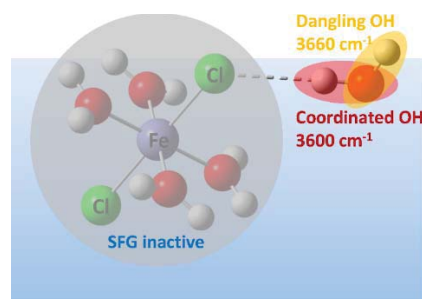


Figure 2. Schematic of the centrosymmetric $\text{FeCl}_2(\text{OH}_2)_4^+$ ion (inside gray circle) that dominates the surface and reduces the VSG intensity. Water molecules in the topmost layer weakly coordinate to chloro of this complex.

Upon experiencing the complicated nuances of bulk iron speciation and how this then impacts the surface speciation, we are now conducting comparative studies of different iron salts to understand the hydration shell in the bulk of Fe(II) and Fe(III) salts (chloride, nitrate and sulfate).

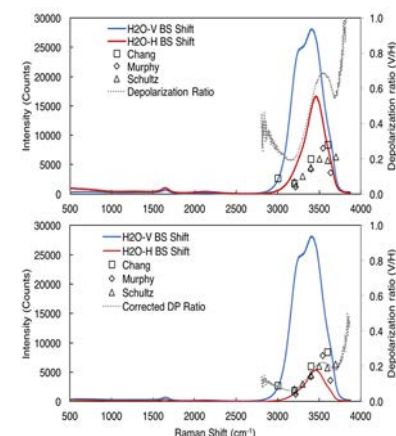


Figure 3. Validation of using Raman polarization ratios for instrument function correction.

These studies incorporate a newly designed polarized Raman spectrometer set up to simultaneously acquire isotropic and anisotropic Raman spectra so that we can then utilize symmetry of the complex in addition to subtraction algorithms to iteratively define the difference spectra for further interpretation. Figure 3, a first step in these experiments, shows water spectra utilizing polarization ratios to correct for the instrument function, and compares this to literature values to validate (Murphy, W. F. *J. Phys Chem.* **1972** 76(8) 1147-1152; Chang, C.H. and Young, L.A.; *IEEE J. Quantum Electronics* **1973** 9(6) 655-655; Schultz, J.W.; *J. Phys Chem.* **1961** 65(12) 2131-2138).

In addition to Raman instrumentation advances, we have been also modifying our surface potential instrument. These modifications arose from the difficulty in normalizing a low- and high-end calibrant to be comparable to literature values. In this process, it has become clear that our newest surface potential design should be patentable

and we have therefore filed an invention disclosure and are working with Ohio State on the patent process.

Future Plans

We are working in several areas to advance our knowledge on hydration and complexation of redox species at aqueous surfaces and in the bulk solution. We plan to investigate other iron salts, as is in play currently using polarized Raman. We intend to further focus on hydration structure and speciation, and a goal is to generate hydration numbers of water in the solvation shell of the iron salt ions. Interest continues in the mechanisms of hydrolysis and speciation, and how this then affects surface speciation. We are continuing our work on surface potential instrumentation as discussed above, and plan to address issues of relative sign of the surface potential. Our current surface potential configuration is susceptible to noise from the salt solution environment and possibly alpha particles decaying from the americium-241 source. We are experimenting with another alternate configuration (of many) to minimize alpha-decay noise from the measurement by introducing a second platinum gauze electrode in the air gap between the source and solution surface. Surface potential instrument development continues to be a major thrust. We have not yet applied the electric field across the air/aqueous interface while probing with VSFG, however, this is tasked to be the next large project of this coming year. Our 2nd method of surface potential measurement was in using second harmonic generation (SHG), and we have recently validated our new SHG optical design and plan to generate several salt system measurements to compare against each other and against the surface potentiostat being built/refined.

Publications (9/2016-present)

1. Iron(III)–Chloro Complex observed at the Air/Aqueous Interface using Vibrational Sum Frequency Generation Spectroscopy, Lu Lin, Stephen M. Bauml, Ka Chon Ng, Tehseen Adel, and Heather C. Allen, Submitted to JACS, September 2018.

Visible light photo-catalysis in charged micro-droplets

DE-SC0016044

Abraham Badu-Tawiah

Department of Chemistry and Biochemistry, The Ohio State University. Columbus, OH 43210

badu-tawiah.1@osu.edu

Program Scope

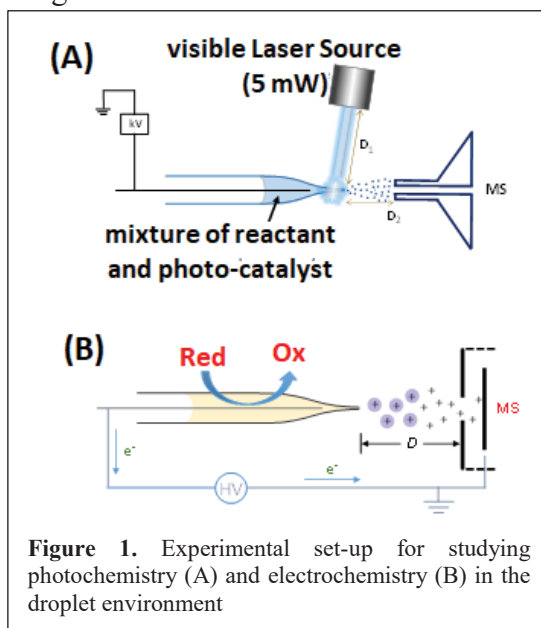
This research program seeks to establish the use of charged micro-droplet environment as a medium for studying photochemical reactions. The confined droplet environment has capacity to accelerate chemical reactions using only picomoles (10^{-12} mol) of reactants. The hypothesis is that the effect of electric fields used during charged droplet generation, the effect of concentration achieved by solvent evaporation from the resultant charged droplets, and the effect of droplet exposure to a highly intense and coherent visible laser source will enable the production of unique, reactive photo-chemical species for novel pathways that might be difficult to access in traditional bulk, condensed-phase conditions. Unlike traditional gas-phase reactions conducted under reduced pressure, the ionic environment of the charged droplets exists at the interface of solution-phase and the gas-phase, yielding information that is directly transferrable to large scale chemical synthesis. The main focus of our work has been the development of novel devices for charged droplet manipulation and real-time product detection by mass spectrometry (MS). Chemical systems of interest involve the study of interfacial oxidation of amines.

Recent Progress

We have developed a novel contained-electrospray (ES) ionization device that is capable of (i) reactant confinement in charged droplets, and (ii) manipulation of the droplet reaction environment with

a variety of stimuli (photons, electrical discharge, and heat). Progress is reported on the effects of photons, electrical energy, and heat on electro sprayed charged droplet reactivity. Experiments were performed using a simplified device (Figure 1B and 1C) involving nano-electrospray ionization (nESI) that mimicked only the outlet portion of the contained-ES apparatus.

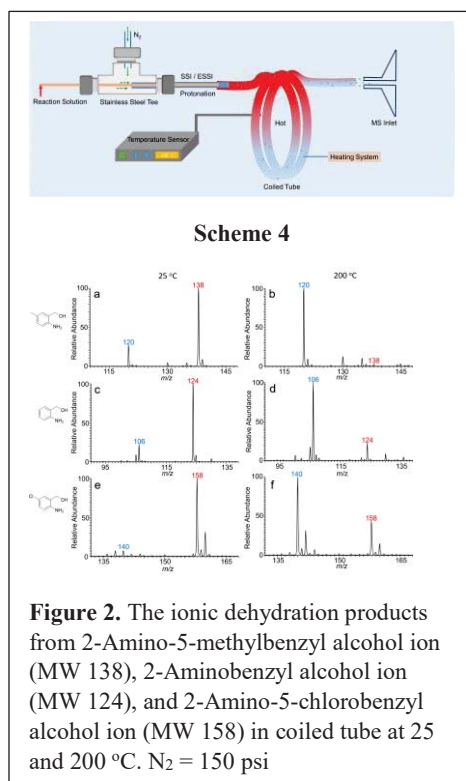
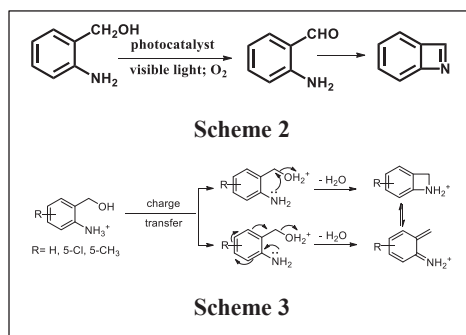
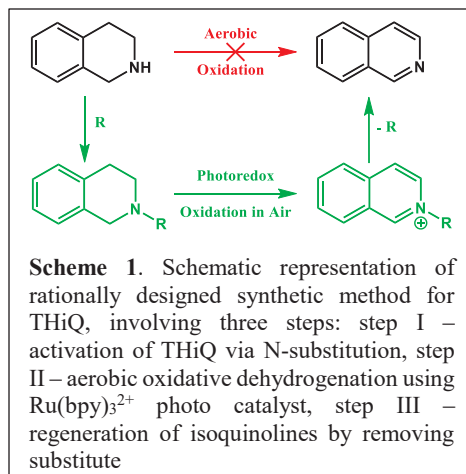
By coupling a portable laser source with nESI MS, we have established the first MS-based picomole-scale real-time photoreaction screening platform. With this approach, we discovered an effective photocatalytic pathway involving the dehydrogenation of 1,2,3,4-tetrahydroquinolines (THQ) to the corresponding quinolines. The reaction was catalyzed by the common visible-light-harvesting complex $[\text{Ru}(\text{bpy})_3]\text{Cl}_2$ (bpy=2,2'-bipyridine) under ambient conditions. Mechanistic



studies revealed that the main active species in the droplet interfacial reaction environment to involve superoxide anions ($O_2^{\cdot-}$) produced during the process of photo-catalyst regeneration. Under this photocatalytic pathway, we observed marked reactivity difference between tetrahydroquinolines and tetrahydroisoquinolines. While tetrahydroquinolines (THQ) underwent full dehydrogenation via the removal of four hydrogen atoms to yield quinolones (>86% yield), tetrahydroisoquinoline (THiQ) produced the dihydroisoquinoline intermediate irrespective of visible light exposure time. Surprisingly, although this reactivity difference between the isomers THQ and THiQ is well-known, the factors governing this inconsistency are incompletely known. Detailed mechanistic investigations using DFT calculation and our real-time reaction screening revealed a high-speed electronic interconversion bottleneck caused by hyper-conjugation. We observed that N-substitution with *pi* and *sigma* donors relieved the hyper-conjugation, freeing THiQs to undergo full hydrogenation. By this insight, a new photocatalytic synthetic strategy was rationally designed to enable large-scale production of isoquinolines from THiQ. This new producer involves three simple steps (Scheme 1): (i) N-substitution of a suitable auxiliary to reduce hyper-conjugation, (ii) photoredox oxidation of N-substituted THiQ using off-the-shelf, visible light harvesting $Ru(bpy)_3Cl_2$ complex under ambient conditions, and (ii) removal of N-substituted auxiliary to generate isoquinoline.

We have now turned our attention to study the reactivity of bi-functional substrates such as amino alcohols. Both the OH and NH_2 groups could act as electron donors for reaction with excited photocatalyst so we seek to study their cooperativity within a single substrate under the droplet reaction conditions. Our expectation was to form strained rings using the reactive droplet environment (Scheme 2). This interest is motivated by the fact that small and strained N-heterocycles such as those found in penicillin offer the prospects of new drug leads. However, less progress has been made for benzazetidines, an azetidine core flanked by benzene ring, due to the significant ring strain in these four-membered scaffolds.

Our previous work showed that droplets effects (concentration and charge) were minimal during photochemistry in the electrospray environment, which allowed effective dehydrogenation. For these bi-functional substrates, however, our initial results indicate a charged directed reaction leading to dehydration (Scheme 3), which is observed to be



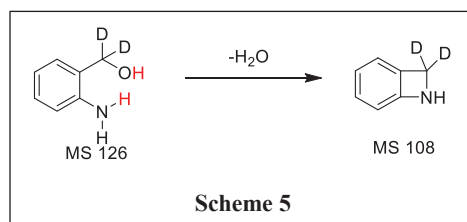
faster than dehydrogenation induced by excited state chemistry. Interestingly, the dehydration reaction is uncatalyzed. Detail mechanistic experiments showed that substrate charging is necessary in this reaction but collisions are more important. Therefore, we introduced heat (Scheme 4) and the corresponding results are shown in Figure 2.

We have also developed a new platform to enable excited chemistry to favorably compete with charge-directed reactions in the droplet environment. In this platform, a multi-phase droplet is formed, with the photocatalyst concentrated at the surface of the droplet. We choose to optimize this reaction platform using organic dye photocatalysts such as pyrylium cations, whose ground state chemistry is distinctly different from the corresponding excited state chemistry. Once optimized, we will go back to studies of small and strained N-heterocycles using both organic dyes and organometallic photocatalysts.

Future Plans

The focus of our work will remain (i) the development and refinement of methodologies to “process” ions at atmospheric pressure, where processing includes ion formation, ion stimulation, ion reaction, and product collection, and (ii) attempts to advance understanding of the fundamentals of photo-redox catalysis, and ion chemistry at interfaces and atmospheric pressure, using these new methodologies. Of particular interests are the elucidation of the complete mechanism governing the photo-redox reaction to enable the creation of new pathways for other substrates.

Our immediate efforts will involve complete structural elucidation and mechanism governing the uncatalyzed thermally-assisted droplet dehydration reaction. This will involve large-scale product collection and characterization by NMR. It is also important to perform isotope labeling experiments to trace the specific hydrogens that are involved in this reaction, as illustrated in Scheme 5.



Detailed experiments are also needed to fully characterize the source of the O₂^{•-} reactive species in droplet-based photochemistry. To be certain of this reaction directions, we will first study the effect that radical scavengers (e.g., benzoquinone) have on the amine oxidation when using [Ru(bpy)₃]²⁺ with blue visible light. Benzoquinone can trap superoxide anions by an electron transfer mechanism and reduced reaction yield is expected. We will also employ 5,5-Dimethyl-1-Pyrroline-N-Oxide (DMPO) as a spin trapping reagent. In this case, DMPO is expected to react with O- and N- centered radicals present in the reaction system to form stable adducts that can be detected and characterized by MS. These experiments will provide both molecular and kinetic information. This result will encourage the development of novel electrospray-based methods that impose electrical discharge on illumination. The combined effect should make it possible to utilize highly abundant first row transition metal (e.g., copper and iron) complexes as catalyst for amine oxidation.

In particular, we are interested in *in-situ* preparation of active catalysts from simple salts (e.g., CuBr₂) and free ligands (e.g., 2,2'-bipyridine). For example, a previous report on a systematic investigation of the effect of different components in the Cu salt/bpy catalytic system showed better performance under basic (e.g., N-methylimidazole (NMI)) and stable radical (e.g., 2,2,6,6-

tetramethylpiperidinyloxy (TEMPO)) conditions.^[82] Spectroscopic investigation suggested the presence of $[\text{Cu}(\text{bpy})(\text{NMI})\text{O}_2]^+$ and oxygen-bound dimer, $[\text{Cu}(\text{bpy})(\text{NMI})(\text{O}_2)\text{Cu}(\text{bpy})(\text{NMI})]^{2+}$, all indicating the importance of reactive oxygen species. Through negative mode electrospray, we will simplify the compositional complexity of this catalytic system. Solvent effects will be studied systematically on-line using the contained-ES apparatus. That novel and highly reactive chemical species can be generated under the charged micro-droplet environment motivates us to screen other first row transition metal salts including those of Ni and Fe. We have unique opportunity to vary a multitude of reaction conditions within a short time period. For this, we will electrospray various selected halides from different solvent compositions. Effects from confinement, photon and electrical discharge is expected to generate different micro-solvated $[\text{ML}_n]^{n+}$ species (L = halide, H_2O , CH_3CN , OCH_3 , OHCH_3 , etc.) with various oxidation states, some of which will be expected to have catalytic activities. Intermediate detection and characterization will be achieved by using a novel transmission-mode desorption electrospray (TM-DESI) ion source, which enables rapidly moving charged droplets, of microseconds lifetimes, to be analyzed by MS.

Recent Publications

1. Suming Chen, Qiongqiong Wan and Abraham K. Badu-Tawiah “Picomole-Scale Real-Time Photoreaction Screening: Discovery of the Visible-Light-Promoted Dehydrogenation of Tetrahydroquinolines under Ambient Conditions” *Angew. Chem. Int. Ed.* **2016**, 55, 9345
2. Kathryn M. Davis and Abraham K. Badu-Tawiah “Direct and Efficient Dehydrogenation of Tetrahydroquinolines and Primary Amines using Ionic Wind Generated on Ambient Hydrophobic Paper Substrate” *J. Am Soc. Mass Spectrom.*, **2017**, 28(4), 647–654
3. Colbert F. Miller, Dmytro S. Kulyk, Jongin W. Kim, and Abraham K. Badu-Tawiah “Re-configurable, Multi-mode Contained-electrospray Ionization for Protein Folding and Unfolding on Milliseconds Time Scale” *Analyst*, **2017**, 142, 2152-2160
4. Qiongqiong Wan, Suming Chen, and Abraham K. Badu-Tawiah “An integrated mass spectrometry platform enables picomole-scale real-time electrosynthetic reaction screening and discovery” *Chemical Science*, **2018**, 9, 5724
5. Sierra Jackson, Devin J. Swiner, Patricia C. Capone and Abraham K. Badu-Tawiah* “Thread Spray Mass Spectrometry for Direct Analysis of Capsaicinoids in Pepper Products” *Analytica Chimica Acta*, **2018**, 1023, 81-88
6. Savithraa Jayaraj and Abraham K. Badu-Tawiah “N-Substituted Auxiliaries for Visible Light-Mediated Dehydrogenation of Tetrahydroisoquinolines: A Theory-Guided Rational Catalytic Design Supported by Real-time Electrospray-based Photoreaction Screening” submitted, 2018

Probing Ion Solvation and Charge Transfer at Electrochemical Interfaces Using Nonlinear Soft X Ray Spectroscopy

L. Robert Baker
100 W. 18th Ave. Newman-Wolfrom Laboratory
Department of Chemistry and Biochemistry
The Ohio State University, Columbus, OH 43210
baker.2364@osu.edu

1. Program Scope

Understanding charge transfer across interfaces is an important challenge with both scientific and technological relevance because these interfacial processes largely determine the performance of batteries, fuel cells, catalysts, opto-electronic devices, and photovoltaics. To significantly improve the efficiency of these energy conversion technologies will require a much better fundamental understanding of the molecular and electronic processes occurring at interfaces that drive energy conversion. Probing the femtosecond dynamics of charge transfer across interfaces with chemical state resolution is crucial for engineering materials with desirable optical and electronic properties for better energy conversion applications.

Toward this goal we have recently developed extreme ultraviolet reflection-absorption (XUV-RA) spectroscopy. This method combines the benefits of X-ray absorption spectroscopy, such as element, oxidation, and spin state specificity, with surface sensitivity and ultrafast time resolution, having a probe depth of only a few nm and an instrument response less than 100 fs. Unlike transmission measurements, XUV reflectivity is not limited by sample thickness, which extends the use of XUV spectroscopy to functional surfaces without restriction to material thickness or substrate. This gives us the ability to track the state of photoexcited charge carriers at a catalyst surface in real time with state-specific precision.

Much more is currently known about molecular photophysics and photochemical reaction dynamics compared to surface photochemistry due to the inability to probe surfaces selectively with sensitivity to oxidation state, spin state, carrier thermalization, lattice distortions, and charge trapping at defect states. Femtosecond XUV-RA spectroscopy developed here is now enabling such studies with the goal of advancing the field of surface chemical physics. It is anticipated that in the future, this technique will also enable the study of ion solvation and de-solvation dynamics at biased electrode–electrolyte interfaces.

2. Recent Progress

Summary of Progress

Using this technique, we have published 6 papers acknowledging this award during the past two years (see Section 4 below). The most recent work includes studies of exciton localization and metal–oxygen bond covalency in transition metal oxide semiconductors,¹ the role of NiO surface defects in mediating charge carrier recombination kinetics,² and preliminary studies of field-driven exciton dissociation and charge transfer at a model heterostructure interface.³ Specific research findings and future plans are summarized below.

Highly Localized Charge Transfer Excitons in Metal Oxide Semiconductors

The valence band of transition metal oxides has a complex electronic structure, composed of M 3d and O 2p states with varying degrees of hybridization. Using time-resolved XUV-RA spectroscopy we have recently shown that we can directly probe the ultrafast localization of photogenerated holes within the hybridized valence band states by simultaneously measuring the metal M_{2,3}-edge and O L₁-edge spectra with femtosecond time resolution.¹ We observe that photoexcited holes localize to O 2p valence band states

within the instrument response time (<100 fs) following photoexcitation. This ability enables us to directly compare the excited state electronic structure of the metal oxide semiconductors, Fe_2O_3 , Co_3O_4 , and NiO .

Figure 1 compares the transient XUV-RA spectra 2 ps following photoexcitation for Fe_2O_3 , Co_3O_4 , NiO and FeS_2 . In each case the shaded background represents the static XUV-RA spectrum of the corresponding material. Analysis of the transient spectra at the Fe, Co, and Ni $M_{2,3}$ -edges reveals that the excited state in each material represents an O $2p \rightarrow M$ 3d charge transfer photoexcitation leading to reduction of the corresponding metal center. In

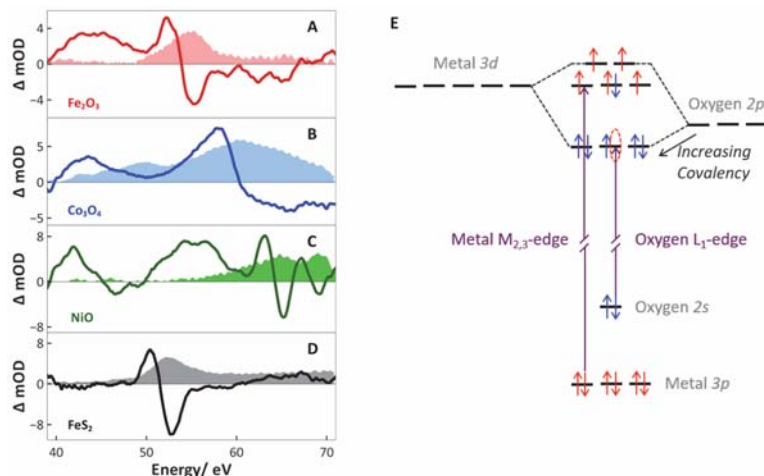


Figure 1 Transient XUV-RA spectra of (A) Fe_2O_3 , (B) Co_3O_4 , (C) NiO , and (D) FeS_2 2 ps following photoexcitation. Shaded plots represent the corresponding measured static XUV-RA spectra. (E) Following a charge transfer photoexcitation, O L_1 -edge absorption is allowed due to the presence of a transient hole on the O $2p$ states.

addition to the spectral features corresponding to the metal $M_{2,3}$ -edge transitions, we observe a broad excited state absorption feature around 42 eV that is common in Fe_2O_3 , Co_3O_4 , and NiO . According to the Henke table, this absorption closely matches the O L_1 -edge transition energy at 41.6 eV. Consequently, we have assigned this positive feature to an additional transient absorption channel at the O L_1 -edge, where the transition occurs from the O $2s$ core state to the photogenerated hole in O $2p$ valence band states as depicted in Figure 1E. To confirm this spectral assignment, we have also measured the transient XUV-RA spectrum of photoexcited FeS_2 (Figure 1D). The spectral feature at the Fe $M_{2,3}$ -edge is similar to Fe_2O_3 ; however, no absorption at ~42 eV is observed. This confirms our spectral assignment of this feature as the L_1 -edge transition in photoexcited metal oxides.

Analysis of the O L_1 -edge for each metal oxide shows that there is a gradual bathochromic shift of the peak position from Fe_2O_3 to Co_3O_4 to NiO . This is the result of varying degrees of hybridization between M $3d$ and O $2p$ in the photoexcited states of Fe_2O_3 , Co_3O_4 , and NiO . Figure 1E shows a simplified molecular orbital picture of the M–O bond depicting how increasing hybridization decreases the O L_1 -edge transition energy, making this transition a direct measurement of M–O bond covalency. Recent studies on water oxidation catalysis speculate that M–O bond covalency has a dominant impact on the reaction kinetics where efficient hybridization between metal $3d$ and O $2p$ reinforces the water oxidation efficiency. However, testing this hypothesis has remained a challenge due in part to the difficulty of determining trends in M–O bond covalency for the late $3d$ transition metal oxides. We demonstrate the ability to directly compare M–O bond hybridization by the transient O L_1 -edge spectrum, which confirms that covalency increases from Fe_2O_3 to Co_3O_4 to NiO . This measured trend is consistent with the efficiency of these materials for water oxidation, affirming the correlation between covalency and catalytic water oxidation kinetics.

Ultrafast Charge Trapping and Defect-Mediated Recombination in NiO

NiO is an important semiconductor serving as a hole transport layer as well as an oxygen evolution electrocatalyst. A number of studies indicate that oxygen vacancies may enhance catalytic performance for photochemical surface reactions while other studies report that oxygen vacancies inhibit catalytic activity by facilitating fast charge carrier trapping and recombination. These reports represent conflicting design parameters for semiconductor engineering and highlight the need to directly measure defect-mediated charge carrier dynamics in real time with chemical state resolution.

In response to this question, we have measured the ultrafast electron dynamics in NiO prepared with varying concentrations of defect states.² Two types of surface defects are identified: one corresponding to a Ni metal phase, which segregates from the oxide during incomplete oxidation and is characterized by a large lattice mismatch at the grain boundary with NiO, and the other corresponding to oxygen vacancy defects. We find that the rate of initial electron trapping occurs on the sub-picosecond timescale and is assigned as electron small polaron formation (Figure 2 A and B). Surprisingly, we find that small polaron formation rates do not depend strongly on defect states in NiO. However, we find that the rate of subsequent recombination scales linearly with the density of Ni metal defects (Figure 2 C and D), indicating that grain boundaries between NiO and Ni metal and not oxygen vacancies are responsible for fast electron-hole pair recombination.

These kinetics can be described by a polaron hopping model as shown in Figure 2C. Detailed analysis of this data provides an absolute measurement of small polaron formation rates, direct versus defect-mediated recombination rates, and the small polaron diffusion coefficient in NiO. These results also reconcile the conflicting design parameters for NiO photoanodes, where the competing role of oxygen vacancies as either a catalytic active center or as a recombination center has not been well understood. In this study we show that oxygen vacancies, which enhance catalytic activity, have no detrimental effect on carrier lifetime. Rather, carrier lifetime can be extended by the elimination of near-surface grain boundaries even in the presence of chemically active oxygen vacancies.

3.Future Plans

Exciton Dissociation and Interfacial Charge Transfer in Model Heterostructures

In a number of recent studies, iron-doped nickel oxide catalysts have been shown to exhibit an exceptional activity for the oxygen evolution reaction during electrochemical water splitting. Mechanistic studies of this system suggest that an optimal iron doping of ~10 percent in nickel oxide increases the formal oxidation state of Ni and changes the electronic structure of the nickel oxide valence band, which in turn enhances the catalytic activity. These observations indicate that charge transfer between iron and nickel is at least partly responsible for the observed catalytic enhancement for water oxidation by NiO upon iron-doping. To investigate the nature of valence band charge transfer in NiO, we have employed XUV-RA spectroscopy to study interfacial hole transfer at a Fe₂O₃/NiO type II heterostructure.³ In these experiments, Fe₂O₃ can be selectively photoexcited because it has a small bandgap compared to NiO. Utilizing the element specificity of XUV-RA spectroscopy, we can simultaneously probe the exciton formation and dissociation dynamics in Fe₂O₃ at the Fe M_{2,3}-edge and subsequent hole transfer to NiO at the Ni M_{2,3}-edge.

The valence band of NiO contains a mixture of O 2p and Ni 3d states. When considering hole transfer to the NiO valence band, it has been shown that the chemical nature of the hole acceptor state strongly influences catalytic activity for water oxidation. Because XUV spectroscopy provides the ability to simultaneously probe the O L₁-edge and the Ni M_{2,3}-edge using XUV spectroscopy, it is possible to comment on the chemical state of hole localization in oxidized NiO. To achieve this goal, we have measured

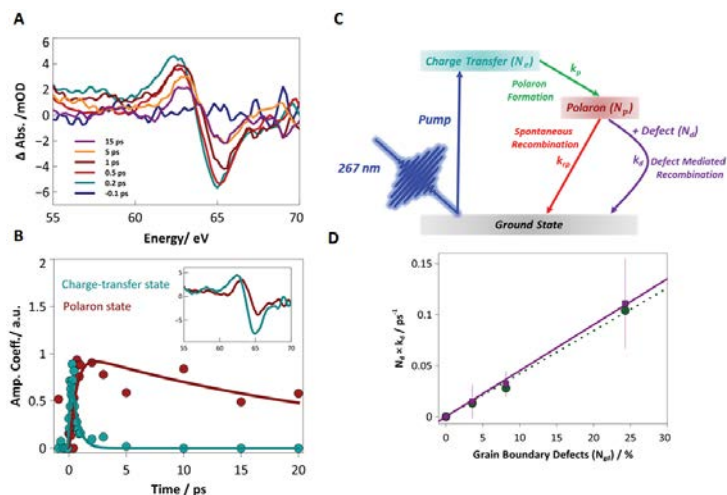


Figure 2 (A) XUV-RA spectra of NiO annealed at 200 °C showing the ultrafast evolution of the charge-transfer state to a small polaron state. (B) Amplitude coefficients of the charge-transfer state and polaron state showing ultrafast small polaron formation followed by recombination. (C) Kinetic model showing grain defect-mediated recombination in which self-trapped electrons diffuse to grain boundaries, which facilitate fast recombination. (D) The recombination rate is linear with the density of Ni-metal sites confirming grain boundary mediated recombination.

the transient kinetics in a Fe₂O₃/NiO type II heterostructure following selective photoexcitation of an underlying Fe₂O₃ substrate. In these experiments, we observe an instantaneous response at the Fe M_{2,3}-edge consistent with direct photoexcitation of the Fe₂O₃ substrate. In contrast to Fe, we observe a delayed response at the Ni M_{2,3}-edge indicating the time scale for hole transfer. Spectral analysis reveals the formation of Ni³⁺ indicating that ultrafast hole transfer occurs in this system to NiO valence band states having significant Ni 3d character as shown in Figure 3A. In these measurements, the rates for field driven exciton dissociation (680 ± 60 fs) in Fe₂O₃ substrate and subsequent hole injection (9.2 ± 2.9 ps) to NiO are independently resolved using a two-step sequential kinetic model depicted in Figure 3B. The ability to independently observe the element specific transient features during ultrafast charge separation and transfer across model heterojunction motivates future experimental studies utilizing XUV-RA spectroscopy. Accordingly, we plan to extend these studies to investigate the chemical details of exciton dissociation and interfacial charge transfer in a variety of semiconductor heterostructures.

An additional important future direction of this work is the study of electron-phonon coupling at surfaces. The dynamics of electron-phonon coupling are known to strongly mediate carrier trapping and relaxation as well as the rates of exciton dissociation and interfacial charge transfer. Ongoing and future studies where phonon coherences are directly probed at semiconductor interfaces will show specific modes that strongly couple to photoexcited states and how the strength of this coupling mediates charge separation kinetics. It is envisioned that this work will lead to a fundamental understanding as well as synthetic control of the primary factors that govern excited state lifetimes and charge separation at semiconductor interfaces. These experiments, which are enabled by the ability to directly observe surface carrier dynamics with element specificity and chemical state resolution, are contributing to a much clearer understanding of the processes occurring at interfaces that mediate charge separation and energy conversion. We anticipate that in the future these methods will continue to advance the field of surface chemical dynamics with important applications for light harvesting and energy conversion catalysis.

An additional important future direction of this work is the study of electron-phonon coupling at surfaces. The dynamics of electron-phonon coupling are known to strongly mediate carrier trapping and relaxation as well as the rates of exciton dissociation and interfacial charge transfer. Ongoing and future studies where phonon coherences are directly probed at semiconductor interfaces will show specific modes that strongly couple to photoexcited states and how the strength of this coupling mediates charge separation kinetics. It is envisioned that this work will lead to a fundamental understanding as well as synthetic control of the primary factors that govern excited state lifetimes and charge separation at semiconductor interfaces. These experiments, which are enabled by the ability to directly observe surface carrier dynamics with element specificity and chemical state resolution, are contributing to a much clearer understanding of the processes occurring at interfaces that mediate charge separation and energy conversion. We anticipate that in the future these methods will continue to advance the field of surface chemical dynamics with important applications for light harvesting and energy conversion catalysis.

4. Publications Acknowledging This Award

1. Biswas, S.; Husek, J.; Londo, S.; Baker, L. R., Highly Localized Charge Transfer Excitons in Metal Oxide Semiconductors. *Nano Letters* **2018**, *18* (2), 1228-1233.
2. Biswas, S.; Husek, J.; Londo, S.; Baker, L. R., Ultrafast Electron Trapping and Defect-Mediated Recombination in NiO Probed by Femtosecond Extreme Ultraviolet Reflection–Absorption Spectroscopy. *The Journal of Physical Chemistry Letters* **2018**, *9* (17), 5047-5054.
3. Biswas, S.; Husek, J.; Londo, S.; Fugate, E. A.; Baker, L. R., Identifying the acceptor state in NiO hole collection layers: direct observation of exciton dissociation and interfacial hole transfer across a Fe₂O₃/NiO heterojunction. *Physical Chemistry Chemical Physics* **2018**.
4. Biswas, S.; Husek, J.; Baker, L. R., Elucidating ultrafast electron dynamics at surfaces using extreme ultraviolet (XUV) reflection–absorption spectroscopy. *Chemical Communications* **2018**, *54* (34), 4216-4230.
5. Cirri, A.; Husek, J.; Biswas, S.; Baker, L. R., Achieving Surface Sensitivity in Ultrafast XUV Spectroscopy: M_{2,3}-Edge Reflection–Absorption of Transition Metal Oxides. *The Journal of Physical Chemistry C* **2017**, *121* (29), 15861-15869.
6. Husek, J.; Cirri, A.; Biswas, S.; Baker, L. R., Surface electron dynamics in hematite (α -Fe₂O₃): correlation between ultrafast surface electron trapping and small polaron formation. *Chemical Science* **2017**, *8* (12), 8170-8178.

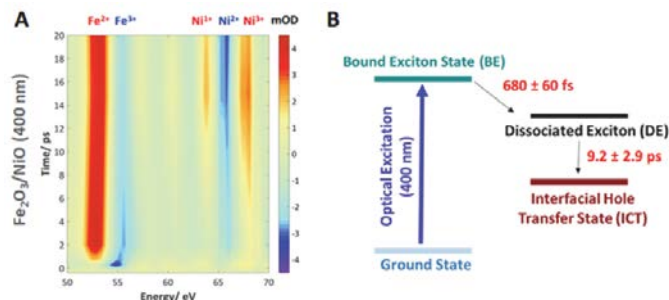


Figure 3 (A) Transient kinetics of NiO/Fe₂O₃ heterojunction pumped at 400 nm, showing the instantaneous transient responses at the Fe M-edge and a delayed response at the Ni M-edge reflecting the rate of interfacial hole transfer. (B) Kinetic model showing measured rates for ultrafast exciton dissociation and subsequent interfacial hole transfer.

Discovering the Mechanisms and Properties of Electrochemical Reactions at Solid/Liquid Interfaces

Ethan J. Crumlin
Lawrence Berkeley National Laboratory
Advanced Light Source
1 Cyclotron Road, MS 6R-2100, CA, 94702
EJCrumlin@lbl.gov

Program Scope

We aim to elucidate the molecular interactions at solid/liquid electrochemical interfaces using a multi-modal approach that combines novel spectroscopy and state-of-the-art microscopy techniques with advanced theoretical modeling and computational science techniques. Our overarching goal is to discover the mechanisms governing interfacial electrochemical properties, in particular the chemistry and electric potentials that will be used to inform the development of more selective, stable, and efficient interfaces for reactions such as water splitting, CO₂ reduction, and N₂ reduction. The primary experimental approach will revolve around the core scientific features of *operando* tender X-ray ($h\nu = 2 \text{ keV} - 6 \text{ keV}$) ambient pressure X-ray photoelectron spectroscopy (APXPS),¹ a technique that is capable of simultaneously probing the electric field,² atomic concentrations,³ and the chemical environment⁴ at solid/liquid interfaces under *operando* conditions. This is largely facilitated by using tender X-ray's that generate photoelectrons with enough energy to escape 10-30 nm of a liquid over layer to study the surface of the underlying solid electrode. We aim to combine this technique with other experimental capabilities such as electrochemical scanning probe microscopy (EC-SPM) and mass spectroscopy (EC-MS) that will be used to characterize nano/microstructure changes and reaction intermediates for the same solid/liquid systems. To further improve our understanding of the solid/liquid electrochemical interface, we will combine these experimental studies with several theoretical and computational techniques,⁵⁻⁶ including *ab initio* molecular dynamic and continuum modeling theoretical simulations, as well as machine learning data mining. Combining experimental approaches with theory, we will iteratively explore the complex molecular interactions of a solid/liquid interface, a strategy that will expedite the discovery of new knowledge enabling future material and device innovations.

Recent Progress

Current efforts have been placed on commissioning the tender X-ray APXPS beamline 9.3.1 at the Advanced Light Source. All of the beamline optics have undergone a complete upgrade including the double-crystal monochromator (DCM). This new DCM can support three-different crystals, with Si(111) serving as the general purpose crystal set to provide a photon energy range between 2.2 keV and 6 keV. Using this beamline in conjunction with APXPS will allow us to probe elemental, chemical, and potential information from the electrochemical solid/liquid interface under *operando* conditions.

Future Plans

We are initiating the beginning of this research program. Therefore a lot of our immediate needs in addition to commissioning the beamline are focused on the hiring of new postdocs for both experimentation and theory efforts. Once the new group members are hired we will begin the process of training to conduct *operando* solid/liquid experiments and theoretical investigations. Our first studies will focus on understanding the metal/liquid interface across a range of pH's to get a detailed comparison of the interfacial properties with respect to the expected thermodynamic properties as suggested by Pourbaix diagrams.

Publications

There are no publications to report because this is a new award, with a start date of September 1, 2019.

References

1. Axnanda, S.; Crumlin, E.; Mao, B.; Rani, S.; Chang, R.; Karlsson, P. G.; Edwards, M. O. M.; Lundqvist, M.; Moberg, R.; Ross, P.; Hussain, Z.; Liu, Z., Using “Tender” X-ray Ambient Pressure X-Ray Photoelectron Spectroscopy as A Direct Probe of Solid-Liquid Interface. *Scientific Reports* **2015**, *5*.
2. Favaro, M.; Jeong, B.; Ross, P. N.; Yano, J.; Hussain, Z.; Liu, Z.; Crumlin, E. J., Unravelling the electrochemical double layer by direct probing of the solid/liquid interface. *Nat Commun* **2016**, *7*, 12695.
3. Favaro, M.; Drisdell, W. S.; Marcus, M. A.; Gregoire, J. M.; Crumlin, E. J.; Haber, J. A.; Yano, J., An Operando Investigation of (Ni-Fe-Co-Ce)O_x System as Highly Efficient Electrocatalyst for Oxygen Evolution Reaction. *ACS Catalysis* **2017**, *7* (2), 1248-1258.
4. Favaro, M.; Valero-Vidal, C.; Eichhorn, J.; Toma, F. M.; Ross, P. N.; Yano, J.; Liu, Z.; Crumlin, E. J., Elucidating the Alkaline Oxygen Evolution Reaction Mechanism on Platinum *J. Mater. Chem. A* **2017**, *5*, 11634-11643.
5. Favaro, M.; Xiao, H.; Cheng, T.; Goddard, W. A. I.; Yano, J.; Crumlin, E. J., Subsurface oxide plays a critical role in CO₂ activation by Cu(111) surfaces to form chemisorbed CO₂, the first step in reduction of CO₂. *PNAS* **2017**, *114* (26), 6706 - 6711.
6. Yu, Y.; Baskin, A.; Valero-Vidal, C.; Hahn, N. T.; Zavadil, K. R.; Eichhorn, B. W.; Prendergast, D.; Crumlin, E. J., Instability at the Electrode/Electrolyte Interface Induced by Hard Cation Chelation and Nucleophilic Attack. *Chemistry of Materials* **2017**, *29* (19), 8504-8512.

Observing the Molecular & Dynamic Pathway of Water Oxidation on Titania Surfaces

Principal Investigator: Tanja Cuk

Associate Professor, Chemistry Department, University of Colorado Boulder
Faculty Fellow, Renewable and Sustainable Energy Institute, University of Colorado Boulder

Chemical transformations have far-reaching impacts for energy utilization, energy storage, and chemical synthesis. The understanding of how chemical transformations occur in real, complex environments is fundamental to our ability to control them and scale them for our needs. Further, at these complex interfaces, chemical transformations occur in a markedly efficient and directed manner and are therefore catalytic, or occur with underpinnings which are understandable and tunable. Yet, while mechanistic pathways of catalysis have been proposed for decades, our ability to follow them directly and along the axis which best defines their trajectory—time—has been limited. Ultrafast chemistry at heterogeneous, condensed phase interfaces (e.g. solid-liquid) develops and applies approaches to reveal how the dynamics of charge across the interface, and between molecular reactants, controls reactivity. In the work proposed here, I will target the following aspects, using water oxidation at the titania/aqueous interface as a model reaction, in three thrusts:

- i. ***Stability and Distribution of O-Radicals*** will reveal the charge dynamics across the solid-liquid interface which defines the stability and distribution of catalytic intermediates (e.g. O-radicals) that re-configure chemical bonds.
- ii. ***O-O Bond Formation from O-Radicals*** will probe the transition state pathways by which catalytic intermediates make and break chemical bonds to form the first chemical bond of the product (e.g. O-O when O₂ evolves).
- iii. ***Dispersive Diffusion at Reactive Aqueous Interfaces*** will probe the interplay between surface charge transport and reactivity, utilizing knowledge from i. and ii.

While elements of heterogeneous water oxidation have been revealed previously by investigating catalysis spectroscopically and *in-situ*, the causal pathway requires truly dynamic probes of diverse molecular reactants and intermediates. In this proposal, multiple dynamic probes that begin at the earliest time steps of the reaction will target the different actors (e.g., trapped charge carriers, radical intermediates, and adsorbed water species) involved in evolving O₂. The strategy is based on merging multi-color, ultrafast transient (optical, mid-infrared, resonance Raman, & X-ray) spectroscopy with highly efficient photo-electrochemistry of the water oxidation reaction. The research aims to reveal the critical steps along the pathway to O₂ evolution and the factor—whether a specific bond breaking event or the surrounding environment—that limits the rate at which each step proceeds to the next.

A major outcome of this DOE grant would be a paradigm by which to resolve how chemical bonds are broken and re-made into new configurations during electrochemical reactions, such that the speed and distribution of evolved products can be tailored by the interface. Depending on the pathway(s) resolved, the tailorable properties include materials choice, electrolyte conditions, and device design, among others. While the focus here is on the water oxidation reaction, this model system provides the critical seed for broader investigations of heterogeneous catalysis at the molecular and dynamic level. It also targets the unique properties of water, important for both energy storing reactions and as a medium for many chemical and life processes.

Voltage-dependent deposition and leaching at electrocatalytic solid–liquid interfaces

Ismaila Dabo (dabo@matse.psu.edu) and Susan B. Sinnott (sinnott@matse.psu.edu)

Department of Materials Science and Engineering
The Pennsylvania State University, University Park, PA 16802

Program Scope

Goal. The electrical response and chemical durability of electrocatalytic metals is primarily controlled by polarization and charge-separation phenomena taking place within the interface region that separates the electrode from the liquid electrolyte (*the electrical double layer*). Despite progress in the description of electrode–electrolyte interfaces from first principles, determining the voltage dependence of the charge accumulated at the interface is still a challenging problem characterized by length scales that are orders of magnitude greater than the typical sizes accessible to density-functional theory simulations. Growing out of the necessity to propose tractable computer models for describing the stability of metal electrodes in aqueous media, the goal of this research is to develop and apply quantum–continuum self-consistent solvation models and voltage-dependent force fields to elucidate the electrochemical stability and the restructuring of these electrodes under applied voltage. The focus is on the electrochemical formation of metal-oxide deposits on gold surfaces and on the voltage-driven leaching of metal cations from gold-based alloys. Guided by the observation that interfacial electrification drives these surface reactions (**Figure 1**), we undertake here a comprehensive computational analysis of the near- and far-equilibrium evolution of the metal–water interface under realistic electrical conditions. Results from simulations will be compared to experimental data from vibrational spectroscopy and potentiodynamic voltammetry for assessing and improving the accuracy of the models.

Methods. We propose to exploit voltage-dependent continuum solvation methods with cluster expansion techniques, and charge-optimized many-body force fields with dynamical control of the voltage. Within the continuum approach, the electrode is described at the quantum-mechanical level and immersed in a continuum medium that includes a diffuse distribution of counterions representing the electrolyte; this implicit model enables one to compute the dependence of the electrode voltage with respect to the surface charge to parameterize a generalized Ising model of the interface free energy for the efficient sampling of the surface configurations (**Figure 2a**). In the charge-optimized model, an electronegativity offset method is used to simulate the effects of an explicit potential on interfacial charge-separation phenomena, enabling the atomistic simulation of an extended surface in contact an aqueous electrolyte, as illustrated in **Figure 2b**.

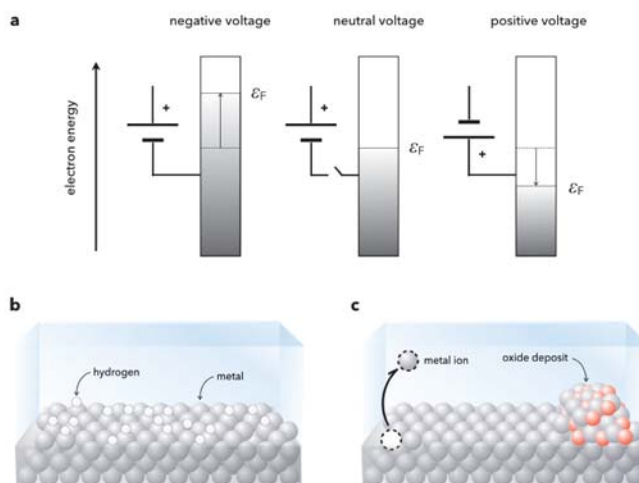
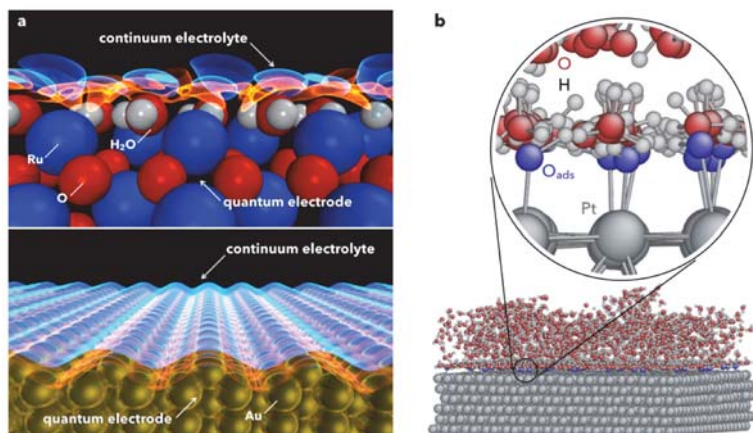


Figure 1 | Voltage-induced deposition and leaching at metal surfaces: The application of a negative (positive) voltage to a metal electrode is accompanied by the accumulation (depletion) of electronic charge at its surface (panel a). The resulting surface charge leads to the adsorption of ions from the solution (panel b), the release of cations in the aqueous medium, or the formation of oxide deposits at the electrode (panel c).



◀ **Figure 2 | (a) Quantum-continuum model** of an oxide surface (top) and metal surface (bottom) using an implicit representation of the electrolyte, which enables an effective description of solvation effects with the possibility to include a few layers of water to improve the accuracy of the model. **(b) Explicit molecular dynamics** of a platinum electrode in contact with an aqueous solution. The calculated interfacial structure confirms the reliability of the newly developed third generation of the charge-optimized many-body model in describing the adsorption of oxygen and hydrogen, and the structure of the water overlayers at the interface.

Recent Progress

To provide a direct assessment of the performance of the proposed models in describing electrochemical stability, we have examined the effects of the voltage on the dealloying of palladium-gold electrodes. Previous experimental studies for electrodeposited palladium-gold surface alloys on gold (111) surfaces have showed a strong enhancement in the surface coverage of palladium monomers relative to palladium multimers. Motivated by these observations, we have applied the quantum-continuum model to examine the effects of solvation and surface electrification on the equilibrium distribution of palladium multimers at PdAu/Au(111) surfaces. Electrochemical enthalpies obtained from the quantum-continuum model were used to fit two-dimensional cluster expansions of the surface alloy for different sets of voltages and differential capacitances. Metropolis Monte Carlo simulations were performed in the canonical ensemble for fixed voltages using non-local spin-exchange moves. Close agreement with experimentally measured palladium multimer coverages was obtained for each case considered. Specifically, we found that at voltages near 0 V vs. SHE (standard hydrogen electrode), palladium monomers are predicted to be stable and tend to adopt locally ordered structures with neighboring palladium atoms occupying second-nearest neighbor positions. At voltages near 0.3 V vs. SHE, we observed that palladium dimers and trimers are stable and homogeneously distributed along the surface when the differential capacitance approaches $60 \mu\text{F}/\text{cm}^2$, but adopts similar low voltage configurations for lower differential capacitances. At voltages near 0.6 V vs. SHE, palladium is observed to exist primarily as monomers along the surface. These results suggest that the applied voltage can provide a driving force for the ordering or clustering of catalytically active multimers within surface alloys, altering the distribution and variety of active sites along the catalyst surface that are available for electrocatalysis under different electrochemical conditions.

Future Plans

This project addresses the main questions surrounding the electrochemical deposition of oxide layers and the voltage-dependent restructuring of gold-based catalytic electrodes. To answer these questions, a database of first-principles surface energies, potentials of zero charge, and interfacial capacitances will be constructed to predict the pH-dependent structure of the interfaces of gold and gold-alloy electrodes with water and to refine the parameterization of the charge-optimized model. This parameterization will then be tested and applied to interpret voltammetry data. In terms of software dissemination, (1) the charge-optimized model will be further developed by implementing a statistically consistent potentiostat as an alternative to the initially proposed charge equilibration scheme in *Lammps*, and (2) the quantum-continuum model will be ported into the *Phonon* code of the open-source *Quantum-Espresso* distribution to interpret experimentally observed voltage-dependent frequency shifts upon surface restructuring.

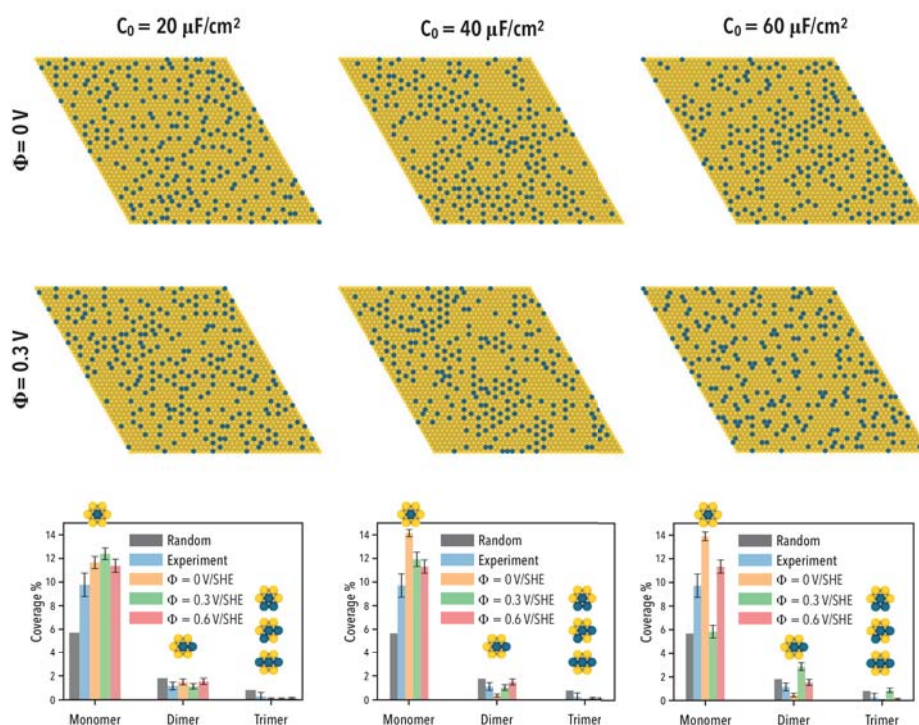


Figure 3 | (a) Monte Carlo configurations of the palladium-gold surface alloy with a palladium surface fraction of $x_{\text{Pd}} = 15\%$ for different voltages and differential capacitances. The surface palladium atoms are shown in blue. Monomer clustering is evident at 0 V and 0.3 V vs. SHE, while dimer and trimer formation can also be clearly seen at 0.3 V. Palladium is found to adopt a dispersed state along the surface at higher potentials. **(b) Average palladium coverage under applied voltage** for different capacitance values. Error bars for the Monte Carlo data are the standard deviations of the coverage distributions. Experimental coverages were obtained by Maroun *et al.* [*Science* 293, 1811 (2001)] by means of scanning tunneling microscopy.

Publications Acknowledging DOE Support

S. E. Weitzner and I. Dabo, Voltage effects on the stability of Pd ensembles in Pd-Au/Au(111) surface alloys, submitted to *Journal of Chemical Physics* (2018).

(There are no publications to report because this is a new award, with a start date of September 1, 2018.)

Rate Theory of Ion Pairing at Liquid Interfaces

Recent Progress and Future Plans

Liem X. Dang
Physical Sciences Division
Pacific Northwest National Laboratory
Richland, WA 93352
liem.dang@pnnl.gov

Background and Significance

The thermodynamics and kinetics of ion pairings at interfaces are fundamental processes encountered in a wide range of physical and chemical systems. The structure and stability of large molecules and membranes depend on the interfacial distribution of ions and counter ions. Moreover, the ion transport mechanism can be an important factor in atmospheric processes, such as molecular uptake at the liquid–air interface. It is also of importance in environmental problems, such as the interaction of contaminated organic solvents in groundwater and separation chemistry performed in binary solvent systems. Considerable progress has been made in understanding the equilibrium and dynamical properties of ion pairings at liquid interfaces. This includes the work of Schweighofer and Benjamin on the thermodynamics and dynamics of NaCl dissociation at the water–1,2-dichloroethane liquid–liquid interface using a variety of statistical mechanical tools, such as the continuum electrostatic model, molecular dynamics free energy calculations, and nonequilibrium dynamic trajectory calculations. Their results indicated that the dissociation of the ion pair at the interface involves a simultaneous transfer of both ions into the aqueous side of the interface. In addition, they found that faster transfer of sodium ions than chloride ions influences the length of time the ion pair spends at the interface. Wick reported a study on the NaCl dissociation rate both in the aqueous bulk and at the air–water interface using the transition path sampling formalism with a polarizable force field. A dissociation rate that was considerably slower at the interface than in the bulk was found. Garde and co-workers used molecular simulations to show that the potentials of mean force between small ions change character dramatically near the water vapor–liquid interface. Specifically, the water-mediated attraction between oppositely charged ions is enhanced relative to that in bulk water. Moreover, they showed that the thermodynamics of ion association are governed by a delicate balance of ion hydration, interfacial tension, and restriction of capillary fluctuations at the interface, leading to nonintuitive phenomena such as water-mediated, like-charge attraction. Interfacial ion pairing has recently been investigated via second harmonic generation experiments by Saykally and coworkers using different kinetic models. They provided insight into how ion pairing influenced anion behavior at the interface, finding that unusually strong surface adsorption is possible at low concentrations. X-ray reflectivity experiments reported by Schlossman and co-workers have shown that the enhancement of ion density near the interface coupled with the effect of capillary waves may lead to layering of Erbium Chloride at the air–water interface. Allen and coworkers carried out surface-sensitive conventional vibrational sum frequency generation and heterodyne-detected spectroscopy studies on the small alkali halide salt at the water liquid–vapor interface. Among other findings, they found that in the conventional VSFG spectra, LiCl and NH₄Cl significantly perturb the hydrogen-bonding network of water. In addition, the direction of the electric field suggests that Cl⁻ ions are always located above the counter cations, even in the case of NH₄Cl salt solution. The main goal of our work, in addition to studying ion-ion PMFs, is to provide detailed kinetic properties of ion pairings at the liquid–vapor interface of water using a variety of rate theory approaches. Moreover, we will determine how the inclusion of polarizable interactions influences the differences that arise at the interface versus bulk. Subsequently, our studies will be expanded to other interfaces, such as liquid–liquid interfaces. Knowledge of free energy profiles and rate theory evaluations is important for understanding a wide range of physical and chemical phenomena for ion solvation and pairing. These also provide a challenging test of the accuracy of the predictive information derived from force field models. Our work is distinguished from earlier contributions by the methodology and the extent in which we have exploited rate theory approaches including classical transition-state theory, the reactive flux formalism, and Grote-Hynes theory. In addition, 1) polarization effects are explicitly included in the potential models, and compared with nonpolarizable models; 2) solvent response at the interface and in the bulk are evaluated using a variety of classical rate theory approaches; and 3) the dissociation lifetimes for the ion pair are computed and compared for different potential models and theories.

Recent Progress

We begin this section by presenting results for the kinetic properties of NaI ion-pair formation at the interface and in the bulk, and continue with the rate theory results determined using the RF and GH formalism/method. At the end of

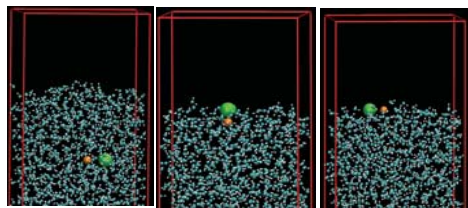


Fig. 1 Schematic descriptions of the NaI–H₂O systems studied. The left panel (a) is the ion pair in the bulk region, and the middle [(b), perpendicular] and right [(c), parallel] panels are the ion pairs at the GDS.

hydrogen networks to accommodate the ion pair at the interface. Moreover, it is well known that I[−] has a larger induced dipole at the interface, which should further strengthen NaI pairing at the interface. Another interesting aspect of the PMF is that the solvent-separated, ion-pair probability (its free energy is lower near 5.0 Å) is slightly enhanced at the interface with respect to the bulk. Overall, this shows that ions are more likely to not just be paired, but to be paired within their first two solvation shells near the interface. The free energy barriers for the ion-pair dissociation are found to be about 3.0 and 1.0 kcal/mol for the interfacial and bulk ion pairs, respectively. The computed rate constants from the PMFs using TST are determined to be 0.55 and 0.06 ps^{−1} for the bulk and interface, respectively. These results show that the 2.0 kcal/mol higher barrier for dissociation at the interface has a major effect on dissociation rate. In Figure 3, we present the computed time-dependent $\kappa(t)$ for both ion-pair locations using the

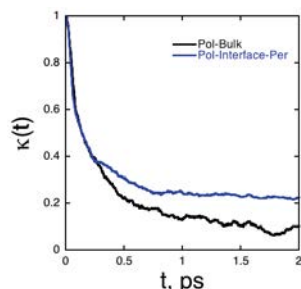


Fig. 3. Computed $\kappa(t)$ using the RF method for the NaI ion pair comparison. In all cases, there are two distinct decay time scales that show first an initial rapid decay, lasting for about 0.1 ps, and then a longer time decay that lasts for a few picoseconds.

The oscillating characteristic of $\zeta(t)$ is reflected in the magnitude of the barrier heights shown in the computed PMFs. For instance, the larger barrier heights correspond to the deeper well-depth in the $\zeta(t)$. The computed transmission coefficients using GH theory are 0.21 and 0.33, respectively, for the bulk and interfacial ion pairs. Using the rate constants from TST, correcting them with the transmission coefficient, and taking their inverses, the relaxation time can be calculated. The bulk and interfacial ion pairs had relaxation times of 9 and 51 ps, respectively. These are somewhat lower than the times calculated from the RF formalism, but they are consistent. Results for the relaxation times obtained from the RF formalism and GH theory unequivocally show that the interface suppresses ion dissociation.

Future Plans

Rate Theory of the Hydrated Proton-Chloride Ion Pairing at the Water Liquid–Vapor Interface

These previous studies included work by Zeng and colleagues on the ion-sign preference of water condensation. Among other computed quantities, they were able to reproduce the experimental observation that the anion is a better nucleator than the corresponding cation. In other work, Kusaka and Oxtoby reported an extensive study on protonated

this section, we compare the results obtained using the different rate theory methods and provide a description of their solvation structures. Figure 1 shows schematic descriptions of the NaI–H₂O systems we studied. Figure 2 shows the computed PMF plots as a function of NaI separation at the interface and in the bulk for the polarizable model. Although the shapes for both of the PMF curves are quite similar, the details of the barriers are different, which may result in dissimilarities in the kinetics of ion pairing. From Figure 2, it is clear that the PMF at the interface has a deeper minimum at the contact ion pair and a larger barrier height to dissociate compared to the corresponding bulk PMF results. This demonstrates that the interfacial ion pair is more strongly associated at the interface, which can be attributed to the rearrangement of the interfacial water

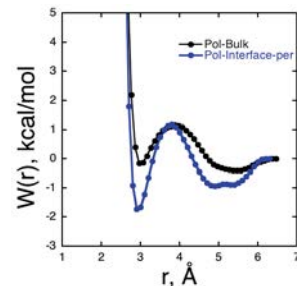


Fig. 2. Computed PMFs for the NaI ion pair in the bulk and at the interface. polarizable

RF formalism. The transmission coefficients, κ_{RF} , are 0.09 and 0.23. We observed that the plateaus of the transmission coefficient curves are very flat after 1.5 ps, and we also noticed that the transmission coefficients decrease from the interface to the bulk. Our results show that in addition to affecting the free energy of solvation, moving ion pairs from the bulk to the surface should significantly influence the kinetics of ion pairing. We found that the relaxation times increased from 20 ps to 72 ps when the ion pair was at the interface in comparison to the bulk. These results confirm that the interface has a significant impact on the kinetics of ion pairing for models with polarizable interactions. We also were interested in using GH theory to calculate a transmission coefficient, κ_{GH} , to compare with the RF results. In Figure 4, we show plots of un-normalized, time-dependent friction kernels of the ion pair at the interface and in bulk water for

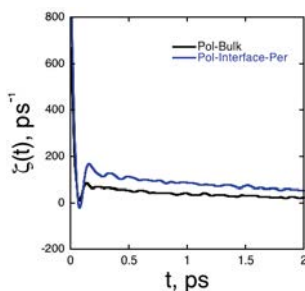


Fig. 4. Computed $\zeta(t)$ using the GH method for the NaI ion pair in the bulk and at the Gibbs dividing surface.

water clusters in which they used grand canonical Monte Carlo simulation techniques and polarizable models. While simulated thermodynamic properties such as free energy, enthalpy, and entropy compared reasonably well with the corresponding experimental data, the study also revealed interesting structural properties of protonated water clusters. For instance, they found that, for larger water clusters, the hydronium ion was on the surface and participated in the hydrogen bond network. This phenomenon has been demonstrated recently for anions with significant polarizabilities. Among other MD studies, with the notable exception of a pioneering study by Voth and co-workers with the use of MS-EVB approach, of a single proton and chloride at the extended air/water interface. Jungwirth and colleagues and studied the molecular structures of acid-base and other systems. They found, in the case of hydrochloric acid both hydronium cations and chloride anions penetrate into the air/solution interface, and there is actually a slight surface ion enhancement of both ions. Note that the hydronium cations are preferentially oriented at the surface, with hydrogens pointing toward the aqueous phase and oxygen toward the air. *Ab initio* MD by Mundy and Tobias on the distribution of HCl, HBr and HI at the aqueous interfaces have provided some insight how the hydrated proton influenced by the solvent solution. We realize that it has been established that dissociation and proton-transfer will influence this phenomenon. Furthermore, the detailed electronic structure of the components may be required to describe the subtle balance between forces. In addition, the collective ion atmosphere, the structure of the electric double layer may have a significant influence on the process. In this preliminary work we focus on the general structure

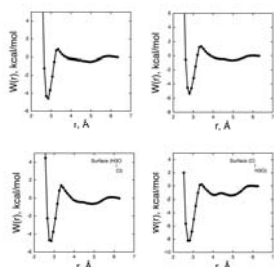


Fig. 5. Computed PMFs for the H_3O-Cl ion pair in the bulk and at the interface. polarizable with various ion pair configurations as shown in Fig. 6.

of the potential of mean force and the time dependent friction for the case of non-simple ions provided by the structure of the hydronium. We expect this to influence the hydrogen bonding network in a non-trivial manner and consequently influence the fluctuations and solvent response to the reactive motion. This work will serve as a foundation for construction of the simplest model that can describe the essential features of the phenomena. To follow, we expect to build a simple dissociable model as well as consider collective ion response to the process. We currently carry molecular simulation studies to examine the thermodynamics and kinetics of ion pair formation of the hydrated proton-chloride ion pair. We compared the process in the bulk and near the water liquid-vapor interface. We calculated potentials of mean force between the ion pair using the constrained mean force approach and calculated the rates using classical transition state theory (Fig. 5). Dynamical solvent effects were taken into account by calculating transmission coefficients computed by the reactive flux method and Grote-Hynes theory. Our results show that both the free energy of ion pairing as well as the kinetics of ion pairing display different behavior in bulk solution when compared to interfacial environments. Estimates of the relaxation time using the reactive flux method and Grote-Hynes theory show that the interface suppresses ion dissociation. The dependence of the rate on the orientation of the hydrated proton-chloride ion pair at the interface was examined.

Develop/apply rate theory methods to study solvation of $Li^+(aq)$ and Li^+ -ion pairings at the graphite-EC solid/liquid interface.

Much effort has been put into LIB system development for electric vehicles, plug-in hybrid electrical vehicles, and other electrical system applications. During LIB operation, a solid electrolyte interphase (SEI) layer forms on the typical graphite anode surface. This SEI is the result of side reactions with the electrolyte solvent and salt. It is accepted that the SEI layer is essential to the performance of LIBs, and it has an impact on initial capacity loss, self-discharge characteristics, cycle life, rate capability, and safety. While the presence of the anode SEI layer is vital, its formation and growth is difficult to control because the chemical composition, morphology, and stability depend on several factors. Such as the type of graphite used, graphite morphology, electrolyte composition, electrochemical conditions, and cell temperature. Thus, SEI layer formation and electrochemical stability over long-term operation should be a primary topic of investigation in further development of LIB technology. Our goal is to develop/apply rate theory methods to study solvation of $Li^+(aq)$ and Li^+ -ion pairings at the graphite-EC solid/liquid interface. Following is a snapshot (Fig. 7) produced from a molecular dynamics study of the graphite-EC solid-liquid interface at 330K. Note that the EC molecules near the interface are less mobile, while molecules at the center have the density of the bulk liquid.

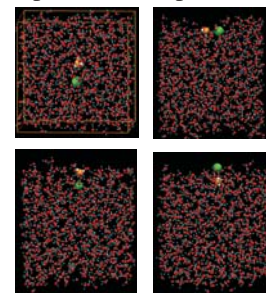


Fig. 6. Snapshots for the H_3O-Cl ion pair in the bulk and at the interface. polarizable with various ion pair configurations.

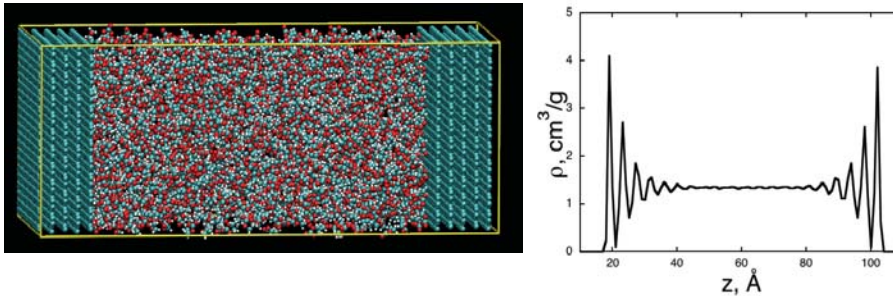


Fig. 7. A snapshot produced from a molecular dynamics study of the graphite-EC solid-liquid interface at 330K

References to publications of U.S. Department of Energy-sponsored research (2017 to the present)

1. The inhibition of methane hydrate formation by water alignment underneath surface adsorption of surfactants. Nguyen, Ngoc N., Nguyen, Anh V. and **Liem X. Dang** *FUEL* 197, 488-496 (2017).
2. Rate Theory of Ion Pairing at the Water Liquid-Vapor Interface. **Liem X. Dang**, Gregory K. Schenter, and Collin D. Wick, *J. Phys. Chem. C* 12, 10018-10026 (2017).
3. Rate Theory on Water Exchange n Aqueous Uranyl Ion. **Liem X. Dang**, Vo N. Quynh, Mikael Nilsson, Nguyen, Hung D. *Chemical Physics Letters*, 671, 58-62 (2017).
4. Interfacial Gas Enrichment at Hydrophobic Surfaces and the Origin of Promotion of Gas Hydrate Formation by Hydrophobic Solid Particles. Ngoc N. Nguyen, Anh V. Nguyen, Karen M. Steel, **Liem X. Dang** and Mirza Galib, *J. Phys. Chem. C* 121, 3830-3840 (2017).
5. Li⁺ Solvation and Kinetics of Li⁺-BF₄⁻/PF₆⁻ Ion Pairs in Ethylene Carbonate. A Molecular Dynamics Study with Classical Rate Theories. Tun-Mei Chang and **Liem X. Dang**. *J. Chem. Phys* 147, 161709 (2017). (Invited)
6. MDS Studies of Nano-bubble Attachment at Hydrophobic Surfaces. J. Jin, J. D. Miller and Liem X. Dang, *International Journal of Mineral Processing*. Volume: 54 Issue: 1 Pages: 89-101 (2018).
7. Rate theory of ion pairing at the water liquid-vapor interface: A case of sodium iodide. Dang, Liem X. and Schenter, Gregory K. *Journal of Chemical Physics* Volume: 148 Article Number: 222820 Published: JUN 14 (2018). (Invited)
8. Water Film Structure during Rupture as Revealed by MDS Image Analysis, *International Journal of Mineral Processing*, Vu N.T. Truong, Liem X Dang, Chen-Luh Lin, Xuming Wang and Jan D. Miller (2018).

Exploring new diamond surfaces with precision chemistry and quantum spectroscopy

Nathalie de Leon (npdeleon@princeton.edu)

Assistant Professor of Electrical Engineering

Princeton University, Princeton, NJ

Program Scope: The aim of the research program is to develop new processing and spectroscopy methods for diamond surfaces, with the goal of creating entirely new surface terminations that are inaccessible with current techniques. Developing new surface terminations for diamond would enable a wide range of future applications based on this material, from classical applications (power electronics, biocompatible devices, electrochemistry, cathodes) to quantum applications (quantum sensors, quantum communication networks, quantum simulators). However, diamond surfaces are particularly difficult to functionalize because the material is chemically inert and difficult to polish. Our approach is to develop a new method of surface termination by first preparing a high quality, reactive, bare surface by thermal annealing in ultrahigh vacuum (UHV) conditions and subsequently exposing the surface to neutral atoms. In order to study these new reactions, we will perform *in situ* measurements using two complementary suites of spectroscopy tools: (1) traditional photoelectron spectroscopy and electron diffraction to study fundamental reaction kinetics, structure, and chemical termination, and (2) quantum spectroscopy using nitrogen vacancy (NV) centers in diamond to probe nanoscale order and magnetic interactions between surface atoms. This project will be enabled by a novel, home-built, UHV cluster tool, which is currently under construction in our group.

Prior Related Work: Our recent work has focused on developing high quality, oxygen-terminated, diamond surfaces to create NV centers within nanometers of the surface that have ultralong coherence times. Many groups have observed that NV spin coherence degrades within 100 nanometers of the surface, suggesting that diamond surfaces are plagued with ubiquitous defects. Prior work on characterizing and reducing near-surface noise has primarily relied on using NV centers themselves as probes; while this has the advantage of exquisite sensitivity, it provides only indirect information about the origin of the noise.

We have taken a different approach: using NV-based nanoscale spectroscopy and traditional surface spectroscopy methods as complementary diagnostic tools to identify sources of noise at the diamond surface. Using this approach, we determined that surface morphology is crucial for realizing reproducible chemical termination, and we used this information to achieve a highly ordered, oxygen terminated surface with suppressed noise and correspondingly longer coherence times for shallow NV centers. Specifically, we have realized a near-atomically smooth oxygen termination that yields NV centers within 5 nm of the surface with coherence times exceeding 100 μ s (Fig. 1), more than an order of magnitude improvement in performance over prior demonstrations.

NV based measurements indirectly suggest that these new surfaces differ in their electronic structure. In order to directly interrogate the electronic structure of the surface, we employed a variety of surface-sensitive spectroscopy techniques. Using X-ray spectroscopy and electron diffraction, we observe that these high quality oxygen-terminated surfaces are highly ordered. In particular, we see that compared to acid processing (the standard procedure in the community), we are able to see a much stronger polarization dependence of the O K-edge in near edge X-ray absorption fine structure spectroscopy (NEXAFS) for oxygen-terminated surfaces,

indicating that the surfaces are highly ordered at the atomic scale (Fig. 2). We also observe that the oxygen terminated surface has a higher positive electron affinity in ultraviolet photoelectron spectroscopy (UPS), as well as a lower density of unoccupied states associated with defects in the C K-edge NEXAFS.

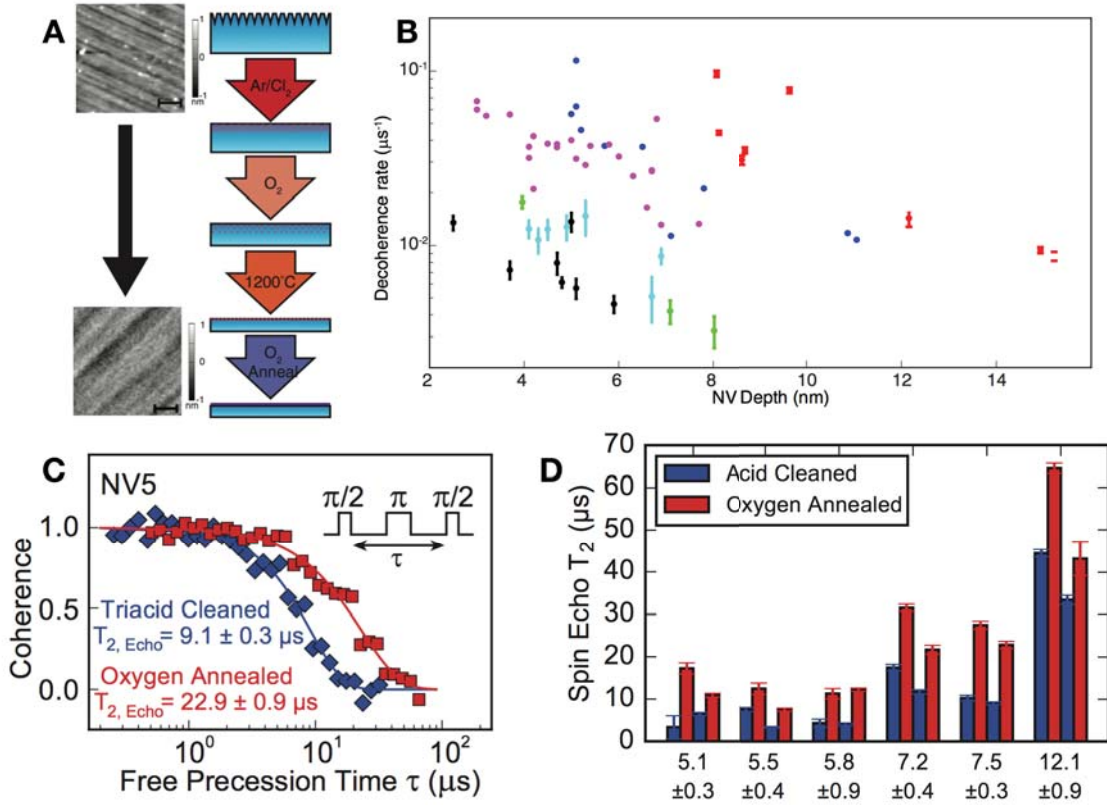


Figure 1: Surface processing for coherent shallow NV centers. (A) Diagram of iterative surface processing. Each step removes the damage caused by the prior step. AFM images of the starting and final surface show that the processing maintains the smooth surface from polishing. (B) Decoherence rate as a function of depth for individual NV centers under different surfaces with varying degrees of subsurface damage (indicated in different colors). The high quality oxygen termination (black) yields NV centers within 5 nm of the surface with 100 μs coherence times. (C) Detailed comparison of Hahn echo T₂ for a single NV between the last two steps of the process, showing an improvement of a factor of 2.4 resulting from the final oxygen anneal. (D) Reversible changes in the coherence time for individual NV centers. Oxygen annealing enhances T₂, while thermal reset and acid cleaning suppresses it. Depths in nm for each NV center are indicated at the bottom of the plot.

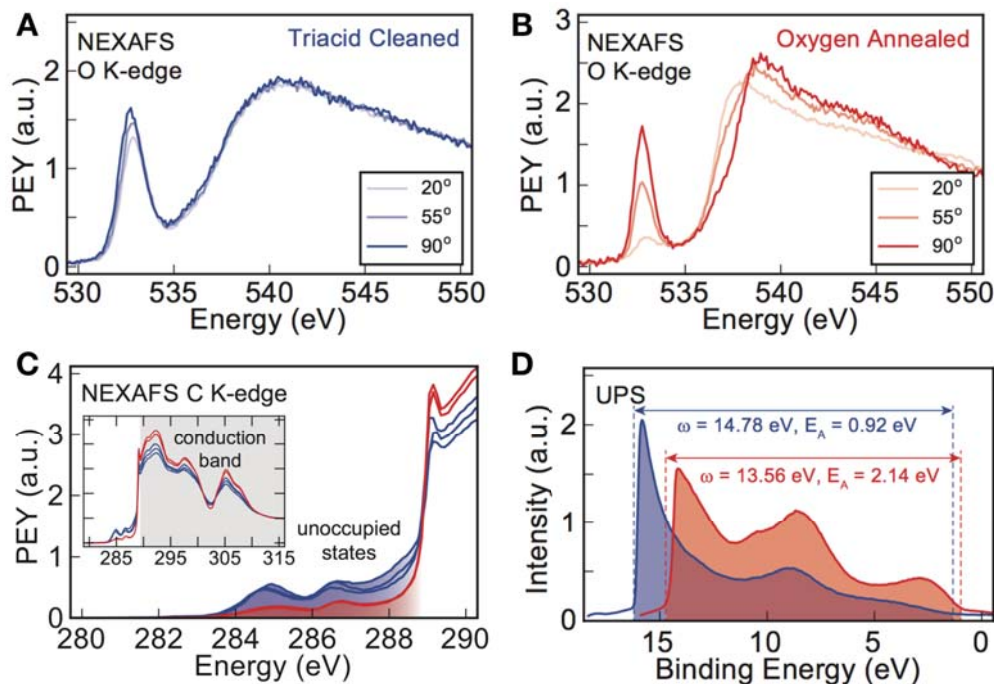


Figure 2: Photoelectron spectroscopy comparisons of the two surfaces, thermally reset and triacid cleaned (blue) and oxygen annealed (red). The O K-edge NEXAFS spectra show qualitatively similar features, but the triacid cleaned surface shows no polarization dependence (A), while the oxygen annealed surface shows a dramatic polarization dependence (B), indicating surface ordering. (C) The C K-edge NEXAFS shows a suppression of defect states in the oxygen annealed surface. (D) UPS shows that the oxygen annealed surface also exhibits a much larger electron affinity.

Recent Progress and Future Plans: Surface chemistry in diamond is difficult because diamond is hard, chemically inert, and sterically hindered. Most available methods involve plasma, which damages the surface morphology. We will develop new techniques for terminating diamond in UHV in a unique apparatus that is currently under construction. UHV allows for the preparation of bare, dangling bond surfaces, which can then be exposed to low energy neutral atoms, minimizing surface damage. Novel surfaces can be prepared and then probed without breaking vacuum, yielding nanoscale information about magnetic and electric field noise at the surface. This instrument is the first of its kind, and it will enable precise chemical control and correspondingly precise spectroscopic interrogation of the diamond surface.

After designing the cluster tool over the first two years of my independent career, the first phase of construction and instrumentation installation began in January of this year, and we have completed the first phase of the project—building the surface preparation and spectroscopy chamber. Using this first chamber, we have primarily focused on developing methods for preparing and measuring reactivity at the diamond surface. Specifically, our preliminary work has focused on oxygen desorption from the diamond surface, as illustrated in Figure 3. Upon heating to 1000°C, we are able to observe almost complete oxygen desorption from the surface using X-ray photoelectron spectroscopy (XPS), as well as subsequent 2x1 reconstruction of the dangling bond surface using low energy electron diffraction (LEED). We are also able to observe

detailed changes in the O1s XPS peak at intermediate temperatures, indicating that different oxygen terminations can form at the surface with incomplete oxygen coverage.

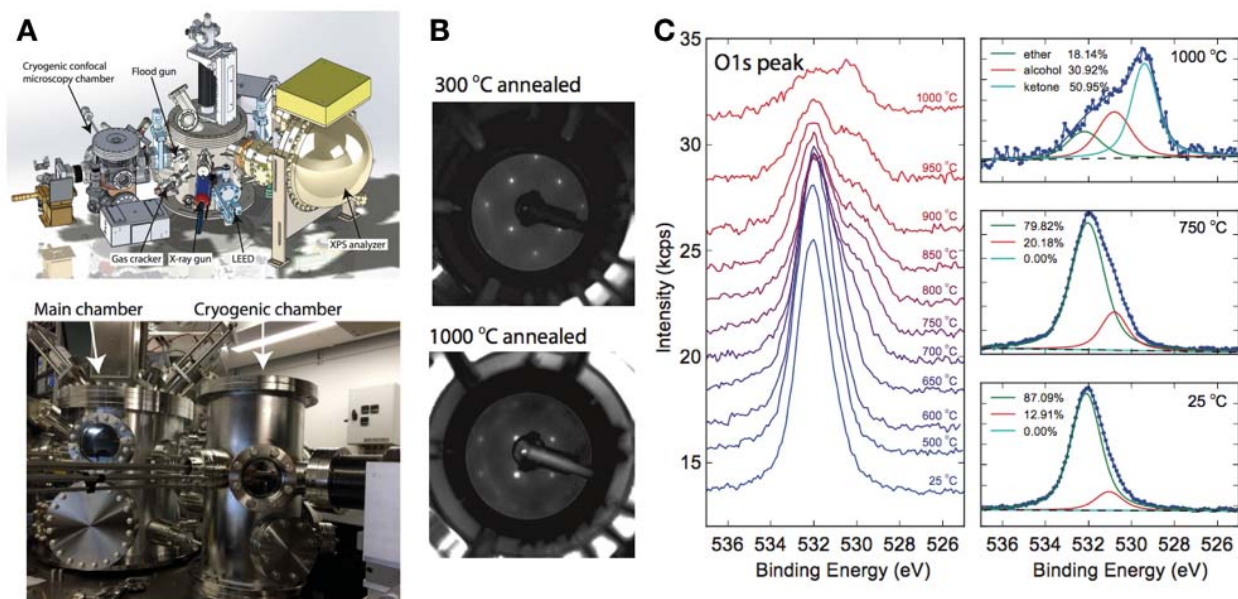


Figure 3: UHV cluster tool for diamond surface science and preliminary data. (A) CAD drawing of the UHV cluster tool and a photograph of the assembled chamber. Construction and installation began in early 2018. (B) LEED patterns showing the change in surface reconstruction upon desorption of oxygen at 1000°C. (C) XPS spectra showing the decreased intensity of the oxygen peak upon desorption. (Right) Detailed XPS spectra at the O1s peak showing that the relative abundance of different surface groups changes during annealing.

Over the next year, we plan to study the reactivity of this bare surface using a thermal gas cracker attached to the chamber to introduce new heteroatoms. We have also begun construction on the second chamber, which will house a cryogenic confocal microscope for performing NV-based surface spectroscopy, and anticipate completion at the end of the calendar year.

There are no publications to report because this is a new award, with a start date of September 1, 2018.

Charge Carrier Space-Charge Dynamics in Complex Materials for Solar Energy Conversion: Multiscale Computation and Simulation

Michel Dupuis

Department of Chemical and Biological Engineering
Computational and Data-Enabled Science and Engineering Program
University at Buffalo, Buffalo USA
mdupuis2@buffalo.edu

Program Scope:

The long term objective of our project is the fundamental characterization of processes and performance of photo-electro-chemical conversion systems in the three phases of ‘light absorption’, ‘carrier transport’, and ‘carrier reactivity’ (Figure 1). Our current efforts focus on ‘carrier transport’, i.e. the modeling of transport of photo-generated electrons and holes in complex crystalline materials for solar energy conversion through combined first principles atomistic computation and mesoscale simulation. To model the space-charge distribution dynamics and activity of charge carriers, we plan to develop original tools for quantum chemical electronic structure computations and of kinetics simulations within a lattice-based Kinetic Monte Carlo framework. We will validate this mesoscale framework with systems for which detailed time-resolved spectroscopy, transport and carrier separation data, and reactivity data are available. The combined modeling has already proven essential for *qualitative* and *quantitative* understanding of how carrier transport affects surface oxidation-reduction activity efficiency.

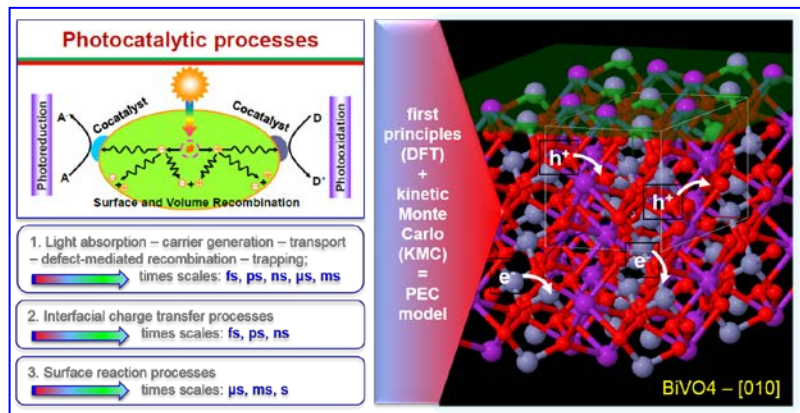


Figure 1. Three phases in solar energy conversion systems. Our project focuses on ‘carrier transport’.

Our overall program deals with timely societal challenges in renewable energy, i.e. the efficient and cost-effective conversion of solar energy to electrical and chemical energies. Current conversion efficiencies, including for solar water splitting, are far from the level needed for practical applications. Our goal is to address how the flow of charge carriers in complex crystalline environments of single phase, multi-phase, and multi-materials semiconductor systems can be tailored to enhance redox reactivity for photo-electro-chemical conversion. This research theme is aligned with BES’ CSGB Division focus areas of ‘charge transport and reactivity’ and ‘chemistry at complex interfaces’.

Our current efforts comprise two thrusts:

a. *Modeling e^-/h^+ carrier dynamics*; the main outcome of this thrust will be the development of a mesoscale Kinetic Monte Carlo (KMC) model informed by first-principles theories to characterize space-charge distribution dynamics. Along the way we will develop original quantum chemical techniques and tools for characterizing carrier transport in single- and multi-

phase crystalline materials. An innovation will be a Marcus/Holstein-like methodology to describe defect-mediated carrier recombination, a key process in loss of efficiency. Targeted systems will be best water oxidation materials, doped and undoped, such as bismuth vanadate BiVO_4 (BVO), tantalum nitride Ta_3N_5 , and other materials, e.g. strontium titanate SrTiO_3 (STO), that exhibit the intriguing phenomenon of *facet selectivity* for oxidation and reduction. One goal will be to establish the theoretical foundation for facet selectivity and homo-junctions, two effective emerging concepts to enhance charge carrier separation and improve solar energy conversion performance.

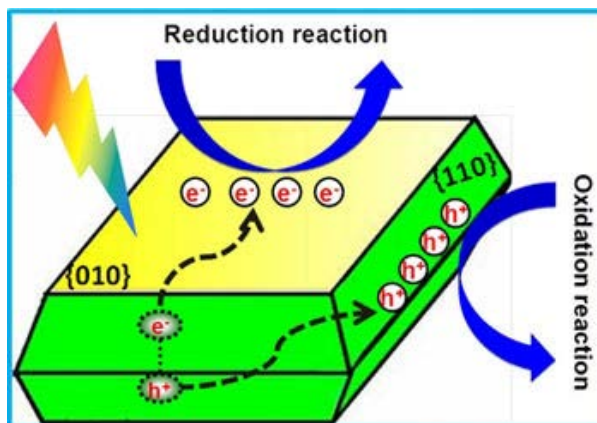


Figure 2. Facet engineering enhances carrier separation and redox reactivity.

b. *Screening photo-active materials*; guided by the dynamics model applied on several classes of materials, we will extract chemical and crystal structural descriptors of good transport and good carrier separation ability to screen materials for improved solar conversion performance.

Recent Progress:

Crystal facet engineering and interface engineering are emerging as highly promising and powerful approaches to enhance carrier separation and overall water splitting efficiency, both for hydrogen evolution and oxygen evolution. At present, synthesis efforts in this field are essentially Edisonian in nature. Our goal is to bring in elements of rational design through computation and simulation.

We recently completed a study of carrier transport in BVO. DFT calculations indicated that thermodynamic stability is not a factor in facet selectivity. An exhaustive characterization of electron and hole hopping pathways in BVO yielded activation energies ~ 0.36 eV for electrons, and, in some cases, much smaller (~ 0.17 eV) for holes. However mesoscale KMC modeling showed that the effective hole mobility is in fact much smaller than what the lower barriers would suggest. The simulations revealed a bi-modal nature of hole transport, with some fast but not transport-efficient hops and some slow but transport-efficient hops. Conductivity in BVO is gated by electron transport.

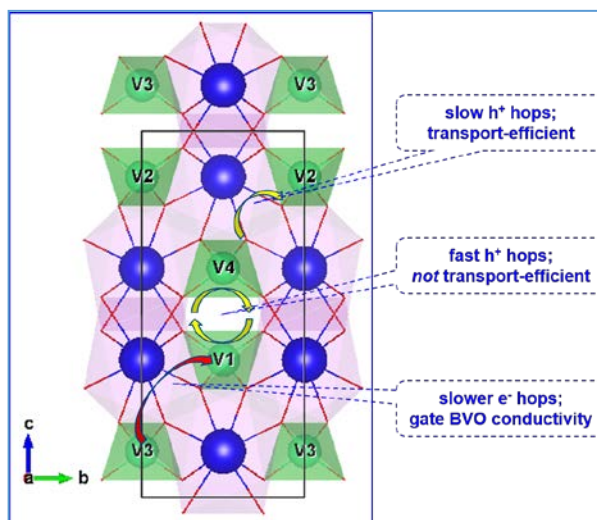


Figure 3. Bimodal h^+ transport in BVO; e^- transport gates BVO conductivity.

These findings illustrate that mesoscale kinetic modeling is essential: it offers a way to capture the critical connection between elementary hopping rates and crystal structure and topology with regard to transport. Interpretations based on elementary hop characterization alone, even if at the quantum level of theory, have the potential to be misleading.

Future Plans:

We are extending this initial work to investigate homo-junctions of layered BVO with a gradient of W/Mo dopant concentrations. Further work will include tunable multi-phase systems such as $(\alpha\text{-}\beta)\text{Ga}_2\text{O}_3$. We also plan to develop methodologies based on accelerated dynamics to replace the Marcus/Holstein approach to computing polaron activation energies, as well as a Marcus/Holstein-like three-state model to describe electron-hole recombination.

CPIMS-sponsored Publications (2016-2018) – There are no publications to report because this is a new award, with a start date of September 15, 2018.

Nanoporous Materials and Ionic Liquids: Dynamics, Structure, and Interactions

Michael D. Fayer

Department of Chemistry, Stanford University, Stanford, CA 94305-5080; fayer@stanford.edu

This program is investigating structural dynamics and intermolecular interactions in complex molecular systems that have mesoscopic structure. In particular, room temperature ionic liquids (RTILs) are being investigated. RTILs are salts that are liquids at room temperature. They are generally composed of complex organic cations and inorganic anions. The complex structure of the cations and anions inhibit crystallization. The cations frequently have long alkyl chains that cause the liquids to segregate into ionic and apolar organic regions, giving the liquids structure on mesoscopic distance scales. In addition, liquids in nanoscopic confinement are being investigated. The liquids include water and RTILs in, e.g., water in the nanochannels of fuel cell membranes or in the pores of hydrogels, RTILs in the pores of polymer membranes in the context of Supported Ionic Liquid Membranes for CO₂ capture. The principal experimental tools for the investigations are ultrafast nonlinear IR methods particularly 2D IR and polarization selective pump-probe experiments (PSPP), fast fluorescence experiments, and optical heterodyne detected optical Kerr effect (OHD-OKE) experiments.

Supported ionic liquid membranes (SILMs) are porous membranes impregnated with ionic liquids (ILs) and used as advanced carbon capture materials. 2D IR and PSPP spectroscopies were used to investigate CO₂ reorientation and spectral diffusion dynamics in SILMs. The SILM contained 1-ethyl-3-methylimidazolium bis(trifluoromethylsulfonyl)imide in the poly(ether sulfone) (PES) membranes with average pore size of ~350 nm. Despite the relatively large pore sizes, the complete orientational randomization of CO₂ and structural fluctuations of the IL (spectral diffusion) in the pores are slower than in the bulk IL by ~2-fold. The implication is that the IL structural change induced by the polymer interface can propagate out from the interface more than a hundred nanometers, influencing the dynamics. This study demonstrates that there are significant differences in the dynamics of ILs in SILMs on a molecular level compared to the bulk IL, and the study of dynamics in SILMs can provide important information for the design of SILMs for CO₂ capture. In addition, the effects of water on the CO₂ and RTIL dynamics in SILMs were investigated because the flue gases from a power plant or other stationary CO₂ sources will contain water vapor. It was found that water speeds up the dynamics in both the SILMs and the bulk RTIL, but the dynamics are still substantially slower in the SILMs.

The structural dynamics of a series of 1-alkyl-3-methylimidazolium bis(trifluoromethylsulfonyl)imide (C_nmimNTf₂, n = 2, 4, 6, 10: ethyl – Emim; butyl – Bmim; hexyl – Hmim; decyl – Dmim) room temperature ionic liquids confined in the pores of PES with an average pore size of ~350 nm and in the bulk liquids were studied. Time correlated single photon counting measurements of the fluorescence of the fluorophore Coumarin 153 (C153) were used to observe the time dependent Stokes shift (solvation dynamics). The solvation dynamics of C153 in the ionic liquids are multiexponential decays. The multiexponential functional form of the decays was confirmed as the slowest decay component of each bulk liquid matches the slowest component of the liquid dynamics measured by OHD-OKE experiments, which is single exponential. The fact that the slowest component of the Stokes shift matches the OHD-OKE data in all four liquids identifies this component of the solvation dynamics as arising from the complete structural randomization of the liquids. Although the pores in the PES membranes are large, confinement on the mesoscopic length scale results in substantial slowing of the dynamics, a factor of ~4, for EmimNTf₂, with the effect decreasing as the chain length increases. By DmimNTf₂, the dynamics are virtually indistinguishable from those in the bulk liquid. The rotation relaxation of C153 in the four bulk liquids was also measured, and showed strong coupling between the C153 probe and its environment.

Proton transfer in the nanoscopic water channels of polyelectrolyte fuel cell membranes was studied using a photoacid, 8-hydroxypyrene-1,3,6-trisulfonic acid sodium salt (HPTS) into the channels. Three fully hydrated membranes, Nafion (DuPont) and two 3M membranes, were studied to determine the impact of different pendant chains and equivalent weights on proton transfer. Fluorescence anisotropy and excited

state population decay data that characterize the local environment of the fluorescent probes and proton transfer dynamics were measured. Measurements of the HPTS protonated and deprotonated fluorescent bands' population decays provided information on the proton transport dynamics. The decay of the protonated band from ~ 0.5 ns to tens of ns is in part determined by dissociation and recombination with the HPTS, providing information on the ability of protons to move in the channels. The dissociation and recombination is manifested as a power law component in the protonated band fluorescence decay. The results show that equivalent weight differences between two 3M membranes resulted in a small difference in proton transfer. However, differences in pendant chain structure did significantly influence the proton transfer ability, with the 3M membranes displaying more facile transfer than Nafion.

Polymeric hydrogels have wide applications including electrophoresis, biocompatible materials, water superadsorbents, and contact lenses. The properties of hydrogels involve the poorly characterized molecular dynamics of water and solutes trapped within the three-dimensional cross-linked polymer networks. Here we apply ultrafast infrared two-dimensional infrared (2D IR) vibrational echo and polarization-selective pump-probe (PSPP) spectroscopies to investigate the ultrafast molecular dynamics of water and a small molecular anion solute, selenocyanate (SeCN^-), in polyacrylamide hydrogels. For all mass concentrations of polymer studied (5% and above), the hydrogen bonding network reorganization (spectral diffusion) dynamics and reorientation dynamics reported by both water and SeCN^- solvated by water are significantly slower than in bulk water. As the polymer mass concentration increases, molecular dynamics in the hydrogels slow further. The magnitudes of the slowing, measured with both water and SeCN^- , are similar. However, the entire hydrogen bonding network of water molecules appear to slow down as a single ensemble, without a difference between the core water population and the interface water population at the polymer-water surface. In contrast, the dissolved SeCN^- do exhibit two-component dynamics, where the major component is assigned to the anions fully solvated in the confined water nanopools. The slower component has a small amplitude which is correlated with the polymer mass concentration, and is assigned to adsorbed anions strongly interacting with the polymer fiber networks.

Many of water's remarkable properties arise from its tendency to form an intricate and robust hydrogen bond network. Understanding the dynamics that govern this network is fundamental to elucidating the behavior of pure water and water in biological and physical systems. In ultrafast nonlinear IR experiments, the accessible time scales are limited by water's rapid vibrational relaxation (1.8 ps for dilute HOD in H_2O), precluding interrogation of slow hydrogen bond evolution in non-bulk systems. Hydrogen bonding dynamics in bulk D_2O were studied from the perspective of the much longer lived (36.2 ps) CN stretch mode of selenocyanate (SeCN^-) using PSPP experiments, 2D IR spectroscopy, and molecular dynamics simulations. The simulations made use of the empirical frequency mapping approach, applied to SeCN^- for the first time. The PSPP experiments and simulations show that the orientational correlation function decays via fast (2.0 ps) restricted angular diffusion (wobbling-in-a-cone) and complete orientational diffusive randomization (4.5 ps). Spectral diffusion, quantified in terms of the frequency-frequency correlation function (FFCF), occurred on two timescales. The initial 0.6 ± 0.1 ps timescale is attributed to small length and angle fluctuations of the hydrogen bonds between water and SeCN^- . The second 1.4 ± 0.2 ps measured timescale, identical to that for HOD in bulk D_2O , reports on the slower collective reorganization of the water hydrogen bond network around the anion. The experiments and simulations provide details of the anion-water hydrogen bonding and demonstrate that SeCN^- is a reliable vibrational probe of the ultrafast spectroscopy of water.

The effects of water concentration and varying alkyl chain length on the dynamics of water in 1-alkyl-3-methylimidazolium tetrafluoroborate RTILs were characterized using 2D IR spectroscopy and PSPP experiments to study the water hydroxyl (OD) stretching mode of dilute HOD in H_2O . Three imidazolium cation alkyl chain lengths, ethyl (Emim^+), butyl (Bmim^+), and decyl (Dmim^+), were investigated. Both the Bmim^+ and Dmim^+ cations have sufficiently long chains that the liquids exhibit polar-apolar segregation, while the Emim^+ ionic liquid has no significant apolar aggregation. While the OD absorption spectra were independent of the chain length, the measured reorientation and spectral diffusion dynamics were chain

length dependent and tend to slow when the alkyl chain is long enough for polar-apolar segregation. As the water concentration is increased, a water-associated water population forms, absorbing in a new spectral region red-shifted from the isolated, anion-associated, water population. Furthermore, the anion-associated water dynamics are accelerated. At sufficiently high water concentrations, water in all the RTILs experiences similar dynamics, the solvent structures having been fluidized by the addition of water. The water concentration at which the dilute water dynamics changes to fluidized dynamics depends on the alkyl chain length, which determines the extent and ordering of the apolar regions. Increases in both water concentration and alkyl chain length serve to modify the ordering of the RTIL, but with opposite and competing effects on the dissolved water dynamics.

Solutions of RTILs and water were studied by observing the reorientational dynamics of the fluorescent probe perylene. Perylene is solvated in the alkyl regions of the RTILs. Its D_{2h} symmetry made it possible to extract dynamical information on both in-plane and out-of-plane reorientation from time resolved fluorescence anisotropy measurements. Perylene reorientation reports on its interactions with the alkyl chains. The RTILs were a series of 1-alkyl-3-methylimidazolium tetrafluoroborates ($C_n\text{mimBF}_4$, where n is the number of carbons in the alkyl chain), and the effects on perylene's dynamics were observed when varying the alkyl chain length of the cation ($n = 4, 6, 8, \text{ and } 10$; butyl, hexyl, octyl, decyl) and varying the water content from pure RTIL to roughly three water molecules per RTIL ion pair. Time correlated single photon counting was used to measure the fluorescence anisotropy decays to determine the orientational dynamics. The friction coefficients for both the in-plane and out-of-plane reorientation were determined to eliminate the influence of changes in viscosity caused by both the addition of water and the different alkyl chain lengths. The friction coefficients provided information on the interactions of the perylene with its alkyl environment and how these interactions changed with chain length and water content. As chain length increased, the addition of water had less of an effect on the local alkyl environment surrounding the perylene. The friction coefficients generally increased with higher water contents; the in-plane orientational motion was hindered significantly more than the out-of-plane motion. The restructuring of the alkyl regions is likely a consequence of a rearrangement of the ionic imidazolium head groups to accommodate partial solvation by water, which results in a change in the arrangement of the alkyl chains. At very high water content, BmimBF_4 broke this general trend, with both in-plane and out-of-plane rotational friction decreasing above a water content of one water per ion pair. This decrease indicates a major reorganization of the overall liquid structure in high water content mixtures. In contrast to BmimBF_4 , the longer chain length RTILs are not infinitely miscible with water, and do not show evidence of a major reorganization before reaching saturation and phase-separating. The results suggest that phase separation in longer chain length BF_4 RTILs is a consequence of their inability to undergo the reorganization of the alkyl regions necessary to accommodate high water concentrations.

The dynamics of the RTIL 1-butyl-3-methylimidazolium bis(trifluoromethylsulfonyl)imide (BmimNTf_2) were investigated with 2D IR spectroscopy and PSPP experiments. The CN stretch frequency of a modified Bmim^+ cation (2- SeCN-Bmim^+), in which a SeCN moiety was substituted onto the C-2 position of the imidazolium ring, was used as a vibrational probe. A major result of the 2D IR experiments is the observation of a long timescale structural spectral diffusion component of 600 ps in addition to short and intermediate timescales similar to those measured for selenocyanate anion (SeCN^-) dissolved in BmimNTf_2 . In contrast to 2- SeCN-Bmim^+ , SeCN^- samples its inhomogeneous linewidth nearly an order of magnitude faster than the complete structural randomization time of neat BmimNTf_2 liquid (870 ± 20 ps) measured with optical heterodyne-detected optical Kerr effect (OHD-OKE) experiments. The orientational correlation function obtained from PSPP experiments on 2- SeCN-Bmim^+ exhibits two periods of restricted angular diffusion (wobbling-in-a-cone) followed by complete orientational randomization on a timescale of 900 ± 20 ps, significantly slower than observed for SeCN^- but identical within experimental error to the complete structural randomization time of BmimNTf_2 . The experiments indicate that 2- SeCN-Bmim^+ is sensitive to local motions of the ionic region that influence the spectral diffusion and reorientation of small, anionic and neutral molecules as well as significantly slower, longer-range fluctuations that are responsible for complete randomization of the liquid structure.

Publications

“Ionic Liquid vs. Li⁺ Aqueous Solutions - Water Dynamics near Bistriflimide Anions,” Chiara H. Giammanco, Patrick L. Kramer, and Michael D. Fayer J. Phys. Chem. B 120, 9997-10009 (2016).

“The Influence of Water on the Alkyl Region Structure in Variable Chain Length Imidazolium-Based Ionic Liquid/Water Mixtures,” Joseph E. Thomaz, Christian M. Lawler, and Michael D. Fayer J. Phys. Chem. B 120, 10350-10357 (2016).

“Water Dynamics in 1-Alkyl-3-Methylimidazolium Tetrafluoroborate Ionic Liquids,” Chiara H. Giammanco, Patrick L. Kramer, Daryl B. Wong, and Michael D. Fayer J. Phys. Chem. B 120, 11523-11538 (2016).

“Dynamics of a Room Temperature Ionic Liquid in Supported Ionic Liquid Membranes vs. the Bulk Liquid: 2D IR and Polarized IR Pump-Probe Experiments,” Jae Yoon Shin, Steven A. Yamada, and Michael D. Fayer J. Am. Chem. Soc. 139, 311-323 (2017).

“Dynamics in a Room Temperature Ionic Liquid from the Cation Perspective: 2D IR Vibrational Echo Spectroscopy,” Steven A. Yamada, Heather E. Bailey, Amr Tamimi, Chunya Li, and Michael D. Fayer J. Am. Chem. Soc. 139, 2408-2420 (2017).

“Dynamics in a Water Interfacial Boundary Layer Investigated with IR Polarization Selective Pump-probe Experiments,” Rongfeng Yuan, Chang Yan, Jun Nishida, Michael D. Fayer J. Phys. Chem. B 121, 4530-4537 (2017)

“Proton Transfer in Perfluorosulfonic Acid Fuel Cell Membranes with Differing Pendant Chains and Equivalent Weights,” Joseph E. Thomaz, Christian M. Lawler, and Michael D. Fayer J. Phys. Chem. B 121, 4544-4553 (2017).

“Water-Anion Hydrogen Bonding Dynamics: Ultrafast IR Experiments and Simulations,” Steven A. Yamada, Ward H. Thompson, and Michael D. Fayer J. Chem. Phys. 146, 234501 (2017).

“Carbon Dioxide in a Supported Ionic Liquid Membrane: Structural and Rotational Dynamics Measured with 2D IR and Pump-Probe Experiments,” Jae Yoon Shin, Steven A. Yamada, and Michael D. Fayer J. Am. Chem. Soc. 139, 11222-11232 (2017).

“Ultrafast to Ultraslow Dynamics of a Monolayer at the Air/Water Interface: 2D IR Spectroscopy,” Chang Yan, Joseph E. Thomaz, Yong-Lei Wang, Jun Nishida, and Michael D. Fayer J. Am. Chem. Soc. 139, 16518-16527 (2017).

“The Influence of Mesoscopic Confinement on the Dynamics of Imidazolium-Based Room Temperature Ionic Liquids in Polyether Sulfone Membranes,” Joseph E. Thomaz, Heather E. Bailey, and Michael D. Fayer J. Chem. Phys. 147, 194502 (2017).

“Influence of Water on Carbon Dioxide and Room Temperature Ionic Liquid Dynamics: Supported Ionic Liquid Membranes vs. the Bulk Liquid,” Jae Yoon Shin, Steven A. Yamada, and Michael D. Fayer J. Phys. Chem. B 122, 2389-2395 (2018).

“Water Dynamics in Polyacrylamide Hydrogels,” Chang Yan, Patrick L. Kramer, Rongfeng Yuan and Michael D. Fayer J. Am. Chem. Soc. 140, 9466-9477 (2018).

“Dynamics and Vibrational Coupling in a Pb-I-SCN Layered Perovskite,” Jun Nishida, John P. Breen, Daiki Umeyama, Hemamala I. Karunadasa, Michael D. Fayer J. Am. Chem. Soc. 140, 9882-9890 (2018).

“Extraordinary Slowing of Structural Dynamics in Thin Films of a Room Temperature Ionic Liquid,” Jun Nishida, John P. Breen, Boning Wu, and Michael D. Fayer ACS Central Science 4, 1065-1073 (2018).

Size Dependence of Liquid-Liquid Phase Separation in Aerosol Particles

Miriam Freedman

Department of Chemistry & Department of Meteorology and Atmospheric Science
205 Chemistry Building, The Pennsylvania State University, University Park, PA 16802
Email: maf43@psu.edu

Program Scope:

The overarching goal of this proposal is to understand how confinement affects phase transitions in particles. We are specifically interested in liquid-liquid phase separation (LLPS) in aerosol particles composed of salts and organic compounds. In these systems, LLPS can occur due to salting out of the organic component, resulting in an organic-rich phase and a salt-rich phase. In experiments, we induce salting out by drying the particles. As the relative humidity surrounding the particles decreases, the salt concentration within the particle increases, driving the phase separation process. We have previously determined that phase separation is inhibited for particle sizes < 50 nm because small particles cannot overcome the activation barrier needed to form a new phase. We focused this initial work on three model systems. Results from these studies have application to understanding myriad processes of aerosol particles in the environment such as heterogeneous chemistry, new particle growth, cloud droplet nucleation, optical properties, etc. At the same time, they have general application to understanding the physical chemistry of this phase transition which results in the formation of an interface within a liquid.

The specific goals of this project are as follows: 1) to extend our initial findings to systems composed of complex mixtures of organic compounds mixed with salts; 2) to investigate LLPS in polymer mixtures to investigate the role of the radius of gyration and the interaction energies on the phase separation behavior; 3) to explore the role of viscosity in the inhibition of phase separation; and 4) to develop experimental phase diagrams for liquid-liquid phase separation as a function of particle size by identifying the approximate location of the binodal curves and the critical point where the binodal and spinodal meet. We have previously captured particles for analysis once phase separation is complete and the particles are dry. We proposed here to capture particles wet and flash freeze them prior to imaging to obtain information on where phase separation occurs as a function of relative humidity. Complementary measurements of surface tension and viscosity of the systems of interest were also proposed. We have currently completed the first year of this grant.

Recent Progress:

Phase Separation in Systems Containing Multiple Organic Compounds and Ammonium Sulfate: We have previously demonstrated that liquid-liquid phase separation is absent at small particle sizes. Our initial systems were succinic acid, pimelic acid, or polyethylene glycol-400 (PEG-400) mixed with ammonium sulfate. In expanding to more complex systems, we observe unexpected behavior. In particular, some of these systems contain three coexisting liquid phases rather than two, in addition to the size dependent morphology. For example, in a system containing only three dicarboxylic acids as well as one containing ten organics with various structures and functional groups, three phases are observed at specific compositions (Fig. 1). Under optical

microscopy, three phases have not been observed for these systems. These results point to a more complex phase diagram for these systems, which we are in the process of mapping. In addition, for some systems, a complex morphology is observed in the dry particles, which has also been seen in the literature on transmission electron microscopy of dried ambient particles. This morphology masks any phase separation. These structures are induced by the solubility difference of the individual compounds within the mixture as well as the salt concentration. We are characterizing the parameters under which these structures are found.

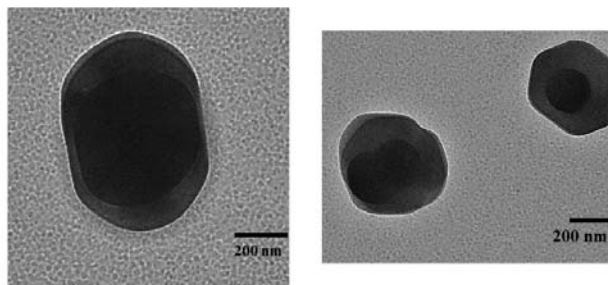


Figure 1. Separation into three phases for a mixture of 10 organic compounds with ammonium sulfate.

Phase Separation in Polymer Nanoparticles: The phase separation of polymers has been studied for decades in many different systems. Our research is unique because we study the phase separation of water-soluble polymers in one dimension through the creation of aerosolized polymer nanoparticles. These experiments can provide insight into the mechanisms behind polymer phase separation and could have potential applications to the energy and medical sciences. The experiments are performed by atomizing aqueous solutions of water-soluble polymers. The particles are dried and impacted on transmission electron microscopy (TEM) grids and imaged using cryo-TEM. The first system studied was polyethylene glycol (PEG) and Dextran, which is a well characterized polymer aqueous two-phase system. Particles composed of PEG-6k and Dextran-10k were found to have a size dependent morphology where particles < 150 nm in diameter are homogeneous and particles > 80 nm in diameter are phase separated. Note that these cutoffs yield three size regimes: only homogeneous particles are found at the smallest diameters, a mixture of homogeneous and phase separated particles are found at intermediate sizes, and only phase separated particles are observed at the largest diameters. The same pattern is seen for PEG-2k/Dextran-10k and PEG-12k/Dextran-10k. For this mixture of polymers, the molecular weight range of PEG was not sufficiently large to observe an effect of changing the radius of gyration or

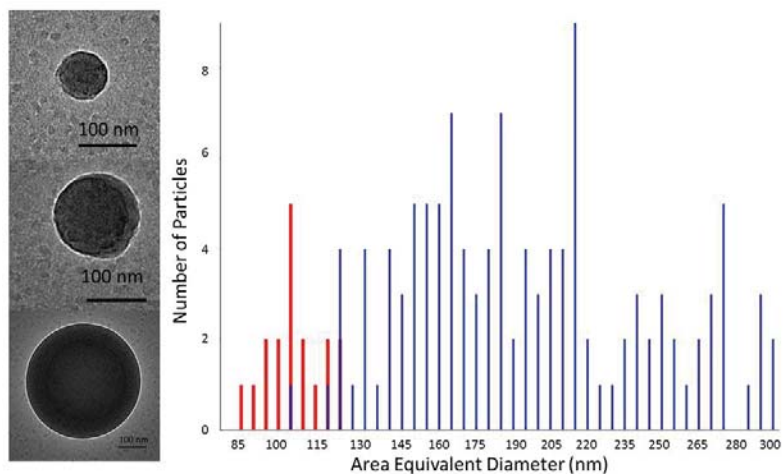


Figure 2. Phase separation behavior of the PVA-145k/PSS-70k system showing TEM images of a small homogeneous particle and two larger phase separated particles and a histogram with homogeneous (red) and phase separated (blue) particles.

the interaction energy χN . In comparison, for polyvinyl alcohol (PVA) and sodium polystyrene sulfonic acid salt (PSS), an effect was observed by changing molecular weight. For PVA-27k and PSS-70k, particles are homogeneous at diameters < 370 nm and phase separated > 220 nm. In comparison, for PVA-145k and PSS-70k, particles are homogeneous at diameters < 125 nm and phase separated at > 100 nm

(Fig. 2). These systems show that region of phase separation can be controlled through changes in the molecular weight, with an increasing molecular weight causing additional phase separation. In this case, we expect that the change in molecular weight of PVA caused an increase in the repulsive interaction of PVA with PSS, causing phase separation to smaller diameters. We have also performed studies of 2-hydroxyethyl cellulose and PEG, which also show a size-dependent morphology. These studies demonstrate that water soluble polymer aqueous two-phase systems have a size dependent morphology when prepared as aerosolized nanoparticles. We are continuing to explore the effect of the interaction energies and the radius of gyration on the phase separation process and size dependence of the morphology.

Fluorescence Recovery After Photobleaching (FRAP): Fluorescence recovery after photobleaching (FRAP) microscopy has been verified as a method to measure viscosity for bulk systems. FRAP was used to find the viscosity of sucrose mixtures at relative humidities from 40-80%. The effect of fluorescent probe concentration was also tested and showed that micromolar concentration does not alter the viscosity of the solution. Thus, studies can be continued at the proposed concentration with relevant organic compounds.

Future Plans:

We are currently working on finishing up the two main projects described above for publication. In addition, the following projects have been started:

Experimentally Constructed Phase Diagrams as a Function of Particle Size: We have built a flow chamber to flash freeze particles at a given relative humidity, deposit them on TEM grids, and image using cryo-TEM. We are currently calibrating the relative humidity within the flow chamber by measuring the efflorescence (crystallization) of several salts. We will then work with a system that phase separates at relative humidities between 70 – 80% in micrometer particles to determine where phase separation occurs as a function of particle size in the submicron regime. The point of phase separation will be determined as the organic:salt composition is varied. An approximation of the critical point will be determined with optical microscopy and confirmed using TEM. Specifically, at the critical point, all particles undergo phase separation rather than having a size dependent morphology. Using this system, we will construct the first experimental phase diagram for LLPS as a function of particle size. We plan to develop a first paper around 2 – 3 systems due to the intensive experiments that will be required.

Effect of Viscosity on Phase Separation: Polymers are being used to study the effect of viscosity on the phase separation of nanoparticles composed of a polymer and an inorganic component (in this case NaCl). These studies follow the same method used to study the phase separation in polymer mixtures. By increasing the molecular weight of the PEG, the viscosity will increase and the effect of viscosity will be studied. Specifically, we are interested in exploring how the diameter below which all particles are homogeneous shifts as the viscosity of the system increases.

Surface Tension Measurements: We have recently begun measurements of bulk surface tensions using a tensiometer. To measure the surface tension of nanometer size particles, we are using a multimode atomic force microscope (AFM). To prepare for these studies, a cover has been

built for the AFM head to ensure that there is minimal contact between the sample and the room air. This cover will allow the relative humidity of the samples to be varied and precisely measured. Specialized tips are used for this measurement. With the AFM setup, we will be able to measure the surface tension of submicron particles as a function of relative humidity.

DOE-Sponsored Publications (since 2017):

D. J. Losey, E.-J. E. Ott, M. A. Freedman, Effects of High Acidity on Phase Transitions of an Organic Aerosol, *Journal of Physical Chemistry A* **2018**, *122*, 3819-3828. doi: 10.1021/acs.jpca.8b00399

Chemical Kinetics and Dynamics at Interfaces
Fundamentals of Solvation under Extreme Conditions

John L. Fulton

Physical Sciences Division
Pacific Northwest National Laboratory
902 Battelle Blvd., Mail Stop K2-57
Richland, WA 99354
john.fulton@pnl.gov

Collaborators: G. K. Schenter, C. J. Mundy, N. Govind, M. Galib.

Program Scope

The primary objective of this project is to describe, on a molecular level, the solvent/solute structure and dynamics in fluids such as water under extremely non-ideal conditions. The scope of studies includes solute–solvent interactions, clustering, ion-pair formation, and hydrogen bonding occurring under extremes of temperature, concentration and pH. The effort entails the use of spectroscopic techniques such as x-ray absorption fine structure (XAFS) spectroscopy, high-energy x-ray scattering, coupled with theoretical methods such as molecular dynamics (MD-XAFS), and electronic structure calculations in order to test and refine structural models of these systems. In total, these methods allow for a comprehensive assessment of solvation and the chemical state of an ion or solute under any condition. The research is answering major scientific questions in areas related to energy, environmental and biological processes including specific areas of relevance to DOE such as mixed hazardous waste processing, power plant chemistry, and geologic carbon dioxide sequestration. This program provides the structural information that is the scientific basis for the chemical thermodynamic data and models in these systems under non-ideal conditions.

Recent Progress

Hydrated structure of Na⁺: The XANES perspective.

The sodium cation (Na⁺) is one of the most common metal ions whose aqueous chemistry plays a crucial role in many geochemical, biochemical and industrial processes. Although the electronic structure is rather simple, the solvation of Na⁺ in water is exceedingly complex due to the delicate balance between ion-water and water-water interactions. In a recent work,³ the Na-O distance in the first solvation shell has been measured with improved precision by both XRD and EXAFS, which has resolved the inconsistency in the Na-O distances reported in the earlier literature (2.38 Å versus 2.44 Å, respectively). A limitation of EXAFS in the case of aqueous Na⁺ is that the photoelectron backscattering of only the water in the first shell can be detected while in contrast the XANES signal for Na⁺ is potentially sensitive to the chemical environment that includes the longer-range interactions. For instance, the Ca K-edge XANES has recently² been used to detect the longer-range structure in solvent-shared ion pairs of Ca²⁺/CO₃²⁻. The Na⁺ K-edge XANES can therefore potentially be used to understand how Na⁺ perturbs the short- and longer-range structure of water.¹

The Na K-edge XANES data (1070.8 eV) were acquired at the Phoenix II, elliptical undulator beamline at the Paul Scherrer Institute (SLS). Measurements were performed in fluorescence mode using a liquid sample cell with a 200 nm thick, Si_3N_4 window. We then used quantum (DFT-based) and classical MD simulations for Na^+ in water to generate structures for the calculation of K-edge XANES spectra for Na^+ solvated by large 35-water clusters using the restricted excitation window time-dependent density functional theory (REW-TDDFT).

To establish the correlations between the local structure and the calculated XANES spectra we evaluated a selection of five suitably-chosen order parameters. Order parameters such as coordination number, hydrogen bond numbers, angular symmetry of the first shell, and the tilt angle of the water have been previously used to describe the local Na^+ structure. Inspired by our own studies¹ on the local structure of water when subject to pressure and the sensitivity of the distribution of interstitial waters to the interaction potential, we introduce the description of the interstitial water molecules between the first- and second shell as an additional order parameter that effectively captures, in a new way, the changes in the local structure of water in the presence of an ion. The interstitial waters are known to play a large role in the understanding of pure water structure, especially when the bulk symmetric structure is perturbed by solute or by applying pressure. If water is seen as a predominately tetrahedral 4-coordinated network, the presence of interstitial waters can be used as a probe for the presence of defects in bulk water or, for instance, defects in the hydration structure about Na^+ .

Overall, the five order parameters included (1) the instantaneous, first-shell Coordination Number (CN) in which the common definition was adjusted to accommodate for each instantaneous configuration, (2) the octahedral order parameter (q_6) that was normalized to give a value of 1 for a perfectly octahedral structure and a value of 0 for a completely disordered system, (3) the number of hydrogen bonds between water molecules in the first and second solvation shell, (4) the tilt angle (θ) defined using the vector between the oxygen and the ion and the water dipole moment, and (5) the new interstitial water parameter (INT_6) for which a value of 0.0 indicates that 6th water is perfectly interstitial while a higher positive value indicates well-separated first and second solvation shells.

Figure 1 compares the experimental Na^+ XANES spectrum to the calculated XANES response to changing 3 of these 5 order parameters. In general, each of these order parameters (CN , q_6 , INT_6) affect the XANES spectrum in different ways. Based upon our prior evaluation of TDDFT XANES for a variety

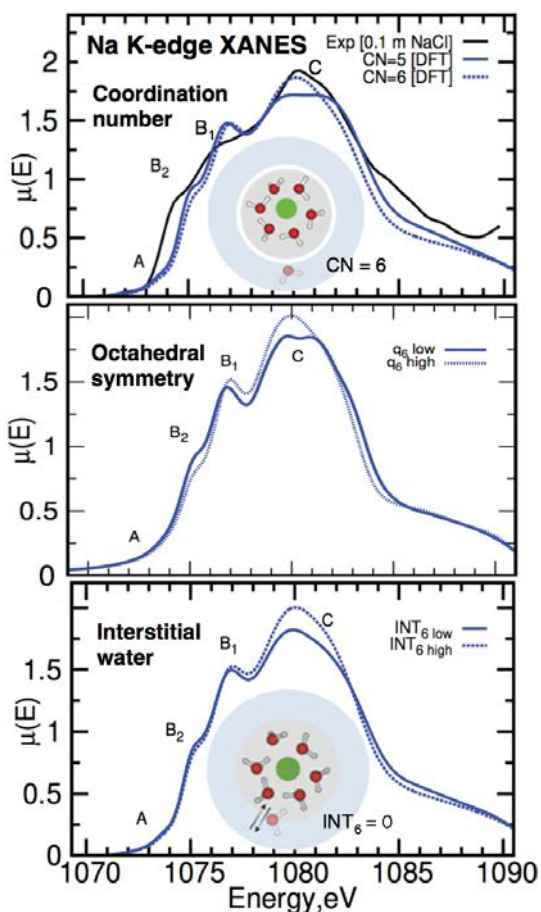


Figure 1. Experimental Na^+ XANES spectrum compared to TDDFT XANES calculations¹ generated from an ensemble of 100 DFT-MD snapshots each containing a 35-water cluster. The effect of three different order parameters (either high- or low-values) on the predicted XANES spectra are shown. Each of the three structural parameters alter the XANES features in different ways.

of different chemical standards, the XANES features have been quantitatively reproduced when the exact molecular configurations are used as input. In Figure 1 (lower panel) the interstitial water parameter (INT_6) significantly affects the XANES spectrum, and demonstrates good sensitivity to this longer-range structure in a way that is different from that of the first-shell order parameters (Figure 1, two upper panels). Results show that the DFT model has much more interstitial character while the classical potential model has mostly separated first and second solvation shells. For both models, more interstitial water moves their calculated XANES spectra closer to the experimental spectrum. The DFT potential, having an explicit electronic structure representation, provides a more realistic model of the interstitial water. A paper summarizing this work¹ will be highlighted as a JCP “Editor's Pick”.

The ion pairing of Cs⁺ with Cl⁻ in concentrated electrolyte.

Concentrated electrolytes have recently emerged as a central interest in various energy storage strategies and for this reason data on the structure of highly concentrated electrolytes is needed. Further, the cation-anion pairing is the starting point for the formation of larger ion clusters that eventually undergo nucleation events leading to the formation nanoparticles or crystals at concentrations above the saturation point. Cs⁺ is the largest ion in the alkali series and as a result it has the weakest hydration shell with the most chaotropic character and the highest potential for ion-pairing. While XRD and ND provide direct structural information on the Cs-Cl ion pair they are hindered by interference from overlapping scattering signals of water-water, water-Cl and water-Cs that are convoluted into a single broad peak. Extended X-ray Absorption Fine Structure (EXAFS) cleanly probes only the radial distribution function around the selected absorber (Cs⁺).

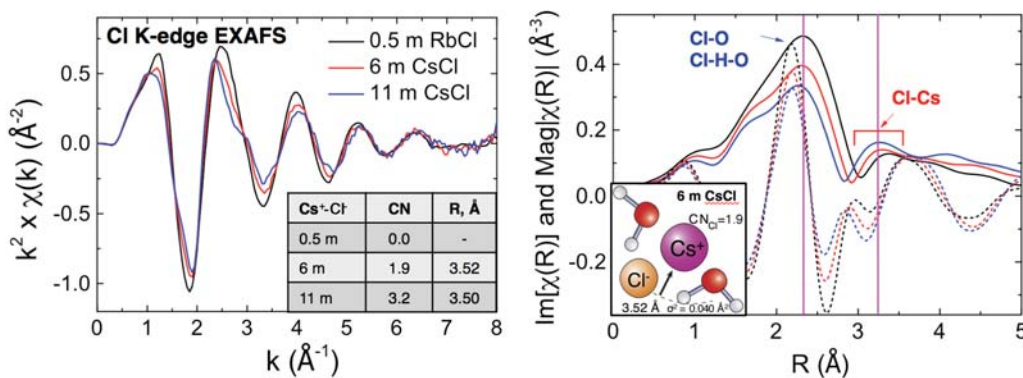


Figure 2. EXAFS spectra for aqueous CsCl solutions up to the saturation point. Tabulated results report the Cs-Cl coordination numbers and Cs-Cl distances for the three different concentrations.

Results for the ion pair structure of aqueous CsCl solutions at 0.5, 6 and 11 mol/kg derived from Cl EXAFS are shown in Figure 2. There is large reduction in the first-shell Cl⁻ waters (7.9 to 5.7 waters) as the concentration is increased from 0.5 to 11 mol/kg. Concurrently, the second peak between 2.7 to 3.5 Å in the R-plot (right panel), increases (from 0 to 3.2 pairs) with increasing concentration consistent with a high degree of Cs⁺/Cl⁻ contact ion pairs in the concentrated solution. The inset of Figure 2 summarizes these details from the simultaneous refinement of EXAFS data for the three solutions.

The Cs⁺ ion, as the largest alkali cation, has the most hydrophobic character allowing a developed water solvent cage having stronger water-water interactions. The weakened Cs⁺-water interaction explains the higher degree of ion-pairing in this aqueous CsCl system.

Future Plans

The objective is to gain a fundamental understanding of the molecular structure that provides the basis for understanding ion chemistry and dynamics. We propose exploring ion-water structure for systems in which the local structure has not yet been measured or the structure is not yet fully understood. Our goal is to identify the underlying structural factors that govern the macroscopic properties of ions that have so far eluded a comprehensive theoretical treatment. The proposed work also involves a comprehensive study of ion pairing in concentrated solutions and at high temperatures. The objective is to describe how the ion-pair structure is governed by a range of different types of solvent interactions.

References to publications of DOE sponsored research (2017 - present)

1. Galib M., G.K. Schenter, C.J. Mundy, N. Govind, and J.L. Fulton. **2018**. "Unraveling the Spectral Signatures of Solvent Ordering in K-edge XANES of Aqueous Na⁺." *Journal of Chemical Physics*. **In press**
2. Henzler K., E. Fetisov, M. Galib, M.D. Baer, B.A. Legg, C. Borca, and J.M. Xto, J. L. Fulton et al. **2018**. "Supersaturated calcium carbonate solutions are classical." *Science Advances* 4, no. 1:eaao6283. doi:10.1126/sciadv.aao6283
3. "Revisiting the hydration structure of aqueous Na⁺", M. Galib, M. D. Baer, L. B. Skinner, C. J. Mundy, T. Huthwelker, G. K. Schenter, C. J. Benmore, N. Govind, J. L. Fulton, **J. Chem. Phys.** 146, 084504, 2017. doi:10.1063/1.4975608
4. Wildman A., E. Martinez Baez, J.L. Fulton, G.K. Schenter, C.I. Pearce, A.E. Clark, and X. Li. **2018**. "Anticorrelated contributions to pre-edge features of aluminate near-edge X-ray absorption spectroscopy in concentrated electrolytes." *Journal of Physical Chemistry Letters* 9, no. 10:2444-2449. doi:10.1021/acs.jpcclett.8b00642
5. Fulton J.L., and T.V. Pham. 2018. "Contact ion-pair structure in concentrated cesium chloride aqueous solutions: an extended X-ray absorption fine structure study." *Journal of Electron Spectroscopy and Related Phenomena*. **In press**
6. Gregory K. Schenter, John L. Fulton, "Molecular Dynamics Simulations and XAFS (MD-XAFS)", In "XAFS Techniques for Catalysts, Nanomaterials, and Surfaces", Yasuhiro Iwasawa, Kiyotaka Asakura, and Mizuki Tada, editors, Springer, New York, Invited Book Chapter, 2017.
7. John C. Linehan, Mahalingam Balasubramanian, John L. Fulton, "Homogeneous catalysis: from metal atoms to small clusters", In "XAFS Techniques for Catalysts, Nanomaterials, and Surfaces", Yasuhiro Iwasawa, Kiyotaka Asakura, and Mizuki Tada, editors, Springer, New York, Invited Book Chapter, 2017.

A cluster approach to understanding solvation effects on ion structure and photochemistry

DE-SC0018902

Etienne Garand

Department of Chemistry, University of Wisconsin-Madison, Madison, WI 53706

egarand@wisc.edu

Program scope

The aim of this proposal is to provide a detailed understanding of solvation effects on the structure and chemistry of molecular ions via spectroscopic interrogation of precisely assembled micro-solvated clusters. Many energy transformation, storage, and transport systems consist of interesting environments that differ from conventional bulk “liquid phase”, such as porous materials with cavity on the nanometer scale. In such environments, chemical behaviors arising from partial solvation and interfaces can play a dominant role in the observed physical characteristics. Even the fundamental chemical properties of a molecule, such as its structure or its acidity, can differ significantly from those found in the isolated molecule or the bulk phase.

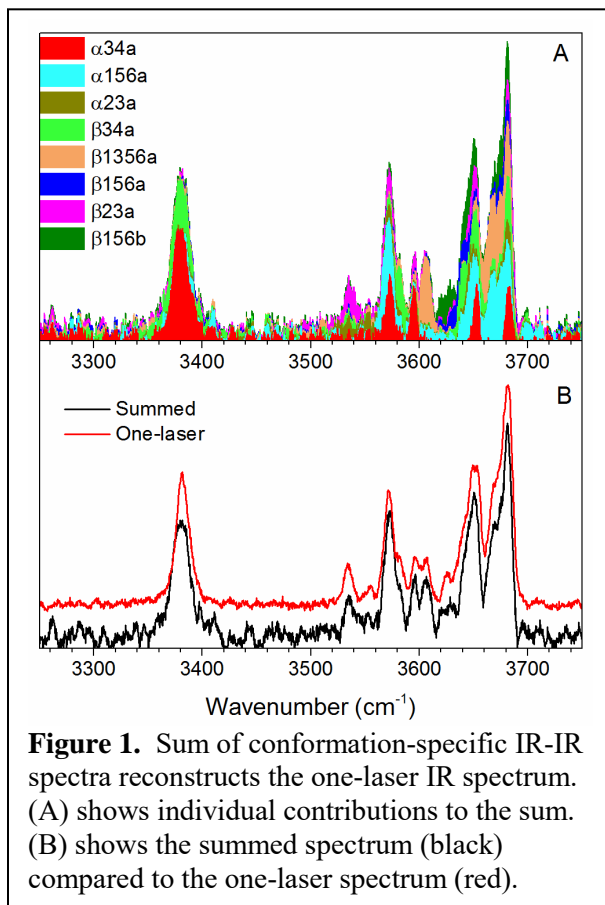
Studies of mass-selected charged clusters are crucial in providing insights into the exact structure of an ion as well as ion-solvent and solvent-solvent interactions. The strength of such mass-selected approach lies in the presence of a well-defined molecular object in which these specific interactions can be highlighted and separated for study. The main challenge here lies in being able to study, at similar levels of detail, clusters with sufficient complexity such that the results from these model systems can be properly translated to condensed phase systems. Recently, experimental progresses made in our lab and others enabled the probing of increasingly complex ionic clusters that are more directly representative of partially solvated ions found at interfaces or of ions present in confined water in nanoscale pores. We recently showed that temperature control in ion traps can be used to efficiently cluster solvent molecules onto almost any ion. Cluster sizes containing up to 50 water molecules can now be readily produced. This unprecedented versatility and cluster size accessibility enables systematic studies of stepwise solvation of illustrative model systems, making it possible for us to build up an in-depth molecular-level understanding of how solvation influence structures via competitive and cooperative interactions. These understandings can then be transferred to more complex systems of various sizes to explain observed phenomena, as these models contain all the basic elements of interactions that are present in the larger systems. Furthermore, results from the proposed studies can serve as crucial benchmarks for theory, where it is still difficult to accurately capture these combinations of non-covalent interactions.

There are several closely interrelated major scientific goals in this proposal. We aim to 1) develop the experimental toolkit necessary to extract molecular structure and non-covalent interaction information from spectroscopy of large solvated ionic clusters. 2) Develop a molecular-based understanding of cooperative and competitive hydrogen-bonding interactions that modulate the conformational space of flexible ions in the presence of water. 3) Understand how the species of the ion can influence the water hydrogen-bonding network surrounding the entire ionic adduct. 4) Probe how photodissociation yield, branching ratio and mechanism can change as a function of the solvation environment around an ionic chromophore.

Recent Progress

With increasing cluster sizes, it quickly became apparent to us that spectral congestions make the analysis and structural determination from the spectral data increasingly difficult. This is illustrated in our studies of $\text{GlyGlyH}^+(\text{H}_2\text{O})_n$ and $[\text{bmim}]^+(\text{H}_2\text{O})_n$ (Ref [1]). Such congestions can stem from the presence of multiple isomers or simply due to the higher density of IR active bands in larger clusters. Therefore, we have implemented two novel experimental approaches to deconvolute spectral complexity present in IR predissociation spectroscopy of weakly bound clusters.

The first approach is an IR-IR two-laser double resonance scheme that can isolate isomer-specific spectral signatures. The details of our IR-IR double resonance implementation are published in Ref [5]. Briefly, our setup has one laser focused directly inside the 10 K tagging trap, while the other functions as a typical predissociation laser. This allows for both an isomer-burning scheme as well as an ion-dip scheme, providing flexibility for tackling different systems of interest. Moreover, the IR-IR spectra correlates closely with the one-laser IR predissociation spectrum acquired using the same instrument, allowing the isomer-specific spectra to tie directly with the overview spectrum. We applied our IR-IR ion-dip double resonance approach to disentangle the vibrational spectrum of $\text{Na}^+(\text{glucose})$, revealing the presence of three α -conformers and five β -conformers, as shown in Figure 1.



The second approach takes advantage of the low-temperature environment in the reaction trap to produce D₂O clusters while preventing H/D exchange with the core ion. When D₂O is introduced at 300 K inside the reaction trap, we observed extensive H/D exchange of the (Gly)₄H⁺ N-H and O-H protons. At 80 K, the results indicate that there is insufficient energy to allow for H/D exchange during the ~10 ms residence time of the ion inside the trap. Our initial spectroscopic results on GlyH⁺(H₂O)_n clusters was published in Ref [6], and the overview spectra are shown in Figure 2. The isotopic substitution allows for the direct identification and separation of the vibrational bands belonging to the ion core from those of the H₂O solvent molecules.

An excellent application of these newly implemented experimental approaches is for the studies of how intermolecular interactions can influence the structures of fluxional molecules, such as a peptide. We first probed the structure of an unsolvated protonated peptide, Gly₃H⁺, detailed in Ref [7]. To accommodate the excess charge, this peptide exists in two distinctly different isomers, revealed via our IR-IR approach. The amine protonated isomer contains an atypical *cis* amide bond as well as a more typical *trans* amide bond. The amide protonated peptide, on the other hand, contains two *trans* amide bonds. Both isomers are found to be the lowest energy structures for their respective protonation site, stabilized by the presence of strong intramolecular hydrogen bonds.

These distinctive gas phase structural characteristics of Gly₃H⁺ immediately beg the question: how many solvent molecules are needed to establish the prevalent solution phase peptide structure? Using IR-IR double resonance and H₂O/D₂O isotopic substitution, we showed that complexation with a single water molecule is already sufficient to yield a global minimum geometry with a protonated amine and all *trans* amide bonds. This result is published in Ref [9]. Based on the experimental results, we further computationally explored possible pathways leading to the observed solvation structure from unsolvated Gly₃H⁺ and found that the solvation energy was sufficient to allow for significant structural changes inside the reaction trap. Our results here suggest that the formation of larger solvated clusters in a cryogenic ion trap can be a viable approach for accessing structures that better represent those found in solution.

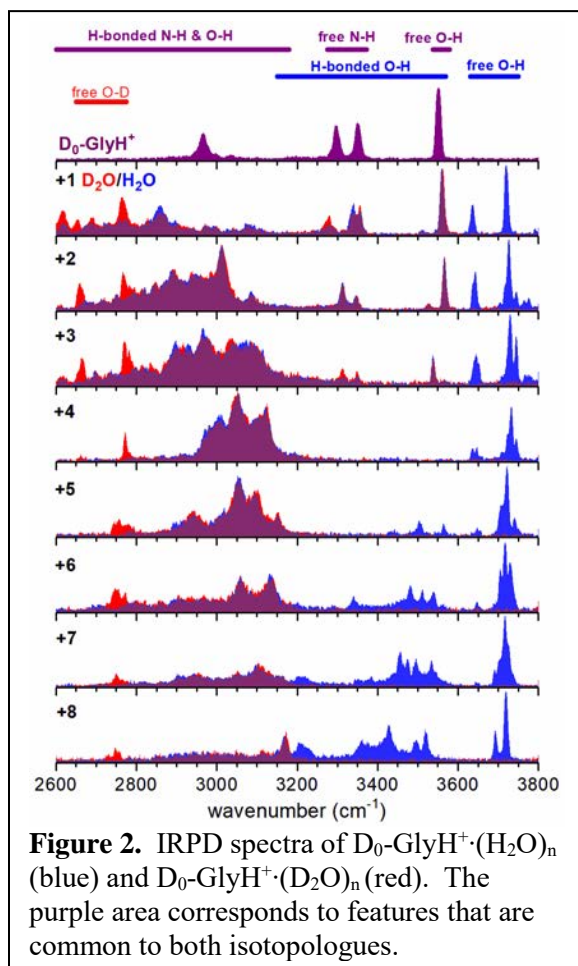


Figure 2. IRPD spectra of D₀-GlyH⁺(H₂O)_n (blue) and D₀-GlyH⁺(D₂O)_n (red). The purple area corresponds to features that are common to both isotopologues.

Future Plans

We are currently working on two major instrumental developments. The first is the addition of two additional reaction traps in series which will enable the synthesis of more complex clusters. The second is the coupling of the reaction trap with an oven source which will enable the formation of clusters with less volatile components. The two next scientific projects involve probing the effects of solvent on the acid-base behaviors of peptides and on the UV photodissociation reaction of conjugated carboxylic acids.

Publications

- 1) J. M. Voss, B. M. Marsh, J. Zhou and E. Garand, *Interaction between ionic liquid cation and water: Infrared predissociation study of [bmim]⁺·(H₂O)_n clusters*, **Phys. Chem. Chem. Phys.**, 18, 18905-18913 (2016)
- 2) S. J. Kregel, G. K. Thurston, J. Zhou and E. Garand, *A multi-plates velocity-map imaging design for high-resolution photoelectron spectroscopy*, **J. Chem. Phys.**, 147, 094201 (2017)
- 3) S. J. Kregel, G. K. Thurston, E. Garand, *Photoelectron spectroscopy of anthracene and fluoranthene radical anions*, **J. Chem. Phys.**, 148, 234306 (2018)
- 4) S. J. Kregel, and E. Garand, *Ground and Low-Lying Excited States of Phenoxy, 1-Naphthoxy and 2-Naphthoxy Radicals via Anion Photoelectron Spectroscopy*, **J. Chem. Phys.**, 149, 074309 (2018)
- 5) J. M. Voss, S. J. Kregel, K. C. Fischer, and E. Garand, *IR-IR conformation specific spectroscopy of Na⁺(Glucose) adducts*, **J. Am. Soc. Mass Spectrom.**, 29, 42-50 (2018)
- 6) J. M. Voss, K. C. Fisher, and E. Garand, *Accessing the vibrational signatures of amino acid ions embedded in water clusters*, **J. Chem. Phys. Lett.**, 9, 2246-2250 (2018)
- 7) J. M. Voss, K. C. Fischer, and E. Garand, *Revealing the structure of isolated peptides: IR-IR predissociation spectroscopy of protonated triglycine isomers*, **J. Mol. Spec.**, 347, 28-34 (2018)
- 8) E. Garand, *Spectroscopy of Reactive Complexes and Solvated Clusters: A Bottom-Up Approach Using Cryogenic Ion Traps*, **J. Phys. Chem. A**, 122, 6479-6490 (2018)
- 9) K.C. Fischer, J. M. Voss, and E. Garand, *Probing the solvation-induced structural changes in conformationally flexible peptides: IR predissociation spectroscopy of Gly₃H⁺(H₂O)*, **J. Phys. Chem. A** (in press)

Methods for addressing strongly heterogeneous and far-from-equilibrium systems

Phillip L. Geissler (plgeissler@lbl.gov),
Teresa Head-Gordon (thg@berkeley.edu), Kranthi Mandadapu (kkmandadapu@lbl.gov), and
Kevin Wilson (krwilson@lbl.gov)

*Lawrence Berkeley National Laboratory, Chemical Sciences Division
1 Cyclotron Road, Berkeley, CA 94720*

Program Scope

A significant gap exists between basic studies of molecular chemical physics and the operation of real devices and natural systems. This effort comprises efforts to establish the chemical methods and insight that will enable understanding of systems that are profoundly complex in composition, heterogeneity, preparation, and organization.

Theoretical and computational aspects of this effort are advanced by Geissler, Head-Gordon, and Mandadapu. Their work aims to provide general techniques for addressing microscopic organization under conditions that profoundly challenge conventional approaches of simulation and analysis. Such behavior typically also presents formidable challenges for experimental measurement. Complementary method development in the laboratory, advanced by Wilson, is thus an important partner to these efforts.

Like theory, experimental advances are needed to develop novel ways for observing reactions in liquids and at their surfaces. In particular, liquids present a substantial challenge for detecting short lived reaction intermediates produced in thermal reactions. Furthermore, in many realistic systems, reactants reside both at the interface as well as the fully coordinated environment of the bulk solution. As laboratory work in other subtasks trends towards systems with slowly relaxing mesoscale disorder, we anticipate growth of the experimental component of this subtask aimed at developing new sample environments and approaches aimed at more robust connections to theory.

Recent Progress

Mandadapu focused on problems related to glassy materials. Dynamical heterogeneity is key to understanding active supercooled liquids on their way to forming inactive glasses. Models of glass formers exhibit an active–inactive dynamical first-order phase transition in trajectory space. Mandadapu studied pre-transition effects in trajectories of a kinetically constrained model of glass formers that exhibits dynamical phase transitions. Analogous to the solvation of hydrophobic solutes in water, “solvating” an inactive region of space–time is governed by a “dynamical interfacial tension”. As a result, two large “solute” effectively attract, in order to minimize the dynamical interfacial free energy.

Mandadapu also studied the nature of the glass transition in atomistic models of glass formers using cooling protocols from a temperature above the onset of glassy dynamics to $T = 0$, which drive the supercooled liquids into a far-from-equilibrium frozen glassy state. Consistent with the kinetically constrained models, it is shown that the relaxation time undergoes a crossover from super-Arrhenius to Arrhenius behavior at a cooling-rate-dependent glass transition temperature.

Head-Gordon performs theoretical studies on strongly heterogeneous and far-from-equilibrium systems such as clay-heavy shales. Anhydrous clays serve as traps for contaminant radionuclides such as Cs-137 that comprise generated nuclear waste and as hosts for vast reserves of fossil methane and shale oil. The mobility of radiocesium in the environment is largely mediated by cation exchange in micaceous clays, in particular illite, a non-swelling clay mineral that naturally contains interlayer K^+ and has high affinity for Cs^+ . Although exchange of interlayer K^+ for Cs^+ is thermodynamically non-selective, recent experiments show that direct, anhydrous Cs^+-K^+ exchange is kinetically viable and leads to the formation of both sharp exchange fronts and phase-separated interlayers (interstratification) through a mechanism that is largely unknown.

Last year we proposed that the sharp exchange fronts arise from a process in which the relaxation dynamics of one of the species induces a metastable phase for the other species, giving rise to a new non-equilibrium idea we have termed “dynamical inversion of the energy landscape” (DIEL).^(1,2) DIEL leads to the observed sharp exchange fronts seen experimentally in illite clays, which cannot be explained by simple diffusion. This year we have developed a clay coarse-grain (ClayCG) model using Iterative Boltzmann Inversion of the all-atom ClayFF model that reproduces features of this proposed feedback mechanism of ion exchange, but with the purpose of understanding the origin of the interstratification of ion species in multiple layers.⁽³⁾ Using ClayCG, we provide evidence that the formation of alternating Cs- and K-illite interlayers (i.e. ordered interstratification) is both thermodynamically and mechanically favorable compared to exchange in adjacent interlayers. Furthermore, contrary to the longstanding theory that ion exchange in a neighboring layer increases the binding of native K in lattice counterion sites leading to interstratification, we find that the presence of neighboring exchanged layers leads to short-range structural relaxations that increase basal spacing and decrease cohesion of the neighboring K-illite layers. This gives more complete insight into the molecular origin of radiocesium mobility.

Geissler is advancing computational techniques that systematically explore the space of dynamical trajectories. Accessing dynamical behavior on time scales much longer than those of basic microscopic motions (say, ps to ns) is a ubiquitous challenge in molecular simulation. A variety of methods have been developed for one-step transformations in relatively simple environments, e.g., elementary chemical reactions in solution. These focus on the existence of a well-defined barrier whose crossing determines long-time dynamics. For much more complex situations that are not dominated by a single barrier, these computational approaches generally fail. From glassy systems to self-assembling nanostructures to systems driven out of equilibrium, examining typical trajectories is a challenge, and examining atypical yet especially informative trajectories is deeply problematic. We are building a new generation of path sampling techniques for this purpose.

Geissler has also adapted path sampling techniques to examine how molecular systems can be driven out of equilibrium with low dissipation. Manipulating chemical kinetics in complex environments, which often feature slow relaxation, essentially requires nonequilibrium driving. Doing so without excessive energy waste is a desirable but highly nontrivial goal. We have formulated a statistical ensemble of driving protocols, biased according to their average dissipation, as a way to explore efficient driving routes and also to quantify their diversity. Analogies with conventional equilibrium ensembles, together with symmetries imposed by the fluctuation theorem, allow a very effective numerical survey of protocols, which we demonstrated in an application that inverts the magnetization of an Ising model. From this survey we identify

which features of time-dependent driving are essential for thermodynamic efficiency and which are unimportant.

Future Plans

Mandadapu plans to study the formation and melting of glasses resulting from cooling protocols or changes in relative humidity. The concept of dynamical interfaces and the associated dynamical interfacial tension will be used to study the formation and melting of glasses in single and multicomponent systems. A theory for nucleation and growth of domains in space–time will be developed by studying two competing factors in the nucleation and growth of a dynamical phase — the dynamical interfacial tension, and the chemical potential difference between the two dynamical phases. This approach will provide microscopic physical mechanisms for glass formation and melting, revealing the existence and size of a critical nucleus in space-time.

While there exist several robust, theoretical interpretations of the temperature or compression-driven glass transition, there is no concrete physical basis for the understanding of glass formation in multi-component systems driven by a change in composition. The prevalent interpretation of mixtures of the viscous materials and water in the literature relies on empirical formulae with no microscopic basis. Mandadapu proposes to develop a physical model for glassy behavior of mixtures, by studying the interplay between dynamical heterogeneity and multicomponent diffusion. The predictions from the model will be tested in experiments performed by Wilson, who has measured the diffusion of water molecules using Raman spectroscopy on levitated droplets of mixtures to ensure rapid mixing times and contactless measurements.

In this next year Head-Gordon plans to explore multi-layer 2D charged interface materials, with control on the inter-plane confinement distances, to simultaneously consider how the sharp ion exchange fronts and interstratification occur dynamically and out-of-equilibrium.

Geissler plans to refine and demonstrate novel path sampling methods, en route to applications involving complex molecular transformations. Model processes will include isomerization of small Lennard-Jones clusters, as well as structural rearrangements within lipid bilayers.

Wilson will work with Saykally and Ahmed to explore a number of rapid mixing approaches that may allow the direct detection of short-lived reaction intermediates in liquid phase chemical reactions. Direct detection of reaction intermediates is an important step in unraveling complex mechanisms in condensed and interfacial systems. Colliding microdroplet reactors currently under development show some promise of achieving very fast inertial mixing times in the microsecond range, which would allow short lived reactive intermediates to be observed directly either by spectroscopy or mass spectrometry. Additionally, we will investigate and quantify the mixing dynamics in colliding "sheet" jets to evaluate whether chemical reactions can be initiated and whether quantitative kinetics can be reliably extracted from the complex mixing dynamics. The use of colliding droplet reactors or liquid "sheets" could allow new studies of condensed phase chemistry using X-ray methods at the Advanced Light Source. Liquid jet sheets have dynamically evolving surfaces, affording the potential to examine the real time evolution of surface chemistry. Additionally, droplets could allow new studies of self-assembly chemistry initiated by surfactant photochemistry at the droplet interface.

Wilson has developed a colliding droplet reactor to measure spontaneous reactions that occur when mixing one reagent with another. The goal of this work is to develop an experimental platform in

which mixing occurs within 1-10 μs and the reaction progress can be monitored using non-time resolved spectroscopic probes. Such rapid mixing allows directly observing transient intermediates needed to better understand aqueous reaction mechanisms.

In the near future we will interface the colliding droplet reactor described above to two main detection methods: Raman Spectroscopy and Mass spectrometry. Each technique gives complementary information about reaction products and intermediates. Once the droplets collide, reaction time and distance become interchangeable kinetic quantities. Thus by measuring Raman or Mass spectra vs. distance fast kinetic timescales can be accessed without needing pulsed lasers. We are building a Raman imaging system to collect spectra vs. distance. Specifically, we will optically couple our colliding droplet reactor with a Princeton Instruments IsoPlane-320 spectrometer. This spectrometer has a zero-astigmatism optical design, allowing high fidelity spectral images as function of distance after the droplets collide and subsequently react.

We will develop new ways of coupling the colliding droplet reactor with atmospheric ionization sources to probe droplet chemistry via mass spectrometry. Under a previous DOE Early Career Award we developed methods for droplet and nanoparticle analysis using electrospray, paperspray and Direct Analysis in Real Time (DART, metastable He^* source) atmospheric ionization mass spectrometry. Here considerable development is needed to collect spectra that preserves the time structure of the droplet train. To do this we propose to use pulsed laser vaporization. An IR laser will be focused to specific locations (e.g. 1 mm or 100 microseconds after the droplet collision) to vaporize the droplet contents for subsequent ionization by DART or electrospray and mass spectrometry analysis. By flash vaporizing the droplets at different distances mass spectra as function of reaction time will be collected during the reaction. We will also explore other non-thermal methods of ionization to evaluate the possible influence of laser heating on the reaction kinetics.

Publications Acknowledging DOE support:

T. R. Gingrich, G.M. Rotskoff, G.E. Crooks, and P.L. Geissler. "Near-optimal protocols in complex nonequilibrium transformations", *Proc. Natl. Acad. Sci. USA* 113, 10263 (2016), doi:10.1073/pnas.1606273113.

G. M. Rotskoff and P. L. Geissler. "Robust nonequilibrium pathways to microcompartment assembly", *Proc Natl Acad Sci USA* 115, 6341 (2018), doi: 10.1073/pnas.1802499115.

L. R. Pestana, K. Kolluri, T. Head-Gordon, and L. Nielsen Lammers (2017). Direct exchange mechanism for interlayer ions in non-swelling clays. *Environ. Sci. & Tech.* 51 (1), 393–400

L. R. Pestana, N. Minnetian, L. Nielsen Lammers, T. Head-Gordon, (2017). Dynamical inversion of the energy landscape promotes non-equilibrium self-assembly of binary mixtures. *RSC Chemical Science*, 9, 1640 - 1646.

K. Schaettle, L. R. Pestana, T. Head-Gordon, L. Nielsen Lammers (2018). A structural coarse-grained model for clays using simple iterative Boltzmann inversion, *J. Chem. Phys.* 148, 222809.

Katira, S.; Garrahan, J. P.; Mandadapu, K. K., Solvation in Space-Time: Pre-transition Effects in Trajectory Space, *Phys. Rev. Lett.* 2018, 120, 260602. DOI:10.1103/PhysRevLett.120.260602

Hudson, A.; Mandadapu, K. K., On the nature of glass transition in atomistic models of glass formers, 2018, arXiv:1804:03769.

Chemical Kinetics and Dynamics at Interfaces

Laser-induced dynamics, reactions and spectroscopy at surfaces

Wayne P. Hess (PI) Alan G. Joly and Patrick Z. El-Khoury

Physical Sciences Division
Pacific Northwest National Laboratory
P.O. Box 999, Mail Stop K8-88,
Richland, WA 99352, USA
wayne.hess@pnnl.gov

Additional collaborators include: Y. Gong, M.T.E. Halliday, D. Hu, A.L. Shluger, P.V. Sushko, V.A. Apkarian, C.J. Cramer, M. Zamkov, A. Tarnovsky, N.D. Browning, R. F. Haglund Jr., P. Abellan, Q.M. Ramasse, I.V. Novikova, A. Bhattarai, G.E. Johnson, J. Laskin, J.E. Evans, E. Aprà, A. Bhattarai, K.T. Crampton, A. Krayev, A. Temiryazev, D. Evplov, C. R. Smallwood, D. L. Hendricks, E. Bylaska, and N. Govind.

Program Scope

The interaction between light, metals, insulators and molecules is fundamentally important in photochemistry, microelectronics, sensor technology, and materials processing. The chemistry and physics of electronically excited solids and surfaces is relevant to the fields of photocatalysis, radiation physics, and solar energy conversion. Irradiation of solid surfaces by UV, or higher energy photons, produces energetic transient species such as core holes and free electrons that subsequently relax to form electron-hole pairs, excitons and plasmons. Specifically, the interaction between light and metal nanostructures can lead to intense field enhancement and strong optical absorption through excitation of surface plasmon polaritons. Such plasmon excitation can be used for a variety of purposes such as ultrasensitive chemical detection, solar energy generation, or to drive chemical reactions. Large electric field enhancements can be localized at particular sites by careful design of nanoscale plasmonic structures. Similar to near field optics, field localization below the diffraction limit can be obtained. Through this field enhancement and localization, surface and tip enhanced Raman spectroscopy (SERS and TERS), capable of single molecule sensitivity, becomes possible. Greater understanding of spectroscopic observables is gained using a combined experiment/theory approach. We therefore use *ab initio* calculations to model results from our SERS and TERS studies. The dynamics of plasmonic excitations is complex and we use finite difference time domain calculations to model field enhancements and optical properties of complex structures including substrate couplings or interactions with dielectric materials.

Approach:

We are developing a combined photoemission electron microscopy (PEEM) and femtosecond laser approach to probe plasmonic nanostructures such as solid metal particles or lithographically produced nanostructures such as gratings, trenches, or nanohole arrays. Finite difference time domain (FDTD) calculations are used to interpret field enhancements measured by the electron and optical techniques. The effects of extreme electric field enhancement on Raman spectra is investigated using plasmonic nanostructures constructed from a metal nanoparticles or metal covered atomic force microscopy (AFM) tips on thin film metal/silica substrates. The Raman scattering from molecules positioned between these structures show greatly enhanced scattering and often highly perturbed spectra depending on nanogap dimensions or whether a conductive junction is created between tip and substrate.

In computational studies we explore non-equilibrium chemical phenomena through *ab initio* molecular dynamics (AIMD)-based Raman spectral simulations. We find that short trajectories, where the accessible phase space is not fully sampled, assist in understanding key features observed in single molecule SERS and TERS measurements. These features, contained in the ensemble-averaged Raman spectrum can be reproduced by averaging several relatively short (3.3 ps) AIMD trajectories. Our results suggest that a complete understanding of single molecule Raman scattering needs to account for molecular conformational flexibility and non-equilibrium chemical phenomena.

Recent Progress

Visualizing surface plasmon polaritons (SPPs) propagation along the metal/dielectric surface requires the use of experimental techniques featuring both high spatial and high temporal resolution. Most existing techniques used to visualize SPPs utilize single-color (degenerate) photon sources. The drawback of such measurements is often that relatively high laser powers are needed to obtain signals from multi-photon photoemission processes, which can result in melting and sample transformation. Information about both spatial and temporal SPP dispersion is often obscured as a result of this requirement. Therefore, processes that enhance the photoelectron yield allow for better imaging sensitivity in experiments and ultimately better signal transmission in plasmonic devices. Time-resolved photoemission electron microscopy (PEEM) images recorded using a combination of ultrafast 800 nm (red) and 400 nm (blue) pulses track surface plasmon polaritons launched from lithographic patterns etched into silver thin films with joint femtosecond temporal and nanometer spatial resolution. The two-color (non-degenerate) scheme is found to significantly enhance the photoelectron yields relative to either nonlinear single-color approach. This enables both enhanced visualization of surface plasmons and more accurate determination of surface plasmon properties compared to single-color measurements. Power dependent photoemission yield measurements reveal that the overall signal is linear with respect to blue excitation, and slightly nonlinear for analogous red excitation. A numerical model based on wave packet propagation reproduces the experimental results and rigorously establishes that the polarization fields from both laser colors and their conjugate surface plasmons account for the observed photoelectron yield enhancement. Tuning the time delay between the red and blue laser pulses allows determination of the group velocity of the blue surface plasmon, in spite of its intrinsically rapid dissipation rate. Numerical analysis of the recorded interference patterns yields a surface plasmon group velocity of $0.70c \pm 0.07c$ at 420 nm.

Plasmonic applications require the ability to launch, focus, and guide SSPs to specific locations. The relative intensities of SPPs simultaneously launched from opposing edges of a symmetric trench structure, etched into a silver thin film, may be controllably varied by tuning the linear polarization of the driving field. This is demonstrated through transient multiphoton PEEM measurements performed using phase-locked femtosecond pulse pairs. Our measurements are rationalized using FDTD simulations, which reveal that the coupling efficiency into SPP modes is inversely proportional to the magnitude of the localized surface plasmon (LSP) fields excited at the trench edges. Additional experiments on single step edges also show asymmetric SPP launching with respect to polarization, analogous to the trench results. Our combined experimental and computational results allude to the interplay between localized and propagating surface plasmon modes in the trench; strong coupling to the localized modes at the edges correlates to weak coupling to the SPP modes. Simultaneous excitation of the electric fields localized at both edges of the trench results in complex interactions between the right- and left-side SPP modes with Fabry-Perot and cylindrical modes. This results in a trench width-dependent SPP intensity ratio using otherwise identical driving fields. A systematic exploration of polarization directed SPP launching from a series of trench structures reveals an optimal SPP contrast ratio of 4.2 using a 500 nm-wide trench.

A square trench structure can be considered an individual element of the toolbox needed for SPP control. The trench structure reveals physical phenomena that are generally neglected in the literature specifically, interplay between LSPs and SPPs. Polarization dependent SPP coupling is a general feature of step edges. For trenches whose edges are separated by a few microns or less, coupling between opposite edges can lead to an increase in SPP launching asymmetry. Similarly, linear polarization may be used to direct SPPs launched from protruded silver spherical cap structures. Experiment and theory reveal that SPP coupling efficiency of spherical caps structures is comparable to conventional etched-in plasmonic coupling structures. Additionally, plasmon propagation direction and coupling using spherical cap structures can be controlled by laser polarization. These results lead directly to application of spherical cap couplers as gate devices. To explain these results we propose a simple geometric model in which the plasmon direction selectivity is proportional to the projection of the linear laser polarization on the surface normal. Overall, our results indicate that protruded cap structures hold great promise as additional elements in the tool-kit for surface plasmon applications.

Future Plans

Future research plans involve fabrication of well-defined plasmonic nanostructures capable of broadcasting the optical response of a single molecule. We stress that nanometric precision in structure is needed to achieve the required local electric fields used for ultrasensitive detection and chemical imaging experiments. This will be achieved through (a) established methods, including modified colloidal syntheses and focused gallium ion beam lithography, and (b) using our state-of-the-art fabrication method of choice for this project, namely helium ion lithography (HIL). All structural motif in these plasmonic constructs consist of interacting nanometric sub-components (e.g. nanometric holes, triangles, rectangles) that cooperatively support optically-accessible LSP resonances. In a recent proof-of-principle application of HIL, we demonstrated that ultrafine plasmonic trenches can be reproducibly etched in metallic thin films. The use of a focused helium ion beam for fabrication will not only afford us plasmonic nanojunctions as fine as a few nm, but will also ensure that the plasmonic properties of the surrounding substrate are not contaminated, e.g., via Ga implantation using standard focused ion beam lithography or by organic contaminants using conventional colloidal sample preparation methods. We now have the tools needed to correlate field enhancement with SERS and TERS response and by adding a two-color photoemission scheme to our PEEM set up, the path opens to an entirely new set of measurements capable of correlating structure and dynamics of a variety of designer plasmonic constructs. These developments will eventually enable us to examine photochemical transformations at the ultimate detection limit of a single molecule in ultrasensitive nanoscale chemical imaging experiments or possibly characterize the atomistic nature of SERS hot spots.

In a similar vein, we will extend our prior work to understand the effect of tailored electromagnetic fields on individual molecules and molecular assemblies. Such comparison will provide insights on emergent behavior in the few molecule and single-molecule regime where the 3D structure (vector components) and absolute magnitude of the local electric field can be inferred from the SERS/TERS spectra/images of carefully selected target molecules. The first step involves engineering and characterizing plasmonic constructs which support LSPs and/or SPPs. The inclusion of HIL into our arsenal now allows sub 10 nm structures to be fabricated enabling correlated femtosecond PEEM with transmission electron microscopy (TEM), tip-enhanced Raman spectroscopy and electron energy loss spectroscopy (EELS). We envision EELS spectroscopy of vibrational and electronic states of molecules adsorbed on such plasmonic metal constructs.

References to publications of DOE BES sponsored research (October 2016 to present)

1. Y. Gong, A. G. Joly, P. Z. El-Khoury, and W. P. Hess, "Enhanced Propagating Surface Plasmon Signal Detection" *ACS Photonics* **3**, 2413 (2016).
2. P. Z. El-Khoury, P. Abellan, Y. Gong, F. S. Hage, J. Cottom, A. G. Joly R. Brydson, Q. M. Ramasse and W. P. Hess, "Visualizing Surface Plasmons with Photons, Photoelectrons, and Electrons", *Analyst* **141**, 3562-3572 (2016).
3. Y. Gong, A. G. Joly, P. Z. El-Khoury, and W. P. Hess "Polarization Directed Surface Plasmon Polariton Launching" *J. Phys. Chem. Lett.* **8**, 49 (2017).
4. S. A. Fischer, E. Aprà, N. Govind, W. P. Hess, and P. Z. El-Khoury, Nonequilibrium Chemical "Effects in Single-Molecule SERS Revealed by Ab Initio Molecular Dynamics Simulations" *J. Phys. Chem. A* **121**, 1344 – 1350 (2017)
5. Y. Gong, A. G. Joly, P. Z. El-Khoury, and W. P. Hess, "Plasmon Coupling and Polarization Control Using Spherical Cap Structures" *J. Phys. Chem. Lett.* **8**, 2695 (2017).
6. I. Novikova, C. R. Smallwood, Y. Gong, D. Hu, L. Hendricks, J. E. Evans, A. Bhattarai, W. P. Hess, P. Z. El-Khoury, "Multimodal hyperspectral optical microscopy" *Chem. Phys.* (2017) **498-499**, 25-32 DOI: 10.1016/j.chemphys.2017.08.011
7. Bhattarai, A.; Joly, A.; Hess, W.; El-Khoury P.Z. "Visualizing Electric Fields at Au(111) Step Edges via Tip-Enhanced Raman Scattering" *Nano Lett.* **17**, 7131-7137 (2017). DOI: 10.1021/acs.nanolett.7b04027
8. A. Bhattarai, A. Krayev, A. Temiryazev, D. Evplov, K.T. Crampton, W.P. Hess, and P.Z. El-Khoury, "Tip-Enhanced Raman Scattering from Nano-Indented Graphene and Graphene Oxide" *Nano Lett.* **18**, 4029-4033, (2018). DOI: 10.1021/acs.nanolett.8b01690
9. A.G. Joly, P.Z. El-Khoury, and W.P. Hess, "Spatiotemporal Imaging of Propagating Surface Plasmons using Two-Color Photoemission Electron Microscopy" *J. Phys. Chem. C* (2018) (ASAP) DOI: 10.1021/acs.jpcc.8b05849
10. E. Apra, A. Bhattarai, K.T. Crampton, E. Bylaska, N. Govind, W.P. Hess, and P.Z. El-Khoury, "Time Domain Simulations of Single Molecule Raman Scattering" *J. Phys. Chem. A* (2018) (ASAP) DOI: 10.1021/acs.jpca.8b05912
11. A.G. Joly, Y. Gong, P.Z. El-Khoury, and W.P. Hess, "Surface Plasmon-Based Pulse Splitter and Polarization Multiplexer" *J. Phys. Chem. Lett.* (submitted August, 2018).

IMPROVED METHODS FOR MODELING FUNCTIONAL TRANSITION METAL COMPOUNDS IN COMPLEX ENVIRONMENTS: GROUND STATES, EXCITED STATES, AND SPECTROSCOPIES

Hrant P. Hratchian (PI, hhratchian@ucmerced.edu), Christine M. Isborn (cisborn@ucmerced.edu), Aurora Pribram-Jones (apribram-jones@ucmerced.edu), Liang Shi (lshi4@ucmerced.edu), and David A. Strubbe (dstrubbe@ucmerced.edu)

University of California, Merced, 5200 N. Lake Rd., Merced, CA 95343

Program Scope. Rapid advances in energy applications require new theory and computational models to provide guidance for interpretation of experimental results and mechanistic understanding. New theory development is necessary to treat systems of increasing complexity, size, and relevance to real applications. Functional transition metal compounds, including molecules, clusters, nanoparticles, surfaces, and solids, provide particular promise for magnetic, optical, and catalytic applications. However, such systems can be exceptionally challenging to model. To make progress in understanding and designing transition metal compounds for energy applications, theory must be able to simulate such systems in complex environments, as well as simulate the spectra of such complex systems to provide direct connections with experiment.

Progress & Future Plans. Leveraging the independent expertise of our team's members, this project will make significant inroads to the theoretical and computational challenges associated with studying transition metal compounds, their reaction chemistry, photophysics and photochemistry, and response to spectroscopic interrogation. In this upcoming first year of the project, team members will begin addressing three central objectives: (1) to develop new electronic ground and excited state methods that will more accurately treat open-shell transition metal compounds; (2) to build models for treating complex environments within ground and excited state calculations; and (3) to implement new theory and methods for simulating modern ultrafast spectroscopies.

The project is focused on developments in chemical computation and theory. Building on the team's track record developing widely used computer programs, new code built as part of this project will be freely available to the research community. Care will be taken to develop intelligent and scalable software capable of handling systems and environments with a broad array of methods and levels of theory. Improved computational efficiency and parallelization will enable calculations at greater length and time scales. Indeed, ccCAT will produce new knowledge and computer programs that will benefit many other groups contributing to the DOE Basic Energy Sciences portfolio.

Publications. There are no publications to report because this is a new award, with a start date of September 1, 2018.

DEVELOPMENT OF APPROACHES TO MODEL EXCITED STATE CHARGE AND ENERGY TRANSFER IN SOLUTION

Christine Isborn¹ (PI), Aurora Clark (co-PI)², Thomas Markland (co-PI)³

1. University of California Merced, Email: cisborn@ucmerced.edu

2. Washington State University, Email: auclark@wsu.edu

3. Stanford University, Email: tmarkland@stanford.edu

The development of next generation energy conversion and catalytic systems requires fundamental understanding of the interplay between photo-excitation and the resulting proton and electron transfer processes that occur in solution. To address these challenges requires accurate and efficient methods to compute ground and excited states, as well as the ability to treat the dynamics of energy transfer in the presence of solvent fluctuations. Our team is developing accurate and efficient theoretical models for solution phase reactions. These developments provide an improved understanding of photo-initiated excitations, electron transfer, and proton coupled electron transfer processes. Our research team brings together expertise in electron and nuclear dynamics (classical and quantum), electronic structure, and analysis of solvation networks. We are developing and validating techniques for modeling condensed phase reactions.

EXCITED STATES IN SOLUTION: One of the goals in our group is accurately modeling absorption spectra in solution. Reproducing experimental condensed phase spectra serves as a good way to validate the ground state sampling of solute-solvent configurations, the ground and excited state methodology, and the importance of what causes spectral broadening, including lifetime and vibronic effects. By gaining a better understanding of which effects are necessary to reproduce absorption spectra, we will know which effects are important for a correct model of condensed phase reactivity. We've explored the accuracy of both the ensemble and Franck-Condon approaches for modeling absorption spectra, and have found that neither approach accurately captures both the full inhomogeneous broadening due to the non-Gaussian solvent distributions along with the vibronic transitions. We have developed a combined approach to model the absorption spectrum of semi-flexible chromophores in solution that includes full sampling of solute-solvent degrees of freedom at the desired temperature using a large QM region for the calculation of vertical excitation energies, and then combines this ensemble sampling with the zero temperature Franck-Condon vibronic shape function to simulate the vibronic contributions to the spectrum at a particular solvent configuration. This combined approach models the full inhomogeneous broadening of the explicit solvent environment and is also able to reproduce the high-energy tail of the spectrum due to vibronic transitions. Our approach with no phenomenological broadening shows

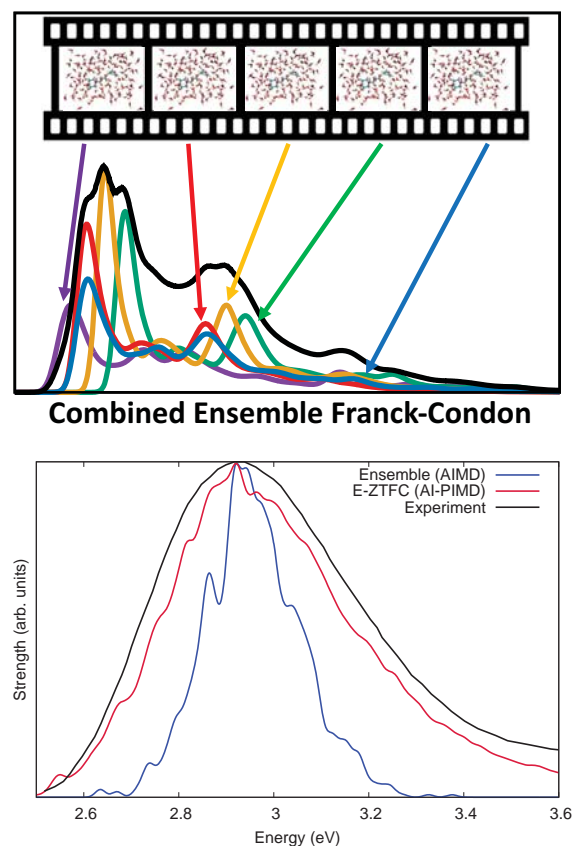


Figure 1: Comparison of the absorption spectra computed from the ensemble approach using AIMD configurations, and from our combined ensemble-zero-temperature Franck-Condon (E-ZTFC) approach using AI-PIMD configurations.

significant improvement in spectral shape compared to the ensemble approach with standard Gaussian broadening (see Figure 1). We are comparing absorption spectra computed from configurations ab initio density functional theory Born-Oppenheimer molecular dynamics (AIMD) that can simulate proton transfer to those including nuclear quantum effects via path integral molecular dynamics (PIMD). Future work includes inclusion of ionic effects and determining the best quantum correction factors for spectra computed from the energy gap autocorrelation function that includes full coupling of solute and solvent degrees of freedom.

ANALYSIS OF PROTON TRANSFER EVENTS IN ACIDIC SOLUTIONS: From path integral molecular dynamics trajectories it is possible to study the shapes of the ring polymers and examine their behavior as a function of different molecular processes. Specifically, we have examined the changes to the topological homology of the ring polymers of hydrogen atoms that are transferred during proton transfer events versus non-reactive hydrogen atoms within solutions of 4M aqueous HCl. Using persistent homology analysis, events that have all beads within the H-atom ring polymer (32 beads) involved in a proton transfer within a 50 fs window were found and their persistent homology compared to H-atoms that did not undergo proton transfer. The Betti numbers were then determined and the Wasserstein distance of the two distributions were compared. As observed in Figure 2, there is significantly more variation in the persistence homologies of the H-atoms that are not undergoing proton transfer relative to those actively transitioning from one eigen/zundel to another. This indicates that the ring polymers actively reacting H-atoms have a more consistent “shape” during the reaction event.

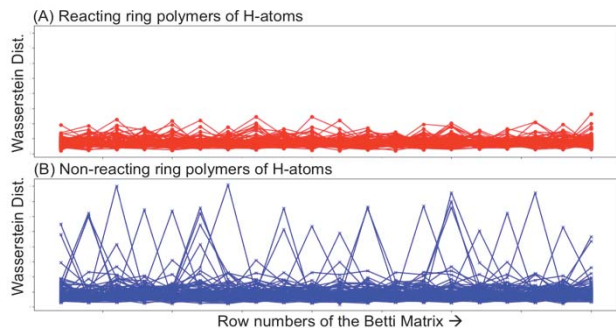
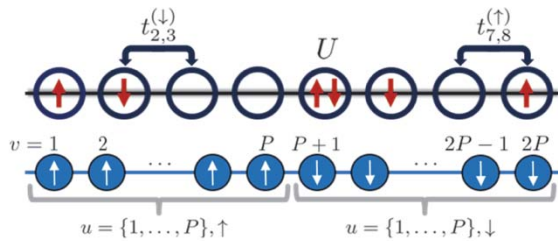


Figure 2: Comparison of the Wasserstein distances from the Betti numbers of the persistent homologies from reacting and non-reacting H-atoms via analysis of their ring-polymer shapes.

EXACT CARTESIAN MAPPING OF FERMIONS FOR INVESTIGATING ELECTRODE PROCESSES: The exact treatment of real time nonadiabatic quantum dynamics in condensed phase chemical systems remains a significant challenge that spurs the ongoing development of approximate methods that are accurate, efficient, and can treat large systems with a wide range of different forms of interactions. Quantum-classical (semiclassical) trajectory-based methods provide some of the most appealing solutions to this problem and offer a hierarchy of approaches with different balances between accuracy and computational cost. We have shown how quantum-classical approaches can be made both more accurate and efficient by combining them with the formally exact quantum master equation framework. This combination of quantum-classical theory and master equation (ME) techniques makes it possible to obtain the accuracy of much more computationally expensive approaches at a cost an order of magnitude lower than even the most efficient trajectory-based approaches, providing the ability to treat the



$$\hat{H} = \sum_u U_u \hat{n}_{\uparrow,u} \hat{n}_{\downarrow,u} + \sum_{u,\lambda} t_{u,u+1}^{(\lambda)} [\hat{c}_{\lambda,u}^\dagger \hat{c}_{\lambda,u+1} + \hat{c}_{\lambda,u+1}^\dagger \hat{c}_{\lambda,u}]$$

$$\text{“} \mapsto \text{”} \sum_u U_u \hat{\eta}_{\uparrow,u} \hat{\eta}_{\downarrow,u} + \frac{1}{2} \sum_{u,\lambda} t_{u,u+1}^{(\lambda)} [\hat{x}_{\lambda,u} \hat{x}_{\lambda,u+1} + \hat{y}_{\lambda,u} \hat{y}_{\lambda,u+1}]$$

Figure 3: Mapping and index ordering for the 1D Hubbard model using our Cartesian mapping approach.

quantum dynamics of atomistic condensed phase systems for long times. Our most recent work has focused on extending the developments of quantum-classical GQME-based dynamics to many-fermion problems where the discrete energy levels are so numerous as to create continua, as is the case for processes near metallic and semiconducting interfaces. To achieve the accuracy benefits from the GQME approach one must have a prescription to generate the initial conditions exactly. In cases where one can write the Hamiltonian in terms of Cartesian positions and momenta, this can usually be achieved straightforwardly using path integral approaches. For Hamiltonians containing discrete states, the Meyer-Miller-Stock-Thoss protocol can be used, however, for those that include fermionic creation and annihilation operators an exact Cartesian mapping has remained elusive. In our recent work, we have therefore derived a rigorous, quantum mechanical map of fermionic creation and annihilation operators to continuous Cartesian variables that exactly reproduces the matrix structure of the many-fermion problem. We have shown how our scheme can be used to map a general many-fermion Hamiltonian and then consider two specific models that encode the fundamental physics of many fermionic systems: the Anderson impurity and Hubbard models. We used these models to demonstrate how efficient mappings of these Hamiltonians can be constructed using a judicious choice of index ordering of the fermions. For example, Figure 3 shows how the 1D Hubbard Hamiltonian can be exactly mapped from its usual form in terms of fermionic creation and annihilation operators to an isomorphic form in terms of Cartesian positions and momenta. Most remarkably in this case, by using an appropriate choice of index ordering, one can eliminate the need to treat the nonlocal operator that imposes the fermionic anticommutivity. This development provides an alternative exact route to calculate the static and dynamical properties of fermionic systems and sets the stage to exploit the quantum-classical and semiclassical hierarchies to systematically derive methods offering a range of accuracies, thus enabling the study of problems where the fermionic degrees of freedom are coupled to complex anharmonic nuclear motion and spins which lie beyond the reach of most currently available methods. These extensions should now allow us to simulate the GQME dynamics using memory kernels generated from a wide variety of quantum-classical approaches for large quantum subsystems coupled to fully atomistic environments. These developments are essential for treating problems such as proton coupled electron transfer in solution and at interfaces.

Award Number DE-SC0014437: Development of Approaches to Model Excited State Charge and Energy Transfer in Solution

Up to Ten Publications Acknowledging this Grant

1. Modeling Absorption Spectra of Molecules in Solution. *T. J. Zuehlsdorff and C. M. Isborn. Int. J. Quant. Chem. e25719. (2018)*
2. Unraveling Electronic Absorption Spectra using Nuclear Quantum Effects: Photoactive Yellow Protein and Green Fluorescent Protein Chromophores in Water. *T. J. Zuehlsdorff, J. Napoli, J. Milanese, T. E. Markland, and C. M. Isborn. J. Chem. Phys., 149, 024107 (2018)*
3. On the exact continuous mapping of fermions. *A. Montoya-Castillo, T. E. Markland. Nature Sci. Rep., 8, 12929 (2018)*
4. The quest for accurate liquid water properties from first principles. *L. R. Pestana, O. Marsalek, T. E. Markland and T. Head-Gordon J. Phys. Chem. Lett., 9, 5009-5016 (2018)*
5. Combining the ensemble and Franck-Condon approaches for calculating spectral shapes of

- molecules in solution. *T. J. Zuehlsdorff and C. M. Isborn. J. Chem. Phys.* 148, 024110 (2018)
6. Nuclear quantum effects enter the mainstream. *T. E. Markland and M. Ceriotti. Nature Rev. Chem.*, 2, 0109 (2018)
 7. Combining Explicit Quantum Solvent with a Polarizable Continuum Model. *M. R. Provorse and C. M. Isborn. J. Phys. Chem. B* 121, 10105-10117 (2017)
 8. Electrostatic control of regioselectivity in Au(I)-catalyzed hydroarylation. *V. M. Lau, W. C. Pfalzgraff, T. E. Markland and M. W. Kanan J. Am. Chem. Soc.*, 139 (11), 4035-4041 (2017)
 9. Convergence of Computed Aqueous Absorption Spectra with Explicit Quantum Mechanical Solvent. *J. M. Milanese, M. R. Provorse, E. Alameda, C. M. Isborn. J. Chem. Theory Comput.* 13, 2159-2171 (2017)
 10. Generalized Quantum Master Equations In and Out of Equilibrium: When Can One Win? *A. Kelly, A. Montoya-Castillo, L. Wang and T. E. Markland, J. Chem. Phys.* 144, 184105 (2016)
 11. Simulating Nuclear and Electronic Quantum Effects in Enzymes. *L. Wang, C. M. Isborn, and T. E. Markland, Methods in Enzymology*, 577, 389-418 (2016)
 12. Unraveling the dynamics and structure of functionalized self-assembled monolayers on gold using 2D IR spectroscopy and MD simulations. *Yan, R. Yuan, W. C. Pfalzgraff, J. Nishida, L. Wang, T. E. Markland, M. D. Fayer, Proc. Natl. Acad. Sci.*, 113 (18), 4929-4934 (2016)

UNMASKING THE MECHANICS OF PROTON DEFECT ACCOMMODATION AND TRANSPORT IN WATER WITH CLUSTER SPECTROSCOPY

DE-FG02-00ER15066 and DE-FG02-06ER15800

Program Managers: Dr. Mark Pederson and Dr. Gregory Fiechtner

K. D. Jordan (jordan@pitt.edu), Dept. of Chemistry, University of Pittsburgh, Pittsburgh, PA 15260

M. A. Johnson (mark.johnson@yale.edu), Dept. of Chemistry, Yale University, New Haven, CT 06520

Program Scope:

Our joint program exploits size-selected clusters as a medium with which to unravel molecular level pictures of key, often transient species in condensed phase and interfacial chemistry. We have intensely focused our recent efforts to unravel the spectral signatures of excess protons in well-defined water networks and to clarify the role of hydrogen bonding in room temperature ionic liquids (ILs). A common theme of our integrated theoretical and experimental programs is that observed spectral behavior very often falls outside the spectroscopy paradigms used to extract structural information about polyatomic molecules. Below we outline several highlights from the past year to illustrate progress in all these areas.

I. Revising the $H^+(H_2O)_{n=2,3}$ systems to understand the strong intermolecular coupling regime

Survey spectra of the $H^+(H_2O)_{n=2-28}$ clusters over the past 15 years have mapped out the large variations in the spectral patterns associated with the excess proton. One curious feature of these band patterns occurs when transitions nominally associated with the OH stretching motions near the center of excess charge approaches the energies associated with the HOH bending motion (in either H_2O or H_3O^+ constituents). This effect is most pronounced in protonated trimer. We therefore carried out a series of experiments to establish the spectra of both $(H^+ \cdot (H_2O)_2)$ and $D^+ \cdot (D_2O)_2$ isotopologues with a newly implemented, two-color IR-IR scheme that eliminates perturbations arising from the usual “tagging” approach to measure vibrational spectra of ions, described in ref. (2). A summary of the data is presented in Fig. 1, which illustrates the need for advanced theory to understand even the qualitative aspects of this system. In this case, full dimensional calculations of the spectra on an accurate potential surface recovered the observed

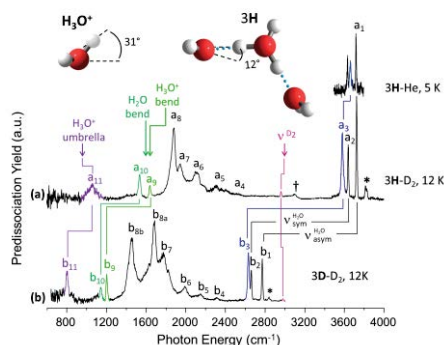


Fig. 1. Vibrational predissociation spectra of (a) $3H-D_2$ and (b) $3D-D_2$ with the free OH region of $3H-He$ on top, where the $3H$ and $3D$ denote the $H^+(H_2O)_3$ and $D^+(D_2O)_3$ isotopologues and $3H-X$ denotes the complexes with $X = He$ or D_2 . Arrows represent the fundamentals of the bare hydronium umbrella (purple) and bending (green) modes as well as the water bending mode (green). $\nu_{sym}^{H_2O}$ and $\nu_{asym}^{H_2O}$ refer to the symmetric and antisymmetric stretches of the OH groups on the flanking water molecules.

trends and indicated that the strong features result from highly mixed states resulting from coupling between bridging proton motion and soft modes that act to break the strong H-bonds to the flanking water molecules. This work was extended to the $\text{H}^+(\text{H}_2\text{O})_4$ system with the resulting manuscript under review at *J. Phys. Chem. A* (ref. 11). Of particular importance in the work on the protonated tetramer is the isolation of the spectral signatures due to a single OH group using another variation of the two-color, IR-IR photoexcitation method.

II. Spectral signatures of single OH oscillators embedded in a three dimensional H-bond network

This past year we have made great progress on the isolation of spectral signatures of single OH groups that are embedded in three dimensional H-bonded networks. This involves introducing a single HDO molecule into the $\text{D}^+(\text{D}_2\text{O})_{20}$ isotopologue. This generates a heterogeneous ensemble of isotopomers based on the location of the single OH group in the pentagonal dodecahedron structure associated with the $\text{H}^+(\text{H}_2\text{O})_{21}$ cluster (inset in Fig. 2). We then acquire the spectrum of this highly diluted OH group in the OH stretching region, indicated in red in Fig. 2. The resulting simplification of the spectrum is dramatic, and will provide a stringent experimental benchmark for theoretical predictions of the structure. Beyond this, however, we have already obtained the first results from isotopomer-selective spectroscopy (using two-color IR-IR photochemical hole burning) to obtain the spectral response of OH groups located at key positions in the PD structure. This information is the first of its kind. For example, these spectra reveal how the homogeneous linewidth of a single OH group evolves across the range of the diffuse OH stretching envelope characteristic of condensed phase water. Comparison of the single OH spectra with that of the $\text{H}^+(\text{H}_2\text{O})_{21}$ isotopologue also provides a direct measurement of the coupling between the two OH groups on the same water molecule when it is embedded in the surface of the clathrate cage.

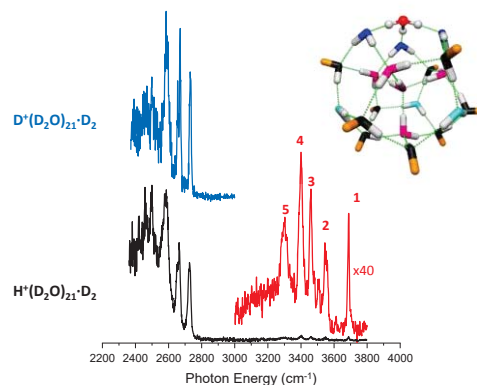


Fig. 2. Vibrational predissociation spectra of D_2 -tagged $\text{D}^+(\text{D}_2\text{O})_{21}$ and $\text{D}^+(\text{D}_2\text{O})_{20}(\text{HDO})$ isotopologues, based on the pentagonal dodecahedron (PD) cage structure in the inset. The expanded region in red highlights the spectrum in the OH stretching region, which results from OH groups residing in various distinct sites in the cage.

III. Characterization of local interactions in functionalized ionic liquids (ILs)

Our expertise in the extraction of structural information from vibrational spectra of H-bonded systems has led to a productive new direction which addresses the role of H-bonding in room temperature ILs. Recent efforts involve the identification of strong, “classical” H-bonds to the $\text{C}_{(2)}\text{H}$ group in imidazole-based (EMIM) ILs through a study of the ternary cationic complexes $(\text{EMIM}^+)_2 \cdot \text{X}^-$. These results were reported in a *J. Chem. Phys. Communication* (ref. 3). We then extended the study to a more complex situation that arises in the functionalization of ILs to tailor their properties. In this case, we engaged a collaboration with Ralf Ludwig’s group in Rostock, which specializes in synthetic manipulations of IL scaffolds. Of particular interest in this regard is their observation that the nominally repulsive cations can undergo a counter-intuitive attractive interaction in hydroxylated derivatives. We identified three isomers in the cationic ternary

complex, one of which adopted such an attractive motif as indicated in Fig. 3. This was reported in *J. Phys. Chem. Letters* (ref. 1), with another manuscript currently under revision (ref. 10).

IV. Adiabatic ID potentials for treating anharmonic effects in ion-water clusters

The OH stretch vibrational spectra of many $X^-(\text{H}_2\text{O})$ clusters display progressions with a spacing of $\sim 75 \text{ cm}^{-1}$. These progressions arise from strong anharmonic coupling between the OH stretch and intermolecular rock vibrations. The large difference between the frequencies of the OH stretch and rock modes allows one to adopt an adiabatic model in which one constructs separate rock potentials for the cluster with zero and one quanta of OH stretch. Fig. 4 reports such adiabatic rock potentials for $\text{HCO}_2^-(\text{H}_2\text{O})$. The lower ($N = 0$) potential was obtained by optimizing at the MP2/aug-cc-pVQZ level the geometry for several values of the rock angle θ and adding the calculated harmonic vibrational zero-point energy (excluding the contribution from the rock mode) at each value of θ . The excited ($N = 1$) potential was then generated by adding, as a function of θ , the calculated harmonic vibrational frequency of one of the OH stretch vibrations. The resulting potential energy curves were fit to sixth-degree polynomials in θ and

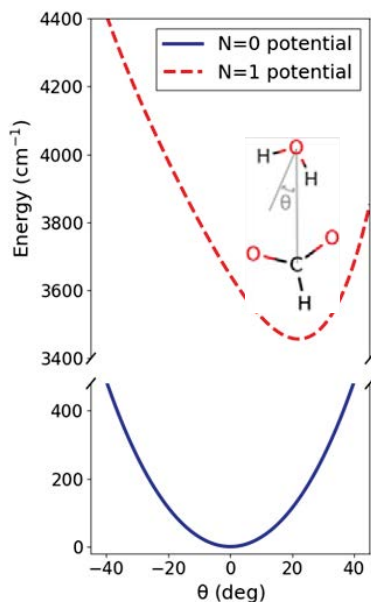


Fig. 4. Adiabatic rock potentials for $\text{HCO}_2^-\cdot\text{H}_2\text{O}$.

V. Plans for the next year

Our primary focus for the next year will be to exploit the new capabilities generated by the two-color, IR-IR measurements of the single OH groups in the protonated $n=21$ water cluster. Most importantly, we intend to leverage our current determinations of the OH signatures of OH occupation in distinct sites to follow the pathways for site-to-site migration as well as

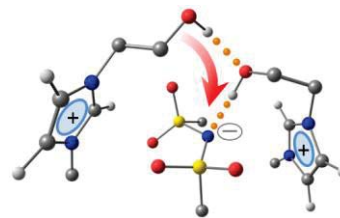


Fig. 3. Schematic structure of the ternary cationic complex formed by the hydroxyl-functionalized EMIM cation with the NTf_2 anion. The attractive interaction between the cations is due to a cooperative H-bonding interaction to the basic N atom in the anion.

the vibrational energy levels associated with the two potentials were calculated by using the Fourier grid DVR method. The spectrum for the $N = 0 \rightarrow 1$ transition was then obtained from the Franck-Condon overlaps between the zero-point level in the rock potential for $N = 0$ stretch and the various levels of the $N = 1$ potential. When the reduced mass is fixed at the value it has at the minimum of the $N = 0$ potential, the resulting vibrational spectrum has spacings of $\sim 125 \text{ cm}^{-1}$ between consecutive members of the progression, much larger than the observed $\sim 73 \text{ cm}^{-1}$ spacings. However, calculations using the Wilson G-matrix procedure show that the reduced mass varies strongly with the rock angle, and when the vibrational spectrum is calculated allowing for this variation of the reduced mass, the resulting spacings are $\sim 75 \text{ cm}^{-1}$, in excellent agreement with experiment. By carrying out calculations with various constraints on the geometrical parameters, it is established that the strong variation of the reduced mass along the θ coordinate is due largely to the increase in the intermonomer separation with growing θ value. This work is described in a paper submitted to the *Journal of Chemical Physics*.^[12]

translocation of the charge defect. This information will yield the first microscopic look at the barriers to proton transport starting from well-defined local structures, as well as the dynamics underlying the diffuse nature of the proton defect in water. We will also continue our work on the local interactions underlying the macroscopic properties of ionic liquids, which is centered around an on-going collaboration with CPIMS colleague James Wishart at BNL.

Papers in the past two years under this grant

1. “Structural Motifs in Cold Ternary Ion Complexes of Hydroxyl-Functionalized Ionic Liquids: Isolating the Role of Cation-Cation Interactions,” F. S Menges, H. Zeng, P. Kelleher, O. Gorlova, M. Johnson, T. Niemann, A. Strate, R. Ludwig, *J. Phys. Chem. Letters*, **9**, 2979–2984 (2018).
2. “Disentangling the complex vibrational spectrum of the protonated water trimer, $H^+(H_2O)_3$ with two-color IR-IR photodissociation of the bare ion and anharmonic VSCF/VCI theory,” C. Duong, O. Gorlova, N. Yang, P. Kelleher, M. A. Johnson, A. B. McCoy, Q. Yu, J. M. Bowman, *J. Phys. Chem. Lett.*, **8**, (2017), pp. 3782–3789
3. “Spectroscopic characterization of a strongly interacting $C_{(2)}H$ group on the $EMIM^+$ cation in the $(EMIM^+)_2X^-$, ($X=BF_4, Cl, Br, \text{ and } I$) ternary building blocks of ionic liquids,” Olga Gorlova, Stephanie M. Craig, and Mark A. Johnson, *J. Chem. Phys. (Communication)*, **147**, (2017), pp. 231101
4. “Spectroscopic Snapshots of the Proton Transfer Mechanism in Water”, C. T. Wolke, J. A. Fournier, L. C. Dzugan, M. R. Fagiani, T. T. Odbadrakh, H. Knorke, K. D. Jordan, A. B. McCoy, K. R. Asmis, and M. A. Johnson, *Science*, **354**, (6316), pp. 1131-1135 (2016).
5. “Characterization of the Primary Hydration Shell of the Hydroxide Ion with H_2 Tagging Vibrational Spectroscopy of the $OH^-(H_2O)_{n=2,3}$ and $OD^-(D_2O)_{n=2,3}$ Clusters”, O. Gorlova, J. W. DePalma, C. T. Wolke, A. Brathwaite, T. T. Odbadrakh, K. D. Jordan, A. B. McCoy, and M. A. Johnson, *J. Chem. Phys.*, *J. Chem. Phys.*, **145**, pp. 134304 (2016).
6. “Gas phase vibrational spectroscopy of the protonated water pentamer: the role of isomers and nuclear quantum effects”, M. R. Fagiani, H. Knorke, T. Esser, N. Heine, C. T. Wolke, S. Gewinner, W. Schöllkopf, M.-P. Gaigeot, R. Spezia, M.A. Johnson, and K.R. Asmis, *Phys. Chem. Chem. Phys.*, **18**, (38), pp. 26743-26754 (2016).
7. “Proton-coupled Electron Transfer in $[Pyridine \bullet (H_2O)_n]^-$, $n = 3, 4$, Clusters”, K. A. Archer, and K. D. Jordan, *Chem. Phys. Lett.*, **661**, 196-199, (2016).
8. “Theoretical Studies of Charged and Neutral Water Clusters”, K. Sen and K. D. Jordan, *Specialist Periodic Reports on Computational Chemistry*, RSC, **13**, 105-131, (2016).

Submitted or currently under review

9. “Tag-Free and Isotopomer-Selective Vibrational Spectroscopy of the Cryogenically Cooled $H_9O_4^+$ Cation with Two-Color, IR-IR Double Resonance: Isolating the Spectral Signature of a Single OH Group in the Hydronium Ion Core,” Chinh H. Duong, Nan Yang, Patrick J. Kelleher, Mark A. Johnson, Ryan J. DiRisio, Anne B. McCoy, Qi Yu, Joel M. Bowman, Bryan V. Henderson, and Kenneth D. Jordan, *J. Phys. Chem. A*
10. “Spectroscopic Evidence for an Attractive Cation-Cation Interaction in Hydroxyl-Functionalized Ionic Liquids: The First H-Bonded Chain-Like Trimer,” T. Nieman, A. Strate, R. Ludwig, H. Zeng, F. Menges, and M. A. Johnson, *Ang. Chem. Int. Ed.*
11. “On the anomalous spectral evolution of the CO stretching bands upon microhydration of the isolated carboxylate anion and $Ca^{2+} \cdot RCO_2^-$ contact ion pair toward those displayed by carboxylic acid monolayers at the air-water interface,” Patrick J. Kelleher, Joanna K. Denton, and Mark A. Johnson, Marcel D. Baer, Shawn M. Kathmann, Christopher J. Mundy, Bethany A. Wellen Rudd, Heather C. Allen, Tae Hoon Choi and Kenneth D. Jordan, *Submitted, J. Phys. Chem. A*
12. “One-Dimensional Adiabatic Models for Calculating Progressions in Vibrational Spectra of Ion-Water Complexes: Application to $HCO_2^-(H_2O)$ ”, Bryan V. Henderson, and Kenneth D. Jordan, *Submitted, J. Chem. Phys.*

Nucleation Chemical Physics

Shawn M. Kathmann
Physical Sciences Division
Pacific Northwest National Laboratory
902 Battelle Blvd.
Mail Stop K1-83
Richland, WA 99352
shawn.kathmann@pnl.gov

Program Scope

The objective of this work is to develop an understanding of the chemical physics governing nucleation. The thermodynamics and kinetics of the embryos of the nucleating phase are important because they have a strong dependence on size, shape and composition and differ significantly from bulk or isolated molecules. The technological need in these areas is to control chemical transformations to produce specific atomic or molecular nanoparticles with specific properties. Computing reaction barriers and understanding condensed phase mechanisms is much more complicated than those in the gas phase because the reactants are surrounded by solvent molecules and the configurations, energy flow, quantum and classical electric fields and potentials, and ground and excited state electronic structure of the entire statistical assembly must be considered.

Recent Progress and Future Directions

Voltage and Field Fluctuations as Crystallization Order Parameters

The observations of luminescence during crystallization as well as electric field induced crystallization suggest that the process of crystallization may not be purely classical but also involves an essential electronic structure component. Strong electric field and/or voltage fluctuations may play an important role in this process by providing the necessary driving force for the observed electronic structure changes. The importance of electric field fluctuations driving electron transfer has been a topic of intense research since the seminal work of Marcus. The main objective of this work is to provide basic understanding of the fluctuations in charge, electric potentials, and electric fields, both classically and quantum mechanically, for concentrated aqueous NaCl electrolytes.

The stability of each ion in a finite cluster depends upon the Madelung voltages of the individual ions, each sensitive to its own crystalline or amorphous environment – see Figure 1, 2 and 4. As the salt clusters approach their ultimate crystal cubic symmetry, they may pass through various non-cubic distorted or amorphous configurations, including the presence of trapped water molecules. Since a unique Madelung potential exists for each stable crystalline polymorph, then the Madelung voltages for each ion

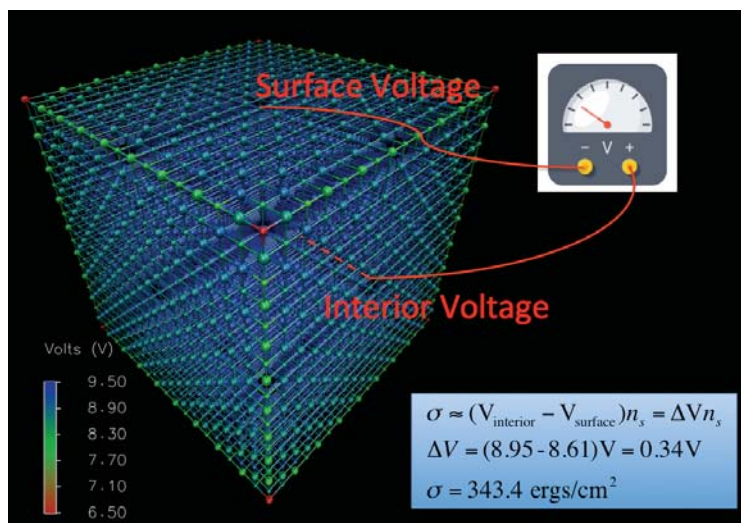


Figure 1. Interfacial surface energy of NaCl (18^3) crystal derived from difference in interior and surface voltages. Interfacial water will lower ΔV to 0.071V yielding an aqueous interfacial surface energy of $\sigma = 67.5 \text{ ergs/cm}^2$.

within a salt cluster may be used as an order parameter (in addition to other order parameters e.g., the distance between ions, the angle between ion triplets, and electric fields at the ion sites) characterizing their progress along various nucleation pathways leading to those polymorphs. Interfacial surface energies can be obtained from differences between interior and surface voltages, including the influence of interfacial water – see Figure 1. Figure 2 shows the progression of Madelung voltages experienced by Na^+ and Cl^- ions due to all other charges within the cubic nanocrystals in a vacuum – large potentials are more stable. By the symmetry of perfect NaCl crystals, the potentials for the Na^+ ions are equal and opposite to Cl^- ions such that the magnitude of both potentials coincide. Conveniently, the size dependent potentials and fields (to be discussed later) can be split into subgroups corresponding to their location in the crystal: interior (*i*), faces (*f*), edges (*e*), and corners (*c*).

Our previous classical molecular dynamics studies of concentrated aqueous NaCl electrolytes showed that the distribution of voltages for all the ions in the solution, including those ions trapped within salt clusters, spanned a broad range that included the bulk Madelung voltages ($\pm 8.95\text{V}$ for ion charges of $\pm 1.0e$). But, in that study we did not separate the voltage distributions between solvated ions and those

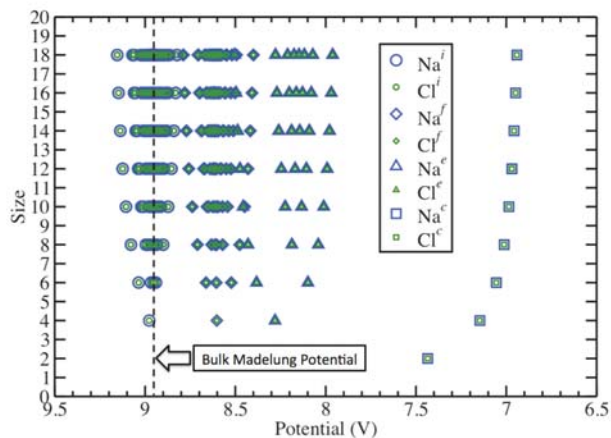


Figure 2. Madelung potentials experienced by ions (Na^+ = blue symbols, Cl^- = green symbols) within even-sized NaCl nanocrystals ($\#$ of ions = Size^3) showing how the electric properties vary with size and subgroup (*i*, *f*, *e*, *c*). Lattice ion-ion distance is 2.81\AA .

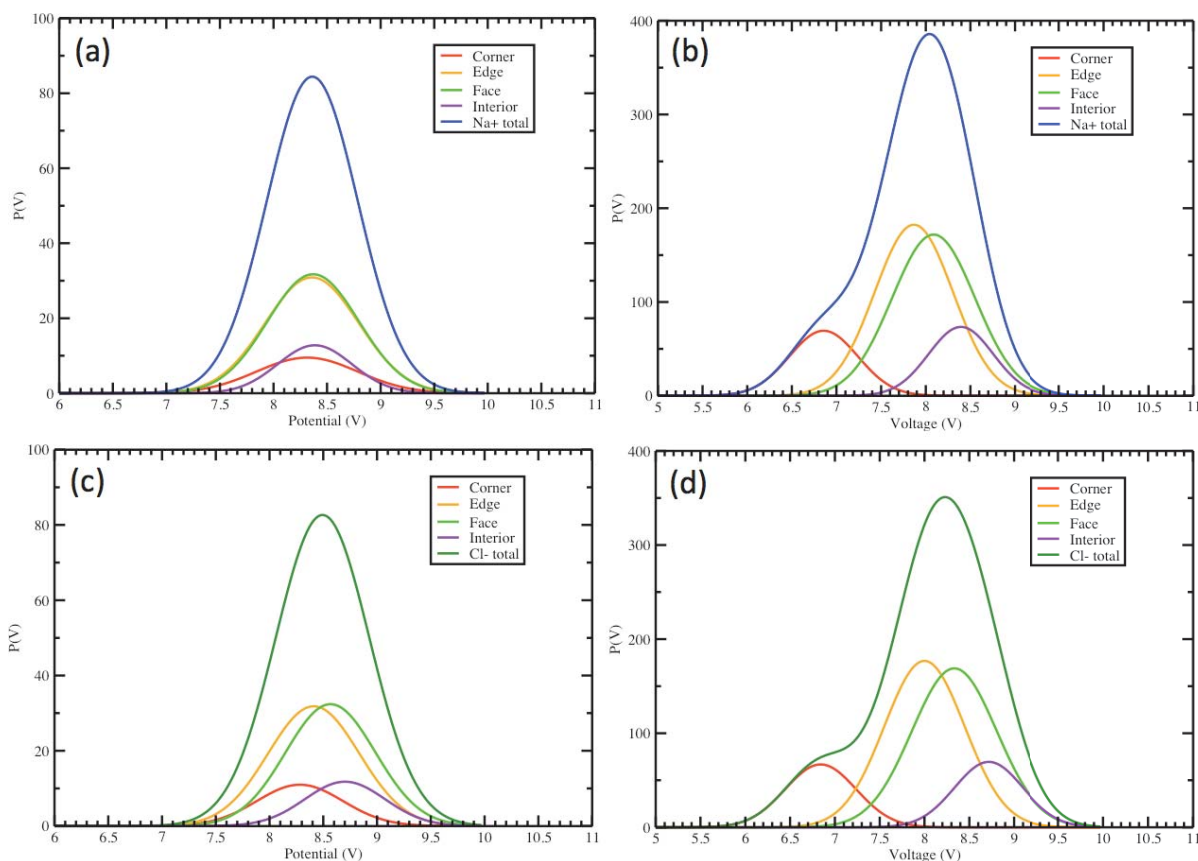


Figure 3. Madelung potentials experienced by ions (Na^+ = blue, Cl^- = green) in a 4^3 NaCl nanocrystal with $[\text{Na}^+(\text{a})$ and $\text{Cl}^-(\text{c})]$ and without $[\text{Na}^+(\text{b})$ and $\text{Cl}^-(\text{d})]$ the influence of the water. The voltage axis is inverted w.r.t. Figure 2.

ions involved in salt clusters. Here we present our results showing how the Madelung voltages are modified for a 4^3 crystal in water taken from a ns trajectory at 300K using the SD + SPC/E interactions. Figure 3 shows the distribution of potentials for Na^+ and Cl^- in water. From these voltage differences we find an aqueous interfacial surface energy of $\sigma = 67.5 \text{ ergs/cm}^2$ including water and an interfacial surface energy of $\sigma = 329.3 \text{ ergs/cm}^2$ without the influence of water. Both of these surface energies compare very well with published simulation and experimental values. Here the water plays a key role in lowering the interfacial surface energy by increasing the voltages on the ions on the crystal faces by 0.35V.

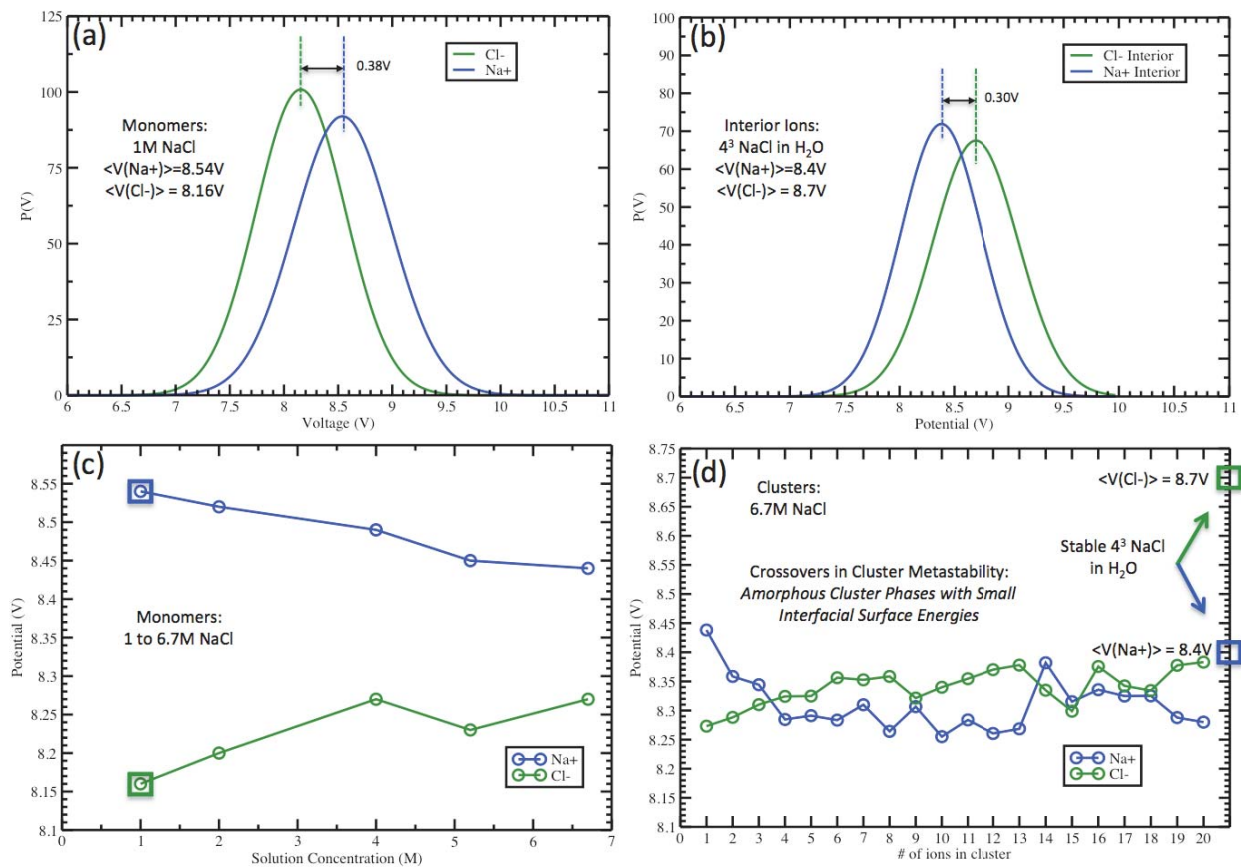


Figure 4. Madelung potentials experienced by ions (Na^+ = blue, Cl^- = green): (a) monomer ions in a 1M NaCl, (b) Interior ions in a 4^3 NaCl nanocrystal in water, (c) monomer ion voltage concentration dependence, and (d) ions in metastable clusters in 6.7M NaCl showing crossover effects compared to a stable 4^3 NaCl nanocrystal in water.

An order parameter, or cluster definition, provides a low-dimensional means of understanding the mechanism of crystallization while differentiating between various amorphous or crystalline pre-critical clusters leading to different nucleation pathways. Furthermore, we anticipate that these order parameters are very sensitive indicators of the structure of salt clusters underlying crystallization.

There is increasing evidence from both simulation and experiment that nanoscale amorphous complexes and phases may play important roles in crystallization. In Figure 4 (a)-(d) we present how the Madelung voltages provide key insights into the metastable pathways leading to crystallization. Fig. 4a shows the voltage distributions for the Na^+ and Cl^- ions in 1M NaCl showing that Na^+ lies at a higher voltage than Cl^- by 0.38V \rightarrow 8.74 kcal/mol. Fig. 4b shows that, in contrast, in a 4^3 NaCl nanocrystal in water the Na^+ lies at a lower voltage than Cl^- by -0.30V \rightarrow -6.9 kcal/mol. Thus, at some intermediate point(s) the voltages experienced by the Na^+ and Cl^- ions must crossover each other. That the ions tend to do so can already be seen in the monomer ions as a function of solution concentration shown in Fig. 4c.

Figure 4d shows the voltages experienced by Na^+ and Cl^- within the clusters in 6.7M NaCl. Clearly, one can see several voltage crossovers as a function of the # of ions in the clusters compared to the voltages experienced by Na^+ and Cl^- ions in the interior of a stable 4^3 NaCl nanocrystal in water. Here, we define clusters to be those ions within a distance of 3.5\AA (i.e., within the 1st peak of the Na-Cl radial distribution function determined from the simulated aqueous electrolytes). Thus, (1) as a function of concentration the ion monomers of Na^+ tend to lower voltages and Cl^- to higher voltages with the Na^+ remaining at a higher voltage than Cl^- , (2) they crossover each other as a function of cluster size, and (3) they finally switch with the Cl^- at a higher voltage than Na^+ in the 4^3 NaCl crystal. A similar crossover between the Na^+ and Cl^- ions is seen in the electric field distributions where Na^+ monomer ions experience stronger fields than Cl^- ions in 1M NaCl by about 0.1 V/\AA whereas in the 4^3 NaCl nanocrystal in water the Cl^- ions experiences a greater field by about 0.1 V/\AA .

Our calculations and analyses provide the first steps toward understanding the magnitude and fluctuations of charge, electric potentials and fields in aqueous electrolytes and what role these fields may play in driving charge redistribution/transfer during crystallization as well as inducing crystal formation itself. Using the Madelung potential and its deviations provide a convenient order parameter to explore various pre-critical amorphous salt clusters and the pathways they take to their ultimate crystalline polymorphs. Moreover, we can use the differences in voltages experienced by the ions in the clusters to quantify the interfacial surface energies to connect with continuum approaches like classical nucleation theory as well as the statistical mechanical formulation of cluster free energies and distribution functions.

It still remains an outstanding challenge to directly connect simulation and experiment. No experiment to date has directly measured the production of critical clusters to yield a true nucleation rate. The particle size distributions relevant to the nucleation event, i.e., those critical clusters being produced as they come over the top of the nucleation barrier, from simulation still remain out of experimental reach. These freshly nucleated particles still need to undergo growth and coagulation to reach the length and times scales probed by conventional laboratory methods. Simulating these processes atomistically quickly becomes computationally intractable. Instead, it is possible to take the particle size distributions relevant to nucleation and model the combined nucleation, growth and coagulation processes through the general dynamic equation. This allows simulators to reach the length and time scales relevant to Small Angle X-ray Scattering (SAXS). On the experimental SAXS side, getting particle size distributions as a function of time suffers from the inverse scattering problem. Current DOE synchrotron X-ray beams as well as the new free electron laser sources of X-rays may be the only way to achieve consistency between measurement and theory of crystallization in condensed phase chemical physics.

Direct PNNL collaborators on this project include G.K. Schenter, C.J. Mundy, S.S. Xantheas, M. Valiev, X. Wang, J. Fulton, L. Dang, and M. Baer and current postdoctoral fellow Evgenii Fetisov. Outside collaborations with Kristian Molhave at the Technical University of Denmark on the connections between electron holography and voltages inside and at the interface of liquid water, Mark Johnson at Yale on connections between electric fields and vibrational spectroscopy have been beneficial.

Acknowledgement: This research was performed in part using the DOE NERSC facility. Battelle operates PNNL for DOE.

Publications of DOE Sponsored Research (2016-present)

C.T. Wolke, J.A. Fournier, E. Miliordos, **S.M. Kathmann**, S.S. Xantheas, and M.A. Johnson, "Isotopomer-selective spectra of a single intact H_2O molecule in the $\text{Cs}^+(\text{D}_2\text{O})_5\text{H}_2\text{O}$ isotopologue: Going beyond pattern recognition to harvest the structural information encoded in vibrational spectra", *Journal of Chemical Physics*, **144**, 074305 (2016).

J.A. Soltis, W.C. Isley III, M. Conroy, **S.M. Kathmann**, E.C. Buck, G.J. Lumetta, "In situ microscopy across scales for the characterization of crystal growth mechanisms: the case of europium oxalate", *CrystEngComm*, **20**, 2822 (2018).

Chemical Kinetics and Dynamics at Interfaces

Structure and Reactivity of Ices, Oxides, and Amorphous Materials

Bruce D. Kay (PI), R. Scott Smith, and Zdenek Dohnálek

Physical Sciences Division
Pacific Northwest National Laboratory
P.O. Box 999, Mail Stop K8-88
Richland, Washington 99352
bruce.kay@pnnl.gov

Collaborators include: G.A. Kimmel, N.G. Petrik, Y. Xu, and C. Yuan

Program Scope

The objective of this program is to examine physiochemical phenomena occurring at the surface and within the bulk of ices, oxides, and amorphous materials. The microscopic details of physisorption, chemisorption, and reactivity of these materials are important to unravel the kinetics and dynamic mechanisms involved in heterogeneous (i.e., gas/liquid) processes. This fundamental research is relevant to solvation and liquid solutions, glasses and deeply supercooled liquids, heterogeneous catalysis, environmental chemistry, and astrochemistry. Our research provides a quantitative understanding of elementary kinetic processes in these complex systems. For example, the reactivity and solvation of polar molecules on ice surfaces play an important role in complicated reaction processes that occur in the environment. These same molecular processes are germane to understanding dissolution, precipitation, and crystallization kinetics in multiphase, multicomponent, complex systems. Amorphous solid water (ASW) is of special importance for many reasons, including the open question over its applicability as a model for liquid water, and fundamental interest in the properties of glassy materials. In addition to the properties of ASW itself, understanding the intermolecular interactions between ASW and an adsorbate is important in such diverse areas as solvation in aqueous solutions, cryobiology, and desorption phenomena in cometary and interstellar ices. Metal oxides are often used as catalysts or as supports for catalysts, making the interaction of adsorbates with their surfaces of much interest. Additionally, oxide interfaces are important in the subsurface environment; specifically, molecular-level interactions at mineral surfaces are responsible for the transport and reactivity of subsurface contaminants. Thus, detailed molecular-level studies are germane to DOE programs in environmental restoration, waste processing, and contaminant fate/transport.

Our approach is to use molecular beams to synthesize “chemically tailored” nanoscale films as model systems to study ices, amorphous materials, supercooled liquids, and metal oxides. In addition to their utility as a synthetic tool, molecular beams are ideally suited for investigating the heterogeneous chemical properties of these novel films. Modulated molecular beam techniques enable us to determine adsorption, diffusion, sequestration, reaction, and desorption kinetics in real-time. In support of the experimental studies, kinetic modeling and simulation techniques are used to analyze and interpret the experimental data.

Recently, in collaboration with Greg Kimmel, we have developed a pulsed laser heating method to investigate deeply supercooled liquids by producing transiently heated films, which become liquids that last for approximately 10 ns per laser pulse. Subsequent rapid cooling due to the dissipation of the heat pulse into the metal substrate effectively quenches the liquid dynamics until the next laser heating pulse arrives. The rapid heating and cooling allows the system to reach previously unattainable supercooled liquid temperatures and return to the amorphous state before significant crystallization can occur.

Recent Progress and Future Directions

Desorption of benzene, 1,3,5-trifluorobenzene, and hexafluorobenzene from a graphene surface: The effect of lateral interactions on the desorption kinetics Understanding the interactions and behavior of adsorbates on graphene substrates is important in a number of areas including catalysis, material science, and astrophysics. The adsorption of aromatic molecules on graphene is of particular interest as a model system to benchmark calculations of van der Waals interactions. These weak interactions are now believed to play an important role in biological systems.

We have previously measured the desorption kinetics and interaction energies for a number of adsorbates on graphene-covered Pt(111). The adsorbates include water, methanol, ethanol, Ar, Kr, Xe, N₂, O₂, CO, methane, ethane, propane, benzene, and cyclohexane. For all, except for benzene, the submonolayer desorption spectra are aligned on a common curve, which is the signature of zero-order desorption kinetics. Surprisingly, for benzene, the submonolayer desorption kinetics are first-order. One explanation for the difference could be that most of the adsorbates listed above are small compared to benzene. However, cyclohexane also exhibits zero-order desorption, and therefore, molecular size cannot be the explanation for the differences in the desorption kinetics. One property of benzene that stands out is its relatively large quadrupole moment ($-33.3 \times 10^{-40} \text{ C m}^2$), which has an absolute magnitude that is more than 10 times larger than that of cyclohexane ($3.0 \times 10^{-40} \text{ C m}^2$). In particular, the polar C–H bonds result in benzene having a partial positive charge around the ring of the molecule. This means that lateral interactions between coplanar benzene molecules are likely repulsive, or at least less attractive than those for cyclohexane. Lateral adsorbate interactions play a key role in determining the desorption order. Submonolayer zero-order desorption kinetics can occur if the adsorbates form two-dimensional islands that are in equilibrium with individual adsorbates diffusing on the surface. The coexistence of the two phases (islands and individual adsorbates) establishes the chemical potential of the system. If equilibrium is maintained during the desorption process, the chemical potential sets the vapor pressure of the system and hence the desorption rate. Thus, the desorption rate will depend only on temperature regardless of the coverage, which is the definition of zero-order desorption.

In a recent paper (6), we compared the desorption kinetics of benzene, 1,3,5 tri-fluorobenzene (TFB), and hexafluorobenzene (HFB) to test the hypothesis that the desorption kinetic order is correlated with the quadrupole moment. The three molecules have nearly the same molecular shape (e.g., all are planar and similarly sized) but have quadrupole moments that range from large and negative for benzene (-33.3) to relatively small for TFB (3.31) and to large and positive for HFB (31.7) (all in units of 10^{-40} C m^2). Thus, these molecules are an ideal set to test the effects of the quadrupole moment on the desorption kinetics.

The temperature programmed desorption spectra for all three species have well-resolved monolayer and second-layer desorption peaks. The desorption spectra for submonolayer coverages of benzene and HFB are consistent with first-order desorption kinetics. In contrast, the submonolayer TPD spectra for TFB align on a common leading-edge, which is indicative of zero-order desorption kinetics. The observed desorption behavior is clearly correlated with the magnitude of the quadrupole moment. The molecules with first-order desorption kinetics (benzene and HFB) have quadrupole moments that are about a factor of 10 larger than the value for TFB. To understand the relationship between the desorption order and the quadrupole moment, one must also take into account how molecular orientation affects adsorbate–adsorbate interactions. Calculations show that the three aromatic molecules studied here lie flat, parallel to the graphene surface. Calculations (second-order Møller-Plesset perturbation and density functional

theory) were done to determine the adsorbate lateral interaction energies. The results show that the potential minimum for coplanar TFB dimers is more than a factor of two greater than that for either benzene or HFB dimers. The calculations support the interpretation that benzene and HFB are less likely to form the two-dimensional islands that are needed for submonolayer zero-order desorption kinetics. The results here illustrate the importance of lateral interactions in systems where the aromatic molecules are constrained and/or on surfaces and also provide theorists with experimental results to test calculations of adsorbates on graphene. Future work will continue to explore more sophisticated systems such as those that include multiple interacting adsorbates on a graphene substrate.

Proton exchange in low temperature co-mixed amorphous H₂O and D₂O films: The effect of the underlying Pt(111) and graphene substrates Proton exchange and mobility are of great importance in a wide range of scientific research areas including astrochemistry, biology, and fuel cell technology, to name a few. The transport of H⁺ ions through solution, membranes, or ices is a critical step underlying many of these processes. The transport of protons has long been described by a Grotthuss or “structural” diffusion mechanism where a proton is passed between adjacent water molecules in a series of hops. The H/D exchange process is thought to occur via a two-step mechanism which involves a proton transfer (hop) followed by the migration of a Bjerrum L defect (turn). Bjerrum defects, also known as orientational defects, are the places where the intermolecular hydrogen bonding is “defective”, where either a hydrogen atom is missing between oxygens (L defect) or where there are two hydrogens (D defect).

In a recent paper (7), in collaboration with Greg Kimmel and Nikolay Petrik, we studied isotopic exchange reactions in mixed D₂O and H₂O amorphous solid water (ASW) films using reflection absorption infrared spectroscopy. Nanoscale films composed of 5% D₂O in H₂O were deposited on Pt(111) and graphene covered Pt(111) substrates. At 130 K, we find that the reaction is strongly dependent on the substrate with the H/D exchange being significantly more rapid on the Pt(111) surface than on graphene. At 140 K, the films eventually crystallize with the final products on the two substrates being primarily HOD on Pt(111) and a mixture of HOD and unreacted D₂O on graphene. The difference in the extent of proton exchange in the co-dosed films could be due to differences in the reactivity of the Pt(111) and graphene surfaces themselves. By pre-dosing H₂ and O₂ on Pt(111) we find that the observed differences in reactivity on the two substrates are likely due to the formation of hydrogen ions at the Pt(111) surface that are not formed on graphene. Once formed the mobile protons move rapidly through the ASW overlayer driving the H/D exchange reaction. Future work will focus on quantifying various aspects of the H/D exchange reaction kinetics and energetics.

Homogeneous Nucleation of Ice in Transiently-Heated, Supercooled Liquid Water Films Understanding ice nucleation in supercooled liquid water is one of the most common and important processes occurring on Earth. However, our understanding of fundamental aspects of ice nucleation, such as the maximum rate of nucleation, the temperature at which this maximum occurs, and the size and initial morphology of the ice nuclei, is still incomplete. Developing a detailed understanding of ice nucleation is impeded by the existence of “no man’s land,” the temperature range from approximately 160 to 230 K in which spontaneous crystallization occurs too fast for most experimental techniques to observe. It is also challenging for molecular dynamics simulations to study ice nucleation due to the low probabilities for forming ice nuclei and the large number of possible molecular configurations. Working in collaboration with Greg Kimmel and Nikolay Petrik we have developed a nanosecond pulsed-laser–heating technique to circumvent the rapid crystallization of supercooled liquid water that occurs between 180 and 262 K. Our approach

is to transiently heat compositionally tailored nanoscale films to the temperature of interest for a brief time (~10 nanoseconds) followed by rapid cooling back to the pre-laser pulse temperature effectively “freezing” the kinetics. Processes that occur at these elevated temperatures are followed via a post-mortem analysis using infrared reflection-absorption spectroscopy (IRAS) and other surface spectroscopic techniques.

In recent work (4), we used this method to investigate the nucleation and growth of crystalline ice in transiently heated water films that are 0.24 μm thick. By varying the temperature distributions within these films, it is possible to control the location within the films where the ice nucleates and grows. In particular, it is possible to suppress nucleation at the water/metal and water/vacuum interfaces and thus measure the homogeneous nucleation rate in the water films. Analysis of the results shows that homogeneous nucleation rates of at least $10^{26} \text{ m}^{-3} \text{ s}^{-1}$ in the temperature range from ~210–225 K are needed to account for our observations. Experiments at lower overall temperatures, where heterogeneous nucleation at the water/metal interface was possible, suggest that the homogeneous nucleation rate is $\sim 10^{29\pm 2} \text{ m}^{-3} \text{ s}^{-1}$. Future work will focus on refining these measurements and exploring other deeply supercooled liquids in regions of the phase diagram that were previously inaccessible due to rapid crystallization.

References to Publications of DOE sponsored Research (October 2016 - present)

- (1) Yuan, C. Q.; Smith, R. S.; Kay, B. D. Surface and Bulk Crystallization of Amorphous Solid Water Films: Confirmation of "Top-Down" Crystallization. *Surf. Sci.* **2016**, *652*, 350-354.
- (2) Xu, Y. T.; Petrik, N. G.; Smith, S.; Kay, B. D.; Kimmel, G. A. Growth Rate of Crystalline Ice and the Diffusivity of Supercooled Water from 126 to 262 K. *Proc. Natl. Acad. Sci. U. S. A.* **2016**, *113*, 14921-14925.
- (3) Yuan, C. Q.; Smith, R. S.; Kay, B. D. Communication: Distinguishing between Bulk and Interface-Enhanced Crystallization in Nanoscale Films of Amorphous Solid Water. *J. Chem. Phys.* **2017**, *146*, 031102.
- (4) Xu, Y. T.; Petrik, N. G.; Smith, R. S.; Kay, B. D.; Kimmel, G. A. Homogeneous Nucleation of Ice in Transiently-Heated, Supercooled Liquid Water Films. *J. Phys. Chem. Lett.* **2017**, *8*, 5736-5743.
- (5) Smith, R. S.; Kay, B. D. Desorption Kinetics of Benzene and Cyclohexane from a Graphene Surface. *J. Phys. Chem. B* **2018**, *122*, 587-594.
- (6) Smith, R. S.; Kay, B. D. Desorption of Benzene, 1,3,5-Trifluorobenzene, and Hexafluorobenzene from a Graphene Surface: The Effect of Lateral Interactions on the Desorption Kinetics. *J. Phys. Chem. Lett.* **2018**, *9*, 2632-2638.
- (7) Smith, R. S.; Petrik, N. G.; Kimmel, G. A.; Kay, B. D. Communication: Proton Exchange in Low Temperature Co-Mixed Amorphous H₂O and D₂O Films: The Effect of the Underlying Pt(111) and Graphene Substrates. *J. Chem. Phys.* **2018**, *149*, 081104.

Probing and Controlling Electronic Correlations and Vibronic Coupling During Ultrafast Intramolecular Electron Transfer in Solvated Mixed Valence Complexes

Munira Khalil

Department of Chemistry, University of Washington, Seattle, WA 98195-1700, mkhalil@uw.edu

Niranjan Govind

Environmental Molecular Sciences Laboratory, Pacific Northwest National Laboratory, P.O. Box 999, Richland, WA 99352.

Robert W. Schoenlein

Linac Coherent Light Source, SLAC National Accelerator Laboratory, Menlo Park, CA 94025

This is a new award (DE-SC0019277) starting in September 2018 and funded under the solicitation, “Research at the Frontiers of X-ray Free Electron Laser Ultrafast Chemical and Material Sciences (DE-FOA-0001904).” The central goal of this project is to directly visualize and quantify how electronic correlations, vibronic couplings, and local solute-solvent interactions control intramolecular electron motion on the femtosecond time scale. The research program will focus on solvated Ruthenium (Ru) based mixed-valence complexes, a prototypical class of transition-metal complexes, which are of significant interest for their potential applications in photochemical energy conversion. Electron movements following photochemical excitation are closely coupled with atomic/vibrational and solvent motion. To disentangle these various components requires tools designed to directly probe electron correlations and vibronic coupling (coherently coupled motions of electronic and vibrational coordinates) on the timescale of electron motion in the solution phase. The proposed X-ray absorption, emission and RIXS spectroscopy experiments will make use of the new technical capabilities of LCLS-II and related upgrades to LCLS, which will provide access to chemical dynamics on the 10s of femtosecond timescale using X-ray pulses in the tender X-ray region (1.5~3 keV) with higher repetition rate and increased spectral stability. The research program will exploit emerging nonlinear X-ray capabilities of XFELs such as stimulated X-ray emission and double-core-hole spectroscopy to achieve new insights into excited-state charge dynamics and correlated phenomena. Along with X-ray experiments, we will utilize new multidimensional vibronic spectroscopies developed by the Khalil group to probe vibronic coupling between the cyanide bridging ligand and the intervalence charge transfer between the Ru sites. Our ability to extract microscopic details from the X-ray experiments hinges on our ability to simulate the linear and non-linear X-ray signals. This project includes the development of computational tools to simulate spectroscopic observables from non-equilibrium chemical dynamics of transition metal mixed valence systems on photo-excited electronic states accounting for explicit solute-solvent interactions. The combined experimental and computational studies will produce data which can be used to develop and validate theoretical models that treat coherent electronic and nuclear dynamics on an equal footing to describe non-equilibrium photochemical dynamics in molecular systems.

The new award described above is based on the progress made in our expiring grant, “Probing Ultrafast Electron (De)localization Dynamics in Mixed Valence Complexes Using Femtosecond X-ray Spectroscopy” with PIs, Khalil, Govind, Schoenlein and Mukamel. This grant is ending in August 2019. The overall goal of the expiring grant is to understand valence electron and vibrational motion following metal-to-metal charge transfer (MMCT) excitation in the following mixed valence complexes dissolved in aqueous solution: $[(\text{NH}_3)_5\text{Ru}^{\text{III}}\text{NCFe}^{\text{II}}(\text{CN})_5]^-$ (**1**, FeRu), *trans*- $[(\text{NC})_5\text{Fe}^{\text{II}}\text{CNPt}^{\text{IV}}(\text{NH}_3)_4\text{NCFe}^{\text{II}}(\text{CN})_5]^{4-}$ (**2**, FePtFe) and *trans*- $[(\text{NC})_5\text{Fe}^{\text{III}}\text{CNRu}^{\text{II}}(\text{L})_4\text{NCFe}^{\text{III}}(\text{CN})_5]^{4-}$ (**3**, FeRuFe, L=pyridine). The project objectives are (i) to observe the time-dependent re-arrangement of *d* electrons across two transition metal sites and the bridging ligand following photoinduced MMCT excitation on a sub-50 fs timescale using femtosecond X-ray pulses generated at LCLS (ii) to simulate femtosecond X-ray absorption and emission spectra of solvated, photo-excited, transition metal mixed valence complexes using a realistic treatment of multi-electron correlations/transitions, spin-orbit coupling and final state lifetime effects and to propose and study the feasibility of nonlinear X-ray experiments on solvated transition metal mixed valence systems using

future X-FEL light sources and (iii) to determine the role of coupled electronic and vibrational motions during ultrafast photoinduced charge transfer.

- ***Development of Two-Dimensional Vibrational-Electronic (2D VE) Spectroscopy.*** We have recently developed a Fourier transform (FT) 2D vibrational-electronic (2D VE) spectroscopy employing a sequence of mid-IR and optical pulses to interrogate coupled vibrational and electronic motions in the condensed phase. We simulated 2D VE spectra using a model Hamiltonian consisting of one anharmonic vibration and two electronic states to outline the selection rules for this experiment. Recently, we have performed polarization-selective 2D VE spectroscopy to measure the relative angles and mode-specific coupling strengths between the cyanide stretching vibrations and the MMCT excitation of FeRu dissolved in formamide.

- ***Equilibrium X-ray Absorption and X-ray Emission Spectroscopy of Transition Metal Mixed Valence Complexes in Solution.*** In order to understand the electronic configuration in the ground state of the transition metal complexes, we have obtained equilibrium X-ray absorption (XA) and X-ray emission (XE) spectra in water for the mixed valence complex complexes, FeRu, FeRuFe, FePtFe, and model complexes Fe(II)CN₆ and Fe(III)CN₆ at the Fe L-edge and the Fe K-edge. The successful collection of equilibrium spectra has allowed us to validate parameters in the simulation/computational codes for correctly modelling the electronic structure of the solvated mixed valence complexes. Our studies reveal the importance of carefully accounting for solute-solvent interactions for core-level spectroscopies. We are currently working on two manuscripts describing our equilibrium results.

- ***Femtosecond X-ray Absorption and X-ray Emission Spectroscopy of Transition Metal Mixed Valence Complexes in Solution.*** We were awarded beam time at LCLS under proposal LJ67 for five shifts in October 2015 and four shifts in December 2016. During 2015, experiments were performed at the X-ray pump probe (XPP) instrument at LCLS using 800 nm laser light to photo excite the sample preceding X-ray measurements. Femtosecond XA and XE spectroscopies were used at the Fe K-edge to directly monitor transient oxidation states and orbital occupancy during charge transfer in a series of solvated mixed-valence complexes. A transition from Fe^{II} to Fe^{III} (as in FeRu) would result in a blue peak shift of ~0.2 eV and broadening of the K α_1 peak consistent with the experimental transient XE result for FeRu. Transient XE spectra for FeRuFe exhibit the opposite, a red peak shift with spectral narrowing consistent with an Fe^{III} to Fe^{II} transition. Fits of the kinetic traces reveal that the initial MMCT from Fe^{II}Ru^{III} to Fe^{III}Ru^{II} and Fe^{III}Ru^{II}Fe^{III} to Fe^{II}Ru^{III}Fe^{III} occurs within the response of the instrument (50 fs) and the back electron transfer (BET) occurs within 100 fs for each compound. In the difference XA signal for FeRu, we see the growth of a transient feature upon MMCT which indicates that a hole is created in the t_{2g} orbital. The other XANES peaks undergo shifts to the blue upon photoexcitation and a change in the linewidth indicating the adjustments of the metal *d* orbitals following the initial MMCT. Simulations of the transient XANES features reveal the extent of electron delocalization during the MMCT process.

- ***Femtosecond X-ray scattering of excited-state structural dynamics of solvated mixed-valence complexes.*** Ultrafast X-ray diffuse scattering (XDS) experiments at LCLS provide important insight to the early structural dynamics of photoexcited FeRu in water, and the coupling of solute-solvent interactions with the MMCT/BET dynamics. Analysis of the XDS data is well advanced, supported with equilibrium and non-equilibrium MD simulations of the solvent response is underway. Preliminary indications are that the change in oxidation state of the FeRu molecule couples to: (1) the bulk dielectric response of the solvent via solvent dipole interactions, and (2) local solvation effects with specific changes in hydrogen bonding between solute ligands and solvent molecules. This is consistent with an interpretation that MMCT/BET dynamics are mediated in part by solute coupling to the solvation shell. Further analysis and comparison with theory is underway, and is expected to lead to more definitive conclusions.

- ***Simulating Valence-to-Core X-ray Emission Spectroscopy.*** Valence-to-Core X-ray Emission Spectroscopy (VtC-XES) is a sensitive tool to identify ligands and characterize ligand valence orbitals in transition metal complexes. We studied how linear-response time-dependent density functional theory (LR-TDDFT) can be extended to simulate K-edge VtC-XES reliably. LR-TDDFT allows one to go beyond the

single-particle picture. Specifically, we developed a “black box” protocol in NWChem to simulate these spectra. We are in the process of calculating of simulating the VtC-XES for the dimer (FeRu) and trimer (FeRuFe) complexes. We have recently applied this technique to solid-state transition metal compounds. Simulating VtC-XES for transient species is also possible with our approach.

- ***Ab Initio Molecular Dynamics/Molecular Mechanics (AIMD/MM), XA, UV/Vis and IR Spectroscopies of Model Transition Metal and Mixed Valence Complexes in Water on the Ground and Electronic Excited States.*** In order to study solvated model $\text{Fe}(\text{CN})_6^{4-}$ and $\text{Fe}(\text{CN})_6^{3-}$ complexes in water, we have performed extensive hybrid AIMD/MM based molecular dynamics simulations with NWChem. The FeRu dimer complex QM/MM model involved the solvation in a simulation box containing the dimer complex with 5000 water molecules to give a density close to 1 g/cm^3 . The FeRuFe and FePtFe complexes contained 7919 and 5842 water molecules respectively to give a density close to 1 g/cm^3 . The QM region in our approach comprises the transition metal complex, while the aqueous environment was treated using a MM representation. The QM region was treated with a hybrid exchange-correlation functional (PBE0). Following the AIMD/MM runs, we extracted snapshots of the complex with an explicit solvation environment of water molecules from the trajectory to perform the XANES, UV/Vis, IR, EXAFS spectra calculations. The Fe K-edge XANES and UV/Vis spectra were calculated with our restricted excitation window (REW) TDDFT approach. We have extended our TDDFT code to capture the quadrupole transitions in the Fe K-edge XANES. For FePtFe, our extensive ground state calculations reveal that the closed-shell singlet configuration is the lowest energy state compared with the triplet configuration in agreement with experiment. This is in contrast to previously published theoretical work on this system that reported a lower triplet state. For the FeRu and FeRuFe complexes, we have developed a new theoretical approach to tackle the transient-XAS to probe the x-ray absorption response of the UV-Vis excited transition metal complex. Our calculations, so far, are in good agreement with experiment. We have also performed VtC-XES calculations on representative clusters of the FeRu and FeRuFe complexes. For these calculations, we treat the solvent environment explicitly, which results in systems of approx. 300-350 atoms. VtC-XES calculations using the ground and excited-state geometries for the FeRu and FeRuFe complexes have also been performed.

- ***Simulations of Core-Resonant Circular Dichroism Signals.*** Core-resonant circular dichroism (CD) signals are induced by molecular chirality and vanish for achiral molecules and racemic mixtures. The highly localized nature of core excitations makes them ideal probes of local chirality within molecules. Our simulations of the circular dichroism spectra of several molecular families illustrate how these signals vary with the electronic coupling to substitution groups, the distance between the X-ray chromophore and the chiral center, geometry, and chemical structure. Clear insight into the molecular structure is obtained through analysis of the X-ray CD spectra. These proof-of-principle results were published in Chemical Science in 2017. Spin-orbit coupling (SOC) of the 2p electrons splits the XANES spectra and the electron-hole exchange interaction blurs the physical picture of the independent particle, thus the experimental intensity branching ratio of the transitions from the $2p_{3/2}$ and $2p_{1/2}$ orbitals may stray far from the ideal value of 2:1. Similarly, SOC should also play an important role in L-edge XCD. We neglected spin-orbit effects in our paper. However, there is every reason to expect that SOC should not affect the most important findings, *i.e.*, for molecules with a chiral center the amplitude of the XCD signals strongly decreases with the distance between the X-ray chromophore and the chiral center if the corresponding excitations are very localized to the excited atom, and that for globally chiral molecules the XCD signals also strongly depend on the chromophore position. A two-component TDDFT approach is under development for future XCD simulations including SOC of large molecules. This development potentially opens up new directions for our project.

- ***Developments and new protocols in NWChem.*** The following enhancements have been implemented or ongoing in the NWChem code over the course of this project:

1. Extensions to the TDDFT code in NWChem to capture quadrupole transitions ($1s \rightarrow 3d$) which are relevant for transition metal K-edge XANES.
2. TDDFT restart capabilities that will allow a user to systematically increase the number of excitations from previously saved calculations.
3. Parallelization enhancements for TDDFT calculations up to 3000 basis functions.

4. "Black Box" valence-to-core x-ray emission spectroscopy (VtC-XES) protocol.
5. New QM/MM protocols for simulations of the model, dimer and trimer complexes in different solvents.
6. New transient XAS protocol to tackle simulations of pump (optical)-probe (X-ray) spectroscopy.
7. Development of TDDFT approach for XCD spectra, spin-orbit effects.

The enhancements described above (2 and 3) are especially relevant for response calculations on the trimer systems where the transition metal complex (solute) plus the explicit water molecules (solvent) can result in system sizes of ~300 atoms or more.

We plan to accomplish the following in the final year of this project: (i) Complete the data analysis and prepare a manuscript incorporating our analysis and modeling of the excited-state structural dynamics of FeRu and FeRuFe in water. (ii) Perform transient IR experiments on FeRu and FeRuFe to follow vibrational relaxation following MMCT excitation. (iii) We are in the process of preparing several manuscripts combining experimental and computational data on the IR, electronic and core-hole spectroscopies on solvated mixed valence complexes. (iv) We will be performing further benchmark studies on our new transient XAS approach. (v) We will focus on the development of theoretical approaches for the calculation of L-edge and transient L-edge and RIXS spectra.

DOE Supported Publications

1. B. E. Van Kuiken, H. Cho, K. Hong, M. Khalil, R. W. Schoenlein, T. K. Kim, and N. Huse, "Time-resolved x-ray spectroscopy in the water window: Elucidating transient valence charge distributions in an aqueous Fe(II) complex", *J. Phys. Chem. Lett.*, **7** (2016) 465-470.
2. K. M. Slenkamp, M. S. Lynch, J. F. Brookes, C. C. Bannan, S. L. Daifuku, and M. Khalil, "Investigating vibrational relaxation in cyanide-bridged transition metal mixed-valence complexes using two-dimensional infrared and infrared pump-probe spectroscopies", *Structural Dynamics* **3** (2016) 023609.
3. B. E. V. Kuiken, M. R. Ross, M. L. Strader, A. A. Cordones, H. Cho, J. H. Lee, R. W. Schoenlein, and M. Khalil, "Picosecond sulfur K-edge x-ray absorption spectroscopy with applications to excited state proton transfer", *Structural Dynamics* **4** (2017) 044021.
4. S. Eckert, J. Norell, P. S. Miedema, M. Beye, M. Fondell, W. Quevedo, B. Kennedy, M. Hantschmann, A. Pietzsch, B. E. Van Kuiken, M. Ross, M. P. Miniti, S. P. Moeller, W. F. Schlotter, M. Khalil, M. Odelius, and A. Fohlich, "Ultrafast independent N-H and N-C bond deformation investigated with resonant inelastic x-ray scattering", *Angew. Chem. Int. Ed.* **56** (2017) 6088-6092.
5. J. D. Gaynor, and M. Khalil, "Signatures of vibronic coupling in two-dimensional electronic-vibrational and vibrational-electronic spectroscopies", *J. Chem. Phys.* **147** (2017) 094202.
6. Y. Zhang, J. R. Rouxel, J. Autschbach, N. Govind, and S. Mukamel, "X-ray circular dichroism signals: a unique probe of local molecular chirality", *Chemical Science*, **8** (2017) 5969-5978.
7. D. R. Mortensen, G. T. Seidler, J. J. Kas, N. Govind, C. P. Schwartz, S. Pemmaraju, and D. G. Prendergast, "Benchmark results and theoretical treatments for valence-to-core x-ray emission spectroscopy in transition metal compounds", *Phys. Rev. B.* **96** (2017) 125136-125145.
8. K. Henzler, E. O. Fetisov, M. Galib, M. D. Baer, B. A. Legg, C. Borca, J. M. Xto, S. Pin, J. L. Fulton, G. K. Schenter, N. Govind, J. I. Siepmann, C. J. Mundy, T. Huthwelker, J. J. De Yoreo, "Supersaturated calcium carbonate solutions are classical", *Science Advances*, **4** (2018), eaao6283, DOI: 10.1126/sciadv.aao6283
9. M. Ross, A. Andersen, Z. W. Fox, Y. Zhang, K. Hong, J-H. Lee, A. Cordones, A. M. March, G. Doumy, S. H. Southworth, M. A. Marcus, R. W. Schoenlein, S. Mukamel, N. Govind, M. Khalil, "Comprehensive experimental and computational spectroscopic study of hexacyanoferrate complexes in water: from infrared to x-ray wavelengths", *J. Phys. Chem. B*, **122**, (2018) 5075-5086
10. M. Galib, G. K. Schenter, C. J. Mundy, N. Govind, J. L. Fulton, "Unraveling the spectral signatures of solvent ordering in K-edge XANES of aqueous Na⁺", *J. Chem. Phys.*, accepted (2018).

Chemical Kinetics and Dynamics at Interfaces

Non-Thermal Reactions at Surfaces and Interfaces

Greg A. Kimmel (PI) and Nikolay G. Petrik

Physical Sciences Division
Pacific Northwest National Laboratory
P.O. Box 999, Mail Stop K8-88
Richland, WA 99352
gregory.kimmel@pnnl.gov

Collaborators include: BD Kay, RS Smith, and Y Xu

Program Scope

The objectives of this program are to investigate 1) thermal and non-thermal reactions at surfaces and interfaces, and 2) the structure of thin adsorbate films and how this influences the thermal and non-thermal chemistry. Energetic processes at surfaces and interfaces are important in fields such as photocatalysis, radiation chemistry, radiation biology, waste processing, and advanced materials synthesis. Low-energy excitations (e.g. excitons, electrons, and holes) frequently play a dominant role in these energetic processes. In photocatalysis, non-thermal reactions are often initiated by holes or (conduction band) electrons produced by the absorption of visible and/or UV photons in the substrate. In addition, the presence of surfaces or interfaces modifies the physics and chemistry compared to what occurs in the bulk.

We use quadrupole mass spectroscopy, infrared reflection-absorption spectroscopy (IRAS), and other ultra-high vacuum (UHV) surface science techniques to investigate thermal, electron-stimulated, and photon-stimulated reactions at surfaces and interfaces, in nanoscale materials, and in thin molecular solids. Since the structure of water near interface plays a crucial role in the thermal and non-thermal chemistry occurring there, a significant component of our work involves investigating the structure of aqueous interfaces. A key element of our approach is the use of well-characterized model systems to unravel the complex non-thermal chemistry occurring at surfaces and interfaces. This work addresses several important issues, including understanding how the various types of low-energy excitations initiate reactions at interfaces, the relationship between the water structure near an interface and the non-thermal reactions, energy transfer at surfaces and interfaces, and new reaction pathways at surfaces.

In collaboration with Bruce Kay and Scott Smith, we have developed a pulsed laser heating method that allows us to investigate deeply supercooled liquids by producing transiently heated films, which become liquids that last for approximately 10 ns per laser pulse. Subsequent rapid cooling due to the dissipation of the heat pulse into the metal substrate effectively quenches the liquid dynamics until the next laser heating pulse arrives. The rapid heating and cooling allows the system to reach previously unattainable supercooled liquid temperatures and return to the amorphous state before significant crystallization can occur.

Recent Progress

The Growth Rate of Crystalline Ice and the Diffusivity of Supercooled Water from 126 K to 262 K

A detailed understanding of supercooled water is crucial to solving many of the remaining mysteries of liquid water. A number of properties exhibit unusual behavior at low temperatures suggesting that there is a temperature, $T_x \sim 228$ K, at which these properties diverge. For example, the diffusivity in normal liquid water, $D(T)$, exhibits Arrhenius behavior. However, upon supercooling the temperature behavior of the diffusivity becomes markedly non-Arrhenius and the diffusivity rapidly decreases. Such a super-Arrhenius

behavior is the hallmark of a so-called “fragile liquid” (In contrast, “strong” liquids exhibit Arrhenius behavior). Supercooled, glass forming liquids have been examined theoretically, and a number of different models have been proposed to explain the anomalous behaviors observed experimentally. Experimental measurements at temperatures near T_x are vital for resolving these outstanding issues. However, rapid homogeneous nucleation of crystalline ice has prevented experiments on bulk water below ~ 232 K.

In collaboration with Bruce Kay and Scott Smith, we have measured the growth rate of crystalline ice, $G(T)$, for $180 \text{ K} < T < 262 \text{ K}$, i.e. deep within water’s “no man’s land” in ultrahigh vacuum conditions.[1] Isothermal measurements of $G(T)$ were also made for $126 \text{ K} \leq T \leq 151 \text{ K}$. The self-diffusion of supercooled liquid water, $D(T)$, was obtained from $G(T)$ using the Wilson-Frenkel model of crystal growth. For $T > 237 \text{ K}$ and $P \sim 10^{-8} \text{ Pa}$, $G(T)$ and $D(T)$ have super-Arrhenius (“fragile”) temperature dependences, but both crossover to Arrhenius (“strong”) behavior with a large activation energy in “no man’s land.” The fact that $G(T)$ and $D(T)$ are smoothly varying rules out the hypothesis that liquid water’s properties have a singularity at or near 228 K at ambient pressures. However the results are consistent with a previous prediction for $D(T)$ that assumed no thermodynamic transitions occur in “no man’s land.” One key assumption of this research involves the use of the Wilson-Frenkel model to relate the $G(T)$ to $D(T)$. Future work will focus on using alternative methods for measuring $D(T)$ in deeply supercooled water, such as tracer diffusion. Those results will then be compared to $D(T)$ extracted from the ice growth rate data.

Homogeneous Nucleation of Ice in Transiently-Heated, Supercooled Liquid Water Films

Understanding ice nucleation in supercooled liquid water is one of the most common and important processes occurring on Earth. However, our understanding of fundamental aspects of ice nucleation, such as the maximum rate of nucleation, the temperature at which this maximum occurs, and the size and initial morphology of the ice nuclei, is still incomplete. Developing a detailed understanding of ice nucleation is impeded by the existence of “no man’s land,” the temperature range from approximately 160 to 230 K in which spontaneous crystallization occurs too fast for most experimental techniques to observe. It is also challenging for molecular dynamics simulations to study ice nucleation due to the low probabilities for forming ice nuclei and the large number of possible molecular configurations.

In collaboration with Bruce Kay and Scott Smith, we recently used our pulsed heating technique to investigate the nucleation and growth of crystalline ice in transiently heated water films that are $0.24 \mu\text{m}$ thick.[3] By varying the temperature distributions within these films, it is possible to control the location within the films where the ice nucleates and grows. In particular, it is possible to suppress nucleation at the water/metal and water/vacuum interfaces and thus measure the homogeneous nucleation rate in the water films. Analysis of the results shows that homogeneous nucleation rates of at least $10^{26} \text{ m}^{-3}\text{s}^{-1}$ in the temperature range from ~ 210 – 225 K are needed to account for our observations. Experiments at lower overall temperatures, where heterogeneous nucleation at the water/metal interface was possible, suggest that the homogeneous nucleation rate is $\sim 10^{29\pm 2} \text{ m}^{-3} \text{ s}^{-1}$. Future work will focus on refining these measurements and exploring other deeply supercooled liquids in regions of the phase diagram that were previously inaccessible due to rapid crystallization.

Proton exchange in low temperature co-mixed amorphous H₂O and D₂O films: The effect of the underlying Pt(111) and graphene substrates

Proton exchange and mobility are of great importance in a wide range of scientific research areas including astrochemistry, biology, and fuel cell technology, to name a few. The transport of H^+ ions through solution, membranes, or ices is a critical step underlying many of these processes. The transport of protons has long been described by a Grotthuss or “structural” diffusion mechanism where a proton is passed between adjacent water molecules in a series of hops. The H/D exchange process is thought to occur via a two-step mechanism which involves a proton transfer (hop) followed by the migration of a Bjerrum L defect (turn).

Bjerrum defects, also known as orientational defects, are the places where the intermolecular hydrogen bonding is “defective”, where either a hydrogen atom is missing between oxygens (L defect) or where there are two hydrogens (D defect).

In a recent paper,[5] in collaboration with Bruce Kay and Scott Smith, we studied isotopic exchange reactions in mixed D₂O and H₂O amorphous solid water (ASW) films using reflection absorption infrared spectroscopy. Nanoscale films composed of 5% D₂O in H₂O were deposited on Pt(111) and graphene covered Pt(111) substrates. At 130 K, we find that the reaction is strongly dependent on the substrate with the H/D exchange being significantly more rapid on the Pt(111) surface than on graphene. At 140 K, the films eventually crystallize with the final products on the two substrates being primarily HOD on Pt(111) and a mixture of HOD and unreacted D₂O on graphene. The difference in the extent of proton exchange in the co-dosed films could be due to differences in the reactivity of the Pt(111) and graphene surfaces themselves. By pre-dosing H₂ and O₂ on Pt(111), we find that the observed differences in reactivity on the two substrates are likely due to the formation of hydrogen ions at the Pt(111) surface that are not formed on graphene. Once formed the mobile protons move rapidly through the ASW overlayer driving the H/D exchange reaction. Future work will focus on quantifying various aspects of the H/D exchange reaction kinetics and energetics.

Diffusion and Photon Stimulated Desorption of CO on TiO₂(110)

Molecular diffusion on surfaces plays a crucial role in many interfacial processes such as adsorption/desorption, catalysis, dissolution, corrosion, and nucleation and growth of nanostructures. Surface diffusion often delivers the reacting molecule to chemically-active surface sites (e.g. defects, adatoms, adsorbed species, etc.) and can limit the overall reaction rate. Therefore, understanding the diffusion of reactive species can be important for developing comprehensive models of catalytic reactions. Recently, we investigated the thermal diffusion of CO adsorbed on rutile TiO₂(110) in the 20 - 110 K range using photon-stimulated desorption (PSD), temperature programmed desorption (TPD) and scanning tunneling microscopy.[4] During UV irradiation, CO desorbs from certain photoactive sites (e.g. oxygen vacancies). This phenomenon was exploited to study CO thermal diffusion in three steps: first these photoactive sites were depleted during an initial UV irradiation, then they were replenished with CO during an annealing step, and finally the active site occupancy was probed in a second UV irradiation cycle. The PSD and TPD experiments showed that the CO diffusion rate correlates with the CO adsorption energy – stronger binding corresponds to slower diffusion. Increasing the CO coverage from 0.06 to 0.44 ML or hydroxylation of the surface decreases the CO binding and increases the CO diffusion rate. Relative to the reduced surface, the CO adsorption energy increases and the diffusion decreases on the oxidized surface. The CO diffusion kinetics can be modeled satisfactorily as an Arrhenius process with a “normal” prefactor (i.e. $\nu = 10^{12} \text{ s}^{-1}$) and a Gaussian distribution of activation energies where the peak of the distribution is $\sim 0.26 \text{ eV}$ and the full width at half maximum (FWHM) is $\sim 0.1 \text{ eV}$ at the lowest coverage. The observations are consistent with a significant electrostatic component of the CO binding energy on the TiO₂(110) surface which is affected by changes in the surface dipole and dipole-dipole interactions.

References to publications of DOE-sponsored research (October 2017 – present)

- [1] Yuntao Xu, Nikolay G. Petrik, R. Scott Smith, Bruce D. Kay and Greg A. Kimmel, “The growth rate of crystalline ice and the diffusivity of supercooled water from 126 K to 262,” *Proc. Nat. Aca. Sci.* **52** (2016) 14921. (DOI: 10.1073/pnas.1611395114).
- [2] Rentao Mu, Arjun Dahal, Zhi-Tao Wang, Zdenek Dohnálek, Greg A. Kimmel, Nikolay G. Petrik, and Igor Lyubinetsky, “Adsorption and Photodesorption of CO from Charged Point-Defects on TiO₂(110),” *J. Phys. Chem. Lett.* **8**, 4565 (2017) (DOI: 10.1021/acs.jpcllett.7b02052).
- [3] Yuntao Xu, Nikolay G. Petrik, R. Scott Smith, Bruce D. Kay and Greg A. Kimmel, “Homogeneous nucleation of ice in transiently-heated, supercooled liquid water films,” *J. Phys. Chem. Lett.* **8**, 5637 (2017), (DOI: 10.1021/acs.jpcllett.7b02685).
- [4] Nikolay G. Petrik, Rentao Mu, Arjun Dahal, Zhitao Wang, Igor Lyubinetsky and Greg A. Kimmel, “Diffusion and photon stimulated desorption of CO on TiO₂(110),” *J. Phys. Chem (C)*, **122**, 15382 (2018), DOI: 10.1021/acs.jpcc.8b03418).
- [5] R. Scott Smith, Nikolay G. Petrik, Greg A. Kimmel, and Bruce D. Kay, “Proton exchange in low temperature co-mixed amorphous H₂O and D₂O films: The effect of the underlying Pt(111) and graphene substrates,” *J. Chem. Phys.* **149**, 081104 (2018), (DOI: 10.1063/1.5046530).

2D IR Microscopy—Technology for Visualizing Chemical Dynamics in Heterogeneous Environments

PI: Amber T. Krummel

Colorado State University, 200 W. Lake Street, Fort Collins, CO 80525

amber.krummel@colostate.edu

1. Program Scope

Chemistries crucial for energy technologies including battery technology, fuel cell technology, and enhanced oil recovery take place in heterogeneous environments. Understanding and predicting chemical dynamics, including solute-solvent interactions, adsorption processes, and transport processes, to name a few, requires the ability to probe these events directly and ultimately visualizing these processes via microscopy. The overarching goal of this project is to develop two-dimensional infrared (2D IR) imaging tools to directly probe chemical interactions in heterogeneous environments, with geochemical systems being our primary target in this project. A combination of experiments directed toward technology development, the exploration of fundamental chemical physics of large macrocycles and acidic oils, and culminating with the direct visualization of chemical interactions in model pore structures. This project builds from our expertise in fabricating IR compatible microfluidic structures, in developing a 100 kHz 2D IR spectrometer, and in probing the nanoaggregates of large macrocycles.

The large number of observables offered by 2D IR spectroscopy allows us to disentangle and quantify complex chemical interactions in ways that were not previously feasible. These observables include the direct measurement of the frequency-frequency correlation function, which is a direct measure of the homogeneous and inhomogeneous contributions to the vibrational lifetime; and the peak positions (both diagonal peaks and cross peaks) and intensities, which are a direct measure of molecular structure. Each of these observables can be spatially resolved. Below the progress made towards imaging dynamics with the 2D IR microscope will be discussed. In addition, the technical details regarding the characterization of the 2D IR microscope will be discussed. During the past year, we have made significant progress toward investigating mesoscale dynamical behaviors in a model room temperature ionic liquid (RTIL).

2. Recent Progress & Current Efforts

In the past 12 months we have completed the characterization of our 2D IR microscope and have applied the technology to investigate the chemical dynamics in a RTIL microdroplet. The 2D IR imaging experiments and the analysis of the data have revealed the chemical dynamics in the microdroplet changing over several micrometers. Our results open new questions regarding heterogeneous dynamics that may exist in mesoscale structures of RTILs.

The layout of the 2D IR microscope we have designed and built is shown in Figure 1. We have been able to improve acquisition rates of 2D IR microscopy images by taking full advantage of our 100 kHz mid-IR laser system that drives our 2D IR microscope. Currently we shape mid-IR pulses and detect the mid-IR signal fields at a 100 kHz repetition rate—the current speed limit of shaping and detection technology. In order to maintain these acquisition speeds we have designed a microscope head to utilize the point scanning geometry.

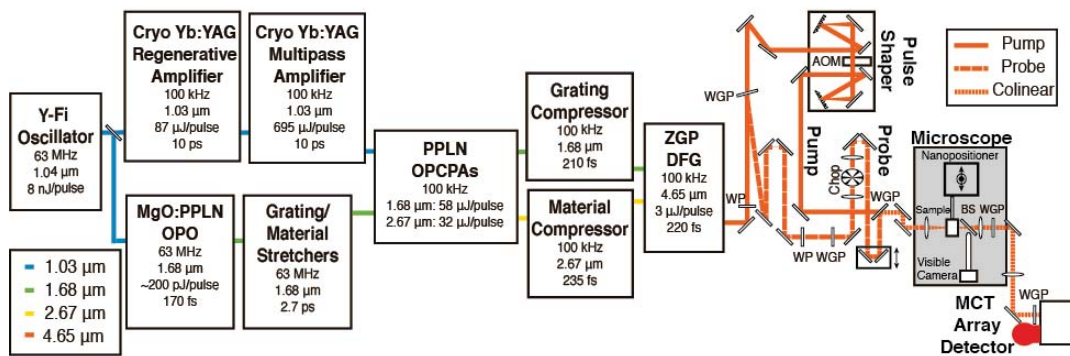


Figure 1. The general layout of 100 kHz mid-IR laser system and 2D IR microscope.

In order to perform 2D IR microscopy, the IR output from the ZGP DFG stage is split into two lines using a $\lambda/2$ waveplate and wire grid polarizer. The polarizer reflects the probe pulse whose polarization is rotated by 90° , creating S-polarization. The P-polarized pump line passes through the polarizer and is sent to a high speed, mid-IR pulse shaper to generate the pump pulse pair with a variable delay at 100 kHz. The pump and probe pulses are recombined using a polarizer that transmits the pump pulses and reflects the probe pulse to create a collinear geometry where 2D IR data is collected in the cross polarization (XXYY) configuration. The three pulses are focused into the sample by a Ge/Si achromatic lens and then re-collimated using a Si lens and sent to the detector. The spot size was measured by scanning a $10\ \mu\text{m}$ pinhole in the X and Y direction at the focal plane and recording the integrated intensity. The full width at half maximum (FWHM) beam diameter was measured to be $19.5\ \mu\text{m}$ in the Y direction and $14.2\ \mu\text{m}$ in the X direction. The Rayleigh range of focus in the direction of propagation is approximately $140\ \mu\text{m}$. The two polarizers before the detector are used to block the pump pulses and transmit the probe and signal. The probe and signal fields are then passed through a monochromator and collected on a 1×64 element, mercury cadmium telluride (MCT) linear array detector operating at the speed limit of detection of 100 kHz. The 2D IR spectra shown in this report were all collected using a series of 510 pump pulse pairs delayed from 0 to 3.57 ps in 7 fs steps. Thus, the spectral resolution along the pump-axis (ω_{pump}) is $4.7\ \text{cm}^{-1}$. Spectra

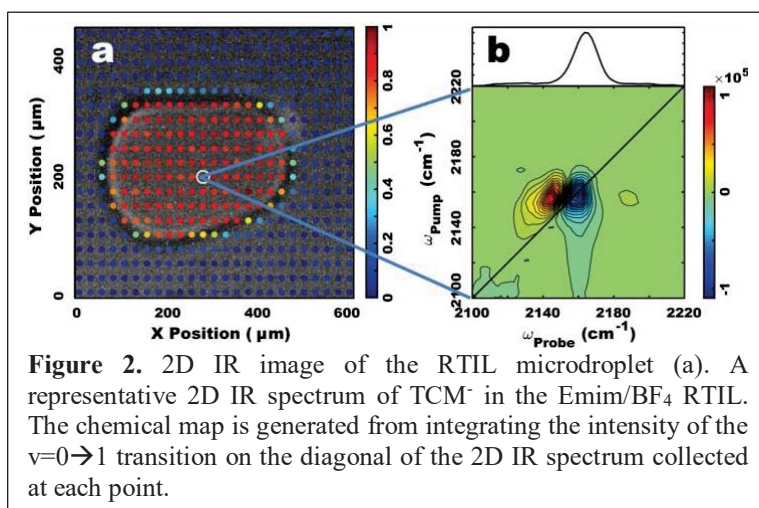


Figure 2. 2D IR image of the RTIL microdroplet (a). A representative 2D IR spectrum of TCM⁻ in the Emim/BF₄ RTIL. The chemical map is generated from integrating the intensity of the $\nu=0 \rightarrow 1$ transition on the diagonal of the 2D IR spectrum collected at each point.

were acquired using a four-step phase cycling scheme with $2000\ \text{cm}^{-1}$ rotating frame for background and scatter removal. The full 2D IR microscopy image of the RTIL microdroplet, shown in Figure 2a, is comprised of a data set of 476 2D IR spectra fully averaged 500 times. The pulse energies utilized were $70\ \text{nJ/pulse}$. The image shown in Figure 2a was collected in 120 minutes with an acquisition rate of 1984 individual 2D IR spectra per minute.

The RTIL microdroplet was produced by drop casting the RTIL in silicon oil. The droplets consisted of 1-ethyl-3-methylimidazolium tetrafluoroborate (EmimBF₄) and 1-ethyl-3-

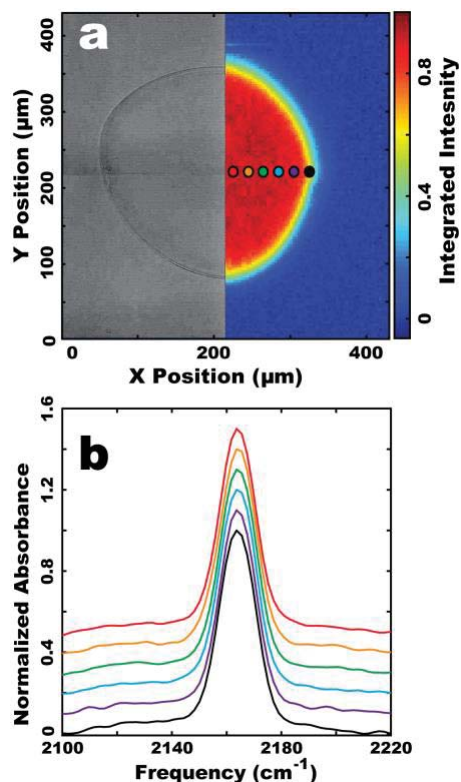


Figure 3. (a) Bright-field and FTIR microscopy image of the RTIL microdroplet. The intensity values on the chemical map are generated by integrating the FTIR spectra of each point from 2146 cm^{-1} to 2186 cm^{-1} . (b) Comparison of FTIR spectra extracted for the set of points across the droplet, indicated in the chemical map above. The FTIR spectra are offset for ease of viewing.

examined. In these experiments, the time delay (T_w) between the second and third pulses is varied and the solvent environment is allowed to evolve after pumping the system. A 2D IR microscopy experiment aimed at extracting the vibrational dynamics of the TCM^- probe was performed over a region of interest (ROI) of the RTIL microdroplet, where at each point 2D IR data were collected as a function of increasing T_w .

We performed nodal line slope analysis of the collected 2D IR spectra to characterize the spectral diffusion dynamics of TCM^- in an RTIL microdroplet. Spectral diffusion dynamics present some parameters, such as correlation times and the fluctuation amplitudes of the frequency fluctuation correlation functions (FFCFs). In Figure 4, the ROI selected is indicated with the white box and the nodal line slope values are plotted as a function of T_w , thus depicting the vibrational dynamics from interfacial and bulk environments within the ROI. It can be seen in Figure 4 that the decay curves at bulk and interfacial regions are significantly different; the 95% confidence intervals for the bulk and interfacial regions are indicated by the gray shadow. In addition, NLS decays at intermediate regions exhibit a combined behavior of the bulk and the interface, but are not included in this plot for clarity. The decays were fit to a biexponential function following the model,

methylimidazolium tricyanomethanide (EmimTCM) RTILs. The EmimTCM is doped into the EmimBF₄ in a 1:500 volume ratio where TCM^- acts as a vibrational probe. A roughly spherical droplet is formed when a very small amount of RTIL (10-20 nL) is casted in silicon oil. The droplet becomes a pancake in shape when placed in between two CaF₂ substrates with a 100 μm spacer to set the sample thickness. The oil is used for stabilization of the RTIL microdroplet as well as removing scatter from the interface because the refractive index of the silicon oil is similar to the RTIL microdroplet. The FTIR chemical map of the RTIL microdroplet is shown in Figure 3a and FTIR spectra collected at several points across the RTIL microdroplet are shown in Figure 3b. The linear IR spectra of TCM^- exhibits an absorption band in the $2100\text{-}2200\text{ cm}^{-1}$ region with a peak appearing at 2164 cm^{-1} corresponding to the degenerate asymmetric stretching vibrations of TCM^- . It can be seen in the chemical map generated from FTIR microscopy that the TCM^- is homogeneously distributed throughout the droplet, as there are no fluctuations of the intensity of the peak associated with the TCM^- throughout the microdroplet. The FTIR spectra at each point have the same FWHM linewidth of $15.5 \pm 0.04\text{ cm}^{-1}$ and center frequency of $2164.0 \pm 0.07\text{ cm}^{-1}$. Thus, any underlying solute-solvent interactions in the RTIL microdroplet remain hidden in FTIR microscopy.

Using both the time and spatial resolution of 2D IR microscopy, dynamics information of different solvation regions across the microdroplet can be

$$C(T_W) = a_1 \exp(-T_W/\tau_1) + a_2 \exp(-T_W/\tau_2) + b$$

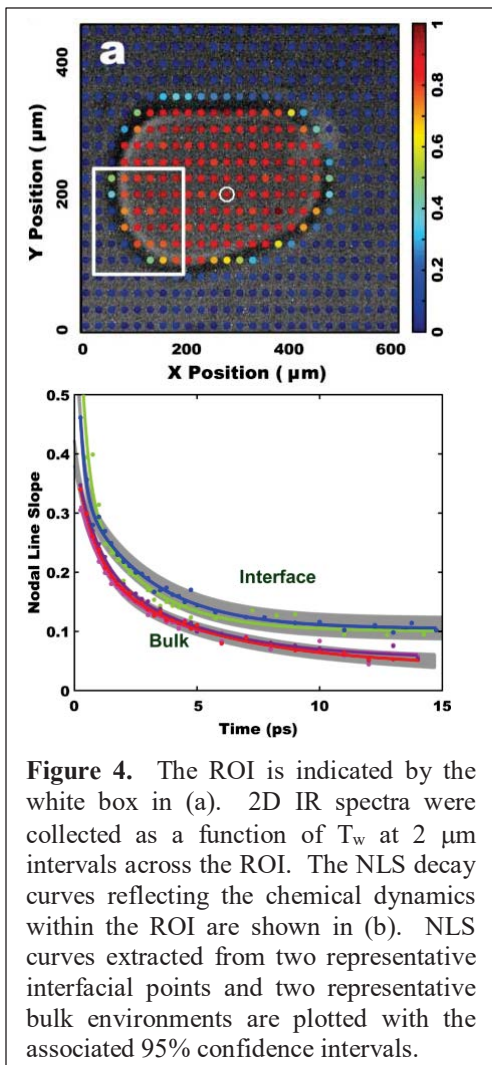


Figure 4. The ROI is indicated by the white box in (a). 2D IR spectra were collected as a function of T_W at $2 \mu\text{m}$ intervals across the ROI. The NLS decay curves reflecting the chemical dynamics within the ROI are shown in (b). NLS curves extracted from two representative interfacial points and two representative bulk environments are plotted with the associated 95% confidence intervals.

The biexponential fit of the bulk region gives a τ_1 of 810 ± 100 fs and a τ_2 of 5.2 ± 1 ps. In contrast, the interface region produces a τ_1 of 210 ± 50 fs and a τ_2 of 2.8 ± 0.25 ps. Therefore, the time components indicate that the dynamics of spectral diffusion is markedly different at the interface than at the bulk environments within the RTIL microdroplets. The data representative of the intermediate regions were collected across the ROI in $2 \mu\text{m}$ steps from the interface, inside the microdroplet. The intermediate regions exhibit a combination of bulk and interfacial behaviors. For example, one such data set collected at $5 \mu\text{m}$ to the interior of the RTIL droplet produces a τ_1 of 650 ± 100 fs and a τ_2 of 5.0 ± 0.6 ps. We are currently working to model the dynamic behaviors that exist in the RTIL microdroplet to assess how the chemical dynamics change across the droplet. These 2D IR measurements made throughout the ROI reveal the complex nature of the chemical dynamics in RTIL microdroplets; the homogeneous and inhomogeneous contributions to the vibrational frequency fluctuations of TCM^- can be used to probe the nature of the chemical dynamics present in the RTIL microdroplet.

3. Future Plans

The third year of this project is focused on continuing the RTIL investigations and moving towards developing a model system to use to explore chemical dynamics that may occur in pore structures encountered in subsurface environments. We expect

to work towards additional tunability of our 2D IR microscope, however it is also crucial to balance instrument development with the need to investigate chemistries applicable to energy technologies.

4. Publications

No publications have been produced under this award, however at this time, one manuscript is submitted, two are in preparation, and a book chapter is also in preparation.

DOE-BES Condensed Phase and Interfacial Molecular Science

Mechanistic investigations of hot carrier induced electrocatalysis by single-particle spectroscopy

Christy F. Landes and Stephan Link

Department of Chemistry, Department of Electrical and Computer Engineering

Rice University, 6100 Main St. Houston, TX 77005

cflandes@rice.edu, slink@rice.edu

Program Scope

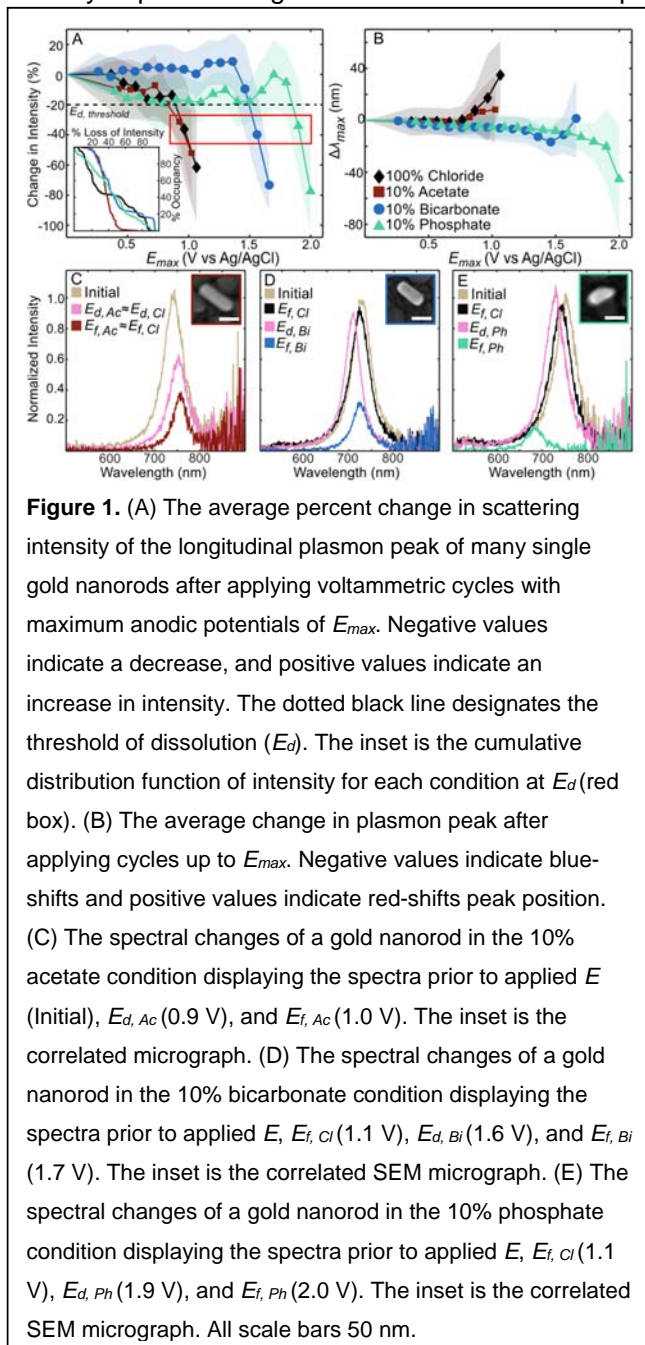
The goal of this project is to mechanistically understand the correlation of activity and stability of plasmonic electrocatalysts to nanoparticle morphology, surface chemistry and 'hot' carrier physics using super-resolved single particle spectro-electrochemical microscopy. The central hypothesis is that catalytic activity, selectivity and stability of plasmonic electrocatalysts can be tuned by controlling the population and dynamics of excited charge carriers, and strongly depend on size, shape, crystal facet and surface chemistry. Furthermore, it is hypothesized that stability can be manipulated through the nanoparticle morphology and plasmon-induced hot carriers. State-of-the-art single particle and single molecule spectroscopic techniques with super-resolution capabilities are employed to probe electrocatalytic activities. Electro-generated chemiluminescence (ECL) microscopy will be used to image the spatial extent of active catalytic sites on single plasmonic nanoparticles and to correlate these sites with the nanoparticle morphology via scanning electron microscopy (SEM). Additionally, single particle plasmon voltammetry is applied to probe electrocatalytic activity of nanoparticles with different morphologies characterized by SEM. Furthermore, the stability of individual nanocatalysts is investigated by ECL and single particle scattering measurements to monitor the kinetics of deactivation and morphology transformation of nanoelectrocatalysts. The following aims are being pursued:

- (1) Investigate the effects of plasmon enhancement on the electrocatalytic activities of single metal nanoparticles and map intraparticle heterogeneity in catalytic activity via super-resolution microscopy.
- (2) Combine single particle voltammetry and super-resolved ECL microscopy to achieve unprecedented level of nanoscale understanding of catalysis using a model $\text{Ru}(\text{bpy})_3\text{Cl}_2$ oxidation reaction.
- (3) Explore the effects of plasmon induced instability of nanoelectrocatalysts and locate the most active and stable sites within particles using model quantum dots (QDs) and CO_2 reduction reactions.

Recent Progress

In the last year, we addressed the project's goal of characterizing the stability of plasmonic electrocatalysts both in the absence and presence of light excitation to create hot carriers. Regulating the electrochemical environment for metal nanoparticles is vital for their longevity in all electrochemical applications. Metal nanoparticles interface with enormously varied and complex chemical environments in technological settings. This range of environments poses critical challenges to corrosion and dissolution prevention in nanoparticle electronics, electrocatalysis, and electrochemical sensing, as no suitable overarching prevention strategy exists. Preventing dissolution is especially critical for expensive metals and for metal nanoparticles with properties that are strongly dependent on size and shape, such as plasmonic noble metal nanoparticles. We

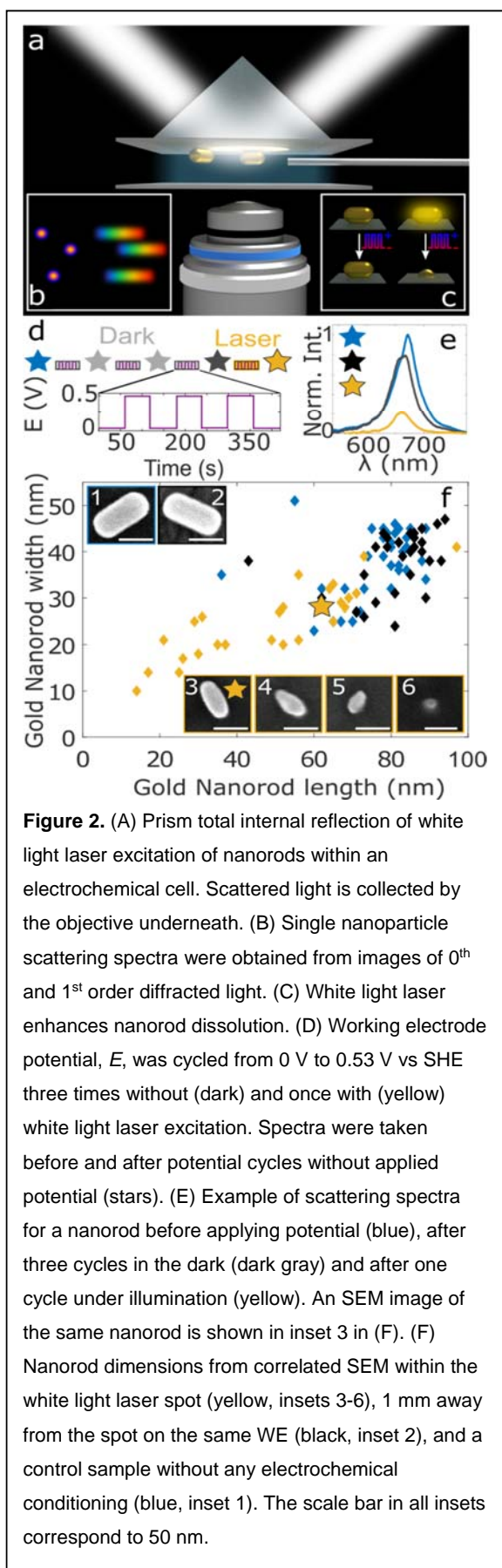
demonstrated that low relative concentrations of certain oxoanions increased the morphological stability of plasmonic gold nanorods under anodic potentials in predominantly chloride-based



aqueous solutions. Single particle hyperspectral dark-field imaging and correlated scanning electron microscopy revealed that low relative concentrations of oxoanions altered the dissolution onset potential, dissolution pathway, and particle reaction heterogeneity, as compared to chloride-only electrolyte solutions. We determined that, in aqueous chloride electrolyte solutions, low relative concentrations (10%) of bicarbonate and phosphate oxoanions inhibited electrodedissolution of gold nanorods by increasing the electrodedissolution potential by 600 mV and 900 mV, respectively (Figure 1). Using single particle analysis, we revealed that a low relative concentration of oxoanions modified the heterogeneity of the electrodedissolution statistics by reducing the emergence of distinct populations which occurred in chloride-only electrolyte solutions. By correlating SEM images with dark-field hyperspectral imaging we determined that partially electrodedissolved gold nanorods in chloride-only electrolyte solution increased in average aspect ratio from 2.7 to 3.0 when the average volume decreased by 36%, whereas the aspect ratio in a 90 mM chloride solution with 10 mM phosphate added, decreased to 2.1 with a volume decrease of 52%. We propose that the main factors contributing to the inhibition of chloride mediated dissolution of nanorods are: coordination, oxoanion concentration, hydroxide

concentration, adsorption energy, and the number of hydroxyl groups. Our interpretations of the observed trends suggest ionicity and the adsorption energy of the oxoanion have the greatest weight in terms of protection of gold nanorods in chloride electrolyte solution. Understanding the impact of complex anion solutions on the stability of metal nanocrystal modified electrodes will improve capabilities of electrochemical sensing and catalysis by increasing the potential window of stability of nanomaterials. This work is currently prepared for publication [1].

When working at electrochemical potentials below the dissolution onset under chloride electrolyte conditions, we explored how optical excitation of gold nanorods affects both the onset



potential and dissolution rate, directly addressing the aim to understand the effects of hot carriers. We indeed found plasmon enhanced dissolution of gold nanorods in a NaCl electrolyte solution (Figure 2) [2]. The onset of nanorod dissolution was observed at similar potential with and without white light laser excitation using average changes in intensity, but the rate of the decrease in intensity due to gold nanorod dissolution was greater with white light laser. The dissolution onset potential corresponded to the chloride adsorption potential of 0.48 V. Above this potential, light induced hot charge carriers enhance the rate of gold oxidation. We employed for these studies our snapshot microspectroscopy setup that we had developed as part of this DOE funded project [3]. The setup is able to measure dark-field scattering spectra in parallel using a transmission grating and a white light excitation laser. This laser is used for probing spectral changes of single gold nanorods and creating hot carriers that drive nanoparticle dissolution. Surface temperature calculations suggests that plasmonic heating was not a major contributor dissolution. The plasmon enhanced dissolution reaction is best described by a plasmon generated hot hole driven mechanism where applied electrochemical potentials are required to adsorb the chloride ion and match the energy of the hole with the HOMO of adsorbed chloride ions. Wavelength dependent studies, where we separated the white light spectrum into a higher energy green and lower energy red part while keeping either total absorbed energy or total absorbed photons the same, showed that hot holes in the d-band from direct interband transitions or transverse mode plasmon decay drive dissolution more efficiently than hot holes from longitudinal mode plasmon decay that are located around the Fermi level. Specifically, these wavelength dependent studies revealed hot holes generated from the absorption of green photons drive the dissolution at almost twice the rate as red photons. This work opens up new insights into hot hole driven photocatalysis on a single particle level, while demonstrating the importance

of single a particle approach for photocatalyst studies.

We also wrote a review article on plasmonic sensing and control of single nanoparticle electrochemistry to summarize the current state of the field [4].

Future Plans

All experiments we have performed so far involve the optical probing of the surface plasmon resonance of single nanoparticles using light to read out electrochemical charging and redox reactions. To decouple the effect of the probing light with electrochemical changes, we have been developing electrogenerated chemiluminescence (ECL) using a model $\text{Ru}(\text{bpy})_3\text{Cl}_2$ oxidation reaction. Polymer stability as the host medium and reproducibility have been issues that we have however now overcome. We have been able to measure the ECL signal as a function of nanoparticle size and shape. Very initial results indicate that the ECL is not only dominated by the total surface area, but also the spectral overlap between the ECL and the plasmon resonance, although the plasmon resonance is not directly excited except for the excited $\text{Ru}(\text{bpy})_3\text{Cl}_2$ species. Our future studies will focus on understanding this enhancement both experimentally and theoretically and testing the effect of enhanced electric fields in the gaps of dimers. Super-resolving the emitted light will furthermore inform us about inter- and intra-particle heterogeneity of single plasmonic electrocatalysts.

Publications

- [1] C. Flatebo, S. S. E. Collins, B. S. Hoener, Y. Cai, S. Link, C. F. Landes *Electrodissolution inhibition of gold nanorods with oxoanions*. To be submitted.
- [2] B. S. Hoener, A. Al-Zubeidi, S. S.E. Collins, W. Wang, S. R. Kirchner, S. A. H. Jebeli, A. Joplin, W.-S. Chang, S. Link, C. F. Landes *Photoelectrodissolution of Single Plasmonic Nanoparticles*. To be submitted.
- [3] S. R. Kirchner, K. Smith, B. S. Hoener, Sean S. E. Collins, W. Wang, Y.-Y. Cai, C. Kinnear, H. Zhang, W.-S. Chang, P. Mulvaney, C. F. Landes, S. Link *Snapshot Hyperspectral Imaging (SHI) for Revealing Irreversible and Heterogeneous Plasmonic Processes*. *J. Phys. Chem. C* 122, 6865 (2018).
- [4] B. S. Hoener, S. R. Kirchner, T. S. Heiderscheit, S. S.E. Collins, W.-S. Chang, S. Link, C. F. Landes *Plasmonic Sensing and Control of Single Nanoparticle Electrochemistry* *Chem* 4, 1560 (2018).

ION SOLVATION AND HYDROGEN BONDING IN LIQUID ELECTROLYTES

Mark Maroncelli¹ and Hyung Kim²

¹Department of Chemistry, The Pennsylvania State University, University Park, PA 16802
maroncelli@psu.edu

²Department of Chemistry, Carnegie Mellon University, 4400 Fifth Ave., Pittsburgh, PA 15213
hjkim@cmu.edu

Program Scope: This goal of this project is to develop a better understanding of hydrogen bonding and solvation of simple ions in liquid electrolytes. The electrolytes considered include dilute salt solutions in conventional dipolar solvents, ionic liquids, and concentrated mixtures of ions and dipolar components such as deep eutectic solvents. Initial efforts will involve be on simple, well-known systems, but the ultimate targets are the more complex electrolyte systems of growing importance in many energy-related technologies, most notably in the areas of Li-ion and related batteries, supercapacitors, and electroplating. Three interrelated projects that combine infrared and NMR spectroscopy and computer simulation are planned.

The first and primary project entails the use of far-infrared (FIR) spectroscopy to study solvation of simple ions such as alkali metal salts in liquid electrolytes. FIR absorption bands of such ions result from rattling motions of the ions within the cage formed by surrounding solvent molecules. The spectra of these ion-solvent vibrations, particularly when augmented with computer simulations as proposed here, provide a direct window on solvation structure and dynamics of these ions in different solvent environments. Although some work of this sort was initiated decades ago, improvements in instrumentation and computational power have greatly enhanced the quality of the spectra obtained as well as our ability to interpret them. Almost no work along these lines has so far been reported in the more complex liquid electrolytes of interest here. This research will therefore explore what new insights can be gained from this type of spectroscopy coupled with modern computational methods.

The second project area involves characterization and use of phosphine oxides as mid-IR solvation probes. The resonance between P=O and P⁺-O⁻ forms in phosphine oxides renders the PO bond highly sensitive to solvent polarity, particularly a solvent's hydrogen bond donating ability. For this reason, the ³¹P chemical shift of triethylphosphine oxide (TEPO) was previously used to establish the well-known acceptor number scale of solvent electrophilicity. Like the ³¹P chemical shift, the frequency of the P=O stretch of TEPO is highly sensitive to its environment. In addition, the IR spectrum of TEPO often shows multiple bands corresponding to differently hydrogen-bonded solvates in protic solvents. Despite the much greater environmental sensitivity of this vibration compared to other vibrational chromophores in current use, this probe has been ignored in vibrational work since the 1980s. Quantum chemical calculations and molecular dynamics simulations will be used to characterize the P=O stretch of trimethylphosphine oxide (TMPO) and create a spectroscopic map based on calibration against experimental data in a number of conventional solvents. IR spectroscopy of TMPO and related molecules will then be used to measure polarity and hydrogen bonding in the liquid electrolytes mentioned above. Classical molecular dynamics simulations, together with the spectroscopic map, will be used to interpret the observed spectra in terms of specific molecular interactions and dynamics.

The final project is a minor extension of the FIR studies of ion solvation. Computer simulations undertaken for the FIR work will be extended to include calculation of the electric field gradient autocorrelation function (EFG ACF), which summarizes the dynamics relevant to quadrupole

relaxation of atomic ions. These functions will be used to predict quadrupole relaxation times of ions both in simple solvents, where experimental times are already available, as well as in electrolyte solvents, which have yet to be studied in this manner. New NMR measurements of relaxation rates will be performed as needed to test these predictions. Comparison of the EFG-ACFs to suitable representations of the dynamics underlying the FIR spectra will be made in order to better appreciate the different perspectives on ion solvation dynamics provided by FIR and NMR spectroscopies.

Recent Progress: The main effort to date has been deciding on the details of the FIR/IR spectrometer that will form the focus of the experimental work.

Future Plans: We hope to have an instrument installed and functional early in the new year. Initial work will entail collecting FIR spectra of dilute Li^+ and Na^+ in simple solvents, both to learn how best to collect such spectra and to provide data with which to test our approaches to spectral modeling. We will also begin to survey more complex electrolyte systems to select those most fruitful for detailed study.

DOE-Sponsored Publications: None since the project start date of 9/15/18.

Intrinsic to collective properties of ions in solution

Christopher J. Mundy
Physical Sciences Division
Pacific Northwest National Laboratory
902 Battelle Blvd, Mail Stop K1-83
Richland, WA 99352
chris.mundy@pnnl.gov

Program Scope

The long-term objective of this research is to develop a fundamental understanding of processes, such as transport mechanisms and chemical transformations, at interfaces of hydrogen-bonded liquids. Liquid surfaces and interfaces play a central role in many chemical, physical, and biological processes. Many important processes occur at the interface between water and interfaces (liquid or solid). Separation techniques are possible because of the hydrophobic/hydrophilic properties of liquid/liquid interfaces. Reactions that proceed at interfaces are also highly dependent on the interactions between the interfacial solvent and solute molecules. The interfacial structure and properties of molecules at interfaces are generally very different from those in the bulk liquid. Therefore, an understanding of the chemical and physical properties of these systems is dependent on an understanding of both the bulk and interfacial solvation structure. The adsorption and speciation of ions at aqueous liquid interfaces are fundamental processes encountered in a wide range of physical systems. In particular, the manner in which solvent molecules solvate ions at the interface is relevant to problems in a variety of areas. Another major focus lies in the development of reduced models of interaction based on the potential of mean force (PMF) and solvation free energies to provide accurate descriptions of both single ion and ion-ion interactions. These reduced models can be used with appropriate simulation techniques for sampling statistical mechanical ensembles to obtain the desired collective properties such as nucleation.

Progress Report

Towards a resolution of the Jones-Ray effect [1] The surface tension of dilute salt water is a fundamental property that is crucial to understanding the complexity of many aqueous phase processes. Small ions are known to be repelled from the air-water surface leading to an increase in the surface tension in accordance with the Gibbs adsorption isotherm. The Jones-Ray effect refers to the observation that at extremely low salt concentration the surface tension decreases in apparent contradiction with thermodynamics. Determining the mechanism that is responsible for this Jones-Ray effect is important for theoretically predicting the distribution of ions near surfaces. We use both experimental surface tension measurements and numerical solution of the Poisson-Boltzmann equation to demonstrate that very low concentrations of surfactant in water create a Jones-Ray effect as shown in **Figure 1**. We also demonstrate that the low concentrations of surfactant necessary to create the Jones-Ray effect are too small to be detectable by surface sensitive spectroscopic measurements. The effect of surface curvature on this behavior is also examined and the implications for unexplained bubble phenomena is discussed. This work leaves open the possibility that the purity standards for water may be inadequate and that the interactions between ions with background impurities are

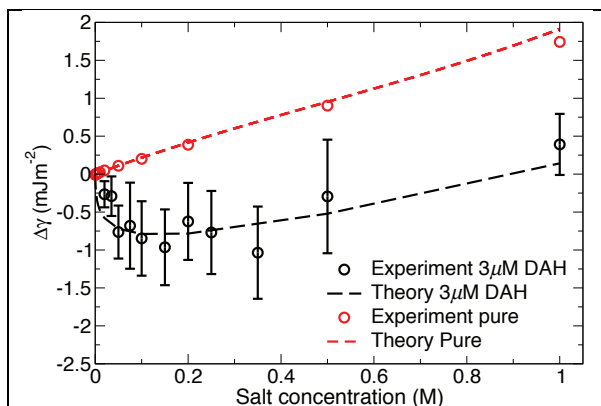


Figure 1: Experimental and theoretical fit of NaCl surface tensions in the presence of a dilute (but measurable) surfactant and the pure salt solution. Clear indication that the presence of a dilute surfactant gives rise to a Jones-Ray-like effect.

important to incorporate into our understanding of the driving forces that give rise to the speciation of ions at interfaces.

A microscopic picture of collective properties of ions in solution [7]: Understanding the nature of ionic hydration at a fundamental level has eluded scientists despite intense interest for nearly a century. In particular, the microscopic origins of the asymmetry of ion solvation thermodynamics with respect to the sign of the ionic charge remains a mystery. We determine the response of accurate quantum mechanical water models to strong nanoscale solvation forces arising from excluded volumes and ionic electrostatic fields as schematically shown in **Figure 2**. This is compared to the predictions of two important

limiting classes of classical models of water with fixed point charges, differing in their treatment of “lone pair” electrons. Using the quantum water model as our standard of accuracy, we find that a single fixed classical treatment of lone pair electrons cannot accurately describe solvation of both apolar and cationic solutes, emphasizing the need for a more flexible description of local electronic effects in solvation processes. However, we explicitly show that all water models studied respond to weak long-ranged electrostatic perturbations in a manner that follows macroscopic dielectric continuum models, as would be expected. The importance of these findings in the context of realistic ion models, using density functional theory and empirical models, and discuss the implications of our results for quantitatively accurate reduced descriptions of solvation in dielectric media.

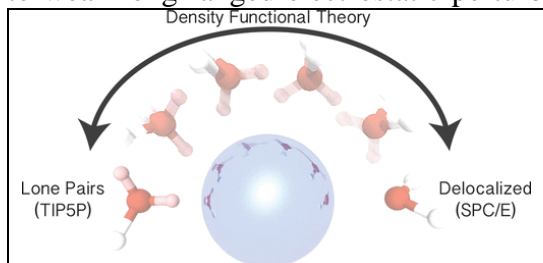


Figure 2: Schematic of the range of solvent response to a charged HS. The extreme on the left is the empirical TIP5P model that contains explicit lone pairs. The extreme on the right is the SPC/E point charge model. Our findings suggest that quantum based descriptions produce a response to a charged HS that interpolates between the two extremes.

Solvation Free Energies: [3,11, 12] Ionic solvation free energies are one of the most fundamental and important properties in physical chemistry and yet there is still debate and uncertainty about what they are. In particular, the contribution from the surface potential of the air-water interface is poorly understood. Our research is aimed at providing clear

and rigorous definition of single ion

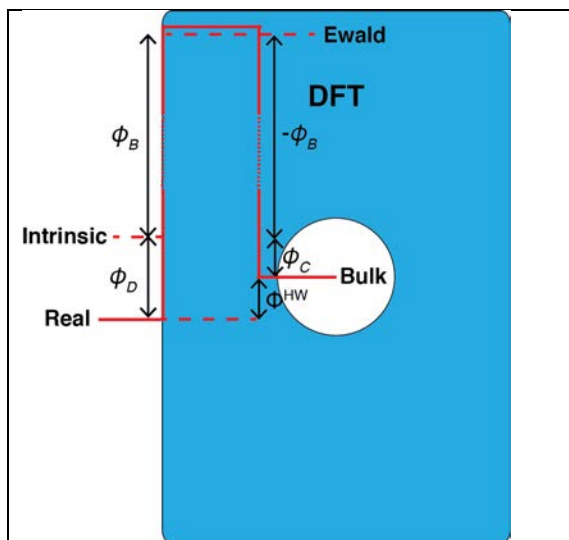


Figure 3: Four different definitions of the electrostatic contributions to the solvation free energies: **Real**, **Intrinsic**, **Ewald** (inherently unphysical because they contain the Bethe potential-- ϕ_B), and **Bulk**. The conversion between each of the definitions is denoted schematically by the addition/subtraction of well-defined potentials, namely the Bethe potential-- ϕ_B , the dipole potential due to the presence of an interface-- ϕ_D , the cavity potential-- ϕ_C . Note, for the case of quantum based potentials such as DFT, ϕ_B is large and positive. See Remsing *et al. J. Phys. Chem. Lett.* **5**, 2767 (2014) for details.

solvation free energies (see **Figure 3**). Starting with model systems we calculate solvation free energies for positive and negative charged hard spheres using interaction potentials based in quantum density functional theory (DFT). For charged hard spheres we show that DFT water responds linearly to the charge in the center of the cavity but exhibits a very large charge hydration asymmetry that is much larger than experimental estimates for real ions. [1] This indicates that real ions, particularly anions, are significantly more complex than the simple charged hard spheres they are often considered to be. We have used these methods developed on model systems to compute single ion free energies of both aqueous Li^+ and F^- . As stated previously, our research suggests that the Li^+ behaves similar to a charged hard-sphere whereas F^- takes on much more complex behavior that relies on an accurate description of the short-range quantum mechanical interaction. [5]

Acknowledgements. This work was performed with Mirza Galib (PNNL), Santanu Roy (PNNL), Tim Duignan (PNNL), John D. Weeks (U. Maryland), Rick Remsing (Temple), Ilja Siepmann (U. Minn.), Greg Schenter (PNNL), Marcel D. Baer

(PNNL), Shawn M. Kathmann (PNNL), Greg Kimmel (PNNL), and John Fulton (PNNL). We also acknowledge computer resources from NERSC. Battelle operates Pacific Northwest National Laboratory for the US Department of Energy. The Molecular Theory and Modeling FWP 16249 is co-managed by CTC and CPIMS programs of DOE Office of Basic Energy Sciences Division of Chemical Sciences, Geosciences, and Biosciences.

Publications with BES support (2017-present):

1. [Invited] T. Duignan, M. Peng, A. Nguyen, Xiu Song Zhao, M.D. Baer, and **CJM**, "Detecting the undetectable: The role of trace surfactant in the Jones-Ray effect" *J. Chem. Phys.* (in press)

2. M. Galib, G.K. Schenter, CJM, N. Govind, and J.L. Fulton, “Unraveling the spectral signatures of solvent ordering in K-edge XANES of Aqueous Na⁺” *J. Chem. Phys.* (in press)
3. T. Duignan, MD Baer, and **CJM**, “Understanding the scale of the single ion free energy: A critical test of the tetra-phenyl arsonium and tetra-phenyl borate assumption,” *The Journal of Chemical Physics* 148, 222819 (2018)
4. Z. Shen, J. Chun, K. Rosso, and **CJM** “Surface Chemistry Affects the Efficacy of the Hydration Force between Two ZnO(1010) Surfaces,” *J. Phys. Chem. C*, 2018, 122 (23), pp 12259–12266
5. A. Prakash, MD Baer, **CJM**, and J. Pfaendtner, “Peptoid Backbone Flexibility Dictates Its Interaction with Water and Surfaces: A Molecular Dynamics Investigation,” *Biomacromolecules*, 2018, 19 (3), pp 1006–101
6. [**Frontiers Article**] S. Roy, M. Galib, G.K. Schenter, and **CJM**, “On the relation between Marcus theory and ultrafast spectroscopy of solvation kinetics,” *Chemical Physics Letters*, 692, 417 (2018)
7. R. Remsing, T. Duignan, M.D. Baer, G.K. Schenter, **CJM**, and J.D. Weeks, “Water Lone Pair Delocalization in Classical and Quantum Descriptions of the Hydration of Model Ions” *J. Phys. Chem. B* 122, 3519 (2018)
8. [**Cover Article**] A. Prakash, J. Pfaendtner, J. Chun, and **CJM**, “Quantifying the Molecular-Scale Aqueous Response to the Mica Surface” *J. Phys. Chem. C* 121, 18496–18504 (2017)
9. S. Roy, MD Baer, **CJM**, G.K. Schenter, “Marcus Theory of Ion Pairing” *J. Chem. Theory Comput.* 13 3470–3477 (2017)
10. [**Editors Choice**] M. Galib, T. Duignan, Y. Misteli, MD Baer, GK Schenter, J. Hutter, and **CJM**, “Mass Density Fluctuations in quantum and classical descriptions of liquid water” *The Journal of Chemical Physics* 146, 244501 (2017)
11. T. Duignan, MD Baer, GK Schenter, and **CJM**, “Electrostatic solvation free energies of charged hard spheres using molecular dynamics with density functional theory interactions” *J. Chem. Phys.* 147, 161716 (2017)
12. T. Duignan, MD Baer, GK Schenter, and **CJM**, “Real single ion solvation free energies with quantum mechanical simulation” *Chem. Sci.* 8, 6131-6140 (2017)
13. M Galib, MD Baer, LB Skinner, **CJM**, T Huthwelker, GK Schenter, CJ Benmore, N Govind, JL Fulton, “Revisiting the hydration structure of aqueous Na⁺” *The Journal of Chemical Physics* 146, 084504 (2017)

Probing the Structure and Dynamics of Water Under Heterogeneous Nanoconfinement Through Ultrafast Vibrational Spectro/microscopy and Many-Body Molecular Dynamics

Francesco Paesani and Wei Xiong

Department of Chemistry and Biochemistry, University of California San Diego

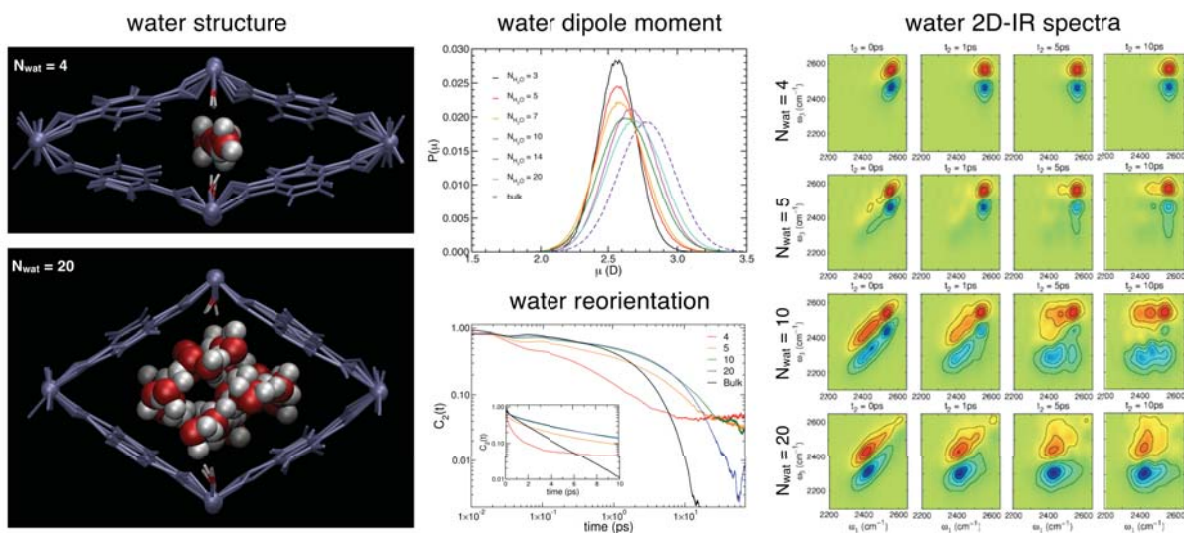
Program Scope.

The goal of this research project is to gain a molecular-level understanding of the structure and dynamics of aqueous solutions in nanoporous materials by integrating state-of-the-art ultrafast vibrational spectroscopy/microscopy with advanced computer simulations based on many-body molecular dynamics.

Specific focus is on identifying the physical mechanisms and characterizing the underlying molecular interactions that determine the adsorption and transport processes of water and small solutes in metal-organic frameworks (MOFs) and β -cyclodextrin (β -CD) polymers - prototypical examples of inorganic porous materials and polymers, respectively, which have recently been proposed for technological applications in water purification. By combining bulk- and surface-sensitive, spatially resolved ultrafast vibrational spectroscopy with many-body molecular dynamics simulations, we aim at gaining broad insight into the structure and mobility of nanoconfined water in MOFs at various length scales. Analogous studies of salt solutions in MOFs will shed light on the molecular mechanisms as well as key solute-framework and water-framework interactions that govern the adsorption and transport of small ions through nanopores with different sizes, shapes, and degrees of hydrophobicity/hydrophilicity. Finally, measurements of spatially-resolved, surface-sensitive vibrational spectra will probe water heterogeneity in β -CD while many-body molecular dynamics simulations will be used to characterize domain-specific, structure-binding affinity relationships.

There are no publications to report because this is a new award, with a start date of September 15, 2018.

Water in Heterogeneous Nanoconfinement



Studies of surface adsorbate electronic structure and femtochemistry at the fundamental length and time scales

Hrvoje Petek (*petek@pitt.edu*)

Department of Physics and Astronomy and Chemistry University of Pittsburgh

We study the dynamical properties of solid surfaces on the femtosecond temporal and atomic spatial scales by time-resolved multiphoton photoemission (TR-mPP) and scanning tunneling microscopy (STM). The chemical and physical properties at molecule-solid interfaces are fundamentally important for energy storage and conversion processes.¹⁻³ We have performed research on *i*) the electronic structure of alkali atom covered graphite surfaces; *ii*) alkali atom promotion of catalytic interactions on metal surfaces; *iii*) metal atom-organic molecule interactions on metal surfaces; *iv*) ultrafast (sub-femtosecond) screening of the Coulomb interaction at metal surfaces; *v*) photoinduced metal-adsorbate charge-transfer dynamics. *vi*) ultrafast coherent dynamics in mPP; *vii*) onset of the non-perturbative mPP. Here we report on *ii*), *iii*) and *vi*).

We have performed scanning tunneling microscopy (STM) on a variety of metal atom-molecule systems. In one direction we investigate 2D topological insulator (TI) properties of a metal-organic honeycomb-kagome lattice that theory predicts to have TI band structure in the absence of support, but our experiment and theory shows that on Ag(111) surface the properties are lost due to the substrate-induced Rhasba effect. We also investigate the interaction of chemisorbed alkali atoms with high energy density molecules, such as O₂. This research is inspiring new research directions in alkali atom promoted Haber-Bosch synthesis of NH₃, and other processes that involve breaking of multiple chemical bonds. We have also applied multidimensional coherent multiphoton photoemission (MDCMP) spectroscopy to study the coherent electron dynamics at Ag(111) surface. We want to develop a theoretical understanding of coherent nonlinear photoemission spectroscopy of solids. Much work has been done on coherent nonlinear *optical* spectroscopy of molecules in a variety of phases, but *photoemission* spectroscopy provides energy and momentum resolved information that is essential in the solid state. We pioneered such spectroscopy in 1997, and are still the only ones with such capability; so also want to the develop the theory. The measurements on Ag(111) have expanded our research in several directions, some of which are described.

Alkali atom promotion of catalytic interactions on metal surfaces. We have investigated interactions of K ions with O₂ molecules on Au(111) surface by low temperature (LT) STM and theory; the inspiration from interesting results, has led us (Prof. J. Zhao's group at USTC) to look into alkali atom-

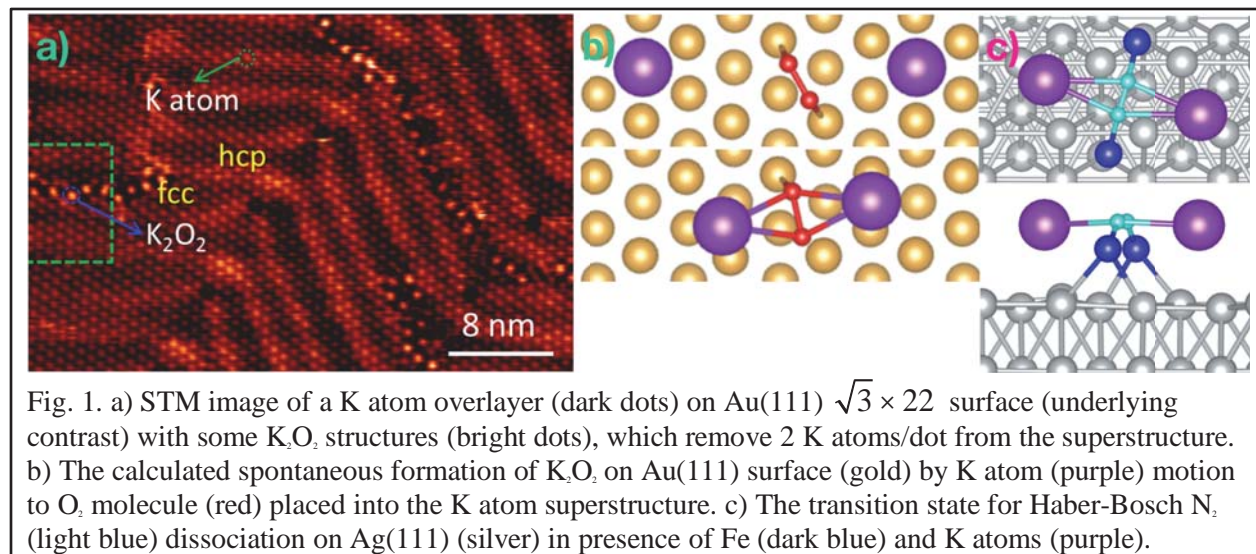


Fig. 1. a) STM image of a K atom overlayer (dark dots) on Au(111) $\sqrt{3} \times \sqrt{3}$ surface (underlying contrast) with some K₂O₂ structures (bright dots), which remove 2 K atoms/dot from the superstructure. b) The calculated spontaneous formation of K₂O₂ on Au(111) surface (gold) by K atom (purple) motion to O₂ molecule (red) placed into the K atom superstructure. c) The transition state for Haber-Bosch N₂ (light blue) dissociation on Ag(111) (silver) in presence of Fe (dark blue) and K atoms (purple).

promoted chemistry on solid surfaces. Alkali atoms on metal surfaces (eg Au(111)) are ionized at submonolayer coverage and form a hexactic liquid structure through the mutual dipole-dipole repulsion, leading to appearance of dots in the LT-STM image in Fig. 1a. Adsorption of a trace O_2 molecules produces brighter dots, where each molecule causes disappearance of two K ions. We conclude with support of DFT calculations that the bright dots correspond to K_2O_2 molecules, where K ions bind to the π -orbitals of O_2 molecules, one on each side (Fig. 1b). Theory and vibrational spectroscopy indicate that this interaction causes $\sim 1 e^-$ to be transferred to sandwiched O_2 molecules, causing the O_2 π -bond to weaken and stretch. K_2O_2 is thought to be a reaction intermediate in alkali-air batteries, but so far there have been no studies at the molecular level. We conclude that one aspect of alkali promotion of catalysis is the attraction of alkali atoms to π -orbitals and the concomitant charge transfers. This led us to investigate whether other π -orbital rich catalytic targets (N_2 , CO_2 , etc.) also experience similar interactions. For example, the rate limiting step for the Haber-Bosch synthesis of NH_3 from N_2 and H_2 is thought to be the dissociation of the N_2 triple bond. It has been proposed that N_2 is sandwiched by alkali atoms from the side, and transition metal atoms from the ends. This indeed is promising; in Fig. 1c when 2K atoms and 2Fe atoms complex N_2 molecule on Ag(111), they cause 1.2-1.3 e^- transfer to the π^* -orbital, and reducing the transition state energy by $\sim 1 eV$.

Metal atom-organic molecule interactions on metal surfaces. We have continued our studies of metal-organic molecule polymers. Previously, we demonstrated that phenylene-diisocyanide (PDI) on Au surfaces forms Au-C bonds with Au adatoms to grow Au-PDI chains. If Au adatoms form such metal-organic polymers, we wondered what happens with other metals. LT-STM studies reveal that alkali atoms bind two PDI molecules, but do not form chains. More interesting, however, is the interaction with Ag atoms on Ag(111) surface. Although Ag is a noble metal like Au, it has a stronger preference for trifold coordination. Indeed, instead of making chains, deposition of PDI molecules on Ag(111) surface leads to formation of a honeycomb-Kagome lattice, with Ag atoms at vertices and PDI molecules forming sides of

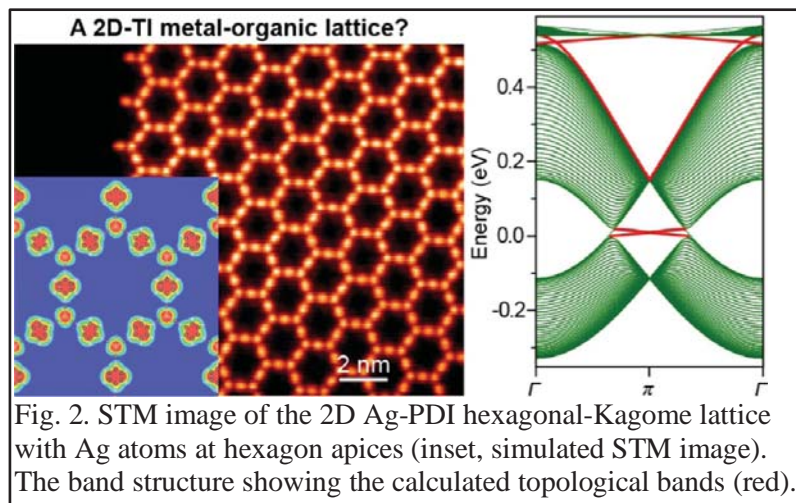


Fig. 2. STM image of the 2D Ag-PDI hexagonal-Kagome lattice with Ag atoms at hexagon apices (inset, simulated STM image). The band structure showing the calculated topological bands (red).

a hexagonal lattice. DFT calculations of an isolated Ag-PDI sheet predict that it should have Dirac points at K and K' points of the Brillouin zone, and the corresponding bands should have 2D topological character, where the edges are conductive and interior of Ag-PDI sheets is insulating. That is not observed experimentally, however. We have shown by theory that a potential at a metal surface introduces a Rashba effect that closes the topological band gaps; in fact, the Ag-PDI sheet is metallic. We expect that the Rashba effect to disrupt most potential 2D topological materials.³

Ultrafast coherent dynamics in mPP. We have applied mPP spectroscopy and interferometric TR-mPP spectroscopy to study the coherent dynamics in Ag(111). To see that the response of a metal is dominantly coherent, one just has to look into a metallic mirror, however, the coherent optical response occurs on a sub-femtosecond time scale; by performing an energy and momentum resolved mPP experiment, we have better chance of resolving the coherent electron dynamics on a more accessible time scale. We have investigated the coherent response of Ag(111) in two different experiments where the photoinduced electronic interactions are minimized and maximized. First, we investigated the coherent, nonresonant 4 and 5 photon photoemission from the occupied Shockley surface (SS state near the Fermi level (E_F) of Ag(111) with IR ($\sim 1.5 eV$) light. The location of SS electrons at a surface near E_F , insures that they have the minimum interactions with the many-body system. We also simulated the interferometric mPP signals by an optical Bloch equation (OBE) model. The interferometric mPP measurements indicate

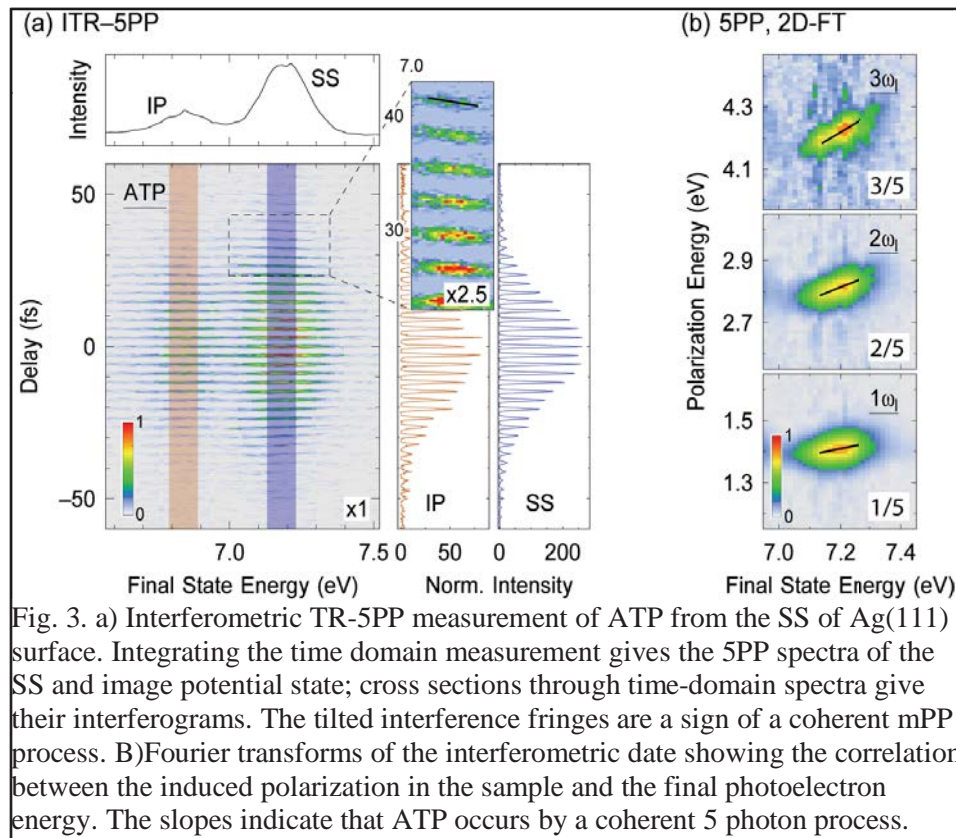


Fig. 3. a) Interferometric TR-5PP measurement of ATP from the SS of Ag(111) surface. Integrating the time domain measurement gives the 5PP spectra of the SS and image potential state; cross sections through time-domain spectra give their interferograms. The tilted interference fringes are a sign of a coherent mPP process. B) Fourier transforms of the interferometric data showing the correlation between the induced polarization in the sample and the final photoelectron energy. The slopes indicate that ATP occurs by a coherent 5 photon process.

that 4 and 5 photon photoemission occurs by excitation of coherent polarizations which oscillate, respectively, at 4ω and 5ω frequencies (Fig. 3). This demonstrates that the multiphoton absorption for a nonresonant process is entirely coherent, and is well suited for the OBE analysis, which gives us a good entry point for theoretically simulating the excitation process. Significantly, we see an above-threshold photoemission (ATP) process where the penultimate level in mPP is above the work function, but SS

electrons absorb one more photon than necessary to induce photoemission. Such ATP signals have been reported before, but have been attributed to a process where electrons are excited to a photoemission state, from where, before escaping into vacuum, they absorb another photon (4+1 photon process). Our study shows that the ATP occurs by the rectification of 5ω polarization (5 photon process) and does not involve the intermediate population of a 4-photon state. Thus, our OBE analysis of the coherent multiphoton interaction is able to distinguish the excitation pathways at metal surface. We are extending such studies to photon energies that increase interactions of the coherent polarizations with intermediate excited states.

In another direction, we also investigated the response of Ag(111) surface to UV light as the excitation is tuned through the $\epsilon(\omega)=0$ region. At $\epsilon(\omega)=0$, the response of a material to the optical field is nonperturbative, and nonlinear processes are strongly enhanced because the lowest order polarization excited in the sample is zero, and higher nonlinear orders of polarizations dominate. The $\epsilon(\omega)=0$ condition determines the bulk plasmon frequency of a metal. At $\epsilon(\omega)<0$, the plasmonic response of a metal screens the external field by setting up an opposing field that reflects the incoming field on the time scale of the inverse plasma frequency (<1 fs). For $\epsilon(\omega)\geq 0$, the optical field propagates through a metal as bulk plasmon excitations, since the electronic system cannot respond fast enough to screen the field. The $\epsilon(\omega)=0$ condition for Ag(111) surface occurs at 3.8-3.9 eV, and the consequent collective plasmonic response is fundamentally related to other plasmonic phenomena of interest to physics, chemistry, and nanotechnology.

We have measured 2PP spectra of Ag(111) surface for $\hbar\omega=2.6-4.5$ eV (Fig. 4). The spectra have surface state contributions, which are not of interest here, and have been studied extensively. In addition, there is signal from two-photon resonant absorption from the lower bulk *sp*-band (L_s) to the upper *sp*-band (U_s); this SP transition is particularly sensitive to the near surface optically induced fields. We find that this signal dominates 2PP spectra for $\hbar\omega=3.4-3.5$ eV, but disappears above $\hbar\omega=3.9$ eV. We conclude that the screening response causes intensification of the near surface fields due to the multipole plasmon screening response below the bulk plasma frequency. Above the bulk plasmon frequency the electronic system cannot respond to intensify the surface field, and the excitation propagates through metal as a charge density wave. At the bulk plasmon frequency, we observe another signal at 7.75 eV, which does not change with $\hbar\omega$ and

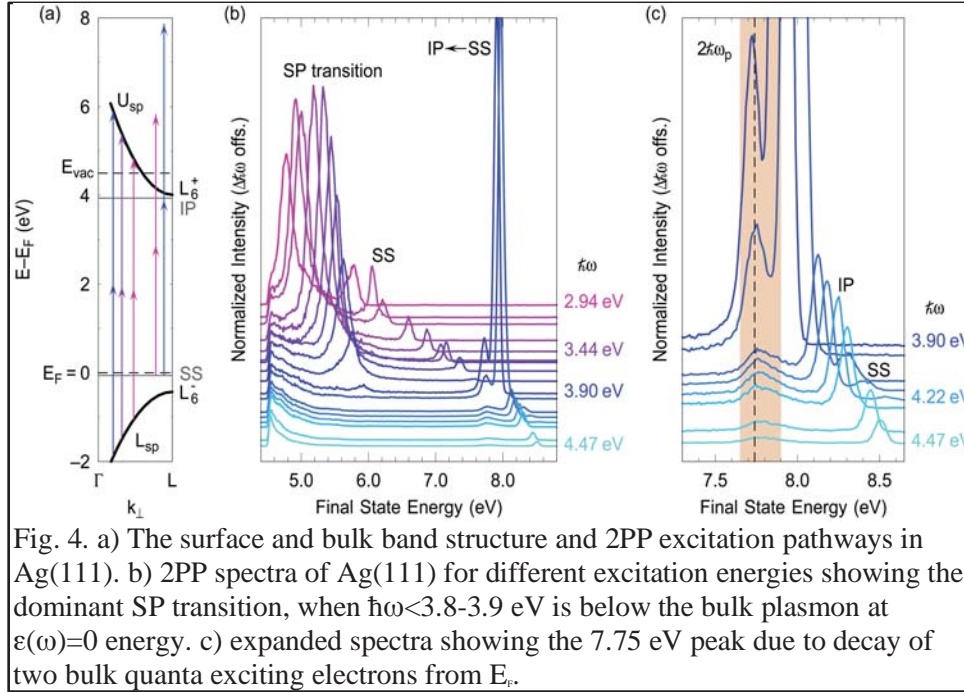


Fig. 4. a) The surface and bulk band structure and 2PP excitation pathways in Ag(111). b) 2PP spectra of Ag(111) for different excitation energies showing the dominant SP transition, when $\hbar\omega < 3.8-3.9$ eV is below the bulk plasmon at $\epsilon(\omega)=0$ energy. c) expanded spectra showing the 7.75 eV peak due to decay of two bulk quanta exciting electrons from E_c .

is most intense for $\hbar\omega=3.9$ eV, the bulk plasmon frequency. This is highly unusual in mPP spectroscopy, and it can signify that the photoemission signal involves the excitation of an energy localized final state, which in the case of Ag(111) surface, does not exist. Instead we assign it to a decay of two bulk plasmons exciting electrons from E_c to produce the $\hbar\omega$ -independent signal at 7.75 eV. Thus, the 2PP measurements in the

$\epsilon(\omega)=0$ region provide information on the collective plasmonic excitation from single-particle spectra.

DOE supported publications 2016-2018.

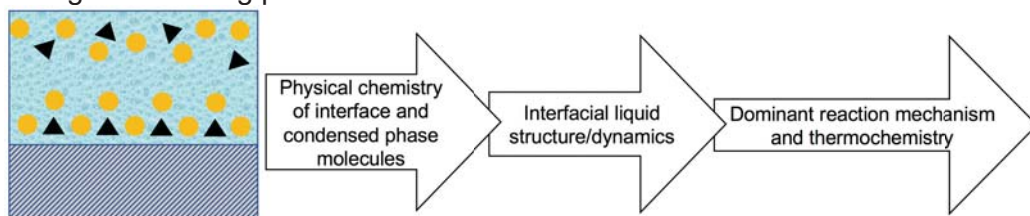
- 1 S. Zhang, C. Wang, X. Cui, Y. Wang, A. Argondizzo, J. Zhao, and H. Petek, Phys. Rev. B **93**, 045401 (2016).
- 2 H. Petek, APS Physics **9**, 123 (2016).
- 3 H. Sun, S. Tan, M. Feng, J. Zhao, and H. Petek, J. Phys. Chem. C **122**, 18659 (2018).
- 4 M. Reutz, A. Li, and H. Petek, Phys. Rev. X (<https://arxiv.org/abs/1807.09164>).
- 5 M. Reutz, A. Li, B. Gumhalter, and H. Petek, Phys. Rev. Lett. (arXiv:1809.02101 [cond-mat.mes-hall]).

Understanding molecular scale chemical transformations at solid-liquid interfaces – computational investigation of interfacial chemistry in electrolytes and charged interfaces

Jim Pfaendtner

University of Washington, Chemical Engineering (100% FTE)
PNNL, Senior Scientist (via UW/PNNL dual appointee program) (0% FTE)
Benson Hall | Seattle, WA 98195-1750 | jpfaendt@uw.edu

Project Motivation: Understanding the molecular and nanoscale mechanisms of chemical reactions occurring at a liquid/solid interface is critically important to a huge range of processes. Compared with homogenous chemistry in a bulk condensed or gas phase, the modeling toolkit for predicting an interface-mediated reaction mechanism is far less developed, with many researchers falling back on individual reaction-by-reaction studies guided by chemical intuition. While very powerful, these methods are often not equipped to handle the challenges of interfacial materials chemistry where intuition can break down, or the enumeration of individual reactions becomes too complex (e.g., as in the growth of a new material via controlled deposition or formation of decomposition products in batteries). This project is precisely motivated by challenges such as this in understanding chemistry at liquid/solid boundaries. Computer simulations can play an important role in developing fundamental molecular understanding and creating predictive models.



Concept: Molecular scale interactions between a solid interface and substituents of a condensed phase give rise to unique structure and dynamics, eventually leading to specificity in the emergent chemical reaction network.

Project Goals: The proposed work will develop new computational approaches that address time scale limitations with a suite of enhanced sampling tools. The work proceeds in three objectives using two types of model systems: electrolyte decomposition in batteries and bio-inspired materials self-assembly (silica and titania) over charged interfaces. Objectives:

1. Probe equilibrium structure and dynamics at interfaces with classical and semi-classical MD methods to study how physical/chemical interactions at an interface combine with the properties of the solvent to guide the final structure.
2. Use a special metadynamics based method for high dimensional sampling to determine reaction networks in the condensed phase at interfaces. We will study the reaction network and mechanism across a wide range of model systems to understand the connection between the interfacial properties and the emergent chemistry. Selected reaction pathways are further studied with kinetics-based approaches to also study the interfacial dependence on rates.
3. Determine how the choice of background ions changes the emergent chemistry at interfaces in selected model chemistries.

There are no publications to report because this is a new award, with a start date of September 15, 2018

Probing Condensed-Phase Structure and Dynamics in Hierarchical Zeolites and Nanosheets for Catalytic Upgradation of Biomass

Neeraj Rai

330 Swalm Chemical, Mississippi State University, Mississippi State, MS, 39762

Email: neerajrai@che.msstate.edu

Program Scope

Understanding complex reactions at the molecular level in systems characterized by multiscale collective coupling across time and space is a significant scientific challenge. This project is guided by the hypothesis that interactions of oligomers, solvents and active sites can be tailored by a suitable choice of solvent and also of pore architecture of solid-acid catalysts to promote chemical transformations during catalytic conversion of biomass. The architecture is determined by the choice of hierarchical zeolites, which provide large channels for macromolecule diffusion and small pores for catalysis. A multiscale computational approach will be used to elucidate physical and chemical interaction across multiple spatial and temporal scales. Furthermore, advanced first principles Monte Carlo algorithms will be developed to efficiently sample configurational space. We will use advanced first principles Monte Carlo and molecular dynamics simulations, and electronic structure calculations to answer fundamental scientific questions pertinent to acid catalyzed hydrolysis and hydrogenolysis of cellulose and lignin, respectively, in ordered mesoporous zeolitic structures. One outcome will be a better understanding of the fundamental interactions of reactant and solid acid catalysts in the presence of solvents, enabling rational design of catalytic systems that can upgrade biomass in a selective and energy efficient manner. Another outcome will be the development of sampling tools essential to detangle interactions in complex, reactive phenomena.

Recent Progress

Diffusion of Glucose Molecules in Nanopores of Beta Zeolite in the Condensed Phase: Our initial focus has been to understand diffusion of glucose and solvent molecules in the nanopores of zeolites Beta.

We have conducted molecular dynamics simulations in *isothermal isobaric ensemble* to elucidate the diffusion mechanism. A model of zeolite supercell was generated and the dangling bonds were saturated with hydrogen atoms. Glucose and solvent molecules were subsequently added to the system. Simulations were started with no solvent and glucose molecules in the nanopores. As the simulation progresses, solvent and glucose molecules diffuse in the pore till the equilibrium is reached. Figure 1) provides snapshot of the system after equilibration. We find that number of glucose molecules in the pores increases as the temperature increased, while the number of water molecules goes down. With respect to the pressure, however, there is not much change in the pore filling. We also find that dynamics of solvent and glucose inside the pores slows down by an order of magnitude compared to glucose solution outside the zeolite framework. Although water molecules are able to diffuse into the smaller pores, glucose molecules reside primarily in the large pores (pore diameter $\approx 0.7nm$).

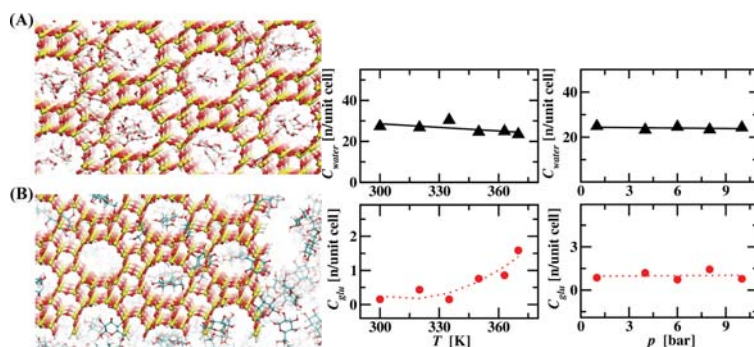


Figure 1. The snapshot of water (A) and glucose (B) molecules in the nanopores of Beta zeolite. Plots on the right show number of glucose or water molecules per unit cell as function of temperature and pressure.

Effect of Nanosheet Surface Termination on Binding Modes of Model Compounds with Ether Linkage:

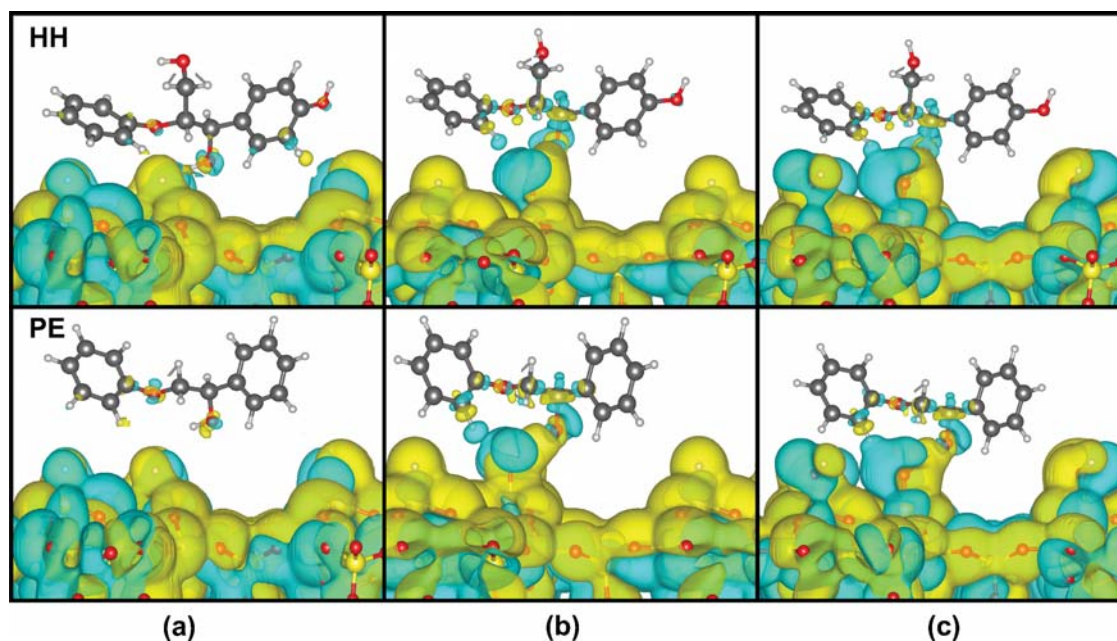


Figure 2. Electron density difference plots during binding of lignin dimer HH and PE on (a) H:OH = 100:0 % , (b) H:OH = 50:50 %, (c) H:OH = 0:100 % terminated surface. Green and yellow represent regions of charge density depletion and accumulation, respectively. The isosurface level is $0.002 e/a_0^3$ (where a_0 is the Bohr radius) for all structures.

We have initiated electronic structure calculations to understand the binding modes of model compounds with β -O-4 linkages (1-(4-hydroxyphenyl) 2-phenoxy-1,3-propanediol (HH) and 2-phenoxy-1-phenylethanol (PE)) on MWW 2D zeolite nanosheets. Brønsted acid site was introduced by replacing one of the silicon atoms with aluminum atom and the charge was compensated by introducing proton on the bridging oxygen (see Figure 2). We have used PW91 and optB88-vdW density functionals for these calculations. The effect of different surface termination ($-H$ vs $-OH$) on electron charge density is shown in Figure 2. Although the binding energies for PW91 functional are 10-15 kcal/mol smaller than the optB88-vdW functional, the qualitative trends are similar, i.e. as we increase the density of $-OH$ group on the surface of MWW 2D nanosheet, the binding energy increases. We have also carried out *ab initio* molecular dynamics simulations in the presence of solvents. We have investigated the effect of different terminated surfaces (H:OH % = 100:0; 50:50; 0: 100 %), different temperatures (323, 353, 373 K), and different solvents (water and methanol) on the binding modes by calculating physical parameters such as bond angles and bond length. Our work shows that binding strength is enhanced by increasing number of hydroxyl groups on the surface, and binding energy varies from 10 to 15 kcal/mol in the gas phase. Also, phenolic dimer shows better binding strength than the non-phenolic dimer and the presence of solvents has significant impact on the binding configuration of both dimers. Overall, MWW framework is characterized by first principles DFT calculations, with the aim of gaining detailed insights into the different binding modes of β -O-4 linkages on the catalytic surface to observe further complete reaction mechanisms for cleavage of β -O-4 linkages of lignin.

Effect of Molecular Structure of Phosphonium Based Ionic Liquids (ILs) on IL/Water Interface :

Phosphonium based phase-separable ionic liquids (PSILs) are promising green solvents for dissolution of cellulose and lignin, a necessary step for conversion of biomass to fuels and chemicals. The knowledge of interfacial behavior of ionic liquid/solvent systems is critical for designing efficient dissolution processes. Molecular dynamics simulations were carried out for aqueous interface of tetraalkylphosphonium ionic liquids with chloride and acetate as anions to investigate IL miscibility with water. The transition zone from miscible to immiscible behavior was observed for alkyl chain lengths of 6 to 8. Emulsion phase was

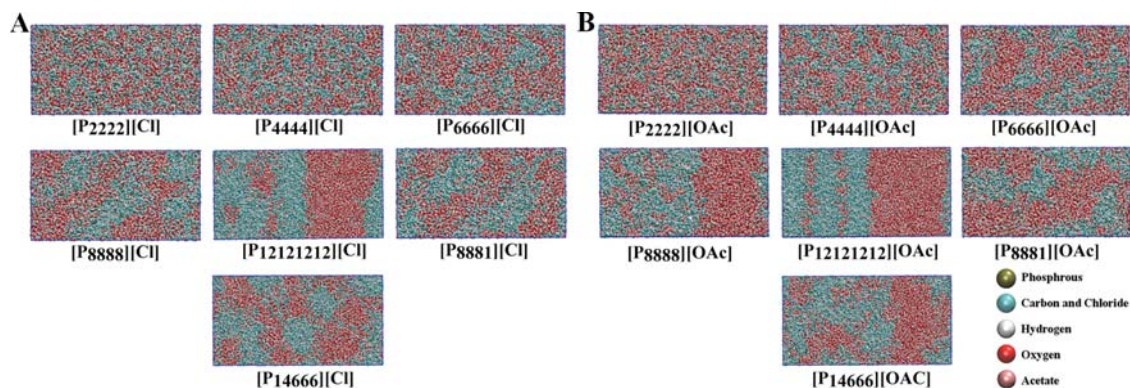


Figure 3. Snapshot at the end of 80 ns of MD simulation of phosphonium chloride (Figure A) and acetate (Figure B) ILs and TIP3P water mixture for alkyl chain length of 2, 4, 6, 8, and 12 (for the alkyl chain length of 12, a snapshot at the end of 190 ns is shown in the figure).

observed for $[P_{8888}]^+$ ion and multiple IL/water interface was observed for $[P_{12121212}]^+$ phosphonium cation. IL/water interface is observed to be enriched with solvated anions with phosphorous atom oriented towards the aqueous phase. The diffusion of chloride and acetate ions into aqueous phase was observed as these ions are better solvated in the aqueous phase. The analysis of selected pair interactions provides insights into the nature of intermolecular forces and the role of the alkyl side chains on the interfacial properties.

Implementing Advanced Monte Carlo Algorithms in CP2K:

Our initial focus has been developing a suitable data structure that will be efficient for first principles simulations. As a result, we are representing complex molecules using graph data structure, where, each atom represents a node of a undirected graph and each bond represents an edge of graph. This approach allows us to efficiently schedule the growth of molecule in condensed phase. Similar to graph traversal mechanisms, we are working on both breadth first search and depth first search approaches to grow the molecule starting from a random atom. A molecule can be decomposed into multiple fragments based on functional groups, backbones and rings. We are using a depth first search algorithm to detect the ring structure in a molecule. In a graph data structure, each fragment corresponds to a node and fragment connectivity represents edge of graph.

Future Plans

In the next year, we will look at the the diffusion mechanism of different solvent and probe molecules in zeolites with topologies. Condensed phase simulations with oligomers will be started to understand the effect of molecular structure on transport. Reaction mechanism for lignin depolymerization in the presence of solvents will be started. We will test the sampling efficiency of advanced Monte Carlo algorithms on the lignin model compounds on the surface of zeolite nanosheets.

List of Publications

This project has not resulted in any publications yet.

MOLECULAR STRUCTURE, BONDING AND ASSEMBLY AT NANOEMULSION AND LIPOSOME SURFACES

PI: Geraldine Richmond, 1253 University of Oregon, Eugene, OR 97403

Email: richmond@uoregon.edu

Program Scope and Definition

Nanoemulsions and microemulsions enable solvation of oil into water (or vice versa), which provides a unique platform for many different biological and industrial applications. Nanoemulsions, unlike microemulsions, have seen little work done to characterize molecular interactions at their surfaces. With time, nanoemulsions destabilize and eventually separate into their respective phases with the process initialized by either coalescence or Ostwald ripening mechanisms. Molecular species, such as surfactants adsorbed to the droplet interface, can significantly extend nanoemulsion stability by increasing the steric hindrance or electrostatic repulsions between droplets, along with lowering the interfacial tension between the two phases. Although there have been many studies of nanoemulsion stability in bulk solutions there is a lack of understanding on a molecular level of how molecules assemble and bond at the oil/water junction at the surface of nanoemulsions.

The objective of these studies is to advance our understanding of the molecular structure, orientation and bonding of surfactants at the surface of nanoemulsions and liposomes, and analyze the bonding characteristics of interfacial water near soft particle interfaces. Our approach involves measuring the surface vibrational spectroscopy of the surfactant coated particle surfaces in-situ using vibrational sum frequency scattering spectroscopy (VSFSS), with related complementary studies of these surfactant systems examined at the more well-defined planar oil/water interface by vibrational sum frequency spectroscopy (VSFS). Classical molecular dynamics (MD) calculations coupled with density functional theory (DFT) methods are employed to assist in spectral assignments and understanding solvation effects. Other experimental techniques such as dynamic light scattering (DLS), zeta potential (ZP), and surface tension (ST) are being used. Our recent publication investigating AOT stabilized nanoemulsions provides a powerful demonstration of our approach.¹

Recent Progress on Synergistic Effects of Polymer-Surfactant Adsorption at Oil/Water

Polymer-surfactant (PS) mixtures stabilize nanoemulsions in drug delivery, food science, and industrial applications, among others. They can be classified into the categories of *weakly* interacting systems, composed of ionic surfactants and non-ionic polymers, and *strongly* interacting systems composed of oppositely charged ionic surfactants and polyelectrolytes. For the former, the dominating intermolecular interactions are hydrophobic, with weak electrostatic contributions. For strongly interacting PS mixtures – the focus of the studies described below – both electrostatic and hydrophobic forces appear to be important. Although the true molecular structure of these strong PS complexes at the nanodroplet surface is still unknown, we have made significant progress studying the assembly of these complexes at the planar oil/water (O/W) interface. Prior research using neutron scattering, x-ray scattering, and surface tension measurements at air/water interfaces suggests that strongly interacting PS systems form ordered interfacial layers. Several groups propose a layer-by-layer growth mechanism, where oppositely charged polyelectrolytes (PEs) are alternatively added to the nanoemulsions to create thicker polyelectrolyte “shells” on top of the pre-existing layered structures. The first layer is thought to be the most crucial with respect to subsequent layer structure. Systems showing multilayer adsorption ($\geq 60 \text{ \AA}$) are classified as “type 1”; those with monolayer of $\sim 20 \text{ \AA}$ are labeled “type

2". Tetramethylammonium surfactants (C_n TAB) coupled with anionic PEs can form either type 1 or 2 depending on the chain length (n). We have chosen two systems for study this past year with the results detailed below.

A. Cetyl trimethylammonium bromide (C_{16} TAB) and Polystyrene Sulfonate (PSS)

The C_{16} TAB and PSS stabilized nanoemulsions are important to study due to their many uses, such as for drug delivery. Our studies of this PSS: C_{16} TAB system² have first examined the stabilization of nanoemulsions using C_{16} TAB alone, where C_{16} TAB forms stable nanoemulsions of ~ 200 nm ZP values near +80 mV. Figure 1 shows a VSFSS spectrum in the CH stretching region of the alkyl chains of C_{16} TAB at the surface of 250 nm nanoemulsions for three C_{16} TAB concentrations. Both methyl and methylene peaks appear, with the intensities of these modes indicating that C_{16} TAB, in the mM concentrations range, the alkyl chains are considerably disordered.

Upon addition of PSS to the 0.1 mM C_{16} TAB emulsions, we find that the polymer readily adsorbs to the nanoemulsions surface, indicated by the decrease in ZP.

When C_{16} TAB and PSS monomers are present at equal concentrations, the ZP is approximately zero, indicating charge neutralization at the interface. With increased PSS, the ZP continues to decline until a PSS: C_{16} TAB ratio of ~ 50 , where the ZP plateaus around -110 mV. The use of deuterated C_{16} TAB allows measurement of only PSS alkyl signal with VSFSS. Figure 2 shows the CH spectrum as a function of PSS: C_{16} TAB ratio. PSS CH modes increase as the ratio moves from 0.1:1 to 100:1. Once the ratio crosses the equimolar region, PSS CH modes appear, indicating that the polymer backbone is relatively well ordered. These studies show that at low PSS concentration C_{16} TAB dominates the interface, but as PSS is added an ordered layer forms, induced by electrostatic interactions. Another interesting observation is the clear time dependence of polymer signal. The CH signal of the polymer at higher PSS/ C_{16} TAB ratios slowly grows in with time, reaching a stable signal after ~ 2 hours. This could be due to slow adsorption to the surface or a gradual

reorientation of the adsorbed polymer, and will be explored in future work. It is clear, however, that we are able to monitor these adsorption processes, allowing us further studies to understand the balance between surface hydrophobic, hydrophilic and electrostatic factors of this important system.

B. C_{16} TAB + Polyacrylic acid (PAA)

Polyacrylic acid (PAA) has been used industrially as a desiccant and emulsifier. PAA's simple structure makes it a model polymer for studies involving carboxylate chelation and fractional polymer ionization. The interfacial activity of PAA at an oil/water interface exhibits pH-tunable behavior.³ Below pH 4.5, PAA forms an initial ordered polymer layer with

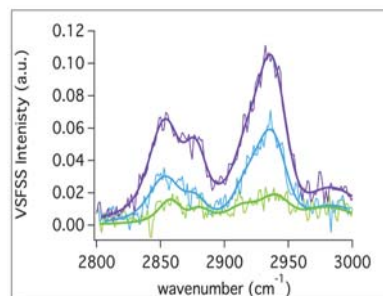


Figure 1. VSFSS (SSP polarization) of 0.1 mM (green), 0.5 mM (blue) and 1.0 mM (purple) C_{16} TAB at the hexadecane nanoemulsion interface. Shown are contributions from the CH methyl and methylene modes.

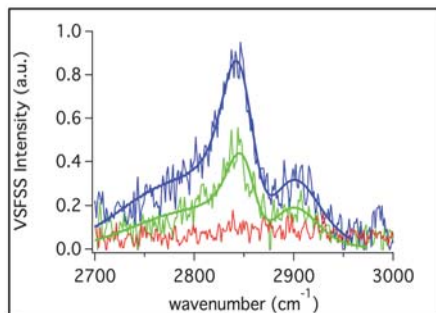


Figure 2. VSFSS (SSP polarization) spectrum of PSS/d- C_{16} TAB stabilized nanoemulsions at concentration ratios of 0.1 (red), 10 (green) and 100 (blue). d- C_{16} TAB concentration constant at 0.1 mM. The peaks are assigned to the CH SS and AS modes of the backbone of the polymer.

subsequent disordered layers. Above pH 4.5, deprotonation of PAA's carboxylic acid groups cause it to remain fully solubilized in the aqueous bulk. C₁₆TAB and PAA exhibit extreme ST lowering at the oil/water interface, which make them promising candidates for emulsion applications. Interfacial studies of PAA/surfactant systems are rare, but indicate the two components interact through a mix of hydrophobic and electrostatic interactions. Furthermore, these interactions are extremely dependent upon concentration and pH, opening the possibility of precise interfacial tuning.

In the most recent publication to come from this grant,⁴ the PAA/C₁₆TAB surface structure was found to be highly dependent upon PAA concentration. By utilizing a fully deuterated surfactant, vibrational modes from each component (polymer, surfactant, and water) were isolated and studied with VSFS. Corroborating ST and ZP were used to thoroughly examine the bulk-to-surface partitioning of this unique system. Ultimately, the system was found to have 3 different "regimes" of interfacial structure, dependent upon PAA concentration, which are represented in Figure 4.

At very low PAA concentration (Regime I), the system exhibits remarkable interfacial synergy, as indicated through a doubling in surface pressure over that of C₁₆TAB alone. In this regime, however, only vibrational signatures from C₁₆TAB and interfacial water are detected. PAA's interfacial presence was revealed through a lowering of the surface tension and interfacial charge compared to C₁₆TAB alone. In Regime I, the surface interactions between PAA and C₁₆TAB are largely hydrophobic, and the dipoles of adsorbed PAA do not have a net orientation. We hypothesize that the structure of adsorbed PAA is that of a loose coil, as it is in bulk. As PAA concentration is increased to the equimolar point, surface tension drops sharply and the system enters Regime II.

In Regime II, an increasing PAA concentration leads to simultaneous decrease of surface tension and interfacial charge, along with an increase in COO⁻, COOH, and CH modes unique to the polymer. The uncoiled polymer has a net orientation at the interface in this and the next regime. C₁₆TAB and PAA primarily interact through electrostatic binding. Though adding more PAA further increases adsorption, only the carbonyl and alkyl modes increase in signal, meaning additional carboxylate moieties exist on charged segments extending into the aqueous phase. At the system's isoelectric point, the interface exhibits the highest degree of adsorption and lowest amount of interfacial charge.

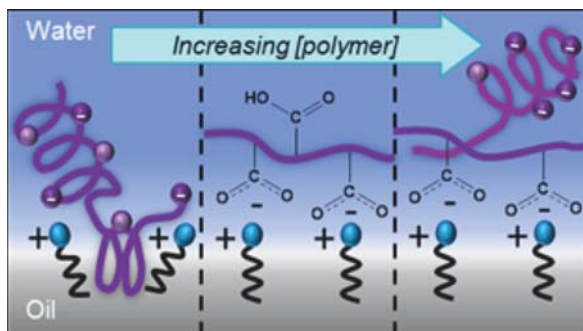


Figure 3. Cartoon depicting the interfacial co-adsorption of PAA and C₁₆TAB for Regime I (left), Regime II (center) and Regime III (right) at the CCl₄/H₂O interface.

Beyond the isoelectric point, the system enters Regime III. A slight pH increase deprotonates PAA, and the net interfacial charge is negative. Like-charge repulsions prevent further PAA adsorption, and may serve to introduce interfacial disorder. However, the strong electrostatic binding between carboxylate and C₁₆TAB headgroups keeps the polymer extended and oriented. At this concentration, the interface is saturated with PAA, and additional PAA stays in bulk.

It is clear from this study that, even at low concentrations, both hydrophobic and electrostatic interactions dictate synergic interfacial properties. Structural observations made herein are relevant for efforts using polymers as emulsion stabilizers or interfacial templates. High polymer/surfactant ratio leads to interfacial overcharging due to a slight pH change, but

there is no evidence of multilayer formation at any concentration of polymer. Further interfacial layers would best interact with PAA's oriented carboxylic acid groups. This summary has only scratched the surface of these findings, which provide much needed molecular details otherwise lacking in previous studies.

Future Studies

In the coming year we will be working on several projects:

- The studies involving C₁₆TAB and PSS described above will be continued as we seek to understand the time dependence in the encapsulation of these C₁₆TAB stabilized nanoemulsions with multiple layers of PSS. The combination of VSFSS, ST and DLS will be important in these time dependent studies.
- Another project currently in progress will examine the co-adsorption of dodecyltrimethylammonium bromide (D₁₂TAB) with PSS. We have begun this project with VSFS studies of co-adsorption at the planar oil/water interface. Extension of these studies to D₁₂TAB/ PSS nanoemulsion interfaces will follow after full spectral interpretation and adsorption characteristics at the planar interface is determined.
- We have just begun a new project involving sodium dodecyl sulfate (SDS) combined with polyethylenimine (PEI). Co-adsorption of this polymer and surfactant can lead to very stable nanoemulsions but there is much uncertainty about the mechanism of adsorption. We are interested in exploring how changes to the pH, ionic strength and temperature affect the interfacial layering on the surface of nanoemulsions through VSFSS, ST and DLW. This is motivated by the broad application of these nanoemulsions in a variety of medical and technological applications.
- We will be continuing our computational studies that augment our VSFSS and VSFS studies and assist in spectral assignments as well as surfactant adsorption characteristics. To this goal we are developing a "stitching" method to compute C₁₆TAB anharmonic frequencies, which will be used in conjunction with MD simulations and DFT calculations to model VSF data.

Publications referenced above that have resulted from the studies sponsored by this grant.

- [1] "Molecular characterization of water and surfactant AOT at nanoemulsion surfaces". J.K. Hensel, A.P. Carpenter, R.K. Ciszewski, B.K. Schabes, C.T. Kittredge, F.G. Moore, G.L. Richmond, *PNAS*, **2017**, 114 (51), 13351
- [2] "Under wraps: molecular details of polyelectrolyte adsorption onto surfactant stabilized nanoemulsions", A.P. Carpenter and G.L. Richmond, *manuscript in preparation*.
- [3] "Come Together: Molecular Details into the Synergistic Effects of Polymer-Surfactant Adsorption at the Oil/Water Interface", B. Schabes, R.M. Altman, G.L. Richmond, *J. Phys. Chem. B*, **2018**, 122 (36), 8582-8590

Enhancing Rare Events Sampling In Molecular Simulations

Ryan DeFever¹, Steven Hall¹, and Sapna Sarupria¹

¹Chemical and Biomolecular Engineering
Clemson University, Clemson SC

Rare events correspond to the events that occur with low frequency. These events usually have potentially widespread impact and are therefore, events of considerable interest. At the molecular level, important transitions such as self-assembly and phase transitions in aqueous systems are rare events – meaning that the waiting time involved to observe even a single event is larger than the typical timescales accessible to molecular simulations. This hinders the ability to calculate the kinetics of these transitions. In our proposed research we focus on developing novel methods and the software infrastructure that implements these methods effectively on high performance computing systems to enable the studies of rare events in molecular simulations. While we motivate our work through studies of heterogeneous ice nucleation, the methods and software infrastructure developed here is applicable to any system.

In our previous work, we developed software called SAFFIRE (previous called Scalable Forward Flux Sampling (ScaFFS)) to perform large scale forward flux sampling (FFS) calculations efficiently and effectively in high performance computing (HPC) infrastructure. In FFS, transitions from state A to state B are sampled through several intermediate transitions by dividing the phase space between A and B into sub-regions marked by interfaces. Several simulations are initiated at a given interface and configurations from those which reach the next interface are harvested. Then several simulations are initiated from the harvested configurations at the “new” interface to obtain configurations for the next interface. This process is continued until the final state is reached. While the process is straightforward, the application of the method to realistic systems can result in large number of simulation jobs and huge amount of data. To handle these large jobs and amounts of data effectively, we have developed SAFFIRE. SAFFIRE represents a collaboration of state-of-the-art techniques in molecular simulations with those from Big Data to enable rare event simulations at massive scales. SAFFIRE is designed to be adaptive, data-intensive, high-performance, elastic, and resilient. SAFFIRE uses Hadoop in a novel manner to handle the millions of simulations performed and files generated in FFS calculations. Through this approach we have been able to address several of the challenges related to implementing FFS.

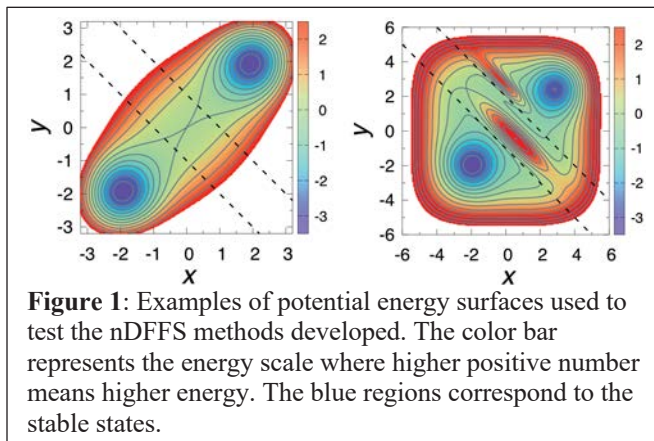
Using SAFFIRE we have performed some of the largest scale FFS studied of ice and hydrate nucleation. We find that even with these extensive simulations, large number of successful transition pathways arise from a handful of configurations at the initial stages of the transition. This is further challenging because it cannot be predicted *a priori* whether the starting configurations will lead to successful transition pathways and therefore, it cannot be corrected for without performing the largescale simulations! This necessitates developing methods that overcome these challenges. In this project we use a multipronged approach to develop methods that address such challenges.

Program Scope and Definition: In our project, we combine state-of-the-art tools in molecular simulations, BigData and multitasking handling systems, and visualization techniques to develop a robust infrastructure for performing rare event simulations. We build FFS to develop multidimensional FFS methods (nDFFS) that will enable us to address the issue of finding appropriate order parameters for any given transition on-the-fly. This methodology has the potential of addressing the major knowledge gap – lack of an ability to find reaction coordinates on-the-fly – in simulations of rare events. We do so by simultaneously developing novel FFS based methods,

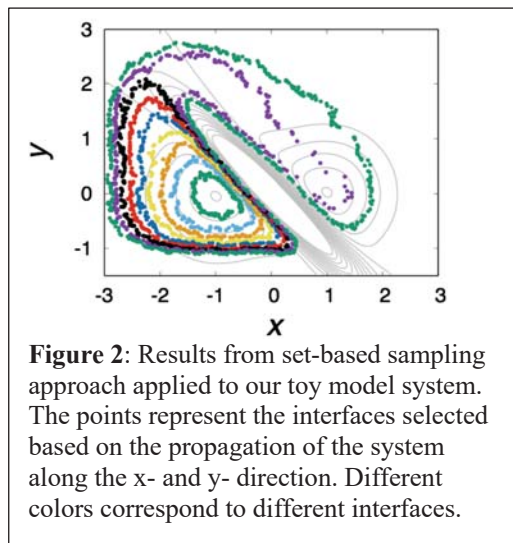
integrating them with machine learning techniques and assimilating it into SAFFIRE to test our methods beyond test cases – on more realistic systems such as ice nucleation.

Recent Progress:

2DFFS methods: We have developed multiple approaches to perform nDFFS calculations and studied them using toy models. Our model test case systems include several analytical two well potential energy surfaces. Examples as shown in Figure 1. Figure 1, left panel is a relatively simple two-well potential while right panel represents a more complicated potential energy surface. Our calculations illustrate that even for such a system it is possible to have “bias in the sampling” of the transition paths when using 1DFFS. We describe two methods we have developed towards performing nDFFS.



Contour Forward Flux Sampling (cFFS): In cFFS sampling, we place the interfaces by following the trajectories in multiple directions (i.e. along multiple order parameters). In this approach, the next interface is placed based on the order parameter sampling obtained from trajectories propagated at any given interface. This enables us to have any “shape” of the interface. An example of sampling from cFFS is shown in Figure. 2. As can be seen, we are able to outline the underlying potential energy surface for the non-simple toy models. We have applied this technique on the transitions with multiple transition tubes and found that cFFS is especially powerful in such cases. FFS fails to capture both transition tubes even with the best order parameter while cFFS samples to get the correct transition path ensemble. To further validate cFFS we have tested the method on the classic problem in the field of rare events – C_{7ax} -to- C_{7eq} conformational change in alanine dipeptide in vacuum. ϕ and ψ backbone dihedral angles were used as the order parameters for cFFS. The transition rate and the transition path ensemble sampled is in good agreement with previous studies.



We also evaluated the computational cost and sampling efficiency of cFFS. We compare the results between 1DFFS with suboptimal order parameter, 1DFFS with optimal order parameter, cFFS and standard Langevin dynamics. We find that in most cases 2DFFS gives us improved sampling for the same or slightly higher computational cost.

LJ nucleation: We have performed largescale FFS simulations of Lennard Jones liquid-to-solid transition. These simulations represent some of the largest FFS simulations of LJ systems. We have performed exhaustive analysis of these results in the context of classical nucleation theory. We are also using the extensive data we have generated to develop efficient

machine learning methods that can characterize the structures obtained during the nucleation process.

Future Work:

In the next year, we will focus on the following aspects of the project:

- cFFS methods: We will apply cFFS method to more challenging problems. We are specifically studying ion pairing which is known to include at least two order parameters in their reaction coordinate and nucleation of organic crystals which are expected to involve two steps.
- We are developing machine learning (ML) methods to identify and characterize the pathways obtained from our FFS studies of LJ and aqueous systems. We will use the insights from the ML techniques to further develop our cFFS methods.

The successful completion of our work will enable simulations to study the kinetics of complex processes -- an aspect that has greatly lagged behind so far. While our work is motivated by phase transitions and assembly processes in aqueous systems, rare events are relevant to a broad span of fields including telecommunications, finance, insurance, physics, chemistry, and biology. The techniques and software program developed here can easily be adapted to these systems. Therefore, our methodology and the simultaneous development of the software infrastructure to implement these methods will provide the broad scientific community with powerful tools to study previous inaccessible processes through molecular simulations.

Grant Number and Title:

DE-SC0015448 Enhancing Rare Events Sampling in Molecular Simulations of Complex Systems

Students: Ryan DeFever (PhD student)

Steven Hall (PhD student)

Equilibrium Structure and Dynamics of Aqueous Solutions and Interfaces

Richard Saykally (RJSaykally@lbl.gov), Musahid Ahmed (mahmed@lbl.gov), Phillip L. Geissler (plgeissler@lbl.gov), Kranthi Mandadapu (KKMandadapu@lbl.gov), and Teresa Head-Gordon (TLHead-Gordon@lbl.gov)

*Lawrence Berkeley National Laboratory, Chemical Sciences Division,
1 Cyclotron Road, Berkeley, CA 94720*

Program Scope:

Solvation of ions and molecules is central for governing chemical transformations in many energy technologies. Key processes include electrochemical transport, ion pair formation and crystallization, corrosion, as well as chemical reactions in solutions and at interfaces. The goal of this work is to develop predictive models of electrolyte behavior in bulk solution, at interfaces and in confined environments.

Recent Progress:

Geissler has derived and verified finite size corrections for molecular simulations of interfacial solvation.¹ These corrections presume that dielectric continuum theory (DCT) accurately describes the polarization response of water at nanometer scales and above. The remarkable accuracy of this approach establishes a simple method for extrapolation to the thermodynamic limit, an important capability for computationally assessing the applicability of simplified theoretical models for ion solvation. Using this method to evaluate nonlinear solvent response to the charging of a solute, we find that DCT fails in important ways to describe the interfacial adsorption thermodynamics of small ions. Together, these results establish a length scale below which DCT breaks down, approximately 1-2 molecular diameters. At larger scales, DCT appears to be a realistic caricature of water even in the heterogeneous environment presented by the liquid-vapor interface.

Saykally and coworkers examined ion adsorption to the model interface formed by water and graphene, comparing the results for this prototypical material interface to those from an earlier study with the Geissler group of the air/water interface.² Deep UV second harmonic generation measurements of the SCN⁻ ion, a prototypical chaotrope, determined a free energy of adsorption within error of that for air/water. However, unlike for the air/water interface, wherein repartitioning of the solvent energy drives interfacial ion adsorption, computer simulations reveal that direct ion/graphene interactions dominate the observed favorable enthalpy change. Moreover, the graphene sheets dampen capillary waves such that rotational anisotropy of the solute, if present, is the dominant (and unfavorable) entropy contribution, in contrast to the air/water interface.

As a route to further clarifying the mechanism that selectively drives ions to and away from the air/water interface, we have developed a new experiment (Deep UV Sum Frequency Generation) for measuring the complete charge transfer to solvent (CTTS) spectrum of interfacial anions, and have applied it to the prototypical cases of the iodide and thiocyanate anions.³ The spectra show significant differences from the bulk CTTS spectra, and provides a new variable for constructing general theoretical models to explain interfacial ion behavior, which are underway in the Geissler group. Our studies of ion adsorption to solid-liquid interfaces were extended to polymer systems in a first study of aqueous ion adsorption to the water-polystyrene interface, using SHG scattering spectroscopy of polystyrene bead solutions.

The powerful atom-selective probing of molecular interactions afforded by soft X-ray spectroscopy has been combined with the surface selective probing capability of second harmonic generation in the first demonstration of both resonant enhancement and surface selectivity of soft X-ray SHG at the Trieste free electron laser facility.^{4 5} The concomitant multiphoton absorption spectra of the carbon target was also quantified by both experiment and theory. These results open the door for the general study of surfaces and interfaces by these powerful new approaches.

Flexible nanoscale confinement of solvent is critical to understanding the role that bending fluctuations play on solvation processes where soft interfaces are ubiquitous.⁶⁷ Head-Gordon and coworkers showed that the phase behavior of water confined between flexible and rigid graphene sheets are remarkably different, since flexible walls introduce a very different sequence of water phases due to the possibility of phase coexistence that is impossible to observe with rigid walls.⁸

Mandadapu seeks to elucidate the complex dynamics of bulk systems and interfaces in and out-of-equilibrium using statistical mechanical principles. Mandadapu's research focus will be on understanding the dynamics of solids, particularly polycrystalline solids, which consists of single crystals oriented in different directions and solid-solid interfaces called grain boundaries. Mandadapu is currently studying the competition between crystallization and vitrification, where the size of the crystals and resulting dynamics of the grain boundaries in polycrystals depend on the formation protocols such as cooling rates. Slower cooling rates produce larger grains while higher cooling rates produce smaller grains and many a times result in glass formation. To this end, Mandadapu group developed a new model called "Arrow-Potts Model" (*In preparation*), which incorporates both the physics behind glassy dynamics and polycrystal dynamics (crystal-crystal and crystal-liquid dynamics). This is being used to study different stages of the coarsening phenomena when the system is quenched or cooled from its liquid state to the crystalline state.

Ahmed seeks to understand nucleation and crystallization from solutions where non-equilibrium pathways for molecular growth may exist and may include multi-ion complexes, oligomeric clusters, crystalline or amorphous nanoparticles and monomer rich liquid drops. X-ray spectroscopy provides a local probe of a sample's electronic structure with elemental and site-specificity and is thus ideally suited for understanding the molecular mechanisms underlying phase separation and the formation of initial solid particles in an aqueous solution, and chemical reactions in aerosols.⁹ We have developed a photoelectron spectrometer to probe the electronic structure of aqueous nanoparticles in vacuum. X-ray photoelectron spectra of organic nanoparticles measured at the carbon K-edge demonstrate a strong low kinetic energy background, explained as emission of secondary electrons caused by inelastic scattering of Auger electrons. The observed spectral features from pure water, 0.038 M NaI solution and gas-phase water molecules were explained in terms of the coexistence of frozen and liquid nanoparticles and the perturbation of tetrahedral molecular coordination by iodide anions in a surface layer of nanoparticles prepared from NaI solution.¹⁰ By varying the pH of an arginine solution, we have provided evidence that the guanidinium group is protonated even in a very basic solution, and explains why the arginine guanidinium group retains its positive charge under all physiological conditions.¹¹ This work has now been extended to probe particle growth via self-assembly when different solutes are introduced into the solution. The valence and core level electronic structure dynamics for arginine solvation is being interpreted by calculations performed by Anna Krylov (USC).

Future Plans:

Theoretical work to date has highlighted our incomplete understanding of charge asymmetry even in the bulk liquid phase. The simpler homogeneous environment already features substantial solubility differences between cations and anions of the same size, differences that dielectric theory cannot explain. Geissler and coworkers have found in simulations that quadrupole contributions can account for this discrepancy, and have identified the geometric relationship between water's dipole and quadrupole as an important source of charge asymmetry. These observations suggest an elaboration of dipole field theory that resolves a microscopic quadrupole field as well. Incorporating constraints between these fields poses a substantial theoretical challenge. As first steps, mean field treatments we will examine as well as models informed empirically from atomistic simulations.

The DUV-SHG experimental approach will be used by Saykally and coworkers to measure CTTS spectra of other surface-enhanced ions, emphasizing the study of counterion effects on the spectra. The goal is to develop a complete model of ion adsorption to aqueous interfaces with the Geissler group. Studies of ion adsorption will be extended beyond graphene-water interfaces to interfaces with both hydrophilic and hydrophobic polymers, and ultimately, to water-metal systems, seeking to quantify entropy and enthalpy effects. The use of the Trieste FERMI soft X-ray free electron laser facility will be extended to the study of liquid interfaces, using the liquid microjet technology developed by this group. The carbonate system previously investigated by X-ray absorption spectroscopy will be the first target.

Head-Gordon and coworkers will continue the study of flexible interfaces, and explore different chemistries of the surfaces using graphene oxide or other 2-D materials, or a heterogeneous mixture of two different confining materials, as well as simulating a wrinkle or modify the bending curvature of graphene to explore steric effects and surface roughness on ion distributions near a solid-liquid interface of polymer systems with Saykally.

Mandadapu plans to study the dynamics of solid-solid grain boundaries in polycrystalline solids. Preliminary results from the group using molecular simulations suggest that high-angle grain boundaries exhibit glassy dynamics, which is also observed in relatively few studies but not characterized. Future work entails detailed characterization of the phase-behaviors and the structure associated with these two-dimensional grain boundary interfaces in solids. To this end, Mandadapu plans to characterize the relaxation times of the motion of the persistent motion of atoms at the grain boundaries with respect to temperatures for different varieties of grain boundaries, which in turn provide us the molecular aspects of their large-scale mobility.

Mandadapu plans to extend the recently discovered orderphobic (Katira et al. [eLife 2016, 5, e13150](#)) effect to study solvation in crystalline materials. Most chemical reactions occur either on the surfaces of polycrystals or at the grain boundaries. It is also well known that many impurities in solids are preferentially localized to the grain boundaries, which may then participate in the associated chemical reactions. Mandadapu group plans to study a novel mechanism by which the solutes may be driven to grain boundaries, primarily due to the competition between the proximity to liquid-crystal phase transition and the existing elastic forces. Drawing from the orderphobic effect, Mandadapu propose that solutes of certain size in a bulk crystalline solid can premelt their surroundings and induce a liquid domain in their vicinity when polycrystalline systems are in proximity to liquid-crystal phase transition. These solutes induce a liquid-crystal interface with a finite line tension, either leading to aggregation in the bulk crystal or being driven to the nearby

interface due to the disorder at the interface. This hypothesis provides an additional effect in comparison to elasticity theories to understand the solvation of impurities in crystalline solids.

To probe the early stages of nanoparticle nucleation processes in solution (a liquid to solid transition), Ahmed proposes a multimodal strategy of interrogating free nanoparticles in space using X-ray spectroscopies coupled to Raman and Terahertz spectroscopy. These spectroscopies are very sensitive to water phase change and will allow for determination of experimental conditions when aqueous aerosols exist either in liquid or in the solid phase. We will explore how the interface changes upon increase of the salt concentration and decrease of amount of water in the nanoparticle. We will utilize the quantitative ability of the recently developed VMI XPS/NEXAFS techniques to measure relative amounts of different chemical elements coupled with the depth profiling to characterize the aerosol interface. The extent of the angular distribution change is proportional to the depth at which the photoelectrons are emitted. Using the unique ability of our VMI apparatus to collect 4π distribution of emitted electrons as well as their angular distribution, we plan to assess electron attenuation lengths for various multiphase systems and use the obtained information to perform depth profiling of free nanoparticles in various stages of nucleation. This will allow for the detection of early stages of salt nucleation on the surface of aerosol nanoparticles. Complementary to Mandadapu's theoretical program, probing nucleation and crystallization on size selected nanoparticles at various rates of formation should allow access to complex dynamics of solids in and out of equilibrium.

Publications Acknowledging DOE support (2017-present):

-
- ¹ Cox, S. J. and Geissler, P.L. "[Interfacial Ion Solvation: Obtaining the Thermodynamic Limit from Molecular Simulations](#)" *J. Chem. Phys.* **2018**,148, 222823. DOI: 10.1063/1.5020563
 - ² McCaffrey, D. L., Nguyen, S. C., Cox, S. J., Weller, H., Alivisatos, A. P., Geissler, P. L., Saykally, R.J. "[Mechanism of ion adsorption to aqueous interfaces: Graphene/water vs. air/water](#)" *Proc. Natl. Acad. Sci.* **2017**, 114 (51), 13369–13373. DOI: 10.1073/pnas.1702760114 (SI).
 - ³ Mizuno, H., Rizzuto, A. M., Saykally, R. J. "[Charge-Transfer-to-Solvent Spectrum of Thiocyanate at the Air/Water Interface Measured by Broadband Deep Ultraviolet Electronic Sum Frequency Generation Spectroscopy](#)" *J. Phys. Chem. Lett.*, **9**, 4753-4757 (2018) (SI)
 - ⁴ Lam, R. K., et al. "[Two-photon absorption of soft X-ray free electron laser radiation by graphite near the carbon K-absorption edge](#)" *Chem. Phys. Lett.*, **703**, pp 112-116 (2018).
 - ⁵ Lam, R. K., et al. "[Soft X-Ray Second Harmonic Generation as an Interfacial Probe](#)" *Phys. Rev. Lett.*, **120**, 023901 (2018)
 - ⁶ E. Jurrus, et al. (2018). [Improvements to the APBS biomolecular solvation software suite](#). *Protein Sci* 27 (1), 112-128.
 - ⁷ A. C. Carr, L. E. Felberg, V. A. Piunova, J. E. Rice, T. Head-Gordon, W. C. Swope (2017). [The effect of hydrophobic core topology and composition on the structure and kinetics of star polymers, a molecular dynamics study](#). *J. Chem. Theory Comput.* 121 (13), 2902-2918.
 - ⁸ L. Ruiz Pestana, L. E. Felberg, T. Head-Gordon (2018). [Coexistence of multilayered phases of nanoconfined water: the importance of flexible confining surfaces](#). *ACS Nano*, 2 (1), 448–454.
 - ⁹ M.I. Jacobs, O. Kostko, M. Ahmed, K. R. Wilson. [Low Energy Electron Attenuation Lengths in Core-Shell Nanoparticles](#), *PCCP* 19, 13372 (2017), DOI: 10.1039/c7cp00663b
 - ¹⁰ O. Kostko, B. Xu, M.I. Jacobs, M. Ahmed, "[Soft X-ray spectroscopy of nanoparticles by velocity map imaging](#)," *J. Chem. Phys.* 147, 013931, (2017), DOI: 10.1063/1.4982822
 - ¹¹ B. Xu, M.I. Jacobs, O. Kostko, M. Ahmed, "[Guanidinium group is protonated in a strongly basic arginine solution](#)," *Chem. Phys. Chem.* 18, 1503 (2017), DOI 10.1002/cphc.201700197

Molecular Theory and Modeling

Gregory K. Schenter

Pacific Northwest National Laboratory

902 Battelle Blvd. Mail Stop K1-83

Richland WA 99352

greg.schenter@pnnl.gov

The Molecular Theory and Modeling group at Pacific Northwest National Laboratory consists of Gregory K. Schenter, Liem X. Dang, Shawn M. Kathmann, Chris J. Mundy, Sotiris S. Xantheas, and Marat Valiev. Please find contributions from individual PIs in the abstract book.

The overarching goals of the Molecular Theory & Modeling Program are: 1) development of a fundamental comprehension of the driving forces, processes and phenomena, such as solvation, nucleation, assembly, transport, and reaction, in complex condensed-phase, heterogeneous and interfacial molecular environments, and 2) development of theoretical and computational methods required to accelerate scientific advances in condensed-phase and interfacial molecular science.

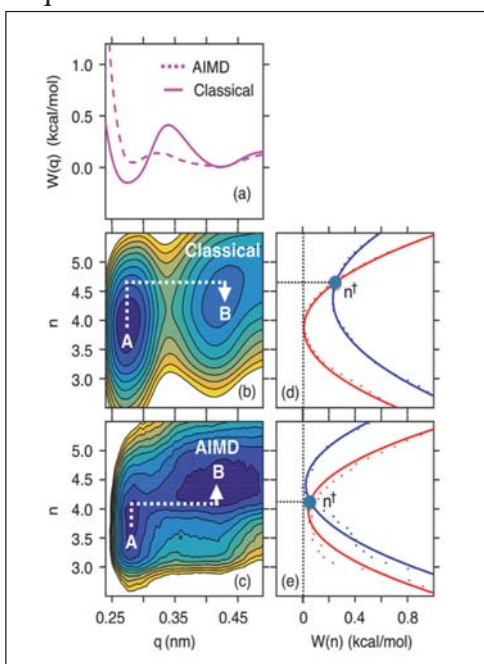


Figure 1. The qualitative features of water exchange about BF_4^- depends on the description of molecular interaction; (top, Classical) empirical vs. (bottom AIMD) electronic structure. q represents ion-water distance, n is the water coordination number. On the right are “Marcus parabola” $W(n)$. The top, $W(q)$, is the potential of mean force along the q motion.

We continue to explore the strengths and limitations of efficient electronic structure coupled to statistical mechanical sampling, constantly balancing accuracy with efficiency. To gain understanding, we generate experimental signals such as XANES to understand the solvation of aqueous Na^+ ions [1,7] as well as EXAFS techniques [12] for assessing solvation structure.

Recently we have focused on model systems to decompose the delicate balance between ion-water and water-water interactions. Many models of molecular interaction have been developed to describe the hydrogen bonding structure and fluctuations of bulk water. We have recently explored the ability of these models to respond to a hard sphere breaking up the solvation structure. [3] This includes both empirical as well as DFT models of molecular interaction. The factors that control the free energy balance of ion solvation involves the balance of this disruption of the hydrogen bonding network with the electrostatic stabilization of the ionic charge. This decomposition has allowed us to better understand the competing processes that lead to a systematic estimate of ion free energies from first principle calculations. [9,10]

In addition to the exploration of molecular interaction we are interested in understanding collective coordinates that lead to rate limiting collective phenomena such as ion pairing and water exchange. In particular, we are interested in exploring how processes change with broken symmetries such as at the water liquid-vapor interface. [2,11] Here we explore reduced

descriptions of dynamics characterized by a Generalized Langevin Equation. Traditionally, ion-water distance is chosen to characterize reactant and product states. Recently we have developed a rate theory in terms of water coordination about ions. The combination of this with the distance coordinate results in a clearer understanding of the reactive process, involving the combination of two steps, water rearrangement and solvation and ion-ion motion. This led to a "Marcus Theory of Ion-Pairing," [6] that provided a clearer picture of the spectroscopy of solvation kinetics. [5] [See Figure 1]

Much of our future efforts will concentrate on characterizing fluctuations, taking advantage of effective potentials of mean force and linear response kernels from density, charge and electromagnetic fluctuations. This will allow us to establish a connection between molecular detail and reduced frameworks for describing phenomena. In our recent work we employed electronic structure descriptions of molecular interaction coupled with statistical mechanical sampling to characterize mass density fluctuations at the vapor liquid interface. [8] Such analysis is essential to elucidate concepts of hydrophobicity.

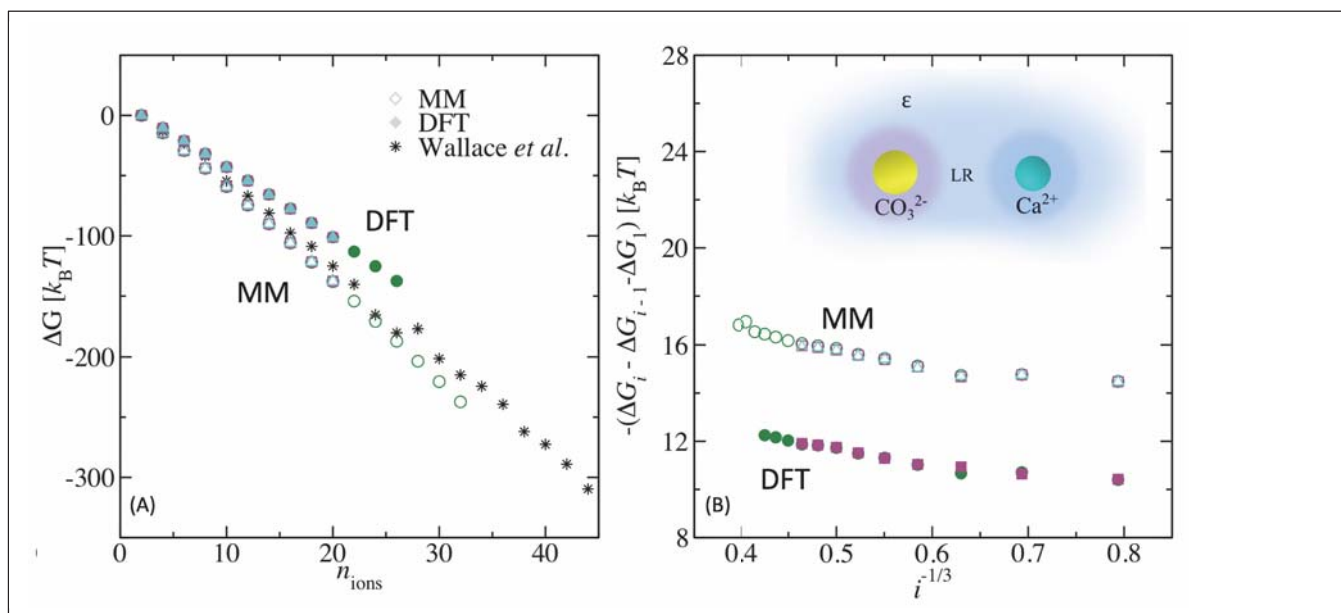


Figure 2. (A) Free energies of $CaCO_3$ cluster formation, comparing empirical potential (MM) to electronic structure (DFT) model of molecular interaction. (B) From the incremental free energies as a function of size, i . (right) the intercept recovers solubility while the slope recovers surface tension.

We will continue to explore mechanisms of nucleation in the condensed phase. In a recent experimental and computational effort, we developed a reduced model of ion interaction in a mean aqueous solvent field. [4] [See Figure 2.] This was combined with state-of-the-art Monte Carlo sampling techniques and an activity model to consider non-ideal solution behavior. The resulting reduced model recovered populations of clusters that were consistent with experimental measurement of XANES spectra. We concluded that the initial stages of nucleation of $CaCO_3$ proceeds through a classical mechanism. In the future we will extend, refine and seek self-consistency of such approach in a variety of solute systems and conditions.

Molecular Theory and Modeling FWP 16249

Postdoc(s): Tim Duignan, Mirza Galib, and Santanu Roy

Acknowledgements: In addition to the postdocs in the group, the work described here was influenced by all members of the Molecular Theory and Modeling group. A majority of the work was performed with Chris Mundy and John Fulton of CPIMS. The Molecular Theory and Modeling FWP 16249 is co-managed by CTC and CPIMS programs of DOE Office of Basic Energy Sciences Division of Chemical Sciences, Geosciences, and Biosciences.

Publications Acknowledging this Grant

Publications of GK Schenter. For other Molecular Theory and Modeling efforts, see contributions Liem X. Dang, Shawn M. Kathmann, Chris J. Mundy, Sotiris S. Xantheas, and Marat Valiev in this abstract book.

1. Galib M., G.K. Schenter, C.J. Mundy, N. Govind, and J.L. Fulton. 2018. "Unraveling the Spectral Signatures of Solvent Ordering in K-edge XANES of Aqueous Na^+ ." *Journal of Chemical Physics*. In Press
2. Dang L.X., and G.K. Schenter. 2018. "Rate Theory of Ion Pairing at the Water Liquid-Vapor Interface: A Case of Sodium Iodide." *Journal of Chemical Physics* 148, no. 22:222820. doi:10.1063/1.5017874
3. Remsing R.C., T. Duignan, M.D. Baer, G.K. Schenter, C.J. Mundy, and J.D. Weeks. 2018. "Water Lone Pair Delocalization in Classical and Quantum Descriptions of the Hydration of Model Ions." *Journal of Physical Chemistry B* 122, no. 13:3519-3527. doi:10.1021/acs.jpcc.7b10722
4. Henzler K., E. Fetisov, M. Galib, M.D. Baer, B.A. Legg, C. Borca, J.M. Xto, S. Pin, J.L. Fulton, G.K. Schenter, N. Govind, J.I. Siepmann, C.J. Mundy, T. Huthwlker, and J.J. DeYoreo. 2018. "Supersaturated calcium carbonate solutions are classical." *Science Advances* 4, no. 1:eaao6283. doi:10.1126/sciadv.aao6283
5. Roy S., M. Galib, G.K. Schenter, and C.J. Mundy. 2018. "On the Relation between Marcus Theory and Ultrafast Spectroscopy of Solvation Kinetics." *Chemical Physics Letters* 692. doi:10.1016/j.cplett.2017.12.041
6. Roy S., M.D. Baer, C.J. Mundy, and G.K. Schenter. 2017. "Marcus Theory of Ion-Pairing." *Journal of Chemical Theory and Computation* 13, no. 8:3470-3477. doi:10.1021/acs.jctc.7b00332
7. Galib M., M.D. Baer, L.B. Skinner, C.J. Mundy, T. Huthwelker, G.K. Schenter, and C.J. Benmore, et al. 2017. "Revisiting the hydration structure of aqueous Na^+ ." *Journal of Chemical Physics* 146, no. 8:084504. doi:10.1063/1.4975608
8. Galib M., T. Duignan, Y.B. Misteli, M.D. Baer, G.K. Schenter, J. Hutter, and C.J. Mundy. 2017. "Mass Density Fluctuations in Quantum and Classical descriptions of Liquid Water." *Journal of Chemical Physics* 146, no. 24:244501. doi:10.1063/1.4986284
9. Duignan T., M.D. Baer, G.K. Schenter, and C.J. Mundy. 2017. "Electrostatic solvation free energies of charged hard spheres using molecular dynamics with density functional theory interactions." *Journal of Chemical Physics* 147, no. 16:161716. doi:10.1063/1.4994912

10. Duignan T., M.D. Baer, G.K. Schenter, and C.J. Mundy. 2017. "Real single ion solvation free energies with quantum mechanical simulation." *Chemical Science* 8, no. 9:6131-6140. doi:10.1039/c7sc02138k
11. Dang L.X., G.K. Schenter, and C.D. Wick. 2017. "Rate Theory of Ion Pairing at the Water Liquid-Vapor Interface." *Journal of Physical Chemistry C* 121, no. 18:10018-10026. doi:10.1021/acs.jpcc.7b02223
12. Schenter G.K., and J.L. Fulton. 2017. "Molecular Dynamics Simulations and XAFS (MD-XAFS)." In *XAFS Techniques for Catalysts, Nanomaterials, and Surfaces*, edited by Y Iwasawa, K Asakura and M Tada. 251-270. Springer International Publishing. doi:10.1007/978-3-319-43866-5_18

Program Title: Understanding Chemical Bond Dynamics in Liquids Using Mixed Quantum/Classical Molecular Dynamics Simulation

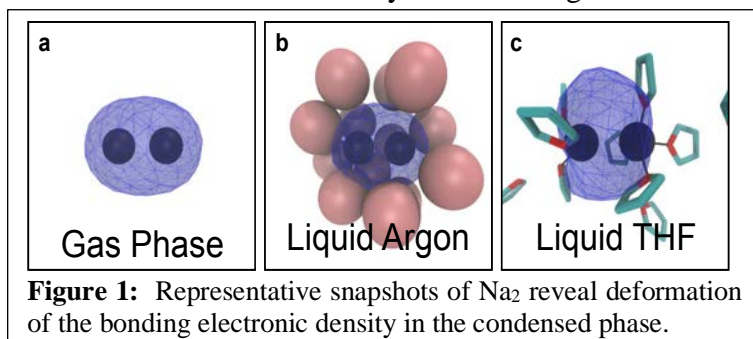
Principal Investigator Info: Professor Benjamin J. Schwartz
Department of Chemistry and Biochemistry
University of California, Los Angeles
Los Angeles, CA 90095-1569 USA
Voice: 310-206-4113; Fax: 310-206-4038
E-mail: schwartz@chem.ucla.edu

Program Scope: One of the central themes of modern physical chemistry is elucidating the elementary steps associated with chemical reactions. In the gas phase, our understanding is becoming largely complete. In principle, knowledge of the potential energy surfaces and the initial reactant trajectories is sufficient to predict the details of the reaction mechanism. In condensed phases, however, changes in reactant charge distribution or size during a reaction are strongly coupled to motions of the solvent molecules: solvent dynamics can stabilize (or destabilize) the energy of the transition state, controlling not only the effective barrier for a reaction but also how long that barrier persists. In addition, ‘caging’ by the solvent can promote recombination of recently-broken chemical bonds. All of these solvent effects, which play a crucial role in determining the rate or possibly even the products of chemical reactions, take place on picosecond or sub-picosecond time scales.

This program presents a description of both short- and longer-ranged studies designed to attack the frontiers of chemical reaction dynamics in the condensed phase. The goal of this projects will elucidate the molecular basis for solvation, non-adiabatic relaxation, and multi-electron quantum mechanical effects in solution-phase chemical reactivity, with emphasis on the critical realms of equilibrium chemical bond dynamics and bond breaking/bond formation.

Recent Progress: We chose to begin our study by focusing on the Na₂ molecule because it can be well described in mixed quantum/classical simulations; the molecule can be thought of as two classical Na⁺ cores that are held together by two quantum mechanical valence bonding electrons. In our simulations, we treat the two quantum mechanical bonding electrons using configuration-interaction-with-singles-and-doubles (CISD),¹ which is equivalent to full CI since only two explicit electrons are involved. The interactions between the bonding electrons and the Na⁺ cores² and the THF³ or Ar⁴ solvent molecules are described using previously-developed pseudopotentials. In this way, we can accurately calculate how immersion of Na₂ in solvents like liquid Ar or THF affects the molecular electronic and vibrational structure of this relatively simple solute.

Because there is relatively little exchange and correlation between the bonding electrons and those in the Na⁺ core, our MQC



description of the Na₂ molecule in the gas phase gives good agreement with high-level quantum chemistry calculations. Fig. 1a shows that the gas-phase Na₂ valence electron density forms a symmetric ovoid around the Na₂ center of mass, as expected from the ideas of

molecular-orbital theory. When we insert the Na_2 molecule into solution, however, interactions with the solvent molecules produce a valence electron density that is deformed relative to that in the gas phase. Fig. 1b shows that when Na_2 is placed in liquid Ar, Pauli repulsion interactions from the surrounding cage of Ar atoms, on average, compress the solute's bonding electronic density leading to a stiffer, tighter chemical bond.⁵

We also inserted the Na_2 molecule into liquid THF, and when we did, we got a surprise.⁶ THF molecules are known to chelate Na^+ in solution, with THF oxygen sites forming metal-oxygen dative bonds with a strength similar to that of a hydrogen bond, about 5 kcal/mol. Figure 1c shows that local interactions with the solvent displace the solute valence electron density to expose part of each Na^+ core for chelation by the THF oxygen sites. The net effect of these dative interactions with the solvent is to cause the solute valence electron density to spill out away from the bond axis, leading to instantaneous dipole moments that are much larger than in liquid Ar. Also in contrast to the bond compression seen in liquid Ar, the THF— Na^+ interactions lead to a large increase in the Na–Na bond length.

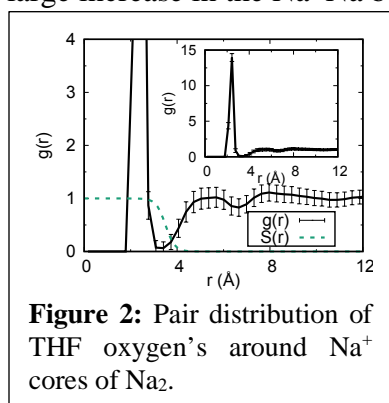


Figure 2: Pair distribution of THF oxygen's around Na^+ cores of Na_2 .

To better understand the local interactions between Na_2 and THF, the black curve in Fig. 2 shows the Na^+ –THF oxygen site radial distribution function, $g(r)$. The large peak at 2.35 Å that dominates corresponds to THF oxygen sites that coordinate the Na^+ core. Integration of $g(r)$ reveals an average coordination of 3.25 THF oxygen atoms making dative bonds per Na cation.

To understand why the THF-solvated Na_2 bond length is longer than in the gas phase or liquid Ar, we introduced a continuous coordination number, defined as the number of THF oxygen sites that lie in the main peak of $g(r)$ around each Na^+ core. We then calculated the free energy of the molecule in THF as a function of this coordination number coordinate, shown in Fig. 3a. The figure shows clearly that there are only a few stable Na_2 coordination states, and that the free energy minima occur precisely at integer coordination numbers. The figure also shows that these stable coordination the number of THFs coordinating one Na^+ core remains fixed while the other Na^+ core either gains or loses a single coordinating THF. Figures 3b,c show 1-D slices along two of the coordination-state conversion pathways, revealing relatively large potential energy barriers ($\sim 8 k_B T$ high) that must be overcome to convert between coordination states. Clearly, the coordination states at each free energy minimum can be thought of as distinct chemical species, with reactive pathways connecting the different species in equilibrium. Thus, even though each Na^+ –THF dative bond has a strength that is similar only to that of a hydrogen bond, the collective interaction of the solute with the solvent produces a variety of new chemical species that are in equilibrium, each of which is distinguished only by the involvement of the solvent.

How unique are the Na_2 chemical species that differ only in their local coordination with the solvent? In Fig. 4

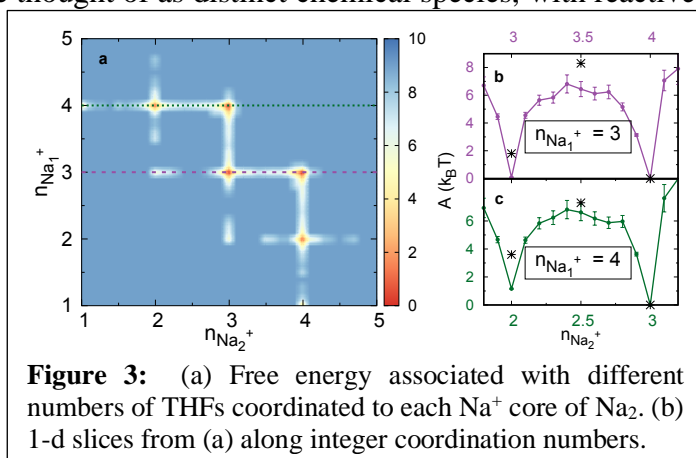
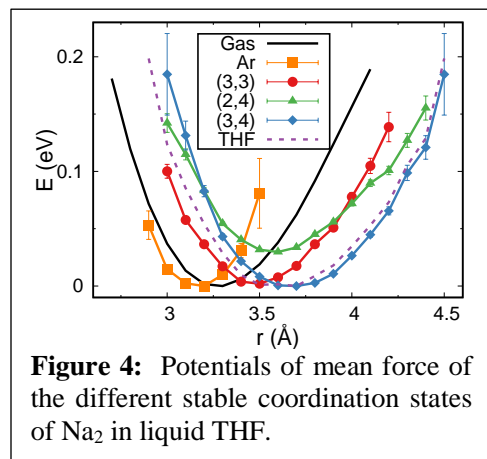


Figure 3: (a) Free energy associated with different numbers of THFs coordinated to each Na^+ core of Na_2 . (b) 1-d slices from (a) along integer coordination numbers.



we compare the potential energy of the gas-phase Na₂ molecule (black curve) to the potentials of mean force (PMFs) for the molecule in liquid Ar (orange curve), in liquid THF on average (purple dotted curve), and for each of the stable THF-solvated coordination states (red, green and blue curves) as a function of the Na–Na bond distance; these are the potential energy surfaces that govern how the two Na atoms move in each of the respective environments. The figure shows clearly that the overall PMF for the sodium dimer in liquid THF is not smooth; there are wiggles at the bottom of the well that result from the presence of the different (and distinct) solvent coordination states. Thus, it makes much more

sense to think of the Na₂THF system as three different molecules in equilibrium: as summarized in Table 1, each THF-coordination state has a different Na–Na bond length (the position of the minimum in the PMF) and a different vibrational frequency (the curvature of the PMF around the minimum), verifying that each is a unique chemical species. Indeed, the calculated UV-Vis and IR spectra for the three coordination states are quite distinct, so that it should be possible to observe them experimentally.⁶

In summary, quantum simulations of Na₂ in liquid THF reveal that the solvent plays an intimate role in the bond dynamics, electronic properties and indeed, chemical identity of simple solutes. There is no simple way to explain the average properties of Na₂ in THF except by thinking of each coordination state as a different molecule that undergoes a series of equilibrium chemical reactions, crossing free energy barriers of $\sim 8 k_B T$ to convert from one stable coordination state to another. Moreover, each coordination species has a unique bond length, distinct bond dynamics, and different IR and UV-Visible absorption spectra, providing an experimental handle to test the idea that interactions with the solvent can induce changes in solute chemical identity. We close by reiterating that the local specific interactions responsible for this behavior, the formation of Na–THF oxygen dative bonds, are no stronger than the hydrogen bonds that help form the secondary structure of peptides and proteins or lead to clathrate formation in aqueous solutions. This suggests that the concept of solvent participation in chemical identity, with chemical reactions converting between different local coordination states, is likely ubiquitous throughout solution chemistry and biochemistry.

Future Plans: For the immediate future, we plan on continuing our exploration of how local specific solvent interactions can alter molecular identity. The fact that the dative bond interactions responsible for changing identity here are comparable to the strengths of H-bonds means that the idea of the solvent playing an explicit role in molecular identity is likely general to any chemical system with local specific interactions of about this strength.

Over the longer term, we plan to address how the solvent alters molecular identity for intrinsically asymmetric molecules such as Na–K, which can be treated with the same level of theory but where the two halves of the molecule have different electron affinities and different sizes, and thus different potentials for chelation.

Over the shorter term, we plan to directly address all the questions discussed under the project scope by simulating the excited-state dissociation dynamics of Na₂⁺. The dimer cation is not only easier to simulate (because CISD is not required), but its lowest singlet excited state is dissociative

(which is not the case for the neutral dimer). By promoting these dimer cations to their lowest dissociative excited-state surface, we can see how the condensed environment, and the local specific interactions present in THF in particular, alter the photodissociation dynamics relative to that in the gas phase. We already have the ground-state simulations completed, and have found (Figure 5) that the nature of the solvent coordination is different than for the neutral dimer (compare Fig. 3a). This likely results from the fact that the solvent is more easily able to push the single bonding electron in the dimer cation out of the way, allowing for higher general levels of coordination. Questions we will address include: Does asymmetric coordination affect which Na⁺ core gets the bonding electron following dissociation? How does coordination affect the probability for recombination and/or subsequent vibrational relaxation? Can we simulate the properties/dynamics of Na₂⁺(THF)_n, which should be readily obtainable experimentally in mass-selected gas-phase molecular beams?

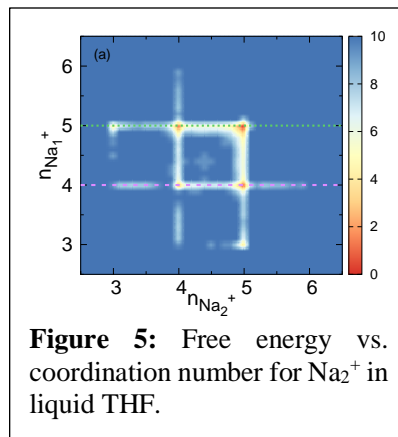


Figure 5: Free energy vs. coordination number for Na₂⁺ in liquid THF.

Publications:

- 1) D. Widmer and B. J. Schwartz, “Solvents can control solute molecular identity,” *Nature Chem.* **S41557-018-066z**, 1-7 (2018). DOI: 10.1038/s41557-018-066-z.
- 2) C.-C. Zho, V. Vlcek, D. Neuhauser and B. J. Schwartz, “Thermal Equilibration Controls H-Bonding and the Vertical Detachment Energy of Water Cluster Anions,” *J. Phys. Chem. Lett.* **9**, 5173-8 (2018). DOI: 10.1021/acs.jpcclett.8b02152.

References:

- ¹ Glover, W. J., Larsen, R. E. & Schwartz, B. J. First principles multi-electron mixed quantum/classical simulations in the condensed phase. I. An efficient Fourier-grid method for solving the many-electron problem. *J. Chem. Phys.* **132**, 144101 (2010).
- ² Glover, W. J., Larsen, R. E. & Schwartz, B. J. The roles of electronic exchange and correlation in charge-transfer-to-solvent dynamics: many-electron non-adiabatic mixed quantum/classical simulations of photoexcited sodium anions in the condensed phase. *J. Chem. Phys.* **129**, 1–20 (2008).
- ³ Smallwood, C. J., Mejia, C. N., Glover, W. R., Larsen, R. E. & Schwartz, B. J. A computationally-efficient exact pseudopotential method. 2. Application to the molecular pseudopotential of an excess electron interacting with tetrahydrofuran (THF). *J. Chem. Phys.* **125**, 9681–9691 (2006).
- ⁴ Gervais, B. et al. Simple DFT model of clusters embedded in rare gas matrix: trapping sites and spectroscopic properties of Na embedded in Ar. *J. Chem. Phys.* **121**, 8466–8480 (2004).
- ⁵ Glover, W. J., Larsen, R. E. & Schwartz, B. J. How does a solvent affect chemical bonds? Mixed quantum/classical simulations with a full CI treatment of the bonding electrons. *J. Phys. Chem. Lett.* **1**, 165–169 (2010).
- ⁶ D. Widmer and B. J. Schwartz, “Solvents can control solute molecular identity,” *Nature Chem.* **S41557-018-066z**, 1-7 (2018).

Development of Metal-Free Photocatalysts

Kevin L. Shuford

Department of Chemistry, Baylor University, One Bear Place #97348, Waco, TX 76798-7348

Kevin_Shuford@baylor.edu

Program Scope

Solar fuels show great promise as clean, sustainable energy sources; however, established technologies are still plagued by high price, toxicity concerns, or low efficiencies. There is a critical need for inexpensive, benign materials that can effectively harness the sun's energy. The overarching objective of this project is to evaluate the compatibility of novel material combinations for use as metal-free, heterojunction photocatalysts. Our central hypothesis is that by tuning the electronic structure of individual components in hybrid composites, via selective chemical modifications and physical stimuli to the interface, we can improve the photocatalytic properties of the overall assembly. We will determine factors that affect energy band gaps and band edge positions in isolated photocatalyst systems as well as explore routes to modulate heterojunction band alignments in composite assemblies. Our results will predict accessible pathways for charge carriers in new composite photocatalysts, facilitating access to more of the solar spectrum via inexpensive, environmentally-friendly material combinations.

Recent Progress

We have completed studies on several two-dimensional (2D) materials including pnictogen-doped graphene, multilayer graphene interacting with halogens, and 1T-TiS₂ under strain. In each case, the electronic properties are altered via interactions at the interface. Chemical dopants and surface adsorbates create a band gap in graphene [1-2], which can be tuned by adjusting the system parameters (e.g. dopant or adsorbate identity and concentration). By controlling these chemical perturbations, the properties of the material can be altered with some degree of selectivity. Mechanical strain also drastically affects the electronic structure of 2D materials. Figure 1 displays the band structure of monolayer 1T-TiS₂ under varying degrees of tensile strain. In the absence of strain (0%), the 2D material is a semimetal, as indicated by energetic overlap of the valence and conduction bands

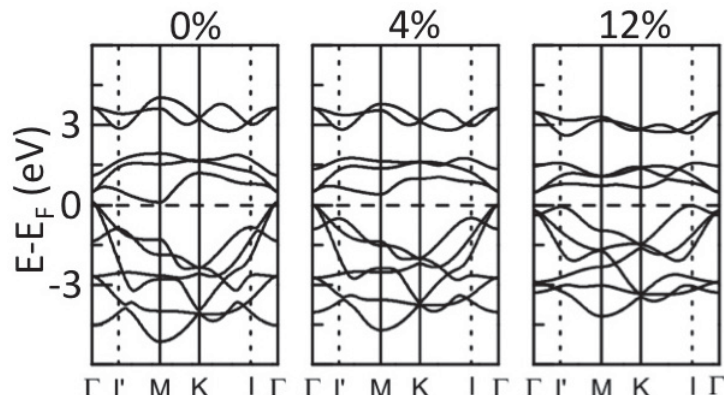


Figure 1: Band structure of monolayer 1T-TiS₂ under tensile strain from 0-12%. The Γ' and I points in the first Brillouin zone marked by dotted lines are not points with high symmetry.

at Γ and M respectively. Applying 4% tensile strain produces a semiconductor with an indirect gap of ~ 0.4 eV. The band edges are affected by strain in different ways. Further straining the monolayer to 9% increases the gap size to 0.64 eV, and the material transitions to a direct gap semiconductor at Γ (band structure not shown). Finally, at 12% strain, TiS₂ transitions back to being an indirect band gap ($I \rightarrow \Gamma$). The transition between valence and conduction bands is a Γ - Γ direct one when strain is 6 - 10%. Outside of this range, an indirect transition is predicted. This provides a way to tune the electronic properties of monolayer TiS₂ by controlling the strain on the monolayer. Lastly, we explored the role that unusual lattice arrangements play in dictating electronic structure. In particular, we have examined ultrathin nanosheets with a (4,8)-

tessellation composed of Boron and Group-V elements (effectively inorganic Haeckelites) [4-5]. This combination results in unique electronic properties and strong optical response at frequencies relevant for solar applications (Fig. 2). The properties evolve upon moving from the standard hexagonal lattice of h-BN to a (4,8) tessellation in H-BN.

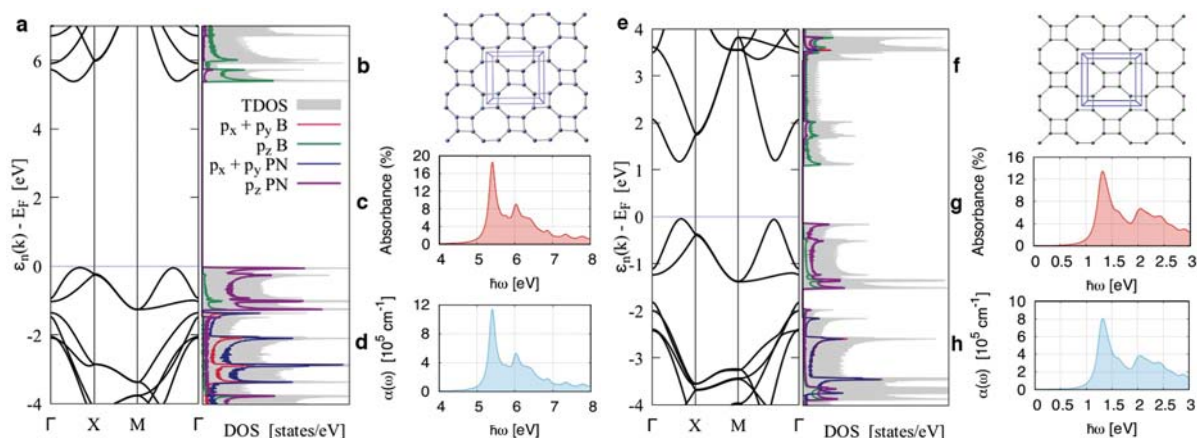


Figure 2: (a,e) Band structure and projected density of states, (b,f) ultrathin film optimized structures, (c,g) absorbance spectrum, and (d,h) absorption coefficient for H-BN and H-BP respectively.

References

1. Paul A. Brown, Chengyong Xu, and Kevin L. Shuford, "Periodic Trends of Pnictogen Substitution into a Graphene Monovacancy: A First Principles Investigation," *Chem. Mater.* **26**, 5735-5744 (2014).
2. Chengyong Xu, Paul A. Brown, and Kevin L. Shuford, "Strain-Induced Semiconductor-to-Semimetal Phase Transition and Indirect-to-Direct Band Gap Transition in Monolayer 1T-TiS₂: A First-Principles Study," *RSC Adv.* **5**, 83876-83879 (2015).
3. Chengyong Xu, Paul A. Brown, Jing Lu, and Kevin L. Shuford, "Electronic Properties of Halogen-Adsorbed Graphene," *J. Phys. Chem. C* **119**, 17271-17277 (2015).
4. Paul A. Brown and Kevin L. Shuford, "Archimedean (4,8)-Tessellation of Haeckelite Ultrathin Nanosheets Composed of Boron and Aluminum-Group V Binary Materials," *Nanoscale* **8**, 19287-19301 (2016).
5. Paul A. Brown and Kevin L. Shuford, "Exceptional Optical Response of Archimedean Boron and Group-V Ultrathin Nanosheets," *J. Phys. Chem. C* **121**, 24489-24494 (2017).

Future Plans

Our recent work demonstrates how chemical dopants, surface adsorbates, and mechanical strain can create and modulate band gaps. By controlling these surface perturbations, the electronic properties of the material can be tuned with selectivity. One can imagine extrapolating these concepts to controlling both energetics in individual materials and band alignments in assemblies to enhance relevant photocatalytic processes that occur at material interfaces. We will use a combination of molecular quantum chemistry and periodic system approaches to determine the fundamental chemical and photophysical properties of emerging photocatalytic materials. Our near-term plans are to focus on the 2D material graphitic carbon nitride. Specifically, we will determine the effects of chemical doping and size-dependent quantum confinement on the electronic structure and optical properties of graphitic carbon nitride. Elemental dopants will be added to graphitic carbon nitride via lattice substitutions and interstitial sites to ascertain changes to electronic structure. Quantum confinement effects in these systems will be gauged by examining absorption properties of zero-dimensional quantum dots up to the bulk material. Later studies will combine graphitic carbon nitride with other materials to form metal-free composites for photocatalysis.

Publications Acknowledging this Grant

There are no publications to report because this is a new award, with a start date of September 1, 2018.

An Atomic-scale Approach for Understanding and Controlling Chemical Reactivity and Selectivity on Metal Alloys

E. Charles H. Sykes (charles.sykes@tufts.edu)

Department of Chemistry, Tufts University, 62 Talbot Ave, Medford, MA 02155

Program Scope:

Catalytic hydrogenations and dehydrogenations are critical steps in many industries including agricultural, chemicals, foods and pharmaceuticals. In the petroleum refining industry, for instance, catalytic hydrogenations are performed to produce light, hydrogen rich products like gasoline. Hydrogen activation, uptake, and reaction are also important phenomena in fuel cells, hydrogen storage devices, materials processing, and sensing. Typical heterogeneous catalysts involve nanoparticles composed of expensive noble metals or alloys based on metals like Pt, Pd, and Rh. Our goal is to alloy these reactive metals, at the single atom limit, with more inert and often much cheaper hosts and to understand how the local atomic geometry affects reactivity.

The CPIMS program has supported Sykes lab work in developing a new class of model alloy catalysts that we have termed *Single-Atom Alloys* (SAAs) and understanding their ability to activate H₂ and enable spillover of hydrogen to the support where ultra-selective reactions can occur. *Spurred by our fundamental studies, many research groups around the world have now shown that our SAA concept is valid in real catalysts working under ambient conditions.* For example, selective hydrogenation of acetylene, butadiene, and acrolein, as well as Uhlmann coupling have been demonstrated. *Our goal is to now push this work beyond hydrogenation chemistry and study the ability of SAAs to perform C-H activation chemistry and dehydrogenation reactions, as well as probing the ability of larger metal alloy ensembles to enable selective oxidations.* Mostly recently we have demonstrated that SAAs are robust and efficient C-H activation and alkane dehydrogenation catalysts as described in detail below.

Recent Progress: PtCu Single-Atom Alloys as coke-resistant catalysts for efficient C-H activation

The recent availability of shale gas has led to a renewed interest in C-H bond activation as the first step towards synthesis of fuels and fine chemicals. Heterogeneous catalysts based on Ni and Pt can perform this chemistry but deactivate easily due to coke formation. Cu-based catalysts are not practical for this chemistry due to high C-H activation barriers, but their weaker binding to adsorbates offers resilience to coking. Methyl iodide (CH₃I) provides a simple method for adding methyl groups to our alloy surfaces and TPR studies of subsequent methane evolution allows us to examine C-H activation energetics. TPR spectra resulting from the reaction of 4.5 Langmuirs CH₃I on pure Cu, 0.01 monolayers (ML) Pt/Cu(111) SAA and 1 ML Pt/Cu(111) are presented in Figure 1c. The major desorption product for each surface is methane. Ethene, ethane, and propene are also produced. Desorption of intact CH₃I is not detected at these exposures. For clarity, only traces for methane and ethene are displayed in Figure 1c. Desorption of these products is reaction rate limited as small hydrocarbons normally desorb from Cu(111) at very low temperatures. The black spectra correspond to the reaction of CH₃I on Cu(111) and agree well with previously published results on this surface. Methane and the larger hydrocarbons desorb at ~450 K. It has been previously demonstrated that the rate limiting step to form these products is the activation of C-H bonds in methyl groups to produce methylene and adsorbed H. Methane is formed by facile hydrogenation of remaining methyl groups, while the coupling of methylene and methyl forms larger hydrocarbons. These coupling reactions allow Cu(111) to avoid coking. The red

spectra in Figure 1c correspond to CH₃I on a 0.01 ML Pt/Cu(111) SAA alloy. On the SAA surface, methane and carbon coupling products desorb at ~350 K, 100 K cooler than on the pure Cu(111) surface. *Because the rate limiting step in methane evolution is C-H activation, this 100 K temperature shift reveals that single Pt atoms in the Cu surface significantly lower the barrier to C-H activation in CH₃.* The formation of ethene, ethane and propene implies the Pt/Cu SAA maintains the ability of Cu to avoid coking via C-C coupling. Experiments adding deuterium to the surfaces verified that C-H activation was still the rate limiting step on the SAA. The blue spectra in Figure 1c correspond to the reaction of CH₃I on a surface where 1 ML of Pt has been deposited on Cu(111). The majority of methane desorbs at ~250 K, a temperature close to that of methyl decomposition on a Pt(111) crystal. Despite activating C-H bonds at a low temperature, on Pt(111) methylene groups do not couple and eventually decompose to surface bound carbon and gas phase H₂. No coupling products are observed at 250 K on the 1 ML Pt/Cu(111) surface, showing that this alloy is more similar to Pt(111) than Cu(111). Hydrogen from methylene decomposition desorbs at high temperature similar to Pt(111). *No hydrogen desorbs from Cu(111) or the Pt/Cu(111) SAA surfaces, confirming their resistance to coking.*

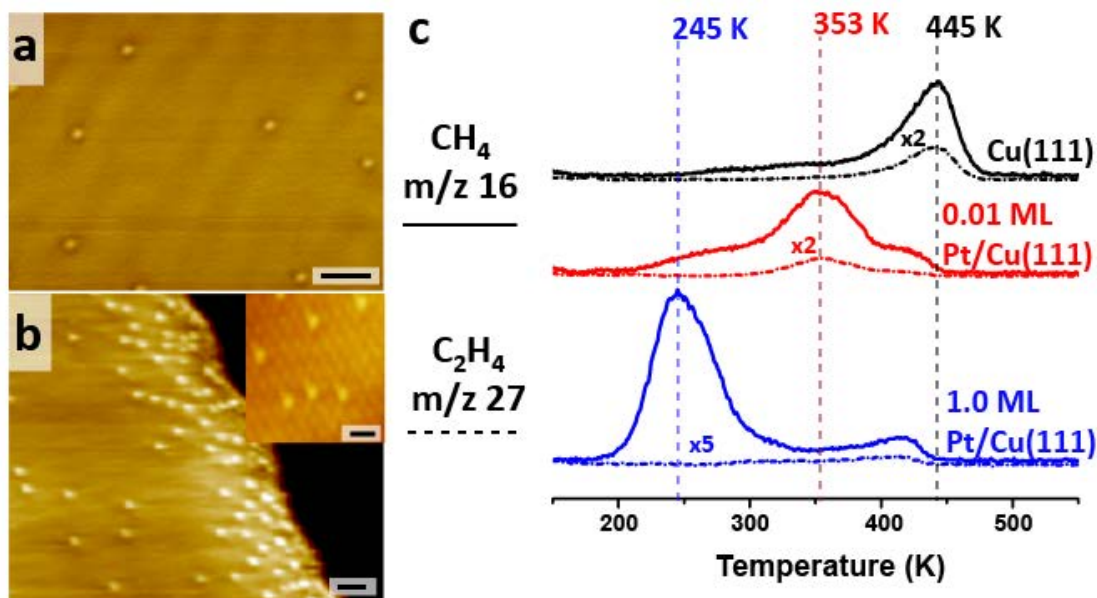


Figure 1. Methane evolution as a reporter for C-H activation in methyl groups, experiment and simulations. (a) STM image of a 0.01 ML Pt/Cu(111) SAA surface. (b) Wide-scale image of the SAA surface showing that Pt is distributed across both terraces and at regions near step edges. Scale bar = 1 nm. Inset shows an atomic resolution image of the alloy surface. Scale bar = 0.5 nm. (c) TPR traces taken with a heating rate of 1 K·s⁻¹ showing the evolution of methane (solid lines) and ethene (dashed lines) from Cu(111) (black), 0.01 ML Pt/Cu(111) (red) and 1.0 ML Pt/Cu(111) (blue) surfaces following deposition of 4.5 L of CH₃I.

We also performed STM experiments to examine reaction intermediates not detectable in the TPR experiments and to confirm that no coke is formed on the Pt/Cu SAA surface. Figure 2a-h shows a series of images taken after annealing the system to progressively higher temperatures for both Cu(111) and 0.01 ML Pt/Cu(111). After an 80 K anneal, below the temperature necessary for C-I bond cleavage, intact CH₃I appears in the images as disordered clusters on both surfaces (Figure 2a and b). Annealing either surface to 120 K results in new ordered structures (Figure 2c and d). On both surfaces there are intermixed bright and dark features arranged in large well-defined 2D clusters forming a $\sqrt{3} \times \sqrt{3}$ R30° structure. The clusters exhibit similar behavior to pure methyl groups formed via pyrolysis of

azomethane on Cu(111). The bright features are iodine atoms while the darker features are CH₃. For the Pt/Cu surface shown in Figure 2d, some individual iodine atoms are separated from clusters, marking positions where iodine is absorbed on Pt atoms. Annealing to higher temperatures between 350-450 K causes notable changes in the adsorbate structures on Cu(111) vs. 0.01 ML Pt/Cu(111) (Figure 2e and f). On Cu(111) both bright and dark features are on the surface, while on Pt/Cu(111) only bright features remain in a $\sqrt{3} \times \sqrt{3} R30^\circ$ structure. *This is consistent with the TPR results which reveal that on 0.01 ML Pt/Cu(111), C-H activation of CH₃ occurs at 350 K followed by immediate desorption of methane and coupling products.* Figure 2f shows that after annealing to 350 K, the Pt/Cu(111) SAA surface contains only patches of iodine atoms which appear as bright protrusions in a $\sqrt{3} \times \sqrt{3} R30^\circ$ structure, in agreement with previous reports. However, annealing the Cu(111) surface to 350 K is insufficient to activate C-H bonds and so methyl groups are still observed in Figure 2e; while for Pt/Cu(111) in Figure 2f, the C-H bond has been activated leaving only adsorbed iodine atoms. Importantly, no other species besides iodine are observed on the Pt/Cu(111) surface, indicating it does not suffer from coking by carbon like pure Pt(111). Annealing the Cu(111) surface further to 450 K (Figure 2g) allows for C-H bond activation, hydrocarbon desorption, leaving only iodine on the surface. On the Pt/Cu(111) surface no change is observed after annealing to 450 K (Figure 2h). Iodine is very stable on Cu(111) and desorbs above 800 K. *Annealing either surface results in a clean Cu(111) surface further demonstrating that the surface is not contaminated by carbon as is the case for Pt catalysts.*

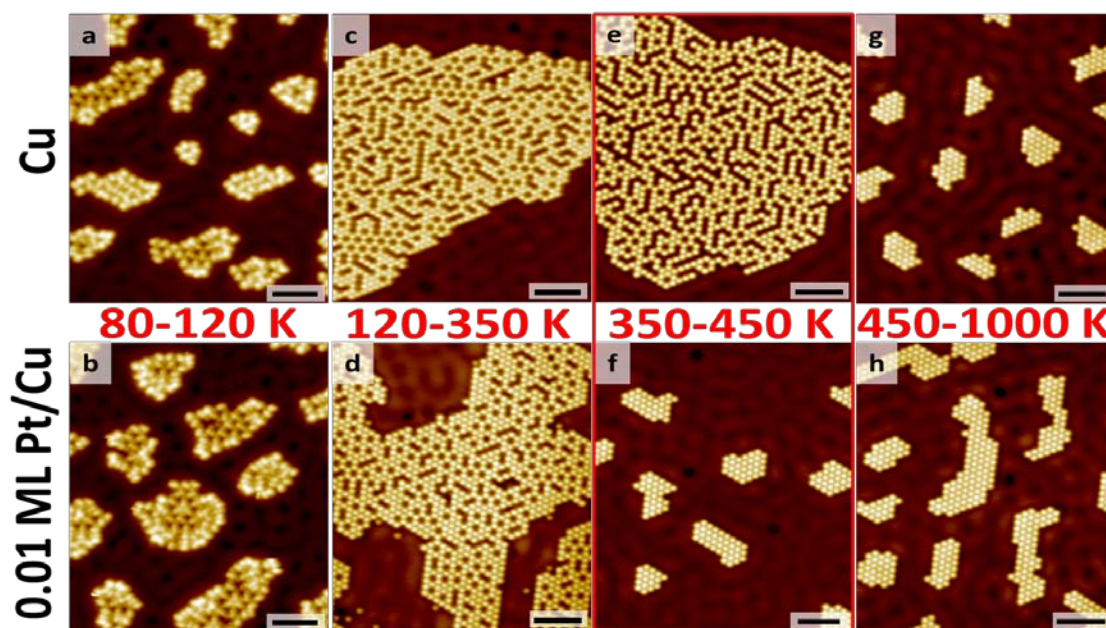


Figure 2. STM imaging of reaction intermediates on Cu(111) and Pt/Cu SAA surfaces revealing lower temperature C-H activation on Pt/Cu SAAs than Cu. (a-h) STM images at 5 K show the various stages of the reaction of CH₃I on Cu(111) and 0.01 ML Pt/Cu(111) surfaces (top and bottom rows respectively) after annealing to various temperatures. Scale bars = 3 nm. Panels a and b show clusters of intact MeI molecules. In panels (c-h) dissociated iodine atoms appears as higher, brighter protrusions, while methyl groups appear as darker protrusions. (i) High resolution STM images of mixed phase methyl (darker protrusions) and iodine (brighter protrusions) after a 120 K anneal on Cu(111) and (j) iodine on Cu(111) after a 450 K anneal. Scale bars = 1 nm for (i) and (j). These STM images confirm what was predicted by the TPR results, namely that the Pt/Cu SAA surface is able to activate C-H bonds in methyl groups at lower temperature than Cu while still avoiding carbon deposition.

Future Plans:

Despite the many heterogeneous catalysis groups that have taken up Single-Atom Alloys we, with the exception of the Trenary group at UIC doing RAIRS, are the only group performing UHV surface science work on SAAs. Our approach offers the opportunity to study the atomic-scale composition and structure of active sites and relate this information to their ability to activate, spillover and react industrially relevant small molecules. We continue to work closely with theorists (Stamatakis and Michaelides at UCL) enabling us to predict and test new SAA combinations in well defined environments and guide the heterogeneous catalysis community. Our future work is aimed at:

- 1) Studying RhCu single-atom alloys which are predicted by DFT to have even lower C-H activation barriers than PtCu.
- 2) Make and test trimetallic SAA model catalysts to investigate if the bifunctional nature we have demonstrated for 2 component SAAs can be extended to “3 site” model catalysts.
- 3) Examining the structure sensitivity (or lack thereof) on SAA surface chemistry by extending the surface science studies to (100) and (110) facets as well as stepped crystals.

DOE-Sponsored Research Publications in the Last Two Years:

- 1) "Pt/Cu Single-atom Alloys as Coke-resistant Catalysts for Efficient C-H Activation" M. D. Marcinkowski, M. T. Darby, J. Liu, J. M. Wimble, F. R. Lucci, S. Lee, A. Michaelides, M. Flytzani-Stephanopoulos, M. Stamatakis, E. C. H. Sykes *Nature Chemistry* 2018, 10 325 (The surface science part of this project (Sykes) was solely funded by CPIMS – collaborator MFS was funded by DOE DE-FG02-05ER15730 for the catalysis side of the project)
- 2) "Lonely Atoms with Special Gifts: Breaking Linear Scaling Relationships in Heterogeneous Catalysis with Single-Atom Alloys" M. Darby, M. Stamatakis, A. Michaelides, E. C. H. Sykes *The Journal of Physical Chemistry Letters* 2018, 9, 5636 [featured cover] (The Sykes lab contribution to this manuscript was funded solely by CPIMS, computational investigations by collaborators at UCL were supported by IMASC EFRC DE-SC0012573)
- 3) "Elucidating the Stability and Reactivity of Surface Intermediates on Single Atom Alloy Catalysts" M. T. Darby, R. Reocreux, E. C. H. Sykes, A. Michaelides, M. Stamatakis *ACS Catalysis* 2018, 8 5038 (computational investigations of this work were supported by IMASC EFRC DE-SC0012573)
- 4) Carbon Monoxide Poisoning Resistance and Structural Stability of Single Atom Alloys" M. T. Darby, E. C. H. Sykes, A. Michaelides, M. Stamatakis *Topics in Catalysis* 2018, 61 428 (The Sykes lab contribution to this manuscript was funded solely by CPIMS, DFT collaborators had European funding)
- 5) "Controlling Selectivity in the Ullmann Reaction on Cu(111)" E. A. Lewis, M. D. Marcinkowski, C. J. Murphy, M. L. Liriano, A. J. Therrien, A. Pronschinske, and E. C. H. Sykes *Chemical Communications* 2017, 53 7816-7819
- 6) "Selective Formic Acid Dehydrogenation on Pt-Cu Single Atom Alloys" M. D. Marcinkowski, J. Liu, C. J. Murphy, M. L. Liriano, N. A. Wasio, F. R. Lucci, M. Flytzani-Stephanopoulos, and E. C. H. Sykes *ACS Catalysis* 2017, 7, 413-420 (The surface science part of this project (Sykes) was solely funded by CPIMS – collaborator MFS was funded by DOE DE-FG02-05ER15730 for the catalysis side of the project)
- 7) "Tackling CO Poisoning with Single Atom Alloy Catalysts" J. Liu, F. R. Lucci, M. Yang, S. Lee, M. D. Marcinkowski, A. J. Therrien, C. T. Williams, E. C. H. Sykes, and M. Flytzani-Stephanopoulos *Journal of the American Chemical Society* 2016, 138, 6396-6399 [featured cover] (The surface science part of this project (Sykes) was solely funded by CPIMS – collaborator MFS was funded by DOE DE-FG02-05ER15730 for the catalysis side of the project)

Excitons in Low-Dimensional Perovskites

William A. Tisdale

Department of Chemical Engineering

Massachusetts Institute of Technology, Cambridge, MA 02139

tisdale@mit.edu

Research Goals

The goal of this research effort is to obtain a deeper understanding of strongly bound excitonic states in low-dimensional halide perovskites. We will study how excitons in these quantum-confined materials move, how they interact with the polar lattice, and how their behavior can be manipulated through chemical or structural modification. This effort will be organized into three parallel thrusts:

- 1) ***Synthesis of low-dimensional perovskites with tunable excitonic properties:*** Using a suite of nanomaterials chemistry approaches, we will synthesize low-dimensional perovskite structures exhibiting varying degrees of quantum and dielectric confinement. In particular, we will compare the excitonic properties of 2D colloidal nanoplatelets to their solid-phase (Ruddlesden-Popper) analogues. Additionally, we propose a series of azulene and chalcogen ring-based organic cations for varying lattice polarizability.
- 2) ***Exciton transport in low-dimensional perovskites:*** Using temperature-dependent transient photoluminescence (PL) microscopy and broadband transient absorption (TA), we will study exciton dynamics in quantum confined perovskite nanostructures of varying dimensionality. We will make extensive use of a superresolution photoluminescence microscopy technique that we developed for spatiotemporal visualization of exciton transport in molecular and inorganic semiconductor films, and back focal plane imaging to determine the transition dipole orientation.
- 3) ***Exciton-lattice interactions in low-dimensional perovskites:*** In metal halide perovskites, charge carrier motion is coupled to the highly polarizable lattice through the formation of large polarons, which contribute to defect-tolerance and long carrier lifetimes. In low-dimensional perovskites – where dielectric confinement promotes strongly bound (0.2-0.5 eV) neutral excitonic states – the role of charge-lattice interactions is less clear. To explore these interactions, we will perform femtosecond stimulated Raman scattering (FSRS) and broadband transient absorption (TA) studies on carefully chosen low-dimensional perovskite structures with varying lattice polarizability and dielectric confinement.

Publications

There are no publications to report because this is a new award with a start date of September 1, 2018.

Structural Dynamics in Complex Liquids Studied with Multidimensional Vibrational Spectroscopy

Andrei Tokmakoff

*Department of Chemistry, James Franck Institute, and Institute for Biophysical Dynamics
University of Chicago
929 E. 57th Street
Chicago, IL 60637
E-mail: tokmakoff@uchicago.edu*

Water's rich hydrogen bonding (H-bonding) dynamics allow ionic species, particularly the proton, to integrate and transport rapidly along the H-bond network. These properties make aqueous systems ideal for alternative energy sources such as fuel cells and water oxidation catalysis. The aim of our research program is to study the molecular details of vibrational energy dissipation and H-bond reorganization in water and how these processes impact the behavior of ions in the aqueous phase.

Research in the past year has focused on revealing structural and dynamical properties of the aqueous excess proton with ultrafast IR spectroscopy, which was enabled by the development and improvement of broadband IR sources spanning the entire mid-IR (1000–4000 cm^{-1}). Additionally, simultaneous collection of the polarization dependence in 2D IR and transient absorption spectra has allowed us to study orientational dynamics of ionic solutes in water, uncovering key details about aqueous charge transport and ion pairing. Reactive classical molecular dynamics simulations from the Voth group (UChicago) have also proven to be an invaluable resource for interpreting IR spectra.

Development of high-quality, broad excitation and detection pulses around 1200 cm^{-1} allowed us to interrogate the IR response of the aqueous proton in this region. We found that the 2D IR feature at 1200 cm^{-1} exhibits an unusual negative anharmonicity, where the excited-state absorption (ESA) is located at higher frequency than the ground-state bleach (GSB). This doublet is consistent with an asymmetric nuclear potential with steep walls and a low barrier. We assigned the feature to the stretching vibration of the excess proton shared between two waters in a Zundel-like arrangement. Based on our results, the potential for this proton stretch mode must be asymmetric with respect to the special pair O-O axis to explain the frequency spacing between the ESA and GSB. Furthermore, this absorption is elongated along the diagonal of the 2D IR spectrum, which indicates a relatively persistent inhomogeneous distribution of environments around the aqueous proton. These characteristics all point to an excess proton that is strongly interacting with two water molecules, with the minimum of the potential residing asymmetrically between the two waters, and a broad distribution of structures that persist beyond the lifetime of the vibrational excitation of ~ 200 fs.

We have extended this measurement to span the entire broadband 2D IR spectrum of $\text{H}^+(\text{aq})$, covering all of the stretching and bending vibrations of the excess proton from 1000–3000 cm^{-1} . Cross peaks appear between all of the different regions of the 2D IR spectrum at the earliest measurable waiting times, which indicates that all proton vibrations are strongly coupled. This implies that the spectrum arises from one dominant structural motif, rather than Eigen and Zundel species coexisting separately in solution and giving rise to different aspects of the spectrum. We additionally observe that the proton continuum that spans the region from ~ 2000 –3000 cm^{-1} in the

linear IR spectrum consists of overlapping features from the proton bend at 1750 cm^{-1} , a particularly broad feature centered at 2400 cm^{-1} from OH stretches of waters flanking the excess proton, and redshifted OH stretches at $\sim 3000\text{ cm}^{-1}$ from waters in the first solvation shells of the aqueous proton complex. Polarization-sensitive detection of 2D IR cross peaks reveal that the shared proton stretch and proton bend exhibit parallel transition dipoles along the Zundel O-O axis and are roughly perpendicular to the flanking water stretches, consistent with assignments for a Zundel-like hydration complex.

One of the distinctive characteristics of the aqueous excess proton is its extremely high polarizability, which results to a significant extent from the large degree of structural reorganization possible in its solvation structure. An important question when studying the structure of the $\text{H}^+(\text{aq})$ complex is the specific role of the counter anions in solution, how they affect the excess proton. If the anion is in close proximity to the excess proton, or if perhaps it is in direct contact, in the form of an ion pair, it might play a significant role in reshaping the solvation structure of the excess proton, and perhaps change its nature entirely. To study this effect, we have performed a series of 2D IR measurements on nitric acid solutions as a function of concentration. At very high concentrations, higher than approximately 4M, we observe a distinct intermolecular cross peak between the asymmetric stretch mode of the nitrate ion and the acid bending mode, indicative of the formation of a significant population of contracted ion pairs. These ion pairs are structurally distinct from undissociated nitric acid molecules, but have a similar concentration dependence. Furthermore, this intermolecular cross peak appears on the high-frequency side of the acid bending band, around 1800 cm^{-1} rather than 1750 cm^{-1} , suggesting that the proximity of the nitrate ion results in the excess proton taking on a more hydronium-like structure as opposed to the more symmetrically shared Zundel-like structure observed when the excess proton is not participating in an ion pair. This demonstrates the structural adaptability of the solvation complex of the excess proton in water.

In addition to disentangling structural information about the excess proton, we have used polarization anisotropy experiments to interrogate proton transfer kinetics. By exciting the bend modes of the aqueous proton and detecting the polarization-sensitive transient absorption, we observe reorientation kinetics that persist on a 2.5 ps timescale, approximately ten times longer than the proton bend vibrational lifetime. The orientational information is preserved in the hot ground state, a spectroscopic signal that arises from the relaxation from the protonated bend into low-frequency modes. Given that the aqueous proton bend dipole is parallel to the O-O axis and the 2.5 ps timescale is consistent with aqueous H-bond reorganization, we conclude that the reorientation of the hydrated proton bend reports on irreversible proton transfer kinetics from one Zundel-like structure to another.

We have expanded the above experiment to multiple temperatures ranging from 5–55 °C and concentrations of 1M–4M to learn about the energetic barriers associated with the proton transfer process. We find that protonated bend reorientation follows Arrhenius kinetics, with barriers ranging from 2.6 kcal/mol in 1M HCl decreasing monotonically to 1.6 kcal/mol in 4M HCl. The 1M HCl reorientation barrier agrees with values of the proton diffusion barrier determined from NMR relaxation experiments (2.4 kcal/mol) and MS-EVB simulations (2.7 kcal/mol), reinforcing the notion that proton bend reorientation reports on proton transfer. The proton transfer barrier is more than 1 kcal/mol less than the barrier for H-bond reorganization in neat water (3.8 kcal/mol), which is counterintuitive given the relatively strong H-bonding around the excess proton. This likely suggests that a low-frequency, low-barrier coordinate such as intermolecular O-O compression significantly contributes to the proton transfer process.

Additionally, the measured proton transfer rate is inversely related with the solution viscosity, consistent with strong coupling to the solvent in accordance with Kramers theory. This suggests that the proton transfer process also relies on a collective solvent coordinate, but the identity of this coordinate has not been determined yet. These findings underscore the dominant role of the aqueous H-bond network in driving proton transfer.

DOE Supported Publications September 2016 to September 2018

1. “Molecular Modeling and Assignment of IR Spectra of the Hydrated Excess Proton in Isotopically Dilute Water,” Rajib Biswas, William Carpenter, Gregory Voth, and Andrei Tokmakoff, *Journal of Chemical Physics*, **145** (2016) 154504-1-12.
2. “IR spectral assignments for the hydrated excess proton in liquid water,” Rajib Biswas, William Carpenter, Joseph A. Fournier, Gregory Voth, and Andrei Tokmakoff, *Journal of Chemical Physics*, **146** (2017) 154507-1-11.
3. “Delocalization and stretch-bend mixing of the HOH bend in liquid water,” William B. Carpenter, Joseph A. Fournier, Rajib Biswas, Gregory A. Voth, and Andrei Tokmakoff, *Journal of Chemical Physics*, **147** (2017) 084503-1-10.
4. “Picosecond proton transfer kinetics in water revealed with ultrafast IR spectroscopy,” William B. Carpenter, Joseph A. Fournier, Nicholas H.C. Lewis, and Andrei Tokmakoff, *Journal of Physical Chemistry B*, **122** (2018) 2792-2802.
5. “Broadband 2D IR spectroscopy reveals dominant asymmetric H_5O_2^+ proton hydration structures in acid solutions,” Joseph A. Fournier, William B. Carpenter, Nicholas H.C. Lewis, and Andrei Tokmakoff, *Nature Chemistry*, **10** (2018) 932-937.

Ab-initio analysis of molecular interactions in clusters and bulk systems

Marat Valiev

Environmental Molecular Sciences Laboratory, Pacific Northwest National Laboratory,
P. O. Box 999, Richland, Washington 993521

Abstract

The goal of our project is to develop fundamental molecular level descriptions of chemical transformations that take place in clusters, interfacial and bulk molecular liquid systems. Of particular interest is understanding how specific molecular features of solvent and solute components at the atomistic scale impact observed macroscopic properties. Our approach revolves around development and application of advanced simulation methods that provide tailored description of the system, which combines electronic structures theories with classical particle and continuum methods. Such hybrid approach retains reliable quantitative description of reactive processes, and at the same time provides simple physically motivated models for rationalizing overall behavior and properties of the complex solution system.

In our analysis of solute, or more generally reactive part of the system, we place a heavy emphasis on high-level electronic structure calculations. The key component of our research efforts in this area is collaboration with experimental photoelectron spectroscopy efforts of Xuebin Wang's group at PNNL. Photoelectron spectroscopy provides a sensitive probe into electronic properties of the molecules and naturally integrates with ab-initio simulations as part of analysis and data interpretation. Following our previous work on proton transfer process bisulfate/formic acid clusters, we have performed combined

experimental and theoretical study bisulfate in complex of benzoic and toluic acids. Our results indicate that similar to formic acid, the benzoic and toluic acids readily transfer the proton to bisulfate despite seemingly prohibitive proton affinity barrier.

Development of systematic statistical mechanics description of bulk molecular liquid solutions continues to remain on of the major focus areas in our project. Molecular liquids play a critical role in vast majority of chemical and biological processes, raising the importance of coherent first principles understanding of these systems. The challenging feature of molecular

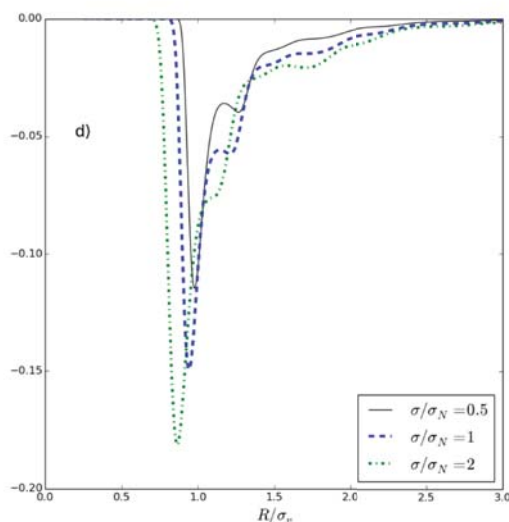


Fig.1 Intra-molecular site-density corrections to RISM description to N_2 molecular liquid solution for various sizes of LJ spherical solute

liquid solutions is the presence of two distinct interaction scales - stiff short-ranged intra-molecular interactions that bind atoms into molecules and long-range inter-molecular correlations that render the overall system "liquid". Simultaneous consideration of the two interaction regimes is exceedingly difficult theoretical task, but yet appears to be essential to capture the observed rich and complex behavior of these systems. As in Chandler's RISM approach, the main variable in our theory is the atomic site-density as the main variable. The difference comes in using general reference system procedure that enables systematic separation of intra- and inter-molecular effects without any approximations. In the current version of our approach, cluster site density functional theory (CSDFT), the intra-molecular part is treated 1-point Mayer cluster expansion. The application of this approach to simple case of N₂ molecular liquid solution (See Fig.1) illustrates the errors of conventional RISM approach in the solute-solvent interface layer.

Project Publications: (2016-present)

Valiev, M.; Deng, S. H. M.; Wang, X. B., How Anion Chaotrope Changes the Local Structure of Water: Insights from Photoelectron Spectroscopy and Theoretical Modeling of SCN⁻ Water Clusters. *J Phys. Chem. B* **2016**, *120* (8), 1518-1525.

Hou, G. L.; Valiev, M.; Wang, X. B., Deprotonated Dicarboxylic Acid Homodimers: Hydrogen Bonds and Atmospheric Implications. *J Phys Chem A* **2016**, *120* (15), 2342-2349.

Qin, Z. B.; Hou, G. L.; Yang, Z.; Valiev, M.; Wang, X. B., Negative ion photoelectron spectra of ISO₃⁻, IS₂O₃⁻, and IS₂O₄⁻ intermediates formed in interfacial reactions of ozone and iodide/sulfite aqueous microdroplets. *J Chem Phys*, **2016**, *145* (21).

T. Pirojsirikul, M. Valiev, A. W. Götz, J. Weare, R. Walker, K. Kowalski, Combined Quantum-Mechanical Molecular Mechanics Calculations with NWChem and AMBER: Excited State Properties of Green Fluorescent Protein Chromophore Analogue in Aqueous Solution. *J. Comp. Chem.*, **2017**, *38*(18), 1631-1639

Hou, G.-L., Zhang, J., Valiev, M., Wang, X.-B., Structures and energetics of hydrated deprotonated cis-pinonic acid anion clusters and their atmospheric relevance *Phys. Chem. Chem. Phys.*, **2017**, *19*, 10676 - 10684

Hou, G.-L., Wang, X.-B., and Marat Valiev, Formation of (HCOO⁻)(H₂SO₄) Anion Clusters: Violation of Gas-Phase Acidity Predictions, *J. Am. Chem. Soc.* **2017** *139* (33), 11321-11324

M. Valiev, G. Chuev, Site density models of inhomogeneous classical molecular liquids. *J. Stat. Mech.: Theory and Experiment*. 2018. 093201. 10.1088/1742-5468/aad6bf.

Chemical Kinetics and Dynamics at Interfaces

Cluster Model Investigation of Condensed Phase Phenomena

Xue-Bin Wang

Physical Sciences Division, Pacific Northwest National Laboratory, P.O. Box 999, MS K8-88, Richland, WA 99352. E-mail: xuebin.wang@pnnl.gov

Collaborators include: GL Hou, Z Yang, SH Deng, J Warneke, ZB Qin, QQ Yuan, L Jiang, WT Borden, SR Kass, CC Cummins, SH Strauss, OV Boltalina, PG Wenthold, AB McCoy, N Govind, SS Xantheas, M Valiev

Program Scope

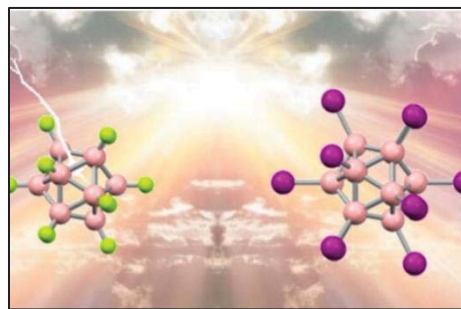
We aim at obtaining a molecular-level understanding of solution chemistry and condensed phase phenomena using gas phase clusters as model systems. Clusters occupy an intermediate region between gas phase molecules and the condensed states of matter and play an important role in heterogeneous catalysis, aerosol chemistry, and biological processes. We use electrospray ionization (ESI) to generate a wide variety of molecular and ionic clusters to simulate key species involved in the condensed phase reactions and transformations, and characterize them using cryogenic negative ion photoelectron spectroscopy (NIPES) and high-resolution velocity-map imaging (VMI) photoelectron spectroscopy. Inter- and intra-molecular interactions and their variation as function of size and composition, important to understand complex chemical reactions and nucleation processes in condensed and interfacial phases can be directly obtained. Experiments and *ab initio* calculations are synergistically combined to

- Explore new concepts and chemistries unique to cluster domain and distinctly different from isolated molecules and bulk;
- Probe ion specific effects in hydrated anion and neutral clusters, and stepwise salt dissolution processes;
- Obtain a molecular-level understanding of the solvation and stabilization of Hofmeister anions important in condensed phases;
- Study temperature-dependent conformation changes and isomer populations of complex clusters;
- Investigate intrinsic electronic structures of environmentally and catalytically important species and reactive diradicals;
- Quantify thermodynamic driving forces resulting from hydrogen-bonded networks formed in aerosol nucleation processes and enzymatic catalytic reactions;
- Unravel new physics of photodetachment of multiply charged anions beyond the prevailing conventional model.

The central goal of this research program lies at obtaining a fundamental understanding of environmental materials and solution chemistry important to many primary DOE missions, and enhances scientific synergies between experimental and theoretical studies towards achieving such goals.

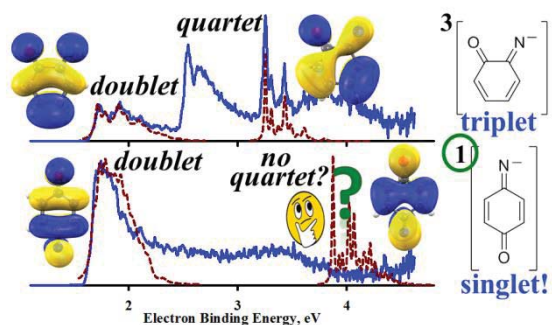
Recent Progress

Electronic Structure and Stability of $[B_{12}X_{12}]^{2-}$ ($X=F-At$): A Combined Photoelectron Spectroscopic and Theoretical Study: The stability and electron loss process of numerous Multiply Charged Anions (MCAs) have been traditionally explained in terms of the classical Coulomb interaction between spatially separated charged groups. An understanding of these processes in MCAs with not well-separated excess charges is still lacking. We report the surprising properties and



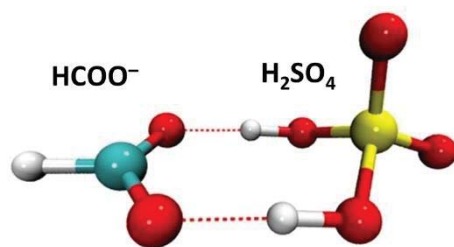
physical behavior of $[B_{12}X_{12}]^{2-}$, $X = F, Cl, Br, I, At$, which are MCAs with not well-separated excess charges and cannot be described by the prevailing classical picture. In this series of MCAs, comprised of a “Boron core” surrounded by a “Halogen shell”, the sign of the total charge in these two regions changes along the halogen series from $X=F-At$. With the aid of experimental photoelectron spectroscopy (PES) and highly correlated *ab-initio* electronic structure calculations, we demonstrate that the trend in the electronic stability of these MCAs is determined by the interplay between the Coulomb (de)stabilization originating from the “boron core” and “halogen shell” and the extent of the overlap between the orbitals from both regions. The second excess electron is *always* taken from the most *positively* charged region, viz. the “Boron core” for $X = F, Cl$, and the surrounding “Halogen shell” for $X = I, At$. This change in the physical behavior is attributed to the position of the Highest Occupied Molecular Orbital (HOMO), which dwells in a region that is spatially separated from the one containing the excess negative charge. The unusual intrinsic electronic structure of the $[B_{12}X_{12}]^{2-}$ MCAs provides the basis for a molecular level understanding of their observed unique physical and chemical properties and a new paradigm for understanding the properties of these MCAs with not well-separated charges that departs from the prevailing model used for spatially separated charges that is based on their classical Coulomb interaction. (*J. Am. Chem. Soc.* **139**, 14749-14756 (2017)).

Photoelectron Spectroscopy Study of Quinonimides. Structures and energetics of *o*-, *m*- and *p*-quinonimide anions ($OC_6H_4N^-$) and quinoniminy radicals have been investigated by using negative ion photoelectron spectroscopy. Modeling of the photoelectron spectrum of the *ortho* isomer shows that the ground state of the anion is a triplet, while the quinoniminy radical has a doublet ground state with a doublet-quartet splitting of 35.5 kcal/mol. The *para* radical has doublet ground state, but a band for a quartet state is missing from the photoelectron spectrum indicating that the anion has a singlet ground state, in contrast to previously reported calculations. The theoretical modeling is revisited, and it is shown that accurate predictions for the electronic structure of the *para* quinonimide anion require both an accurate account of electron correlation and a sufficiently diffuse basis set. Electron affinities of *o*- and *p*-quinoniminy radicals are measured to be 1.715 ± 0.010 and 1.675 ± 0.010 eV, respectively. The photoelectron spectrum of the *m*-quinonimide anion shows that the ion undergoes several different rearrangements, including a rearrangement to the energetically favorable *para* isomer. Such rearrangements preclude a meaningful analysis of the experimental spectrum (*J. Am. Chem. Soc.* **139**, 11138-11148 (2017)).



Formation of $(HCOO^-)(H_2SO_4)$ Anion Clusters: Violation of Gas-Phase Acidity Predictions:

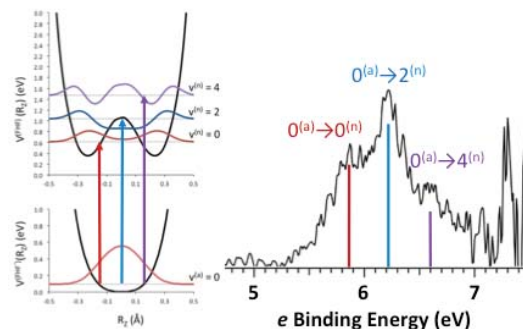
Sulfuric acid is commonly known to be a strong acid and, by all counts, should readily donate its proton to formate, which has a much higher proton affinity. This conventional wisdom is challenged in this work, where temperature-dependent negative ion photoelectron spectroscopy and theoretical studies demonstrate the existence of a $(HCOO^-)(H_2SO_4)$ pair at an energy slightly below the conventional $(HCOOH)(HSO_4^-)$ structure. Analysis of quantum-mechanical calculations indicates that a large proton affinity difference (~ 36 kcal/mol), favoring proton transfer to formate, is offset by a gain in inter-molecular interaction energy between $HCOO^-$ and H_2SO_4 through the electron delocalization and formation of two strong hydrogen bonds.



However, this stabilization comes with a severe entropic penalty, requiring the two species in precise alignment. As a result, the population of $(\text{HCOO}^-)(\text{H}_2\text{SO}_4)$ drops significantly at higher temperatures, rendering $(\text{HCOOH})(\text{HSO}_4^-)$ as the dominant species. This phenomenon is consistent with the photoelectron data, which shows depletion in the spectra assigned to $(\text{HCOO}^-)(\text{H}_2\text{SO}_4)$, and has also been verified by *ab initio* molecular dynamics (AIMD) simulations. (*J. Am. Chem. Soc.* **139**, 11321-11324 (2017)).

Experimental and Theoretical Studies of the $\text{F}^\bullet + \text{H-F}$ Transition-State Region by Photodetachment of $[\text{F-H-F}]^-$: The transition-state (TS) region of the simplest heavy-light-heavy type of reaction, $\text{F}^\bullet + \text{H-F} \rightarrow \text{F-H} + \text{F}^\bullet$, is investigated in this work by a joint experimental and theoretical approach.

Photodetaching the bifluoride anion, $[\text{F}\cdots\text{H}\cdots\text{F}]^-$, generates a negative ion photoelectron (NIPE) spectrum with three partially resolved bands in the electron binding energy (*eBE*) range of 5.4 – 7.0 eV. These bands correspond to the transition from the ground state of the anion to the electronic ground state of $[\text{F-H-F}]^\bullet$ neutral, with associated vibrational excitations. The significant increase of *eBE* of the bifluoride anion, relative to that of F^- , reflects a hydrogen bond energy between F^- and HF of ~46 kcal/mol. Theoretical modeling reveals that the antisymmetric motion of H between the two F atoms, near the TS on the neutral $[\text{F-H-F}]^\bullet$ surface, dominates the observed three bands, while the F-H-F bending, F-F symmetric stretching modes, and the couplings between them is calculated to account for the breadth of the observed spectrum. From the NIPE spectrum, a lower limit on the activation enthalpy for $\text{F}^\bullet + \text{H-F} \rightarrow \text{F-H} + \text{F}$ can be estimated to be $\Delta H^\ddagger = 12 \pm 2$ kcal/mol, a value below that of $\Delta H^\ddagger = 14.9$ kcal/mol, given by our G4 calculations (*J. Phys. Chem. A.* **121**, 7895-7902 (2017)).



Future Directions

The main thrust of our BES program will continue to be on cluster model studies of condensed phase phenomena in the gas phase. The experimental capabilities that we have developed give us the opportunity to attack a broad range of fundamental chemical physics problems pertinent to ionic solvation, solution chemistry, homogeneous / heterogeneous catalysis, aerosol chemistry, biological processes, and material synthesis. The ability to cool and control ion temperature and wavenumber energy resolution of VMI capability enable us to study different isomer populations and conformation changes of environmentally important hydrated clusters. Another major direction is to use gaseous clusters to model ion-specific interactions in solutions, ion transport, inert compound activation, ion-receptor interactions in biological systems, and initial nucleation processes relevant to atmospheric aerosol formation.

References to Publications of DOE CPIMS Sponsored Research (Oct. 2016 – Sept. 2018)

1. Evgeny V. Beletskiy, Xue-Bin Wang, and Steven R. Kass. “Anion Binding of One-, Two-, and Three-Armed Thiourea Receptors Examined via Photoelectron Spectroscopy and Quantum Computations”, *J. Phys. Chem. A* **120**, 8309-8316 (2016).
2. Zhengbo Qin, Gao-Lei Hou, Zheng Yang, Marat Valiev, Xue-Bin Wang. “Negative ion photoelectron spectra of ISO_3^- , IS_2O_3^- , and IS_2O_4^- intermediates formed in interfacial reactions of ozone and iodide/sulfite aqueous microdroplets”, *J. Chem. Phys.* **145**, 214310 (2016).
3. Xue-Bin Wang. “Cluster Model Studies of Anion and Molecular Specificities via Electrospray Ionization Photoelectron Spectroscopy”, *J. Phys. Chem. A* **121**, 1389-1401 (2017) (**Invited Feature Article, noted on the Cover, awarded as ACS Editors’ Choice**).

4. Gao-Lei Hou, Jun Zhang, Marat Valiev, and Xue-Bin Wang. "Structure and energetics of hydrated deprotonated cis-pinonic acid anion clusters and their atmospheric relevance" *Phys. Chem. Chem. Phys.* **19**, 10676-10684 (2017).
5. Gao-Lei Hou, Bo Chen, Wesley J. Transue, Zheng Yang, Hansjörg Grützmacher, Matthias Driess, Christopher C. Cummins, Weston Thatcher Borden, and Xue-Bin Wang. "Spectroscopic Characterization, Computational Investigation, and Comparisons of ECX⁻ (E = As, P, and N; X = S and O) Anions" *J. Am. Chem. Soc.* **139**, 8922-8930 (2017).
6. Ekram Hossain, Shihu M. Deng, Samer Gozem, Anna I. Krylov, Xue-Bin Wang and Paul G. Wenthold. "Photoelectron Spectroscopy Study of Quinonimides" *J. Am. Chem. Soc.* **139**, 11138-11148 (2017).
7. Gao-Lei Hou, Xue-Bin Wang, and Marat Valiev. "Formation of (HCOO⁻)(H₂SO₄) Anion Clusters: Violation of Gas-Phase Acidity Predictions" *J. Am. Chem. Soc.* **139**, 11321-11324 (2017) (communication).
8. Jonas Warneke, Gao-Lei Hou, Edoardo Aprà, Carsten Jenne, Zheng Yang, Zhengbo Qin, Karol Kowalski, Xue-Bin Wang, and Sotiris S. Xantheas. "Electronic Structure and Stability of [B₁₂X₁₂]²⁻ (X=F-At): A Combined Photoelectron Spectroscopic and Theoretical Study", *J. Am. Chem. Soc.* **139**, 14749-14756 (2017).
9. Gao-Lei Hou, Xue-Bin Wang, Anne B. McCoy, and Weston Thatcher Borden. "Experimental and Theoretical Studies of the F^{*} + H-F Transition-State Region by Photodetachment of [F-H-F]⁻", *J. Phys. Chem. A.* **121**, 7895-7902 (2017).
10. Long K. San, Sarah N. Spisak, Cristina Dubceac, Shihu H. M. Deng, Igor V. Kuvychko, Marina A. Petrukhina, Xue-Bin Wang, Alexey A. Popov, Steven H. Strauss, and Olga V. Boltalina. "Experimental and DFT Studies of the Electron-Withdrawing Ability of Perfluoroalkyl (R_F) Groups: Electron Affinities of PAH(R_F)_n Increase Significantly with Increasing RF Chain Length", *Chem. Eur. J.* **24**, 1441-1447 (2018).
11. Gao-Lei Hou, Niranjan Govind, Sotiris S. Xantheas, Xue-Bin Wang. "Deviation from the *trans*-Effect in Ligand-Exchange Reactions of Zeise's Ions PtCl₃(C₂H₄)⁻ with Heavier Halides (Br⁻, I⁻)", *J. Phys. Chem. A.* **122**, 1209-1214 (2018).
12. David A. Hrovat, Xue-Bin Wang, and Weston Thatcher Borden. "Calculations of the Relative Energies of the Low-lying Electronic States of 2,7-Naphthoquinodimethane and 2,7-Naphthoquinone. Substitution of Oxygen for CH₂ Is Predicted to Increase the Singlet-Triplet Energy Difference (ΔE_{ST})", *J. Phys. Org. Chem.* e3824 (2018).
13. Zheng Yang, David A. Hrovat, Gao-Lei Hou, Weston Thatcher Borden, and Xue-Bin Wang. "Negative Ion Photoelectron Spectroscopy Confirms the Prediction of the Relative Energies of the Low-Lying Electronic States of 2,7-Naphthoquinone", *J. Phys. Chem. A.* **122**, 4838-4844 (2018).
14. Qinqin Yuan, Zheng Yang, Renzhong Li, Wesley J. Transue, Zhipeng Li, Ling Jiang, Niranjan Govind, Christopher C. Cummins, and Xue-Bin Wang. "Magnetic-bottle and velocity-map imaging photoelectron spectroscopy of APS⁻ (A = C₁₄H₁₀ or anthracene): electron structure, spin-orbit coupling of APS^{*}, and dipole-bound state of APS⁻", *Chin. J. Chem. Phys.* **31**, 463-470 (2018).
15. Gao-Lei Hou, Wei Lin, Xue-Bin Wang. "Direct Observation of Hierarchic Molecular Interactions Critical to Biogenic Aerosol Formation" , *Communications Chemistry*, **1**: 37 (2018) (DOI: 10.1038/s42004-018-0038-7 (highlighted in Phys.org "**Researchers find intermolecular forces stabilize clusters, promote aerosol production**" <https://phys.org/news/2018-08-intermolecular-stabilize-clusters-aerosol-production.html>))
16. Qinqin Yuan, Xiang-Tao Kong, Gao-Lei Hou, Ling Jiang, and Xue-Bin Wang. "Photoelectron spectroscopic and computational study of [EDTA•M(III)]⁻ complexes (M = H₃, Al, Sc, V-Co)" *Phys. Chem. Chem. Phys.* **20**, 19458-19469 (2018).
17. David Hrovat, Xue-Bin Wang, Weston T. Borden. "Calculations on 1,8-Naphthoquinone Predict that the Ground State of this Diradical Is a Singlet" *J. Computational Chemistry* (accepted) (2018).

Nonequilibrium Properties of Driven Electrochemical Interfaces

PI: Adam P. Willard

Massachusetts Institute of Technology, Department of Chemistry

77 Massachusetts Ave., Cambridge, MA 02139

awillard@mit.edu

Program Scope:

The influence of nanoscale disorder on individual electrochemical processes is an important problem that remains to be completely understood. Disorder due to variations in local electrolyte composition or irregular interfacial geometries can influence chemical dynamics and thereby lead to heterogeneous chemical reactivity. It is difficult to assess the importance of this heterogeneity using traditional theoretical approaches (such as those based on the developments of Gouy, Chapman, and Stern) because these approaches are primarily based on mean field approximations, and thus omit the explicit effects of molecular/nanoscale disorder. The development of theoretical techniques that are capable of modeling these effects and quantifying their influence on chemical processes thus have the potential to provide important new physical insight.

Reactive electrochemical systems are inherently out of equilibrium. Active processes, such as interfacial electron transfer, influence both the static and dynamic properties of the interfacial environment, and ultimately drive the flux of reactive species across the electrochemical interface. Understanding and characterizing the nonequilibrium response of the interfacial environment is thus essential for predicting and quantifying these effects. The primary goal of this program is to investigate the static and dynamic properties of electrochemical interfaces driven out of equilibrium, and to determine how these nonequilibrium systems are affected by the presence of nanoscale disorder.

Our approach utilizes all-atom molecular simulation and coarse grained modeling to explore the properties of electrolytes under changing conditions of the electrostatic environment. We utilize general phenomenological models that provide the capability to explicitly evaluate the theoretical assumptions that underlie traditional electrochemical theories. Unlike traditional theoretical frameworks our models do not rely on the assumption that the electrochemical environment is a rapidly relaxing homogeneous continuum. Instead, our models explicitly treat the spatial fluctuations of charged species that drive individual electrochemical processes.

Our simulations also include a stochastic model of interfacial charge transfer to simulate active model electrochemistry. This allows us to explicitly evaluate the interplay between charge mobility within the electrolyte and charge creation/annihilation at the electrochemical interface. By exploring this interplay, and how it is affected by nanoscale disorder at the interface, we aim to reveal fundamental physical insight into the microscopic processes that drive reactivity at driven electrochemical interfaces.

Recent Progress:

We have made progress in this program on two scientific fronts. The first is the development of simulation tools that are capable mapping the nonequilibrium response of electrolytes in both space and time. The second is the development of a phenomenological model for simulating nanoscale electrochemical cells under driven electrochemical conditions. Both of these developments are described in more detail below.

Simulation tools for measuring nonequilibrium electrostatic potentials in electrolyte solutions:

We are currently developing of a new set of techniques that can be used for quantifying the nonequilibrium response of liquid electrolytes from molecular simulation. These techniques are designed to map the space and time dependent properties of the electrostatic environment. We quantify these properties based on the Madelung potential, $U_i(t)$, which describes the time dependent value of the

electrostatic potential experienced by the i th particle within a point-charge system. The Modeling potential is defined as,

$$U_i(t) = \frac{e}{4\pi\epsilon_0} \sum_{j \neq i} \frac{q_j(t)}{|\vec{r}_i(t) - \vec{r}_j(t)|},$$

where e is the elementary unit of charge, ϵ_0 is the vacuum permittivity, the summation is taken over all other particles in the system, each with charge $q_j(t)$ and position $\vec{r}_j(t)$. This definition of the potential provides an instantaneous and species specific snapshot of the electrostatic environment.

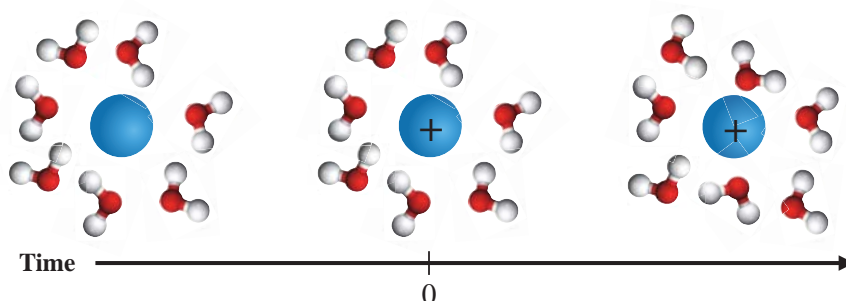


Figure 1. A schematic illustration of a simulation scheme for studying water's nonequilibrium response to electrostatic perturbations. In this scheme an originally neutral particle is assigned a permanent charge of +1 at time zero.

Our simulation tools provide the statistics of $U_i(t)$ for specific species within an electrolyte solution before, during, and after a non equilibrium perturbation. With these statistics we can characterize the equilibrium and nonequilibrium properties of electrolyte systems. Our initial efforts have focused on the simple nonequilibrium perturbation that is illustrated in Fig. 1. Specifically, we simulate a single Lennard-Jones (LJ) particle immersed in bulk liquid water. The system is initially equilibrated under the condition that the LJ particle is neutral and then, at time $t = 0$, the charge on the LJ particle is changed. This change puts the system out of equilibrium, which initiates a subsequent relaxation. By computing $U_i(t)$ for the oxygen atoms in the system, we can quantify how the system feels the initial nonequilibrium perturbations and the dynamics of the systems subsequent response.

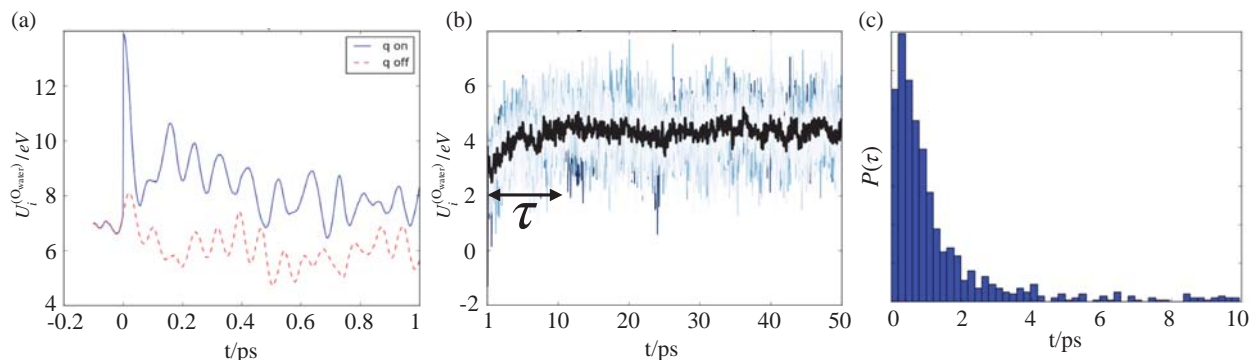


Figure 2. Probing the electrostatic relaxation in water around a point charge particle. (a) The dynamics of the Madelung potential on a single water oxygen near a LJ particle with variable charge. The blue line shows the case where the charge on the LJ particle changes from 0 to +1 at time $t=0$ and the red line shows the dynamics from the same initial configuration but without the change in charge. (b) Averaging the dynamics over many trajectories, each started from the same initial configuration (i.e., isoconfiguration averaging) enables smooth relaxation curves to be generated for each oxygen in the system. (c) A histogram of relaxation times for water molecules in the first solvation shell of the LJ particle.

Figure 2 illustrates our approach with data generated for water oxygens around a LJ particle that is spontaneously charged to be either positive, as in panel (a), or negative, as in panel (b). Individual trajectories feature large fluctuations that are difficult to analyze, as illustrated in Fig. 2(a). We have found that by performing isoconfigurational averaging, in which we run many trajectories each launched from the same nuclear configuration (but with slightly different momenta), we can converge the relaxation dynamics that are inherent to a given configuration, as illustrated in Fig. 2(b). By sampling over many individual initial configuration we can generate statistics of relaxation dynamics that directly characterize the effects of molecular heterogeneity within the system, as illustrated in Fig. 2(c).

Coarse grained model of a driven electrochemical interface:

We are developing a theoretical framework for simulating the dynamics of active electrochemical interfaces. This framework explicitly describes both the effects of molecular disorder that are inherent to dilute electrolyte systems and the dynamic effects of interfacial charge transfer. The model also includes an explicit description of interfacial charge transfer, and thus offers a realistic simulation of the driving forces that control the flow of current in an electrochemical cell. As illustrated in Fig. 3(a), our model combines three basic ingredients: (1) a constant potential electrode, (2) an explicit model of an electrolyte, and (3) an empirical model of interfacial charge transfer. We combine these three ingredients, as illustrated in Fig. 3, to simulate the flow of current in model electrochemical cells.

In our model, we formulate the interfacial electron transfer rate as a function of the applied electrode potential and of the characteristics of the local electrostatic environment. This means that different micro-environments can yield different rates of charge transfer, as illustrated in Fig. 3(b). As a result, heterogeneity in the local rate of electron transfer occurs naturally in our system due to fluctuations in the local composition of the ionic environment. Furthermore, our model can describe how the distribution of interfacial electron transfer rates changes when current is flowing across the electrode.

With this model we simulate the static and dynamic properties of electrochemical system under different conditions. To illustrate the capability of our model to simulate nonequilibrium dynamics we consider an electrochemical system, originally equilibrated under neutral electrodes, that is subject to a gradient in

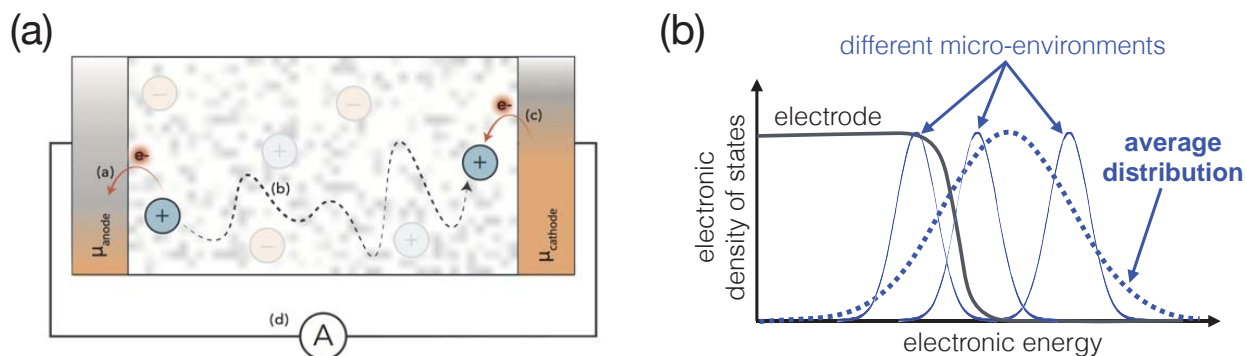


Figure 3. (a) A schematic illustration of our coarse grained model of a driven electrochemical cell. The model contains variable potential electrodes that are capable of exchanging electrons with redox-active model species in the electrolyte region. The dynamics of these species thus mediate the flow of charge through the model system. (b) Variations in micro-environment lead to variations in charge transfer rates. This figure shows the distribution of electronic energy levels in the electrode (grey line) and the average over all Li-ions (dashed blue line). The distribution for individual ions (solid blue lines) can differ from the average distribution due to variations in micro-environment, for example arising from differences in local ionic coordination. Our methodology will treat these variations explicitly, so that local configuration directly influences charge transfer rates.

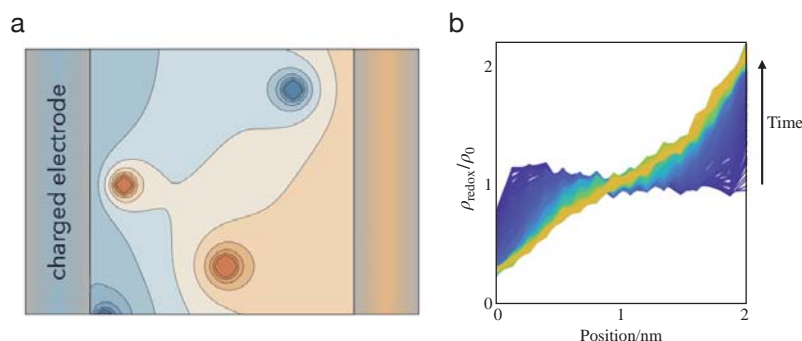


Figure 4. (a) Snapshots from our model reveal heterogeneity in the electrostatic potential (as indicated by shading). Ions perturb this potential and ultimately arrange themselves to screen the influence of charged electrodes. (b) The density profile of a redox active species after the application of a constant electrochemical driving force between electrodes at position 0nm and 2nm. At early times (dark blue) the density profile is roughly uniform and at later times (yellow) the density profile reflects the presence of a electrode-induced chemical potential gradient.

applied electrode potential. Figure 4 (a) illustrates the electrostatic potential computed along a slice through the system. The electrodes impose potential gradient across the system and the ion positions shape this potential gradient. Figure 4(b) contains a plot of the density of redox active species after the potential is applied. This efficient coarse grained model can be used to simulate the dynamics of experimentally relevant systems. For example, Fig. 4 shows the evolution of the cell-wide ion density field in a model potential jump experiment.

Future Plans:

Future plans for this program will combine our newly developed simulation tools and coarse grained model to explore the properties of driven electrochemical systems. Specifically, we will focus on investigating the structural and dynamical properties of the electrochemical double layer, and how these properties vary when systems are out of equilibrium. We will apply our newly developed simulation tools and coarse grained models to study the screening response of electrolytes systems, such as that illustrate in Fig. 5, that are forced out of equilibrium by some external bias.

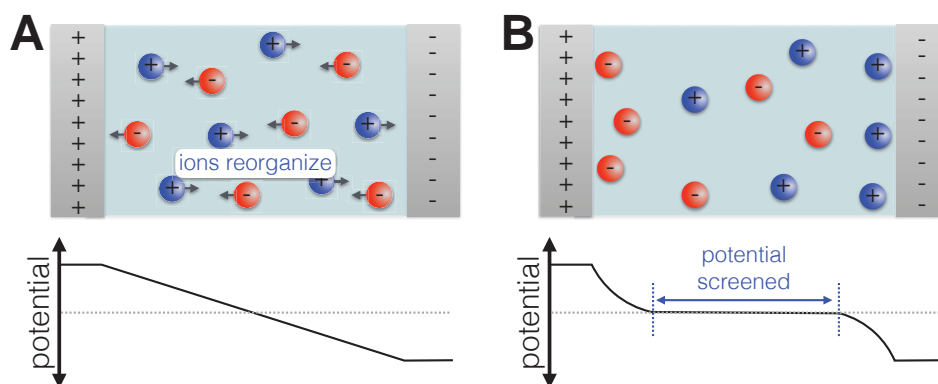


Figure 5. The screening response of an electrolyte confined between two constant potential electrodes. (A) When an applied electrode potential is introduced to an electrolyte that is initially at equilibrium, a linear potential gradient drives the flow of ions. (B) The equilibrium response of the electrolyte to an applied potential includes a buildup of excess ionic charge at each electrode compensates the electrode charges, screening the potential gradient in the regions away from the electrode surfaces.

Publications:

We have not yet produced any publications under this award.

Non-Empirical and Self-Interaction Corrections for DFTB: Towards Accurate Quantum Simulations for Large Mesoscale Systems

Bryan M. Wong

Department of Chemical & Environmental Engineering and Materials Science & Engineering Program, University of California-Riverside, Riverside, CA 92521

E-mail: bryan.wong@ucr.edu, Web: <http://www.bmwong-group.com>

1. Program Scope

This project is comprised of two complementary (but parallel) thrusts: (1) implementing massively-parallelized computing hardware (with new computational hardware that may replace GPUs) for calculating the electron structure and dynamics of large chemical systems, and (2) introducing self-interaction corrections for improving the accuracy of the density functional tight binding (DFTB) approach. While classical molecular dynamics can handle hundreds of thousands of atoms, it cannot provide a first-principles based description of mesoscale systems at the quantum level. At the other extreme, conventional Kohn-Sham DFT methods can probe the true quantum mechanical nature of chemical systems; however, these methods cannot tackle the large sizes relevant to mesoscale dynamics and length scales. The DFTB formalism utilized in this project provides a viable approach for probing these mesoscale systems at a quantum mechanical level of detail. However, to utilize the DFTB approach for accurate calculations of electronic properties, it is crucial to incorporate *quantum-based non-empirical corrections* in DFTB since exchange-correlation effects can still remain very strong in these large systems. At the same time, enhancing the computational efficiency of DFTB is also essential since optimal computational performance is required for addressing the large size scales associated with mesoscale systems. As such, the new non-empirical corrections and computing hardware enhancements implemented in this project will enable accurate *and* computationally efficient approaches to directly probe electronic properties in these large, complex systems.

2. Recent Progress

The start date of this project was 08/15/2016, and during the past two years we have devoted half of our initial efforts to massive parallelization (with additional chemical applications) of the electron dynamics code and the other half of our focus to an in-house (i.e., from scratch) implementation of self-interaction corrections (SICs). One of the chemical/material systems that we have applied our real-time, time-dependent DFTB (RT-TDDFTB) approach is large metallic nanocluster systems and arrays. Since our last progress update, Niranjana Ilawe (a graduate student funded by this DOE project) graduated with a Ph.D. this year and published his last paper on RT-TDDFTB simulations of a large plasmonic antenna, which is described further below.

One of the recurring issues with the practical application of these plasmonic ensembles is that the propagation distance of energy transfer remains too short. A possible solution for increasing this propagation distance in plasmonic chains is to (naturally) decrease the interparticle spacings, which results in stronger plasmon couplings. As the interparticle distance is decreased, however, various hybridized plasmon resonances emerge as a result of interactions between the individual plasmon resonances of the elementary nanoparticles. For example, the Bonding Dipole hybridized Plasmon (BDP) is characterized by in-phase charge oscillations in each of the nanoparticles. Another hybridized plasmon mode, the Charge Transfer Plasmon (CTP), is observed in the structure when the nanoparticles touch each other or a conductive junction is established between

them, allowing for a direct charge transfer from one nanoparticle to the other. The onset of these hybridized plasmon resonances drastically modify the near and far field properties of the systems, resulting in new mechanisms to modulate energy/charge transfer in these plasmonic ensembles.

To augment our previous 2017 CPIMS progress report (which reported on *long-range* energy-transfer mechanisms), we have made new progress in investigating extremely *small inter-particle spacings*, where quantum effects play an essential role and are beyond the scope of classical finite-difference time domain (FDTD) methods. In addition, to make closer contact to relevant chemical systems of interest to experimentalists, we have moved beyond the simple sodium nanoparticles used in our previous report to large silver nanoparticle arrays. In these new studies, we first characterized the plasmon resonance energy of a single silver nanoparticle containing 55 atoms and having an icosahedral shape. As can be seen in **Fig. 1**, a prominent peak, corresponding to the plasmon resonance is observed around 3.23 eV, which is in good agreement with a time-dependent density functional theory (DFT) calculation of 3.6 eV and a recent experimental result of 3.8 eV for similar-sized Ag nanoparticles.

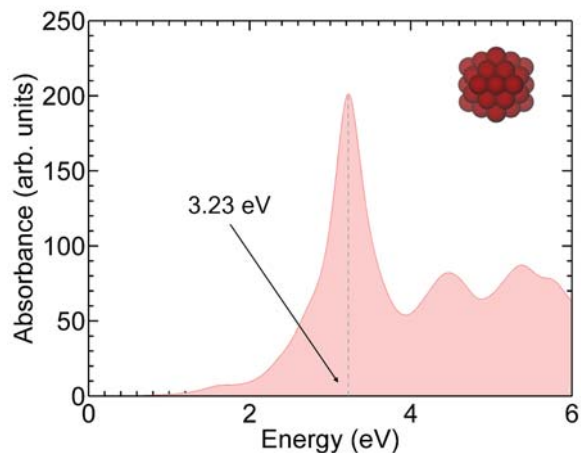


Figure 1. Absorption spectra of a 55-atom icosahedral silver nanoparticle obtained with RT-TDDFTB. A prominent plasmon resonance peak is observed around 3.23 eV.

With the energy of a single Ag nanoparticle (NP) characterized, we proceeded with an analysis of energy transfer in plasmonic NP assemblies, each containing 8 Ag NPs and with varying interparticle spacings (ranging from 5 to 0.5 Å). All of these chains are extremely large systems with each containing a total of 440 atoms, as shown in **Fig. 2**. To simulate energy transfer along the NP chains, we excite only the first Ag NP in the chain using a monochromatic laser with an energy equal to the plasmonic resonance energy of a single Ag NP (3.23 eV), and the entire system is allowed to evolve in time via the RT-TDDFTB propagation. To quantify the energy-transfer efficiency along the chain, we computed the electric field intensities, $I \propto |\mathbf{E}|^2$, where \mathbf{E} is the total electric field between each of the NPs along the axial direction of the chain.

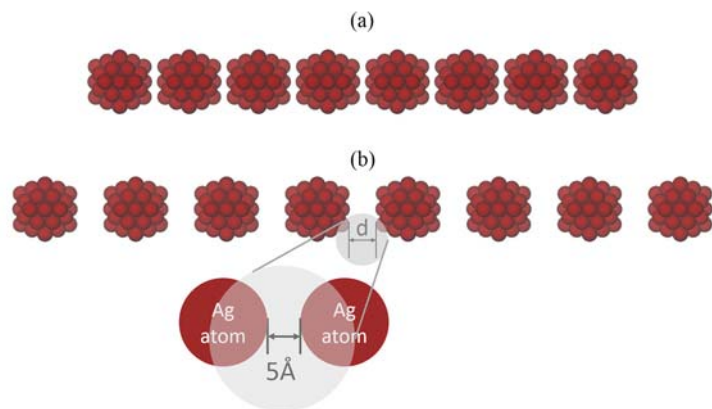


Figure 2. Pictorial representation of two of the nanoparticle chains with interparticle (edge-to-edge) distances equal to (a) 1 Å and (b) 5 Å.

We have chosen this metric of computing electric field intensities along the NP chain since this allows a direct comparison of energy transfer efficiencies that were used in previous studies. **Fig. 3** on the following page shows the trends in the intensities of the NP chains with interparticle distances ranging from 0 to 5 Å. From the trends in **Fig. 3**, we observed a monotonic increase in energy transfer efficiency (i.e. the slope of the intensity lines and transmission loss factor both decrease)

as the interparticle distance is reduced from 5 Å to about 2 Å. This result is in qualitative agreement with results obtained by previous studies on similar systems using classical electrodynamic methods and can be attributed to an increase in capacitive coupling between the Ag NPs as the interparticle distance between them is reduced. This phenomenon is analogous to a charged capacitor, where the capacitance of a capacitor increases as the charged plates are brought closer together. However, as the interparticle distance is further reduced below 2 Å, we observed an opposite trend – a sudden drop in energy-transfer efficiency occurs for interparticle distances below 2 Å (i.e. the slope of the intensity line increase), which is qualitatively opposite to what has been predicted by previous

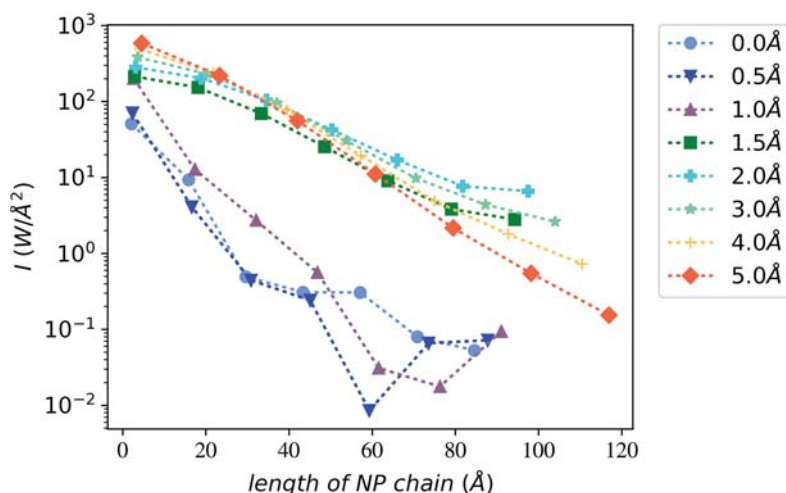


Figure 3. Field intensities along silver NP chains with varying interparticle distances. The first nanoparticle in each of the chains is excited at the plasmon resonance energy, and the intensity values are computed at the interparticle gaps of the NPs as shown in Figure 2. The excitation energy used in the simulation is equal to the plasmon resonance energy of the single Ag nanoparticle. A drastic drop in the field intensity is seen for Ag chains with interparticle spacings less than 2 Å.

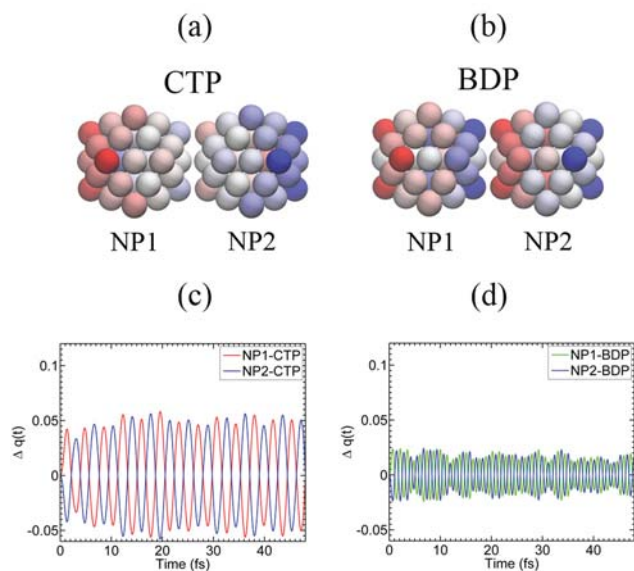
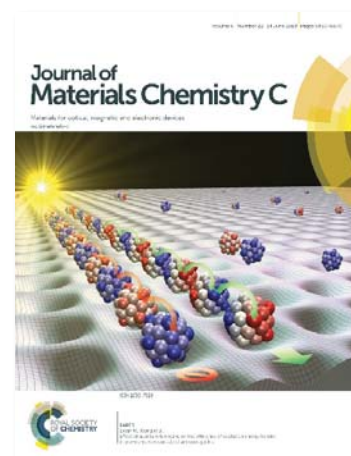


Figure 4. Snapshot of charge distributions at one instance in time for a silver NP with an interparticle distance of 1 Å. The CTP is characterized by a charge separation between the two NPs, whereas the BP shows dipolar charge distributions within each of the NPs.

computational studies. Specifically, previous studies have observed a decrease in energy transfer when the interparticle distance is reduced to a distance where the NPs directly touch each other. In contrast, we observe a decrease in energy-transfer efficiency even before the instance when the NPs touch each other. We attribute this decrease to competing mechanisms between a Bonding Dipole hybridized Plasmon (BDP) and another hybridized plasmon mode, the Charge Transfer Plasmon (CTP), described briefly below.

Fig. 4 shows both the charge distributions and their time-dependent behavior for a NP dimer with an interparticle spacing of 1 Å. In contrast to a “pure” BDP mode (which we described in our previous 2017 CPIMS progress report), the hybridized BDP mode shown in **Fig. 4** shows some degree of charge transfer from one NP to the other. In short, at

subnanometer interparticle spacings, the hybridized BDP allows for a small charge transfer between NPs and, therefore, reduces the capacitive coupling between the NPs. Going back to the capacitor analogy used previously, this is analogous to a leaking capacitor which reduces the overall efficiency of the entire antenna (and, more importantly, cannot be predicted by classical approaches). Consequently, our study has two important ramifications on EET in plasmonic nanosystems: (1) while classical methods based on solving Maxwell's equations have long been used to analyze a variety of nanoantenna systems, our findings show that the inclusion of quantum effects has a nontrivial effect on EET dynamics, especially in plasmonic nanoantennas with subnanometer interparticle spacings, and (2) decreasing the interparticle spacing beyond a certain limit may not have the intended effect of increasing EET efficiency and, therefore, a more careful consideration of other strategies may be necessary in improving energy transfer in plasmonic devices fabricated with subnanometer dimensions. This work was prominently featured as a front cover of the *Journal of Materials Chemistry C*.



3. Future Plans

We intend to focus much of this remaining fiscal year's effort into massive parallelization of our real-time approach (with new computational hardware that may replace GPUs) for calculating the electron structure and dynamics of large chemical systems. We hope to have an update on this second phase of the project at the upcoming 2019 CTC meeting. In addition, two manuscripts detailing our progress in self-interaction corrections have already been submitted and are undergoing peer review. This DOE Grant has supported 1 Postdoctoral Associate, 2 PhD students, and 2 MS students.

Grant Number and Title: DE-SC0016269: "Non-Empirical and Self-Interaction Corrections for DFTB: Towards Accurate Quantum Simulations for Large Mesoscale Systems"

Publications acknowledging DOE grant DE-SC0016269 in the last two years:

1. A. A. Barragan, N. V. Ilawe, L. Zhong, B. M. Wong, and L. Mangolini, "A Non-Thermal Plasma Route to Plasmonic TiN Nanoparticles." *Journal of Physical Chemistry C*, **121**, 2316 (2017).
2. S. Pari, I. A. Wang, H. Liu, and B. M. Wong, "Sulfate Radical Oxidation of Aromatic Contaminants: A Detailed Assessment of Density Functional Theory and High-Level Quantum Chemical Methods." *Environmental Science: Processes & Impacts*, **19**, 395 (2017). (Invited Paper)
3. L. N. Anderson, M. B. Oviedo, and B. M. Wong, "Accurate Electron Affinities and Orbital Energies of Anions from a Non-Empirically Tuned Range-Separated Density Functional Theory Approach." *Journal of Chemical Theory and Computation*, **13**, 1656 (2017).
4. N. V. Ilawe, M. B. Oviedo, and B. M. Wong, "Real-Time Quantum Dynamics of Long-Range Electronic Excitation Transfer in Plasmonic Nanoantennas." *Journal of Chemical Theory and Computation*, **13**, 3442 (2017).
5. L. N. Anderson, F. W. Aquino, A. E. Raeber, X. Chen, and B. M. Wong, "Halogen Bonding Interactions: Revised Benchmarks and a New Assessment of Exchange vs Dispersion." *Journal of Chemical Theory and Computation*, **14**, 180 (2018).
6. N. V. Ilawe, M. B. Oviedo, and B. M. Wong, "Effect of Quantum Tunneling on the Efficiency of Excitation Energy Transfer in Plasmonic Nanoparticle Chain Waveguides." *Journal of Materials Chemistry C*, **6**, 5857 (2018).

Intermolecular Interactions in the Gas and the Condensed Phase

Sotiris S. Xantheas

Advanced Computing, Mathematics & Data Division,
Pacific Northwest National Laboratory, PO Box 999, MS K1-83, Richland WA 99352
sotiris.xantheas@pnl.gov

Program Scope: The overarching themes of this research component of the Molecular Theory & Modeling Program are:

- establish accurate benchmarks for archetypal intermolecular interactions, aqueous clusters and guest – host interactions relevant to energy applications,
- incorporate the appropriate physics into models (classical or quantum) that explicitly account for the desired behavior,
- elucidate the molecular level factors that control complex behavior,
- understand the interplay between the molecular level information and the macroscopic properties of complex aqueous environments.

The ultimate goal of the program is *to develop accurate descriptions of intermolecular interactions for complex environments that include molecular level detail.*

Recent Progress: In recent work, we have focused on revisiting the Many-Body Expansion (MBE) for water-water and ion-water interactions by examining the effects of the basis set, including those resulting from the Basis Set Superposition Error (BSSE) correction, on the various terms for selected sizes of water clusters of selected clusters in the range $n = 7 - 21$. The analysis is performed at the second order Møller-Plesset (MP2) perturbation theory with the family of augmented correlation consistent basis sets up to five zeta quality for the $(\text{H}_2\text{O})_n$, $n = 7, 10, 13, 16$ and 21 clusters, for which we report either the complete MBE ($n = 7, 10$) or the one through the 5-body term ($n = 13, 16, 21$). Our results suggest that any sizeable contributions to the total cluster binding energy arising from the 5-body and larger terms are solely an artifact of the finite basis set. Indeed, all terms above the 4-body converge to practically zero at the Complete Basis Set (CBS) limit and this finding is accurately reproduced even with the smaller basis set of the series (aug-cc-pVDZ) once the BSSE correction is considered. The same level of theory (MP2/aug-cc-pVDZ, BSSE-corrected) also accurately reproduces the magnitude of the 3- and 4-body terms, for which we also find that the effects of electron correlation are quite small. Our results unquestionably demonstrate that the MBE for water-water interactions converges monotonically

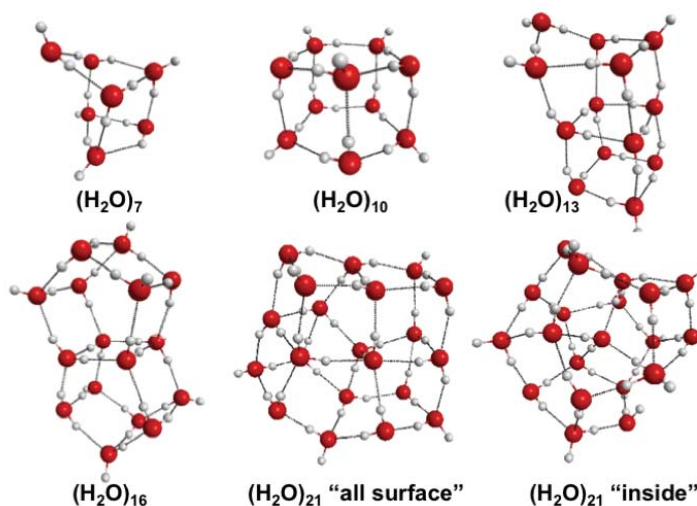


Figure 1. Water clusters used in the MBE analysis.

and can be safely truncated at the 4-body term. We expect these findings to have important consequences in the pursuit of accurate many-body molecular dynamics simulations for aqueous systems.

Extensive benchmark CCSD(T) Complete Basis Set (CBS) estimates of the binding energies, structures and harmonic frequencies of $\text{H}_3\text{O}^+(\text{H}_2\text{O})_n$ clusters, $n=0-5$, including all currently known low-lying energy isomers, were performed in order to establish the baseline for the development of a many-body Potential Energy Surface (PES) for aqueous hydronium. A new 4-body $\text{H}_3\text{O}^+-\text{H}_2\text{O}-\text{H}_2\text{O}-\text{H}_2\text{O}$ term was added to a previously reported many-body (up to 3-body interactions) CCSD(T)-based PES for the hydrated proton. The new term is aimed at refining the relative energies of isomers of the $\text{H}_3\text{O}^+(\text{H}_2\text{O})_n$, $n=4-5$ clusters. In addition, the previous 3-body interaction was refit using additional ab initio energies and also shifted by a small constant to account for BSSE, which improves both the absolute and relative cluster binding energies. The harmonic frequencies of the various cluster isomers obtained from the new PES were also compared to the ones obtained from the highest level of ab initio calculations, several of which are reported for the first time, the differences between the two being at most 30 cm^{-1} . These tests confirm the high accuracy of the new PES for aqueous hydronium. The harmonic frequencies of the new PES differ by $< 10-20\text{ cm}^{-1}$ from those obtained from a previous version of the PES without the modified 3-body and the new 4-body terms. This new extended PES is appropriate to study the dynamics of larger protonated water clusters. In addition, the new binding energies and harmonic frequencies provide important benchmarks that can be used to assess the accuracy of more approximate, efficient electronic structure methods. Notably, tests can now be performed of the large number of DFT functionals that have already been used in numerous studies of the structure, energetics, and spectroscopy of protonated water clusters as well as condensed environments involving the hydrated proton.

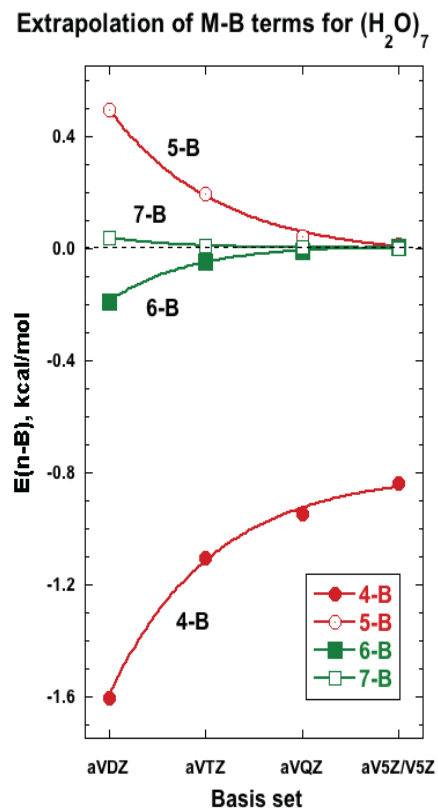


Figure 2. Convergence of the uncorrected 4- through 7-body terms in the many-body expansion of $(\text{H}_2\text{O})_7$ for the various basis sets.

well as condensed environments involving the hydrated proton.

Future Work: We will investigate the interactions associated with the process of CO_2/CH_4 exchange in a hydrate lattice. We will attempt the first CCSD(T) calculation for the interaction of H_2 , N_2 , CH_4 , and CO_2 inside hollow $(\text{H}_2\text{O})_{20}$ and $(\text{H}_2\text{O})_{24}$ cages with a triple zeta quality set. Preliminary calculations at the MP2 and B3LYP+D levels will be performed. It should be remembered that at the DFT level the guest [H_2 , CH_4] + host [$(\text{H}_2\text{O})_{20}$] system lies *above* the asymptote of the empty cage + the gas-phase molecule, whereas at the MP2 or CCSD(T) level it lies *below* the asymptote, i.e., it is more stable than the two isolated fragments. This finding further justifies the necessity of using high-level electronic structure calculations in order to quantify the relevant interactions in those systems. Additional calculations for the accommodation of CO_2 and CH_4 inside the small and large cages of the structure I (sI) hydrate

lattice will focus on understanding their exchange mechanism between adjacent cages in the hydrate lattice by computing the barrier for that exchange between adjacent cages in the lattice.

Furthermore, we will extend our previous studies of weak π - π interactions in an attempt to establish an accurate interaction energy for the Coronene dimer, a polyaromatic hydrocarbon (PAH) with 7 perifused benzene rings that has been used as a molecular model for the interactions between graphene sheets, at the MP2 and CCSD(T) levels of theory. Due to the technological applications of the electrical properties of graphene sheets and associated carbon-based functionalized nanomaterials, the magnitude of the interaction in the Coronene dimer has recently received a lot of attention. Most calculations have been performed to date using various density functionals, the accuracy of which is difficult to assess, since an accurate benchmark is currently not available. Following the same protocol we have established earlier for the benzene dimer, we expect that CCSD(T) single-point energy calculations with the cc-pVDZ and cc-pVTZ basis sets (1,775 basis functions) will provide an accurate binding energy for the Coronene dimer. We will finally extend our work on weak intermolecular interactions to the C₆₀ dimers and trimers. To date, the interaction between two C₆₀ molecules as well as the simulation of their phase diagram has been reported using either classical potentials or various Density Functional Theory approaches and their variants. We will compute the interaction between two and three carbon nanoparticles up to C₆₀ at the MP2 and CCSD(T) levels of theory in order to obtain accurate dimer potential energy curves as well as the magnitude of the respective 3-body term. Of particular importance is the investigation of the long-range part of the interaction potential and the ability of MP2 to provide accurate 1/R behavior when compared to CCSD(T). For this purpose, we will also consider corrections to the c₆ coefficient at long range proposed by Head-Gordon. The ab initio potentials will be fitted to the simple PEFs developed during the past award period and will provide accurate pairwise additive and 3-body potentials that can be used to model the aggregation and phase diagram of those carbon nanoparticles. The nature of bonding both in and between those nanoparticles will be investigated using a recent analysis based on molecule-intrinsic quasi-atomic, bonding, and correlating orbitals. Subsequent studies will be extended to the interaction between carbon nanoparticles, starting from C₂₄ and extending all the way to C₆₀.

Publications Acknowledging this Grant in the last 3 years

1. J. S. Moore, S. S. Xantheas, J. W. Grate, T. W. Wietsma, E. Gratton, A. E. Vasdekis, "Modular Polymer Biosensors by Solvent Immersion Imprint Lithography", *Journal of Polymer Science, Part B: Polymer Physics* **54**, 98 (2016)
2. E. Miliordos and S. S. Xantheas, "The origin of the reactivity of the Criegee intermediate: implications for atmospheric particle growth", Communication to the Editor, *Angewandte Chemie International Edition* **55**, 1015 (2016). Designated as "Hot paper"
3. S. Yoo Willow, X. Cheng Zeng, S. S. Xantheas, K. S. Kim and S. Hirata, "Why is MP2-Water 'Cooler' and 'Denser' than DFT-Water?", *Journal of Physical Chemistry Letters* **7**, 680 (2016)
4. C. T. Wolke, J. A. Fournier, E. Miliordos, S. M. Kathmann, S. S. Xantheas, and M. A. Johnson, "Isotopomer-selective spectra of a single intact H₂O molecule in the Cs⁺[(D₂O)₅·H₂O] isotopologue: Going beyond pattern recognition to harvest the structural information encoded in vibrational spectra", *Journal of Chemical Physics* **144**, 074305 (2016)
5. S. Iwata, D. Akase, M. Aida and S. S. Xantheas, "Hydrogen-Bonded Networks in Polyhedral Water Clusters (H₂O)_n, n = 8, 20 and 24" *Physical Chemistry Chemical Physics* **18**, 19746 (2016)

6. E. Miliordos, E. Aprà and S. S. Xantheas, "A New, Dispersion - Driven Intermolecular Arrangement for the Benzene – Water Octamer Complex: Isomers and Analysis of their Vibrational Spectra", *Journal of Chemical Theory and Computation* **12**, 4004 (2016)
7. T.-M. Chang and S. S. Xantheas, A. E. Vasdekis, "Mesoscale Polymer Dissolution probed by Raman Spectroscopy and Molecular Simulations" *Journal of Physical Chemistry B* **120**, 10581 (2016)
8. S. S. Xantheas, "Spying on the neighbors' pool: Spectral signatures are obtained for the movement of protons in cold water clusters", invited Perspective, *Science* **354**, 1101 (2016)
9. G. E. Doublerly, R. E. Miller and S. S. Xantheas, "Formation of Exotic Networks of Water Clusters in Liquid Helium Droplets Facilitated by the Presence of Neon Atoms", *Journal of the American Chemical Society* **139**, 4152 (2017). Included in *Science* **355**, 1388 (2017) under *Research in Other Journals*
10. S. Yoo Willow and S. S. Xantheas, "A Molecular Level Insight of the Effect of Hofmeister Anions on the Interfacial Surface Tension of a Model Protein", *Journal of Physical Chemistry Letters* **8**, 1574 (2017)
11. T. B. Ward, E. Miliordos, P. D. Carnegie, S. S. Xantheas, M. A. Duncan, "Ortho-Para Interconversion in Cation-Water Complexes: The Case of $V^+(H_2O)$ and $Nb^+(H_2O)$ Clusters", *Journal of Chemical Physics* **146**, 224305 (2017)
12. P. Hamm, G. S. Fanourgakis, S. S. Xantheas, "A surprisingly simple correlation between the classical and quantum structural networks in liquid water", *Journal of Chemical Physics*, **147**, 064506 (2017)
13. J. Warneke, G.-L. Hou, E. Aprà, C. Jenne, Z. Yang, Z. Qin, K. Kowalski, X.-B. Wang and S. S. Xantheas, "Electronic Structure and Stability of $(B_{12}X_{12})^{2-}$ ($X = F - At$): A Combined Photoelectron Spectroscopic and Theoretical Study", *Journal of the American Chemical Society* **139**, 14749 (2017)
14. G.-L. Hou, N. Govind, S. S. Xantheas, X.-B. Wang, "Deviation from the *trans*-Effect in Ligand-Exchange Reactions of Zeise's Ions $PtCl_3(C_2H_4)^-$ with Heavier Halides (Br^- , I^-)", *Journal of Physical Chemistry A* **122**, 1209 (2018)
15. A. Mukhopadhyay, S. S. Xantheas, R. J. Saykally, "The Water Dimer II: Theoretical Investigations", Frontiers Article (invited), *Chemical Physics Letters* **700**, 163 (2018). Journal Cover
16. J. P. Heindel, Q. Yu, J. M. Bowman, S. S. Xantheas, "Benchmark electronic structure calculations for the $H_3O^+(H_2O)_n$, $n=0-5$, clusters and tests of an existing 1,2,3-body potential energy surface with a new 4-body correction", *Journal of Chemical Theory and Computation* **14**, 4553 (2018)
17. G. Liu, E. Miliordos, G. Liu, S. N. Ciborowski M. Tschurl, U. Boesl, U. Heiz, X. Zhang, S. S. Xantheas, and K. H. Bowen, "Water Activation by Single Metal-Atom Anions" *Journal of Chemical Physics* accepted for publication (2018)

The emergent photophysics and photochemistry of molecular polaritons: a theoretical and computational investigation

DE-SC0019188

Joel Yuen-Zhou

Department of Chemistry and Biochemistry, University of California San Diego, La Jolla, CA 92093

joelyuen@ucsd.edu

Program scope. This project aims to develop a comprehensive theoretical and computational framework to address a new class of emergent room-temperature photophysical and photochemical processes afforded by molecular polaritons (MPs), namely, hybrid states arising from the strong coupling of organic dye electronic/vibronic excitations and confined electromagnetic modes. Recent experimental progress on MPs prompts for the development of robust theoretical tools that can describe the novel phenomenology afforded by these systems under realistic dissipative conditions. Our project aims to fill this gap. The molecular or photonic components of MPs can be tuned to rationally modify the physicochemical properties of molecular matter. In this work, we will first pioneer formalisms based on open-quantum systems theory to address the low-energy dynamics of MPs in the presence of room-temperature realistic conditions such as in the presence of static and dynamic molecular disorder as well as absorptive losses in the electromagnetic environment. This framework will allow

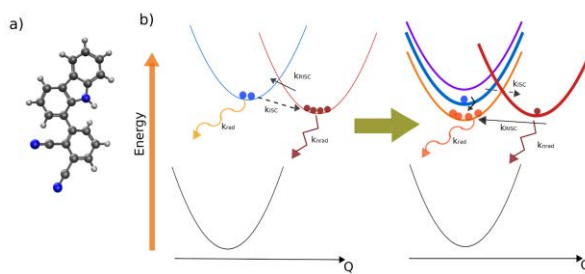


Fig. 1. Schematic of polariton-assisted triplet harvesting. a. Electrical injection of excitons produces statistical populations of 75% triplet and 25% singlet excitons. The former do not emit light unless they can transfer their population into singlet states. **b.** Strong coupling an optical cavity with the singlet excitons generates a lower polariton which has sufficiently low energy to harvest population from the triplets, thus potentially enhancing the electrical to photon conversion efficiency.

us to harness MPs to design control strategies of great interest to the missions of DOE-BES such harvesting of triplet excitons (Fig. 1, work in progress), or even exotic paradigms for the remote control of chemical reactions (Fig. 2, work in progress) in condensed

phases. Given the emergent many-body flavor of the problems of interest where many electrons, vibrations, and photons interact with one another, our approach will construct effective Hamiltonian theories that can capture the essential dynamical features of the problems in question. To ensure relevance to experiments, we will routinely supplement our models with parameters obtained from computational quantum chemistry and from spectroscopic data in the literature or from our experimental collaborators.

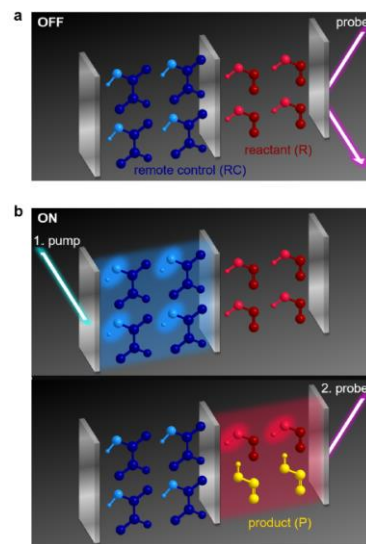
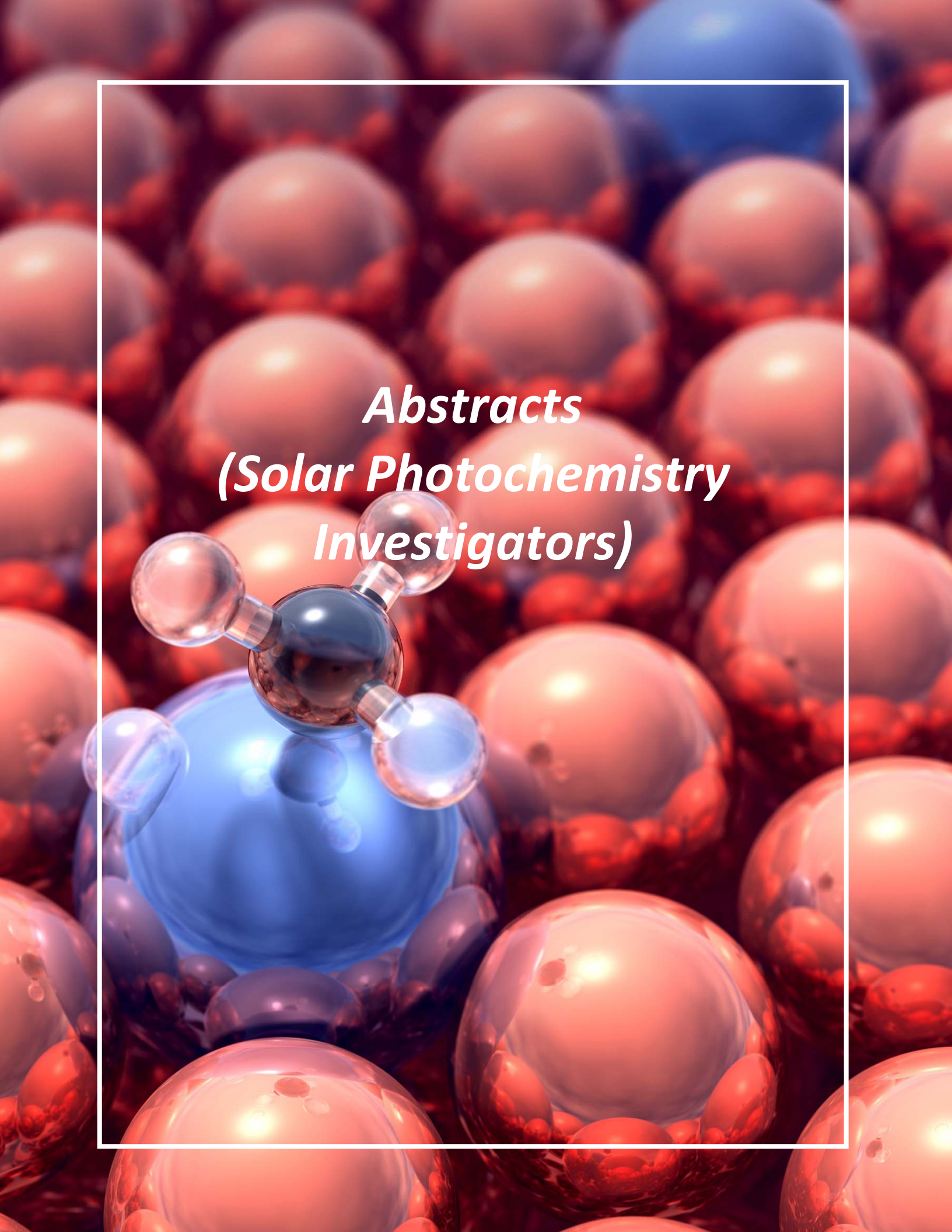


Fig. 2. Schematic of remote control of infrared-induced conformational isomerization of HONO. a. Without excitation of 'remote catalyst' (RC, blue) Tc-glyoxylic acid, the 'probe' laser pulse impinging on the mirror of the cavity containing reactant (R, red) *cis*-HONO is reflected; the reaction does not occur. **b.** First, a pump laser pulse impinging on the mirror of the RC cavity excites a polariton whose character is predominantly this cavity and the strongly coupled OH (light blue) stretch of RC. Within <100 ps, coupling between this vibration and solvent modes induces relaxation from the eigenstate to optically uncoupled (dark) RC states. Next, the 'probe' pulse efficiently excites a polariton whose character is predominantly the impinged cavity and the strongly coupled OH (light red) stretch of R; R is subsequently converted into the product (P, gold) *trans*-HONO.

There are no publications to report because this is a new award, with a start date of September 1, 2018.



***Abstracts
(Solar Photochemistry
Investigators)***

FUNDAMENTAL ADVANCES IN RADIATION CHEMISTRY

Principal Investigators:

DM Bartels (bartels.5@nd.edu), I Carmichael, I Janik, JA LaVerne, S Ptasińska
Notre Dame Radiation Laboratory, University of Notre Dame, Notre Dame, IN 46556

SCOPE

- *Research in fundamental advances in radiation chemistry is organized around two themes. First, energy deposition and transport seeks to describe how energetic charged particles and photons interact with matter to produce tracks of highly reactive transients, whose recombination and escape ultimately determine the chemical effect of the impinging radiation. The work described in this part is focused on fundamental problems specific to the action of ionizing radiation. Particular projects include completion of a radiolysis model for high temperature water, experimental and theoretical investigation of the VUV spectra of liquids up to supercritical conditions, chemistry of highly excited states in spur and track recombination in aromatic hydrocarbon liquids, and quantitative characterization of a novel radiation source, the atmospheric pressure plasma jet. The second thrust deals with structure, properties and reactions of free radicals in condensed phases. Challenges being addressed include the experimental and theoretical investigation of solvated electron reaction rates, determination of the redox potentials of hyper-reduced transition metal ions, analysis of the structure and reactivity of aqueous halide ion oxidation products; and characterization of the structure and properties of the CO_2^- radical.*

PROGRESS AND PLANS

In previous years it has been demonstrated that the equilibrium (1) $\cdot\text{OH} + \text{H}_2 \rightleftharpoons \text{H}_2\text{O} + \text{H}^\cdot$ is the most critical in controlling the radiolytic production of corrosive oxidizing species in pressurized water-cooled nuclear reactors, by the addition of excess H_2 to the water. Last year we reported an extensive series of experiments using high dose rates from 2.5 MeV electrons, in the range 0.5 to 8 kGy/s, to measure the steady state H_2 in neat water from room temperature to 350°C. We have a tentative value for the equilibrium constant (K_1) at 250-350°C. The value of K_1 is smaller than we previously considered possible, on the assumption that the ΔG_{hyd} for OH radical would be smaller (less negative) than that of water itself at all temperatures. This makes intuitive sense given that water can make four hydrogen bonds but OH can only make three, and it agrees very well with room temperature data. The implication of the new measured equilibrium constant above 250°C, is that OH radicals are more strongly solvated than water molecules at these high temperatures. This calls for some simulation of the OH radical solvation in high temperature water, presumably with ab initio MD methods.

The steady state H_2 produced at pH 11 in our high dose rate radiolysis experiment, starting just above room temperature, is much larger than can be accounted for with the accepted radiolysis mechanism. This pH was chosen to help determine the reaction rate (2) for $(e^-)_{\text{aq}}$ with $\cdot\text{O}_2^-$, which has only been reported at room temperature. The assumption has always been that the immediate product is $\text{O}_2^{\cdot-}$, which then is neutralized by proton transfer from water giving HO_2^- and OH^- . However, the H_2 measurements in our experiment require more oxidation of $\cdot\text{O}_2^-$. We tentatively concluded from our modeling that an oxidation of $\cdot\text{O}_2^-$ by $(e^-)_{\text{aq}}$ is the only reaction that can explain our observations, i.e. $(e^-)_{\text{aq}} + \cdot\text{O}_2^- \Rightarrow \text{O}_2 + \text{H}_2 + \text{OH}^-$. In the past year we carried out experiments in alkaline aerated formate solutions to test this hypothesis. The experiment made use of a burst of microsecond electron pulses from our linac, and involved measuring the $(e^-)_{\text{aq}}$ absorbance during the pulses as O_2 was converted quantitatively to $\cdot\text{O}_2^-$. Up to 100°C, the rate constant k_2 is found to be slightly smaller than the reaction rate for $(e^-)_{\text{aq}}$ with

O₂. Measurement of the H₂ product at 100°C in this chemical system failed to demonstrate the “oxidation” mechanism that we postulated. We are left at this time with no explanation for the large steady state H₂ concentrations measured at alkaline pH.

To probe the mechanism of halide oxidation by OH radicals, transient DC conductivity with simultaneous detection of optical absorption signals in (pseudo)halide solutions (Cl⁻, Br⁻, I⁻, SCN⁻) was carried out for the first time. For that purpose we designed and constructed a tandem fast DC conductivity/optical flow cell/setup. No conductivity change is observed in chloride solutions. Bromide, iodide and thiocyanate OH-induced oxidation in acidic solutions resulted in decrease of apparent transient conductivity due to proton and double (pseudo)halide ion uptake, offset by X₂⁻ formation (X=Br, I, SCN). Qualitative comparison of kinetic traces of optical/conductivity change in acidic and basic solutions of (pseudo)halides indicates that bromide solutions undergo a slightly different mechanism of OH-induced oxidation. The conductivity signal decrease in acidic bromide solutions, unlike in iodide or thiocyanate solutions, does not produce an optical signal growth. Moreover, quantitative DC conductivity signal increase did not account for 100% conversion of OH radicals into OH⁻. We propose that 92% of OH radicals react with Br⁻ via electron transfer and the remaining 8% of OH radicals add to Br⁻, which is reflected in fast optical growth of BrOH⁻ at 350 nm. Quantitative interpretation of the kinetics obviously requires accurate dosimetry of the conductivity signals. We recognized in the course of these experiments that chloromethane as well as DMSO dosimetry used routinely in past studies were giving unphysical results. MeCl undergoes gradual decomposition during storage in commercial containers. DMSO requires reevaluation of earlier reported radiation chemical yields of proton formation. We found that both thiocyanate and iodide solutions can be used as convenient dosimeters in acidic conditions instead of the problematic MeCl and DMSO dosimeters.

Partial molar volume changes in formation of hemibonded symmetric and asymmetric (pseudo)halide radical anions were measured at room temperature for the first time. To do this we designed and constructed an optical flow cell/setup for pulse radiolysis studies operating at pressures up to 2kbar. It has been found that in the reaction of di(pseudo)halide radical anions $X^{\bullet} + X^{-} \rightleftharpoons X_2^{\bullet -}$ (X=Br, I, SCN, SeCN), the partial molar volume of the products decreases by a few cc/mol in relation to the respective substrates. Following our recent reevaluation of the equilibrium for ClOH⁻ formation in water, we examined the pressure effect on the $Cl^{\bullet} + OH^{-} \rightleftharpoons ClOH^{\bullet -}$ equilibrium constant. The partial molar volume of ClOH⁻ was determined as 41.83 cc/mol which is almost 30% larger than the sum of [•]OH (14.4 cc/mol) and Cl⁻ (17.83 cc/mol) partial molar volumes. This confirmed that ClOH⁻ is a very loosely bound radical and qualitatively agrees well with our earlier temperature studies as well as a number of prior literature computational reports.

The temperature dependence of the vacuum ultraviolet charge-transfer-to-solvent (CTTS) absorption spectra of aqueous halide and hydroxide ions was measured up to 300 °C in subcritical water. With increasing temperature, absorption spectra are observed to broaden and redshift, much in agreement with previous measurements below 100 °C. These changes can be described alongside classic cavity models of the solvated species, where a gradual increase in cavity size is observed as a function of temperature while the Gibbs energy of hydration is largely unaffected. The changes in solvation properties can be considered in the context of recent studies of the ultraviolet spectroscopy of subcritical water and earlier investigations into the CTTS absorption.

For further characterization of the atmospheric-pressure plasma jet (APPJ) being used in many applications, we explored the possibility of applying an interferometry technique. We investigated the influence of plasma discharge in He gas flow in the APPJ using a Michelson interferometer and compared results with Schlieren photography. Both cases showed that the plasma discharge followed the He flow in the open atmosphere; however, the plasma discharge also affected the gas flow, indicating a transition from laminar to turbulent flow. One possible explanation of this effect may be gas heating; however, to achieve this increase in flow, the gas temperature must be significantly increased. The optical emission spectroscopy of the gas temperature ruled out thermal heating as a major or sole cause of this transition, indicating that more complex phenomena such as electrodynamic coupling of the applied electrical field and ions are likely to be involved. Currently, we are continuing introducing advanced techniques to better characterize APPJs, e.g., acoustic characterization, which will lead to deeper understanding of low-energy interactions in APPJ.

To tackle the challenge of short-lived plasma species characterization, we have developed *in situ* absorption spectroscopy with an acidified ferrous sulfate (Fricke) solution as a molecular probe of oxidative species formed due to plasma interaction. Our experimental results indicated that the total number of reactive species formed increased with plasma frequency and voltage, but decreased with increased frequency per pulse. To obtain a better understanding of the processes and species involved in the chemical reactions due to plasma exposure, we performed calculations for several scenarios in which the most likely reactive species were involved. In addition, to correlate the effects observed in Fricke solution with biological effects, we performed a study, in which other molecular probes such deoxyribonucleic acid was irradiated by plasma. These studies allowed us to investigate plasma-induced chemistry under different plasma experimental conditions in order to verify the usefulness of both the Fricke solution as a molecular probe to characterize plasma for future applications.

One thrust of work at the NDRL is to provide a comprehensive understanding of low-energy electron interactions, with a particular focus on dissociative electron attachment (DEA) to model biomolecular systems in the gas phase. The majority of biomolecules studied in the last decade consist of 5- or 6-membered rings. Therefore, it is important to indicate what factors drive the specific fragmentation reactions initiated by DEA to those ring compounds. Our study commenced with an investigation of imidazole, the simplest heterocyclic compound having a 5-membered aromatic ring with two nitrogen atoms, and was performed in collaboration with the Innsbruck group. In this study, the most abundant fragment was a dehydrogenated anion formed via H loss at the N1 position. This process occurred at electron energies of ~ 1.5 and ~ 2 eV, while other anions were formed dominantly above 7 eV. Among these anions, multiple dehydrogenation reactions were observed resulting in the loss of 2, 3 or 4 hydrogens, leading to a complete dehydrogenation of the imidazole molecule. Quantum chemical calculations revealed that these multiple dehydrogenation reactions were responsible for ring opening. We also studied DEA to a more complex compound, *i.e.*, nicotine, which is a bicyclic compound containing 5- and 6-membered rings linked to each other as well as to its two individual component fragments, *i.e.*, pyridine and methylpyrrolidine. DEA to nicotine did not result in the formation of a stable dehydrogenated molecular anion as was the case for other similar biomolecules. However, it was prone to complex dissociation pathways involving the cleavage of the pyrrolidine ring and isomerization mechanisms. Furthermore, for each dissociation channel in nicotine, an analogous pathway in *N*-methylpyrrolidine was observed. Based on this mass spectrometric study and quantum chemical calculations, we proposed possible fragmentation pathways for each fragment.

Our results showed that the pyrrolidine ring is particularly susceptible to fragmentation due to low-energy electron impact. In contrast with nicotine and *N*-methyl-pyrrolidine, the dominant pathway in DEA to pyridine was dehydrogenation. These results provide important new information about the stability of nicotine and its constituent parts, that can further advance our understanding of other ring compounds. Further systematic investigations are underway for gas phase 5-membered rings (e.g., oxazole, isoxazole, thiozole) in which positions of hetero atoms vary in their isomers.

PUBLICATIONS WITH BES SUPPORT SINCE 2016

- Sterniczuk M.; Bartels D.M. *J. Phys. Chem. A* **2016**, *120*, 200-9. Source of molecular hydrogen in high-temperature water radiolysis.
- Sterniczuk M.; Yakabuskie P.A.; Wren J.C.; Jacob J.A.; Bartels D.M. *Radiat. Phys. Chem.* **2016**, *121*, 35-42. Low LET radiolysis escape yields for reducing radicals and H₂ in pressurized high temperature water.
- Walker J.A.; Mezyk S.P.; Roduner E.; Bartels D.M. *The Journal of Physical Chemistry B* **2016**, *120*, 1771-9. Isotope dependence and quantum effects on atomic hydrogen diffusion in liquid water.
- Janik I.; Tripathi G.N.R. *J. Chem. Phys.* **2016**, *144*, 154307-7. The nature of CO₂⁻ radical anion in water.
- Huang W.; Ptasińska S. *Appl. Surf. Sci.* **2016**, *367*, 160-6. Functionalization of graphene by atmospheric pressure plasma jet in air or H₂O₂ environments.
- Adhikari E.; Ptasińska S. *Eur. Phys. J. D* **2016**, *70*, 180-7. Correlation between plasma induced DNA damage level and helium atmospheric pressure plasma jet (APPJ) variables.
- Arjunan K.; Obrusnik A.; Jones B.; Zajickova L.; Ptasińska S. *Plasma Proc. and Polym.* **2016** *13*, 1089-105. Effect of additive oxygen on the reactive species profile and microbicidal property of a helium atmospheric pressure plasma jet.
- Marin T.M., Janik I., Bartels D.M., Chipman D.M., *Nat. Commun.* **2017**, *8*, 15435. Vacuum ultraviolet spectroscopy of the lowest-lying electronic state in subcritical and supercritical water.
- Janik I., Carmichael I., Tripathi G.N.R., *J. Chem. Phys.*, **2017**, *146*, 214305. Transient Raman spectra, structure and thermochemistry of the thiocyanate dimer radical anion in water.
- Sargent, L., Sterniczuk, M., Bartels, D.M., *Radiat. Phys. Chem.* **2017**, *135*, 18-22. Reaction rate of H atoms with N₂O in hot water.
- A Ribar, K Fink, Z Li, S Ptasińska, I Carmichael, L Feketeová, S Denifl. *Phys. Chem. Chem. Phys.* **2017**, *19*, 6406-6415. Stripping off hydrogens in imidazole triggered by the attachment of a single electron.
- Z. Li, A.R. Milosavljević, I. Carmichael, S. Ptasińska. *Phys. Rev. Lett.*, **2017**, *119*, 053402. Direct observation and characterization of neutral radicals from a dissociative electron attachment process.
- J. Gorfinkiel, S. Ptasińska. *J. Phys. B: Atomic, Molecular, Optical Physics*, **2017**, *50*, 182001. Electron scattering from molecules and molecular aggregates of biological relevance.
- M. Ryszka, E. Alizadeh, Z. Li, S. Ptasińska. *J. Chem. Phys.* **2017**, *147*, 094303. Low-energy electron-induced dissociation in gas-phase nicotine, pyridine, and methyl-pyrrolidine.
- S. Ptasińska, M.A. Śmiałek, A.R. Milosavljević, B. Sivaraman *Eur. Phys. J. D*, **2017**, *71*, 264. Low-energy interactions related to atmospheric and extreme conditions.
- Li Z.; Carmichael I.; Ptasińska S. *Phys. Chem. Chem. Phys.* **2018**, *20*, 18271-8. Dissociative electron attachment induced ring opening in five-membered heterocyclic compounds.
- V. Samara, S. Ptasińska. *J. Vac. Sci. Technol. A*, **2018**, *36*, 04F402. Interferometry of plasma bursts in helium atmospheric-pressure plasma jets.
- E.R. Adhikari, V. Samara, S. Ptasińska. *J. Phys. D: Appl. Phys.*, **2018**, *51* 185202. Influence of O₂ or H₂O in a plasma jet and its environment on plasma electrical and biochemical performances.
- E.R. Adhikari, V. Samara, S. Ptasińska. *Biolog. Chem.*, **2018**, doi: 10.1515/hsz-2018-0203. Total yield of reactive species originating from an atmospheric pressure plasma jet in real time.

Radiation Stability of Aromatic Compounds

Jay A. LaVerne
Notre Dame Radiation Laboratory, University of Notre Dame
Notre Dame, IN 46556
laverne.1@nd.edu

Program Scope

The radiation chemistry of organic compounds can vary widely because of the vast variety of elemental compositions and yet some aspects of their decomposition can be obtained by observations of the fundamental processes occurring. This program elucidates the complete decomposition scheme of selected simple organic compounds with the goal of finding simple trends that can be applied to general classes of compounds in order to give predictive capability of their overall radiation stability. All radiation-induced processes in organic compounds are initiated by ionization, which is followed by neutralization to populate the whole manifold of excited states. These excited states and their subsequent reactions are responsible for product formation. The lowest energy triplet states of aliphatic compounds tend to readily decompose to a wide variety of radical species. These compounds are quite sensitive to radiation as exhibited by the high yields of products. On the other hand, aromatic compounds are thought to be radiation inert because of the low yields of final products. (Roder 1981) Recent studies from our laboratory have shown that aromatic compounds can in fact undergo extensive radiolytic decomposition under certain conditions. (Baidak, Badali et al. 2011; La Verne and Baidak 2012) The radiation stability of aromatic compounds can now be questioned. This program seeks to understand the mechanism underlying how aromatic compounds decompose when exposed to ionizing radiation and to identify the final products formed and their variation under different radiolytic conditions. Characterization of the conditions under which aromatic compounds are likely to be sensitive to radiation is an important part of this effort. Mixed organic compounds are found throughout the DOE complex. They are vital components of resins used in radioactive waste separations and the polymers used in construction components and waste storage containers. Aromatic entities are found in many of the solvents used in extraction processes including the newer “designer solvents” made from ionic liquids. Many building blocks of cells including DNA contain aromatic components so this research is also important for radiation protection purposes. The research focuses on the radiation chemistry of a variety of simple aromatic liquids containing different heteroatoms or aliphatic side chains. Molecular hydrogen production is the primary probe of radiation sensitivity, but a wide variety of spectroscopic and chromatographic techniques are also used to obtain detailed mechanisms on a few select compounds. This effort differs substantially from the conventional radiation chemical approach in that heavy ion radiolysis is used extensively as a tool for the elucidation of mechanisms.

Recent Progress

Aromatic compounds are found to be radiation inert when exposed to conventional gamma rays, but under certain heavy ion radiolysis conditions they exhibit substantial decomposition. This program tries to identify the characteristics under which aromatic compounds decompose and the mechanism involved. Since the decomposition of aromatic compounds is observed under heavy ion radiolysis this program relies extensively on exploiting the detailed characteristics of the track structure of radiation to probe the mechanisms involved. Ionizing radiation deposits energy along its path in localized regions

leading to a nonhomogeneous distribution of reactive species that constitutes the radiation track. The general effects of track structure on the radiolysis of materials in the condensed phase are reasonably well understood. (LaVerne 2004) With increasing linear energy transfer (LET, equal to the stopping power, $-dE/dx$) the density of energy deposition becomes greater about the particle path. This increase in local energy density leads to higher concentrations of reactive species than are obtained using conventional fast electron or gamma radiolysis. Yields of products that are formed due to second order reactions will be enhanced with increasing LET while those due to first order processes will be unaffected. Therefore, the yield dependence on LET can be used as a convenient probe of mechanisms in radiolysis. These so-called track effects elucidate the dominant process from the many possible pathways for product formation in the radiolysis of organic compounds. Studies on benzene and its analogs found a substantial increase in the production of H_2 on increasing the LET of the incident radiation. (LaVerne and Araos 2002; Enomoto, LaVerne et al. 2007) Organic radiolysis is primarily initiated by C-H bond breakage so the observation of H_2 implies that modification to the parent molecule decomposition must be occurring.

Previous work on molecules consisting of an aromatic and an aliphatic component found that with increasing aliphatic fraction the yield of H_2 also increased signifying an increase in radiation sensitivity. However, the total decomposition was still far below that observed with aliphatic compounds. For instance, the yield of H_2 with benzene is only 0.04 molecules/100 eV while that of cyclohexyl-benzene increases to about 0.3 molecules/100 eV, which is far below the value of 5.6 molecules/100 eV found for cyclohexane itself. The results suggest that even though the probability of initial energy deposition in the cyclohexyl-benzene is equal for the aliphatic and aromatic components, the energy is shifted to the aromatic moiety, which drives the subsequent chemistry. A mixture of 50% hexane and 50% benzene gives an almost identical yield of H_2 as the cyclohexyl-benzene. Although the energy deposition between the aromatic and aliphatic moieties are similar, one system involves intermolecular energy transfer while the other is an intramolecular energy transfer. Surprisingly, these two energy transfer are equally efficient. The results at LET definitely show that the process leading to H_2 formation is second order in aromatic compounds. (Baidak, Badali et al. 2011) The data further suggests that high-energy excited states are leading to H_2 formation, which is contrary to contemporary thought that the lowest level excited states are responsible for radiolytic decomposition. The increase in local concentration of excited state species within the particle track is promoting a substantial amount of reaction between them before they would normally decay to ground. The implication of this observation is that high-energy excited states can undergo extensive chemistry, but that chemistry can be somewhat restricted because of the short lifetimes of these states.

Previous studies with aromatic compounds containing heteroatoms was limited to pyridine and aniline. Both of these compounds have about the same radiation sensitivity as benzene, and toluene, respectively, suggesting that it is the aromatic nature of the compound that is leading to the observed effects and not the heteroatom. This work was further extended by the examination of radiation sensitivity of cyclic rings of different sizes by comparing six member rings (pyridine, pyrimidine, and piperidine) with five member rings (pyrrole, imidazole, and pyrrolidine). Radical scavengers I_2 and CCl_4 were used to elucidate reaction mechanisms of the H atoms. The pyridine and pyrrole show no dependence of H_2 on H atom scavenger concentration suggesting the H atom is not a precursor to H_2 but rather the pathway involves high-energy excited states. The H_2 yield with pyrrole is low as expected with an aromatic compound, but still about an order of magnitude higher than for pyridine possibly because of the increased strain in the smaller ring structure. On the other hand, piperidine and pyrrolidine have high H_2 yields comparable to a simple aliphatic like cyclohexane indicating their relative sensitivity to radiation. Both compounds show a strong dependence of H_2 yields on H atom scavengers suggesting the strong role of H atom abstractions reactions as the leading mechanism. The

aliphatic compounds, piperidine and pyrrolidine show no LET dependence while pyrrole and pyridine show the typical significant increase in H₂ yield with increasing LET indicating the role of second order reactions of high-energy excited states.

DNA bases are composed of aromatic rings with N atom heteroatoms. Some of them also contain O atoms, the effects of which on the relative radiation sensitivity of aromatic compounds have not yet been examined. As expected from the work with simple aromatic compounds with N heteroatoms in the ring, the DNA bases do not significantly decompose in gamma radiolysis. The yields of H₂ in the gamma radiolysis of the bases, adenine, guanine, cytosine, thymine, and uracil are about an order of magnitude lower than found with pyridine indicating their extreme stability to radiation. However, as the LET is increased the production of H₂ increases dramatically, much in the same trend as found with pyridine and benzene. Clearly, the DNA bases are not radiation inert under all radiolytic conditions. The increased sensitivity of the bases with the higher LET radiation is of the same order as the radiation quality factor and may be the reason that the relative biological effectiveness increases with increasing LET.

Future Plans

A wide variety of types of aliphatic and aromatic compounds has been examined and several trends noted. The LET dependence clearly shows that the H₂ is due to a second order reaction but the nature of the precursor is still unknown. The rate of transfer of energy from an aliphatic to an aromatic entity is extremely fast and independent of intermolecular or intramolecular processes. The initial state and the mechanism for energy transfer lies at the core of the radiation stability of aromatic compounds and fundamental approaches will be used to elucidate the mechanisms involved. The higher energy states are extremely short lived and present a challenge to experimental and theoretical methods. Deuterated mixtures may shed some information on the underlying processes. The goal is to examine the isotopic distributions of hydrogen in order to determine the site of H₂ production especially at high LET where the aromatic entity seems to dominate the productions of H₂.

The N heteroatomic aromatic molecules follow the same trends with LET as the simple carbon atom analogs suggesting similar mechanisms are involved. Many molecules in nature also have oxygen heteroatoms and a sample of these species will be examined to see if they generally follow the same trend as nitrogen and carbon atom analogs.

References

- Baidak, A., M. Badali, et al. (2011). "Role of the Low-energy Excited States in the Radiolysis of Aromatic Liquids." *Journal of Physical Chemistry A* **115**: 7418-7427.
- Enomoto, K., J. A. LaVerne, et al. (2007). "Heavy Ion Radiolysis of Liquid Pyridine." *Journal of Physical Chemistry A* **111**(1): 9-15.
- La Verne, J. A. and A. Baidak (2012). "Track Effects in the Radiolysis of Aromatic Liquids." *Radiation Physics and Chemistry* **81**: 1287-1290.
- LaVerne, J. A. (2004). *Radiation Chemical Effects of Heavy Ions. Charged Particle and Photon Interactions with Matter*. A. Mozumder and Y. Hatano. New York, Marcel Dekker, Inc: 403-429.
- LaVerne, J. A. and M. S. Araos (2002). "Heavy Ion Radiolysis of Liquid Benzene." *Journal of Physical Chemistry A* **106**(46): 11408-11413.
- Roder, M. (1981). *Aromatic Hydrocarbons*. In *Radiation Chemistry of Hydrocarbons*. Amsterdam, Elsevier.

DOE Sponsored Publications in 2016-2018

- M. T. Postek, D. L. Poster, A. E. Vladar, M. S. Driscoll, J. A. LaVerne, Z. Tsinas and M. I. Al-Sheikhly (2018) "Ionizing radiation processing and its potential in advancing biorefining and nanocellulose composite materials manufacturing", **Radiation Physics and Chemistry** 143, 47-52.
- J. A. La Verne, N. A. I. Tratnik and A. Sasgen (2018) "Gas Production in the Radiolysis of Poly(dimethylsiloxanes)", **Radiation Physics and Chemistry** 142, 50-53.
- K. Iwamatsu, S. Sundin and J. A. LaVerne (2018) "Hydrogen Peroxide Kinetics in Water Radiolysis", **Radiation Physics and Chemistry** 145, 207-212.
- J. Schofield, J. A. La Verne, D. Robertson, P. Collon and S. M. Pimblott (2017) "Material Dependence on the Mean Charge State of Light Ions in Titanium, Zirconium and copper", **Physical Chemistry Chemical Physics** *submitted*.
- S. C. Reiff and J. A. LaVerne (2017) "Radiolysis of water with aluminum oxide surfaces", **Radiation Physics and Chemistry** 131, 46-50.
- J. A. LaVerne and S. R. Kleemola (2017) "Hydrogen Production in the Radiolysis of Dodecane and Hexane", **Solvent Extraction and Ion Exchange** 35, 210-220.
- G. P. Horne, S. M. Pimblott and J. A. LaVerne (2017) "Inhibition of Radiolytic Molecular Hydrogen Formation by Quenching of Excited State Water", **Journal of Physical Chemistry B** 121, 5385-5390.
- S. Feister, D. R. Austin, J. T. Morrison, K. D. Frische, C. Orban, G. Ngirmang, A. Handler, J. A. La Verne, E. A. Chowdhury and W. M. Roquemore (2017) "Relativistic Electron Acceleration by mJ-class kHz Lasers Normally Incident on Liquid Targets", **Optics Express** 25, 18736-18750.
- J. Schofield, S. C. Reiff, S. M. Pimblott and J. A. La Verne (2016) "Radiolytic hydrogen generation at silicon carbide - water interfaces", **Journal of Nuclear Materials** 469, 43-50.

Radiation Chemical Impacts on Nuclear Power

Jay A. LaVerne and David M. Bartels

Notre Dame Radiation Laboratory, University of Notre Dame, Notre Dame, IN 46556

laverne.1@nd.edu, bartels.5@nd.edu

Program Scope

Advances in the development of nuclear power and in the maintenance of our present fleet of reactors requires fundamental radiation chemistry studies on complex systems containing water, organics, and interfaces. This program is an extension of studies on fundamental radiation chemical effects in homogeneous media that have been and continue to be a major effort at the NDRL. The extensive knowledge obtained for water, aqueous solutions, and organic liquids is being expanded to more directly address specific needs in the nuclear power industry. The program probes reactor water chemistry at operating conditions of BWR and PWR reactors, as well as the radiation chemistry at the molecular level occurring on interfaces. Development of newer separation systems that are more efficient and economic are being aided by fundamental studies on the organic separation media as well as the aqueous phases containing the high concentration of salts commonly associated with these systems.

Recent Progress and Future Plans

Oxidation of reactor components by H_2O_2 produced in the radiolysis of the water coolant is of major concern in the nuclear power industry. One of the more common methods for mediation of the production of H_2O_2 employs the addition of H_2 in order to suppress the combination reactions of OH radicals to form H_2O_2 . The kinetics of the formation and reaction of H_2O_2 in the long time gamma radiolysis of water is examined using a combination of experiment with model calculations. Escape yields of H_2O_2 on the microsecond time scale are easily measured with added radical scavengers even with substantial amounts of initial added H_2O_2 . The gamma radiolysis of aqueous H_2O_2 solutions without added radical scavengers reach a steady state limiting concentration with increasing dose, and that limit is directly proportional to the initial concentration of added H_2O_2 . The dose necessary to reach that limiting H_2O_2 concentration is also proportional to the initial concentration, but dose rate has a very small effect. The addition of H_2 to aqueous solutions of H_2O_2 leads to a decrease in the high dose limit that is linear with the initial H_2 concentration, but the amount of decrease is not stoichiometric. Proton irradiations of solutions with added H_2O_2 and H_2 are more difficult to predict because of the decreased yields of radicals; however, with a substantial increase in dose rate there is a sufficient decrease in radical yields that H_2 addition has little effect on H_2O_2 decay. More studies with selective radical scavengers will be employed to piece out their relative contributions and high LET (Linear Energy Transfer = $-\text{dE}/\text{dx}$) radiolysis will be performed. An extensive deterministic modeling effort is currently underway to help elucidate the underlying mechanisms involved in these systems.

A major source of water radiolysis in light water reactors comes from the $^{10}\text{B}(\text{n},\alpha)^7\text{Li}$ reaction. Borate is used as a “shim” for fine control of the neutron flux, and this fission reaction can amount to 30% of the total dose at the start of a new fuel cycle. Astonishingly there has been no measurement of the yields of product (g values) from the high-energy alpha and lithium recoil ions. In the last year we have been able to measure the room temperature g value for H_2 molecule production using low energy neutrons from the NIST neutron imaging facility. Irradiation of a 0.1M borate solution with low energy neutrons was carried out for up to several hours, and then

dissolved H₂ was measured with the mass spectrometric technique used at Notre Dame for many years. The neutron exposure was measured by including Na⁺ ions to capture some neutrons in the borate solution, and then counting the ²³Na gamma signal the day after the experiment. Using well-known neutron cross-sections, this technique gives the number of fission events the water was exposed to. Division of the H₂ produced by the total fission energy gives the room temperature g-value for H₂ as 1.35±0.03 molecules/100 eV. For these high LET fission particles, the yield of H₂O₂ in the water is probably equal to the H₂, with virtually no free radicals escaping the tracks. We expect in the next beam period to be able to make measurements at the reactor temperatures of interest, 200-350°C.

Systems for the separation of various metals from radioactive wastes are often mixed aqueous-organic phases in which the element of choice is dissolved in a concentrated nitric acid solution and then extracted into an organic liquid phase using selective ligands. Separation systems involve an aqueous phase of dissolved metals of interest with very high (up to 6M) nitrate concentrations. Nitrites formed from the radiolytically induced dissociation of the nitrates have been suggested to interfere with many of the ligands currently in use and for several of those proposed for future use. High nitrate concentration can also modify water radiolysis from that observed in the more commonly used dilute solutions. The role of excited states in the radiolysis of water can become important at high nitrate concentrations. Comparison of experimental measurements of the yield of H₂ produced in the gamma radiolysis of water and aqueous nitrate solutions with predictions of a Monte Carlo track chemistry model shows that the nitrate anion scavenging of the hydrated electron, its precursor, and hydrogen atom cannot account for the observed decrease in the yield at high nitrate anion concentrations. Inclusion of the quenching of excited states of water (formed by either direct excitation or reaction of the water radical cation with the precursor to the hydrated electron) by the nitrate anion into the reaction scheme provides excellent agreement between the stochastic calculations and experiment demonstrating the existence of this short-lived species and its importance in water radiolysis. Energy transfer from the excited states of water to the nitrate anion producing an excited state provides an additional pathway for the production of nitrogen containing products not accounted for in traditional radiation chemistry scenarios. Such reactions are of central importance in predicting the behavior of liquors common in the reprocessing of spent nuclear fuel and the storage of highly radioactive liquid waste prior to vitrification. Further experiments will explore the results with high nitric acid concentrations at high LET.

Most of the focus on the radiolysis of separation systems has concerned the aqueous phase. Organic radiolysis has mainly examined the stability of the ligands used to extract the actinides and lanthanides. However, a major portion of these systems is the organic solvent, which has traditionally been kerosene with the more modern systems using dodecane. A program to examine the radiation chemistry of dodecane has been started. Initial focus has been on the production of H₂ because it gives a measure of the overall sensitivity of the medium and the data is useful for establishing safety working limits due to its flammability. The yields of H₂ have been measured in the radiolysis of dodecane and hexane following radiolysis by gamma rays and a variety of heavy ions. Hexane has been examined because there are previous studies on it that can be used to verify experimental protocols. Measured yields with gamma rays are found to be slightly higher than literature values and decrease by about 25% on aeration of the sample. Increasing the LET from gamma rays to radiolysis with protons results in a decrease of H₂ yields by about 15% due to the increased importance of second order H atom combination reactions. A further increase in LET results in a slight increase in hydrogen yields. Scavenging of radical precursors using I₂ resulted

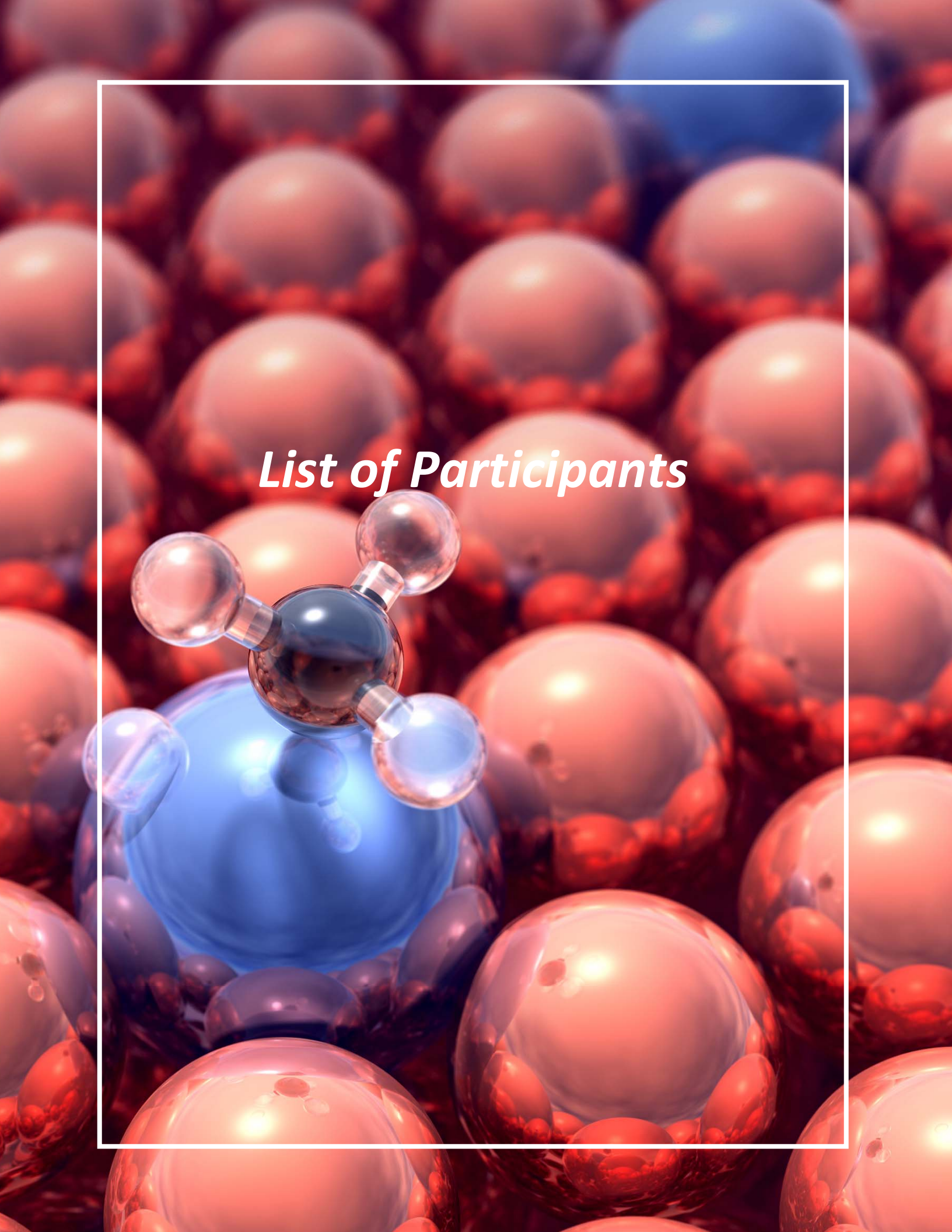
in a net loss of H₂, but the corresponding quantitative yields of HI were not reproducible. The formation of HCl in scavenging reactions of CCl₄ seems to indicate that both H atom combination and H atom abstraction reactions are occurring with the latter being more dominant.

There is a renewed interest in the radiolysis of aqueous solutions of highly concentrated chlorides and bromides due to the possible use of seawater as a coolant in emergency conditions. The main concern is the reaction of halogens with H₂O₂, which is the main stable oxidizing species produced in water radiolysis. Simple addition of halogens to aqueous solutions of H₂O₂ leads to its decomposition due to a thermal reaction that may well be acid catalyzed. For instance the half-life of H₂O₂ with 2 M bromide is about 400 hours. Further efforts are underway to determine the dependence of H₂O₂ on bromide and acid concentration and model studies will be used to determine rate constants. Initial efforts to examine the radiation dependence of H₂O₂ concentration on bromide concentration found an increase in H₂O₂ production with increasing bromide concentration. Bromide reacts with the OH radical and should decrease H₂O₂ production. Further examination determined that Br₂ or Br₃⁻ produced in radiolysis interferes with the iodide method used to determine H₂O₂. Other methods to circumvent this obstacle are being explored. Pulse radiolysis of concentrated bromide solutions found that the normally expected kinetics at low halogen concentration is different at higher concentrations. An equilibrium, Br₂ + Br⁻ ⇌ Br₃⁻, is quickly established that seems to control much of the observed kinetics. Further pulse radiolysis will be used to establish the exact mechanisms and models will be developed to extract the kinetics.

Publications with BES support (2016-2018)

- M. T. Postek, D. L. Poster, A. E. Vlarar, M. S. Driscoll, J. A. LaVerne, Z. Tsinas and M. I. Al-Sheikhly (2018) "Ionizing radiation processing and its potential in advancing biorefining and nanocellulose composite materials manufacturing", **Radiation Physics and Chemistry** 143, 47-52.
- J. A. La Verne, N. A. I. Tratnik and A. Sasgen (2018) "Gas Production in the Radiolysis of Poly(dimethylsiloxanes)", **Radiation Physics and Chemistry** 142, 50-53.
- K. Iwamatsu, S. Sundin and J. A. LaVerne (2018) "Hydrogen Peroxide Kinetics in Water Radiolysis", **Radiation Physics and Chemistry** 145, 207-212.
- J. Schofield, J. A. La Verne, D. Robertson, P. Collon and S. M. Pimblott (2017) "Material Dependence on the Mean Charge State of Light Ions in Titanium, Zirconium and copper", **Physical Chemistry Chemical Physics** *submitted*.
- L. Sargent, M. Sterniczuk and D. M. Bartels (2017) "Reaction Rate of H Atoms with N₂O in Hot Water", **Radiation Physics and Chemistry** 135, 18-22.
- S. C. Reiff and J. A. LaVerne (2017) "Radiolysis of water with aluminum oxide surfaces", **Radiation Physics and Chemistry** 131, 46-50.
- J. A. LaVerne and S. R. Kleemola (2017) "Hydrogen Production in the Radiolysis of Dodecane and Hexane", **Solvent Extraction and Ion Exchange** 35, 210-220.
- G. P. Horne, S. M. Pimblott and J. A. LaVerne (2017) "Inhibition of Radiolytic Molecular Hydrogen Formation by Quenching of Excited State Water", **Journal of Physical Chemistry B** 121, 5385-5390.
- S. Feister, D. R. Austin, J. T. Morrison, K. D. Frische, C. Orban, G. Ngirmang, A. Handler, J. A. La Verne, E. A. Chowdhury and W. M. Roquemore (2017) "Relativistic Electron Acceleration by mJ-class kHz Lasers Normally Incident on Liquid Targets", **Optics Express** 25, 18736-18750.

- J. Schofield, S. C. Reiff, S. M. Pimblott and J. A. La Verne (2016) "Radiolytic hydrogen generation at silicon carbide - water interfaces", **Journal of Nuclear Materials** 469, 43-50.
- M. Sterniczuk and D. M. Bartels (2016) "Source of Molecular Hydrogen in High-Temperature Water Radiolysis", **Journal of Physical Chemistry A** 120, 200-209.
- M. Sterniczuk, P. A. Yakabuskie, J. A. Jacob and D. M. Bartels (2016) "Low LET Radiolysis Escape Yields for Reducing Radicals and H₂ in Pressurized High Temperature Water", **Radiation Physics and Chemistry** 121, 35-42.



List of Participants

14th Condensed Phase and Interfacial Molecular Science Research PI Meeting
October 14 – 17, 2018
Participant List

Musahid Ahmed
Lawrence Berkeley National Laboratory
mahmed@lbl.gov

Anastassia Alexandrova
University of California, Los Angeles
ana@chem.ucla.edu

Abraham Badu-Tawiah
Ohio State University
badu-tawiah.1@osu.edu

Marcel Baer
Pacific Northwest National Laboratory
marcel.baer@pnnl.gov

Robert Baker
Ohio State University
baker.2364@osu.edu

David Bartels
Notre Dame Radiation Laboratory
bartels.5@nd.edu

Chris Bradley
U.S. Department of Energy/BES
chris.bradley@science.doe.gov

Ian Carmichael
Notre Dame Radiation Laboratory
carmichael.1@nd.edu

Aurora Clark
Washington State University
auclark@wsu.edu

Ethan Crumlin
ALS/Lawrence Berkeley National Laboratory
ejcrumlin@lbl.gov

Tanja Cuk
University of Colorado, Boulder
tanja.cuk@colorado.edu

Ismaila Dabo
Pennsylvania State University
dabo@psu.edu

Liem Dang
Pacific Northwest National Laboratory
Liem.Dang@pnnl.gov

Michel Dupuis
University at Buffalo
mdupuis2@buffalo.edu

Patrick El-Khoury
Pacific Northwest National Laboratory
patrick.elkhoury@pnnl.gov

Michael Fayer
Stanford University
fayer@stanford.edu

Christopher Fecko
U.S. Department of Energy/BES
christopher.fecko@science.doe.gov

Gregory Fiechtner
U.S. Department of Energy/BES
gregory.fiechtner@science.doe.gov

Miriam Freedman
Pennsylvania State University
maf43@psu.edu

John Fulton
Pacific Northwest National Laboratory
john.fulton@pnnl.gov

Etienne Garand
University of Wisconsin, Madison
egarand@wisc.edu

Bruce Garrett
U.S. Department of Energy/BES
Bruce.Garrett@science.doe.gov

Niranjan Govind
Pacific Northwest National Laboratory
niri.govind@pnnl.gov

Wayne Hess
Pacific Northwest National Laboratory
wayne.hess@pnnl.gov

Christine Isborn
University of California, Merced
cisborn@ucmerced.edu

Ireneusz Janik
Notre Dame Radiation Laboratory
ijanik@nd.edu

Mark Johnson
Yale University
mark.johnson@yale.edu

Kenneth Jordan
University of Pittsburgh
jordan@pitt.edu

Shawn Kathmann
Pacific Northwest National Laboratory
Shawn.Kathmann@pnnl.gov

Bruce Kay
Pacific Northwest National Laboratory
bruce.kay@pnnl.gov

Munira Khalil
University of Washington
mkhalil@uw.edu

Greg Kimmel
Pacific Northwest National Laboratory
gregory.kimmel@pnnl.gov

Jeffrey Krause
U.S. Department of Energy/BES
jeff.krause@science.doe.gov

Amber Krummel
Colorado State University
amber.krummel@colostate.edu

Christy Landes
Rice University
cflandes@rice.edu

Jay LaVerne
University of Notre Dame Radiation Lab
laverne.1@nd.edu

Stephan Link
Rice University
slink@rice.edu

Kranthi K. Mandadapu
Lawrence Berkeley National Laboratory
kranthi@berkeley.edu

Mark Maroncelli
Pennsylvania State University
maroncelli@psu.edu

Christopher Mundy
Pacific Northwest National Laboratory
Chris.Mundy@pnnl.gov

Francesco Paesani
University of California, San Diego
fpaesani@ucsd.edu

Mark Pederson
U.S. Department of Energy/BES
Mark.Pederson@science.doe.gov

Hrvoje Petek
University of Pittsburgh
petek@pitt.edu

Jim Pfaendtner
University of Washington
jpfandt@uw.edu

Neeraj Rai
Mississippi State University
neerajrai@che.msstate.edu

Geraldine Richmond
University of Oregon
richmond@uoregon.edu

James Rustad
U.S. Department of Energy/BES
james.rustad@science.doe.gov

Sapna Sarupria
Clemson University
ssarupr@g.clemson.edu

Gregory Schenter
Pacific Northwest National Laboratory
Greg.Schenter@pnnl.gov

Benjamin Schwartz
University of California, Los Angeles
schwartz@chem.ucla.edu

Viviane Schwartz
U.S. DOE/Basic Energy Sciences
Viviane.Schwartz@science.doe.gov

Liang Shi
University of California, Merced
lshi4@ucmerced.edu

Wade Sisk
U.S. Department of Energy
wade.sisk@science.doe.gov

Charles Sykes
Tufts University
charles.sykes@tufts.edu

William Tisdale
Massachusetts Institute of Technology
tisdale@mit.edu

Andrei Tokmakoff
University of Chicago
tokmakoff@uchicago.edu

Marat Valiev
Pacific Northwest National Laboratory
marat.valiev@pnnl.gov

Xue-Bin Wang
Pacific Northwest National Laboratory
xuebin.wang@pnnl.gov

Adam Willard
Massachusetts Institute of Technology
awillard@mit.edu

Kevin Wilson
Lawrence Berkeley National Laboratory
krwilson@lbl.gov

Bryan Wong
University of California, Riverside
bryan.wong@ucr.edu

Sotiris Xantheas
Pacific Northwest National Laboratory
Sotiris.Xantheas@pnnl.gov

Wei Xiong
University of California, San Diego
w2xiong@ucsd.edu

Joel Yuen-Zhou
University of California, San Diego
joelyuen@ucsd.edu